Open Research Online

Investigating the Behavioural and Molecular Functions of *Cry1* and *Cry2* Using Mouse Mutants

Thesis

oro.open.ac.uk

The Open University

Investigating the Behavioural and Molecular Functions of *Cry1* and *Cry2* using mouse mutants

A thesis presented for the degree of Doctor of Philosophy

Sneha N. Anand (BSc., MSc.)

Mammalian Genetics Unit, Medical Research Council, Harwell
The Open University
November 2011

DATE OF SUBMISSION : 17 NOVEMBER 2011
DATE OF AWARD : 13 FEBRUARY 2012

To My Dear Family

Thank you Aai for your constant support, encouragement and love.

Nitish, thank you for your understanding, patience and co-operation.

Thank you Papa and Mummy for being so supportive.

Last but not the least thanking Amma, Aatya, Bhavaji, Mausaji and Mausiji.

No words are enough to thank you all...........

ABSTRACT

Investigating the Behavioural and Molecular Functions of
Cry1 and _Cry2_ using mouse mutants

Sneha N. Anand
MRC Harwell and The Open University, 2011

Endogenous circadian clocks generate rhythms of physiology and behaviour that are synchronised to the environment, principally through the light-dark cycle. In mammals, the circadian clock is dependent on interlocked feedback loops that involve several clock elements such as cryptochromes (_Cry1_ and _Cry2_). Post-translational modifications control intracellular trafficking, functionality and degradation of CRY proteins which are keys to the functioning of the clock. CRY protein levels are dependent upon their timely degradation by F-box proteins. This has recently been shown in the afterhours _(Afh)_ mutant carrying a mutation in the F-box gene, _Fbxl3_. _Afh_ has been shown to lengthen circadian period by stabilising levels of CRY proteins across the circadian cycle. To understand the specific roles of each of the two CRY proteins in circadian regulation, we generated compound mouse mutants to investigate the behavioural and molecular consequences of stabilising either CRY1 or CRY2 protein levels in mice lacking the alternative form of _Cry_. The circadian wheel-running activity assessed in light:dark and constant environmental conditions for both $Cry1^{-/-};Fbxl3^{Afh/Afh}$ and $Cry2^{-/-};Fbxl3^{Afh/Afh}$ (stabilising CRY2 and CRY1 protein levels respectively); clearly show a gradual increase in period length in constant darkness as the dosage of $Fbxl3^{Afh}$ is increased. This would suggest that stabilisation of either CRY protein can lengthen the clock, presumably as a result of a prolonged phase of transcriptional repression by either protein. This effect seen in the compound mutants was confirmed at the gene and protein levels and it was concluded

that *Cry1* and *Cry2* can both act as transcriptional repressors, but that *Cry1* plays the predominant inhibitory role in the cerebellum and peripheral organs.

Subsequently it has been shown that FBXL21, the closest homologue of FBXL3, also binds to CRY1 and impairs its repressive action towards the transcriptional activators, CLOCK-BMAL1 presumably by degrading CRY1. Due to differences in their expression *Fbxl3* and *Fbxl21* may have overlapping roles. *In-vitro* and *in vivo* analysis in mutants generated in *Fbxl21;* revealed CRY2 as a preferable target of FBXL21 and that this may contribute to the lower repressive function of *Cry2*. Further investigation into the genetic interactions between the two F-box genes showed that *Fbxl3* is epistatic to *Fbxl21*.

Finally, *Fbxl21* has been shown to be associated with schizophrenia in humans. In our hands mutant mouse *Fbxl21* showed no such associations, instead indicating an association with anxiety and/or defects in sensorimotor gating.

ACKNOWLEDGEMENTS

TABLE OF CONTENTS

LIST OF FIGURES

LIST OF TABLES

ABBREVIATIONS

5-HT	5-hydoxytryptamine
Ach	Acetylcholine
Afh	afterhours
AVP	Arginine vasopressin
bHLH	Basic helix-loop-helix
Bmal1	Brain and Muscle ARNT-like protein 1
CALR	Calretinin
CaMK	Ca^{2+}/Calmodulin-dependent protein kinase
CCGs	Clock controlled genes
cDNA	Complementary DNA
CHL	Chlorambucil
CHX	Cyclohexamide
CK1ε	Casein kinase 1ε
CK2	Caesin kinase 2
CLC	Cardiotrophin-like cytokine
Clock	Circadian Locomotor Output Cycles Kaput
CRE	Ca2+/cAMP response element
CREB	cAMP response element binding protein
Cry1	Cryptochrome 1
Cry2	Cryptochrome 2
Cyc	Cycle
dB	Decibels
Dbt	Double time
DD	Constant darkness
dHPLC	Denaturing high-performance liquid chromatography
DMEM	Dulbecco's Modified Eagle Medium
DMSO	Dimethyl sulfoxide
DNA	Deoxyribonucleic acid
Dpc	Days post coitum
E.coli	*Escherichia Coli*
Ebd	earlybird
Enu	*N-ethyl-N-nitrosourea*
ES cells	*Embryonic stem cells*

FAD	Flavin adenine dinucleotide
FBS	Fetal Bovine Serum
Fbxl21	F-box and leucine rich repeat protein 21
Fbxl3	F-box and leucine rich repeat protein 3
FRQ	Frequency
GABA	Gamma amino butyric acid
GHT	Geniculohypothalamic tract
GLU	Glutamate
GRP	Gastrin releasing peptide
GSK3β	Glycogen synthase kinase 3β
Gtp	Guanosine triphosphate
hr	Hour
IEGs	Immediate early genes
IGL	Intergeniculate leaflet
ipRGCs	Intrinsically photosensitive retinal ganglion cells
IVF	*In-vitro* fertilisation
KOMP	Knockout mouse project
LB	Luria broth
LD	Light:dark
LL	Constant light
LRR	Leucine rich repeats
MAPK	Mitogen activated protein kinase
Mbp	Mega base pair
mENK	Met-enkephalin
mGLU	Metabotropic glutamate
MOP3	Member of PAS superfamily
ms	Millisecond
NE	Norepinephreine
NMDA	N-methyl-D-aspartate
NPAS2	Neuronal PAS domain protein 2
NPY	neuropeptide Y
NR1D1	Nuclear receptor subfamily 1 Group D Member 1
NT	Neurotensin
Opa1	Optic atrophy
Ovt	Overtime

PACAP	pituitary adenyl cyclase-activating peptide
PAS	period-arnt-single-minded
PBS	Phosphate Buffered Saline
PBST	Phosphate Buffered Saline with Tween 20
PCR	Polymerase Chain Reaction
Per1	Period1
Per2	Period 2
Per3	Period 3
PFA	Paraformaldehyde
PHR	Photolyase related
PK2	prokineticin
PKA	Protein kinase A
PP5	Protein phosphatase 5
PRC	Procabazine
PVDF	Polyvinylidene Fluoride
PVN	paraventricular nucleus
PWS	Prader-Willi syndrome
rd	Retinal degeneration mutation
RGC	Retinal ganglion cells
RHT	Retinohypothalamic tract
RORE	Retinoic acid- related orphan nuclear receptor response elements
Rorα	Retinoic acid- orphan receptor α
RPL13	Ribosomal protein L 13a
SCF	Skp/Cullin-1/F-box protein complex
SCN	Suprachiasmatic nucleus
SDS	Sodium Dodecyl Sulfate
sg	Staggerer
Sgg	Shaggy
SS	Somatostatin
TBST	Tris Buffered Saline with Tween 20
TGCE	Temperature gradient capillary electrophoresis
TGF-α	Transforming growth factor-α
TILLING	Targeted induced local lesions in genomes
TIM	Timeless
TOC1	Timing of CAB expression 1

TTX	Tetradotoxin
Ub	Ubiquitin
VIP	Vasoactive intestinal polypeptide
VPAC2	Vasoactive intestinal peptide receptor 2
WD	Tryptophan-Aspartate (Trp-Asp) repeats
Ztl	Zeitlupe
ZT	Zeitgeber time
β-Trcp1	Beta-transducin repeat-containing protein1
β-Trcp2	Beta-transducin repeat-containing protein2

1 CHAPTER ONE: Introduction

1.1 INTRODUCTION TO CIRCADIAN RHYTHMS

1.1.1 Circadian rhythms

The study of the temporal organisation of living organisms exposed to dynamic changes in the environment is called chronobiology. Many of these changes are rhythmic and are called biological rhythms. Under constant conditions, these biological rhythms are classified into circadian rhythms – endogenously generated rhythms with a period of ~24hrs, ultradian rhythms – recurrent periods generated at regular intervals throughout 24hrs eg. hormone release, and infradian rhythms – rhythms with a frequency less than one cycle occurring in 28hrs eg. seasonal rhythms and breeding. Amongst the three classified rhythms, circadian rhythms are the most characterised and widely studied.

Circadian rhythms exist across a wide range of organisms including vertebrates, plants, fungi and prokaryotes. The term "circadian" is derived from the Latin words "*circa*" meaning "about" and "*dies*" meaning "day". Thus, circadian rhythms are defined as endogenously generated self-sustained rhythms that are synchronised to the external environment with a period of ~24hrs. The beauty of these rhythms lies with the endogenous clock, the suprachiasmatic nucleus (SCN), which enables the organism to adapt to the external environment but still operate under constant conditions and in the absence of external cues (Lucas and Foster 1999; Wager-Smith and Kay 2000; Gachon, Nagoshi et al. 2004).

In mammals the circadian clock system is controlled in a hierarchial way, where the SCN receives photic (light) and non-photic input (social interaction, availability of food) from the environment. These responses are then processed in the SCN via the core oscillators,

involving complex genetic interactions, which are finally relayed into different output pathways.

1.1.2 Molecular basis of mammalian circadian core oscillators

Every living organism is able to exhibit rhythms with a period of ~24hrs. The molecular basis of circadian rhythms in a variety of species such as fungi, cyanobacteria and mammals have become clearer over the past few years. Although certain genes may have specific functions in different species, rhythms are generated with similar mechanisms of transcriptional-translational feedback loops (Reppert and Weaver 2001; Ko and Takahashi 2006).

The mammalian autoregulatory feedback loop is depicted in Figure 1.1. The positive regulators of the transcriptional-translational feedback loop are Circadian Locomotor Output Cycles Kaput (*Clock*) (or Neuronal PAS domain protein 2, *NPAS2*, a functional paralogue of *Clock*) and Brain and Muscle ARNT-like protein 1 (*Bmal1*) (also called Member of PAS superfamily, *MOP3*). The negative regulators are the three period (*Per1, Per2* and *Per3*) and two cryptochrome (*Cry1* and *Cry2*) genes. During early circadian day the two basic helix-loop-helix (bHLH) and PAS (period-arnt-single- minded) containing transcription factors, CLOCK and BMAL1 heterodimerise and bind to E-box *cis*-regulatory elements present in the promoter regions of clock controlled genes (CCGs), including *Per* and *Cry*. The binding of the complex facilitates the transcription of *Per* and *Cry*. Over the course of the day, PER and CRY proteins are translated; heterodimerise and translocate back and accumulate in the nucleus. From the beginning of the subjective night, the CRY proteins within the heterodimer, interact

with the CLOCK-BMAL1 complex and repress *Per* and *Cry*, thus creating a negative feedback. Since transcription of *Per* and *Cry* is inhibited due to the accumulated protein levels in the nucleus, translation of PER and CRY proteins is also inhibited. Thus, over time the levels of accumulated PER-CRY complex diminish, releasing the negative feedback. As a result a new cycle of transcription-translation is inititated (Griffin, Staknis et al. 1999; Kume, Zylka et al. 1999; van der Horst, Muijtjens et al. 1999; Shearman, Sriram et al. 2000; Ko and Takahashi 2006).

In addition to the above mentioned feedback loop, a secondary feedback loop exists which also involves the CLOCK-BMAL1 heterodimeric complex. The complex initiates transcriptional activation of retinoic acid-related orphan receptor α (*Rorα*) and nuclear receptor *Rev-erbα* (also called Nuclear Receptor Subfamily 1 Group D Member 1, *NR1D1*). The translated RORα and REV-ERBα proteins regulate the activation and suppression of *Bmal1* respectively by binding to retinoic acid-related orphan nuclear receptor response elements (ROREs) present in the *Bmal1* promoter. Additionally, when CRY proteins from the primary feedback loop accumulate in the nucleus, they are also able to inhibit the expression of *Rev-erbα*. As a result, there is activation of *Bmal1* transcription (Oishi, Fukui et al. 2000; Shearman, Sriram et al. 2000; Preitner, Damiola et al. 2002; Reppert and Weaver 2002; Ueda, Chen et al. 2002; Ko and Takahashi 2006) . Thus, the positive and negative transcriptional feedback loops are initiated by the CLOCK-BMAL1 heterodimer and are tightly regulated by the dynamic levels of clock proteins.
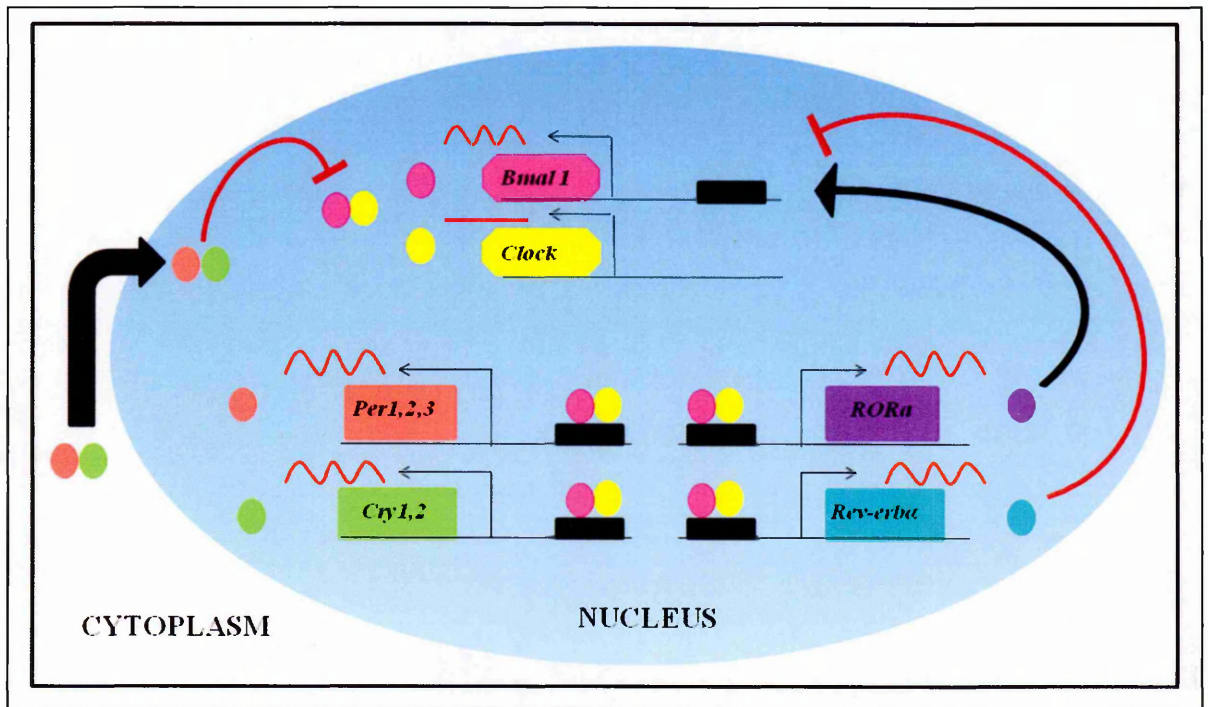
Figure 1.1: A simplified model describing the molecular mechanisms of the mammalian circadian clock. The circadian oscillations in mammals are composed of interlocked feedback loops consisting of the positive regulators, *Clock* and *Bmal1*, protein products of which (yellow and pink circles respectively) form a CLOCK-BMAL1 heterodimer. This heterodimer binds to the E-box elements (black boxes) present on the promoters of the three period (*Per1, Per2 and Per3*) and two cryptochrome (*Cry1* and *Cry2*) genes, activating their transcription. The translated PER (orange circle) and CRY (green circle) proteins form a heterodimer in the cytoplasm that translocates into the nucleus and inhibits their own transcription forming a negative loop. In addition to this loop is a secondary stabilising loop involving the retinoic acid related orphan nuclear receptors, *RORa and Rev-erbα* which are E- box regulated clock genes. While RORa (purple circle) activates *Bmal1*, REV-ERBα (aqua circle) suppresses the transcription of *Bmal1*. The timely regulation of these clock genes makes the mammalian circadian oscillator very robust.

1.1.3 Posttranslational modifications

The expression of clock genes, as seen previously, is controlled by interacting transcriptional-translational feedback loops. One of the critical processes involved in the regulation of these loops is the 24hr oscillating levels of clock gene RNA and proteins that are under tight circadian control. In order to maintain the loops at equilibrium, it is necessary to maintain the synthesis and degradation of dynamic clock protein levels. There are a number of processes that control the translated protein levels to avoid reaching steady state levels. Post-translational control of clock proteins includes processes like phosphorylation followed by ubiquitination, acetylation and sumoylation, of which phosphorylation is the most well studied in mammals.

Phosphorylation determines the cellular location and contributes to the stability of clock proteins. This is a critical process which is involved in generating time delays in clock mechanisms (Edery, Zwiebel et al. 1994; Dunlap 1999; Young 2000; Denault, Loros et al. 2001; Lee, Etchegaray et al. 2001). This is known from reports showing mutations in clock genes in appropriate domains result in either accelerating or delaying the clock.

The transcription of the *Per* and *Cry* genes results in the translation of PER and CRY proteins in the cytoplasm which form the negative core complex (Figure 1.1). In mammals, PER proteins are known to be phosphorylated in the cytoplasm during the day by casein kinase 1ε (CK1ε), first identified as a homolog of double-time (*Dbt*) in *Drosophila*. Studies carried out in *Drosophila* show that mutations in *Dbt* can result in either a shorter (Bao, Rihel et al. 2001) or longer circadian period (Price, Blau et al. 1998) by modulating the protein kinase activity of CK1ε. Moreover, in Syrian hamsters, a semidominant spontaneous mutation in CK1ε results in a significant shortening of circadian period length (Lowrey, Shimomura et

al. 2000). This was further confirmed in the targeted $CK1\varepsilon^{tau/tau}$ mouse mutant that displays a significantly short period of ~20hrs. Period shortening was shown to be associated with hyperphosphorylation of PER and accelerated destabilisation and degradation of PER *in vivo*. This was in contrast to the mild long circadian period observed in the targeted $CK1\varepsilon^{-/-}$ null mutant mouse (Meng, Logunova et al. 2008) .

In-vitro studies by Eide et al. (2005) further confirmed the binding and phosphorylation of PER by CKIε. Their studies confirmed the basis of the long circadian period observed in the $CK1\varepsilon^{-/-}$ mice *in-vitro*. They identified that inhibition of CK1ε resulted in the inhibition of PER protein degradation, thus lengthening the circadian period. *In-vitro* studies also showed interaction of CRY and CK1ε, however phosphorylation of CRY only took place when both CRY and CKIε are bound to PER (Eide, Vielhaber et al. 2002). Based on these studies, the following model was suggested. When CKIε-mediated phosphorylation of PER proteins take place, the CK1ε-PER complex is able to interact with CRY. The PER-CRY complex thus formed is translocated to the nucleus where the CRY proteins from the PER-CRY complex repress their own transcription by inhibiting the binding of CLOCK-BMAL heterodimer to the E-boxes (Griffin, Staknis et al. 1999; Eide, Vielhaber et al. 2002). This suggests that CK1ε promotes nuclear translocation of PER. On the other hand, Eide et al. (2005) confirmed that CK1ε also promotes the recruitment of a ubiquitin ligase necessary for PER degradation. Such opposing views suggest that if CK1ε regulates degradation of PER proteins, there may be other kinases (mentioned below) that are involved in re-localising PER from the nucleus to the cytoplasm.

Apart from CK1ε, there are various other kinases that are involved in the phosphorylation of clock proteins. Kinases that may regulate the phosphorylation-mediated degradation of clock proteins include mitogen activated protein kinase (MAPK) (Sanada, Harada et al. 2004)

involved in the phosphorylation of BMAL1(Sanada, Okano et al. 2002) and glycogen synthase

kinase 3β (GSK3β) (Gallego and Virshup 2007) that have several substrates including REV-

ERBα (Yin, Wang et al. 2006), CLOCK (Spengler, Kuropatwinski et al. 2009), PER2 (Iitaka,

Miyazaki et al. 2005), and CRY2 (Harada, Sakai et al. 2005). In addition to kinases,

phosphatases are also important for clock function. It has been shown that protein phosphatase

5 (PP5) removes the autoinhibitory phosphorylation and activates CKIε. PP5 is itself regulated

by an interaction with CRY (Gallego and Virshup 2007), indicating that PP5, CK1ε and CRY

dynamically regulate the mammalian clock (Partch, Shields et al. 2006). The functions of

kinases and phosphatases involved in the phosphorylation of CRY need to be investigated as

phosphorylation is an important process which can affect dimerisation, changes in localisation,

and degradation of clock proteins, therefore adding more complexity to the regulation of

circadian clock proteins.

1.1.4 Proteasomal degradation

Apart from phosphorylation, another requirement for efficient and timely reactivation of

the CLOCK-BMAL1 heterodimer is the degradation of the clock proteins which inhibit their

own transcription. Eukaryotic proteolysis is regulated by E3 ubiquitin ligases. One class of the

E3 ubiquitin ligases is the Skp/Cullin-1/F-box protein (SCF) complex as shown in Figure 1.2

Within this complex, Cullin-1 acts as a scaffold protein that interacts with the RING-domain

interacting molecule, Roc1, through its carboxyl-terminus. On the other hand, the amino-

terminus of Cullin-1 interacts with Skp that is associated with F-box proteins. The carboxyl-

terminus of F-box proteins is able to bind to phosphorylated substrates recruiting them to the

complex. Roc1 then recruits Ubiquitin-conjugated E2 enzymes that transfer ubiquitin to the

substrates. Once the substrates are polyubiquitinated, they undergo proteasomal degradation. While this interaction set up remains constant, it is thought that the specificity of the complex lies in the F-box protein. The F-box protein itself consists of two motifs, the F-box motif, made up of ~ 50amino acids, linking the F-box protein to the SCF complex, and the secondary motif involved in binding to the targeted phosphorylated substrates. Based on the secondary motifs, F-box proteins are divided into three groups: Fbw (containing Trp-Asp or WD repeats), Fbxl (containing leucine rich repeats or LRR) and Fbxo (containing "other" motifs) (Kipreos and Pagano 2000). Proline-rich regions, cyclin domains and zinc finger domains are amongst those associated with the Fbxo group.
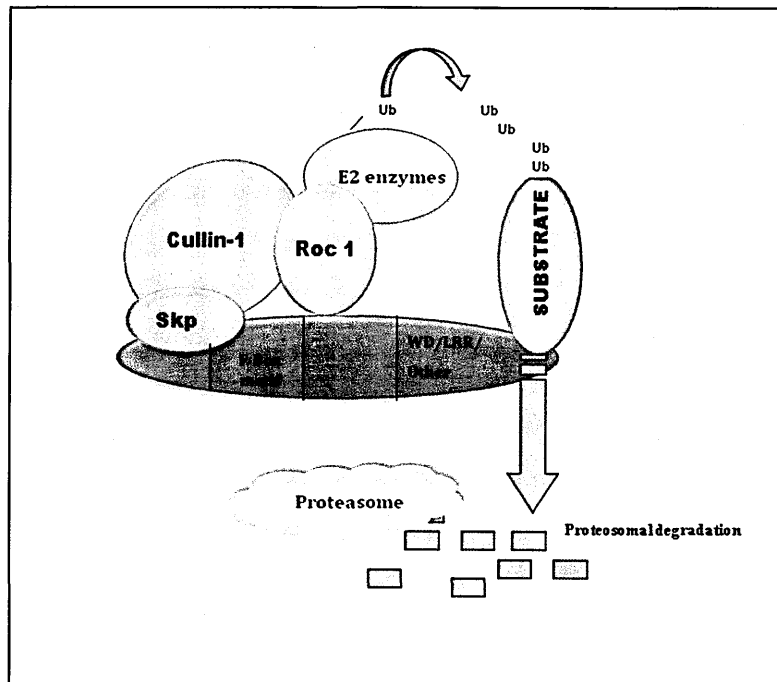
Figure 1.2: A schematic representation of the mammalian Skp/Cullin-1/F-box complex. Within the
Skp/Cullin-1/F-box protein complex, Cullin-1 acts as a scaffold protein and interacts with Roc-1 through its C-
terminus and with Skp through the N-terminus. Skp interacts with the F-box motif of the F-box protein. The C-
terminus of the F-box protein associates with specific phosphorylated substrates through either WD, leucine rich
repeats or any other motif. Once bound to the substrate, Roc-1 then interacts with E2 Ubiquitin conjugated
enzymes and transfers ubiquitin molecules on the substrate. Once is the substrate is polyubiquitinated, it
undergoes proteasomal degradation.

One of the first evidences confirming the importance of F box proteins was with the identification of zeitlupe (*Ztl*), an F-box protein found in *Arabidopsis*, required in the degradation of TIMING OF CAB EXPRESSION 1 (TOC1). A mutation in *Ztl* causes a reduced interaction of ZTL and TOC1 resulting in constitutive expression of TOC1 (Mas, Kim et al. 2003). Subsequently an F-box protein in *Neurospora*, *Fwd1*, was identified. FWD1 was found to regulate degradation of the clock protein FREQUENCY (FRQ) (He, Cheng et al. 2003). It was after the identification of *Fwd1* that orthologues of F-box proteins in different species were identified. The orthologue of *Fwd1* in *Drosophila, Slimb*, was identified as the F-box protein required for the timely degradation of PER and TIMELESS (TIM) (Grima, Lamouroux et al. 2002; Ko, Jiang et al. 2002). There are two mammalian orthologues of *Slimb*, beta-transducin repeat containing protein 1 (*β-Trcp*1) (also called *Fbw1a*) and beta-transducin repeat containing protein 2 (*β-Trcp*2) (Ohsaki, Oishi et al. 2008). Since most of the genes in the mammalian clockwork were identified as *Drosophila* homologues, it was thought that the β-TRCP proteins would also have a similar function of degrading phosphorylated PER proteins in mammals. *In-vitro* studies involving the mutagenesis of *β-Trcp1* resulted in stabilisation of PER proteins, thus resulting in a long circadian period (Reischl, Vanselow et al. 2007). Thus, a common mechanism of clock protein degradation was found across species. However an *in-vivo* model of an F box protein regulating degradation was not known until the identification of the afterhours (*Afh*) and overtime (*Ovt*) mutants (both have point mutations in *Fbxl3*) (Godinho, Maywood et al. 2007; Siepka, Yoo et al. 2007). Both these mutants, with point mutations in the secondary motif (LRRs), of the F-box protein, *Fbxl3*, were identified as circadian phenodeviants in an ENU based forward genetic screen in mice. Mass spectrometry analysis of endogenous FBXL3 associated proteins expressed in HeLa-S3 cells demonstrated the F-box-CRY interaction (Busino, Bassermann et al. 2007). Studies showed that when

NIH3T3 cells were infected with retroviruses encoding FLAG-tagged F-box proteins and immunoprecipitated, only FBXL3 interacted with the clock proteins, CRY1 and CRY2. This interaction was also confirmed by the stabilisation of CRY in the absence of FBXL3 (Busino, Bassermann et al. 2007). Expression studies in the *Afh* mutant showed a reduced interaction between FBXL3 and CRY proteins resulting in stabilised levels of CRY across time. Consequently, high levels of CRY were found during the daytime leading to an extended CRY transcriptional repression which ultimately contributes to the long circadian phenotype *in vivo*. Thus, it was identified that FBXL3 is important for the degradation of CRY, necessary for the normal functioning of the clock (Godinho, Maywood et al. 2007; Siepka, Yoo et al. 2007).

Forty-seven mammalian F-box proteins have been reported in 1999 which are encoded by mammalian genes (Jin, Cardozo et al. 2004). Recently another member of the F-box family, *Fbxl21*, the closest paralogue of *Fbxl3* has been shown to have circadian oscillations in the SCN with very low expression patterns in peripheral tissues. Similar to *Fbxl3*, it has been shown that *Fbxl21* is also involved in the interaction with and degradation of CRY proteins, suggesting that the two F box proteins may contribute to the opposite phenotypes of *Cry1*$^{-/-}$ (short phenotype) and *Cry2*$^{-/-}$ (long phenotype) mutant mice (Dardente, Mendoza et al. 2008)

1.1.5 Diversity of Clock genes

Systematic approaches to study the circadian clock mechanisms were initiated more than 20 years ago in the fruitfly *Drosophila melanogaster*. These studies were fast paced and were soon applied to investigate mechanisms in other species. Not surprisingly, the mechanisms of the circadian clock in mammals were also formulated based on the *Drosophila* clock (Hall 1995; Reppert and Weaver 2002). This was possible only due to the identification of gene

homologues in mammals. With the majority of the core mammalian clock genes identified, it can be said that a reasonable diversity in terms of gene functions exists among species. However, the backbone of the core oscillator works on the same principle of interacting transcriptional-translational positive-negative feedback loops among different species. With the mammalian core oscillator mechanism already described in section 1.2, the diversity between specific genes is described below with cryptochromes (*Cry*) as an example.

1.1.5.1   *Cryptochromes*

Cryptochromes (*Cry*) were first identified as photoreceptors belonging to the family of DNA photolyases (including both class I and class II photolyases). Photolyases are enzymes that use blue light to repair DNA damage induced by ultraviolet rays (Kanai, Kikuno et al. 1997; Sancar 2003). The *Arabidopsis thaliana* gene *Hy4* was known to encode CRY1. Studies carried out in the mutant *Hy4* and their human homologues showed that *Cry* had a similar sequence as photoloyases but lacked the repair activity. Hence *Cry* was classified as a separate class of blue light photoreceptor (Ahmad and Cashmore 1993). In addition to the sequence similarity between CRY1 and class I photolyases, CRY1 was also found to bind to the same co-factors, flavin adenine dinucleotide (FAD) and 5, 10-methenyltetrahydrofolate, as the photolyases (Lin, Robertson et al. 1995; Malhotra, Kim et al. 1995)

Cryptochromes have been identified in a range of organisms with high similarity in their sequence. Plant, *Drosophila* and mammalian cryptochromes are described below, showing the diversity of a single gene mainly in terms of its function.

1.1.5.2   *Plant Cryptochromes*

The plant kingdom is very broad and includes ferns, moss, angiosperm and algae. It is known that cryptochromes are found in each one of the species belonging to the plant kingdom (Lin and Shalitin 2003) and contain two main domains; an N-terminal domain related to photolyase function (PHR) and the C-terminal domain that is known to vary in size across species (Todo 1999). The PHR domain is involved in the binding of chromophores whereas the C-terminal domain is involved in protein-protein interactions and plays an important role in the nuclear or cytosolic localisation of CRY. Although cryptochromes are present in most of the plant species, and are similar in their PHR domains, there are two known *Cry* genes, *Cry1* and *Cry2*, in *Arabidopsis thaliana*. The number of *Cry* genes varies for each plant species. For example there are five known *Cry* genes in ferns (Imaizumi, Kanegae et al. 2000) and three in tomato (Perrotta, Ninu et al. 2000). The PHR domains are, however, very similar with all the differences present only in the C-terminal regions of *Cry* genes. Amongst the *Cry1* and *Cry2* paralogues of *Arabidopsis*, there is 58% similarity in the PHR domain whereas within the C-terminus *Cry1* and *Cry2* have a sequence similarity as little as 13%. The C-terminus varies largely amongst species from a 380 amino acid sequence in *Arabidopsis* to no C-terminal region in white mustard (Batschauer 1993; Malhotra, Kim et al. 1995) indicating that this region may have distinct functional roles in different species.

It has been found that *Arabidopsis* CRY1 and CRY2 mediate the majority of blue light responses and are involved in physiological functions like inhibition of hypocotyl elongation, affecting flowering time (Ikegawa, Masuno et al. 1999; Imaizumi, Kanegae et al. 2000) and anthocyanin accumulation (Deng and Quail 1999; Banerjee and Batschauer 2005). CRY proteins are also known to undergo phosphorylation in the C-terminus in response to blue-

light exposure and this is shown in the *Cry1* mutant where *Cry1* fails to be phosphorylated, suggesting that CRY1 plays an essential role in photoreception. *Arabidopsis* CRY1 and CRY2 are known to interact with phytochromes (red far-red receptors) and together play a role in the entrainment of the *Arabidopsis* clock (Bagnall, King et al. 1996).

1.1.5.3   *Drosophila Cryptochromes*

For several years now, genetics has provided a lot of insight into the key regulators of the circadian oscillations as most of the species studied, such as *Drosophila, C. elegans, Neurospora crassa,* and *Cyanobacteria,* possess circadian rhythms (Hardin, Hall et al. 1990). The first clock gene identified in *Drosophila* was the period (*Per*) gene in a mutagenesis screen (Konopka and Benzer 1971; Bargiello, Jackson et al. 1984). With data obtained from *Neurospora crassa,* it was predicted that *Per* participates in a negative feedback regulation that was shown to be the central regulatory mechanism (Hardin, Hall et al. 1990; Aronson, Johnson et al. 1994; Marrus, Zeng et al. 1996; So and Rosbash 1997). Similarly, the second clock gene identified was timeless (*Tim*) (Myers, Wager-Smith et al. 1995; Sehgal, Rothenfluh-Hilfiker et al. 1995). Further studies by Emery et al. (1998) in a *Drosophila* mutant with an ablated eye led to the identification of *Drosophila Cry* that predominantly act as a photoreceptor (Sehgal, Rothenfluh-Hilfiker et al. 1995). *Cry* regulates the *Drosophila* circadian clock by interacting with and degrading TIM present in the PER-TIM complex, thus releasing the negative feedback (Emery, So et al. 1998; Stanewsky, Kaneko et al. 1998; Ceriani, Darlington et al. 1999). Being predominantly nuclear, *Drosophila Cry* is known to regulate the circadian clock through light (Emery, So et al. 1998; Stanewsky, Kaneko et al. 1998). The molecular mechanism of the circadian clock in *Drosophila* is briefly described

below. It involves the formation of the CLOCK/CYCLE heterodimer that bind to E-boxes of *Per*, *Tim* and *Cry*. PER and TIM form a heterodimer, enter the nucleus and inhibit the binding of the clock proteins, forming a negative feedback loop which is in turn suppressed by CRY. In the presence of light, CRY binds to TIM and forms a heterodimer which ultimately promotes ubiquitination followed by proteasomal degradation of TIM, thus releasing the inhibitory effects (Ceriani, Darlington et al. 1999).

The photoreceptor role of *Cry* was evident from studies in the hypomorphic *Cryb* mutant line that lack *Cry* function and showed a reduced entrainment in light:dark (L:D) and light conditions (Stanewsky, Kaneko et al. 1998; Helfrich-Forster, Winter et al. 2001). This was also supported by recent studies where the clock neurons were tested for their ability to entrain to out-of-phase light and temperature cycles. The results from these studies show that, similar to *Cry* null mutants, the *Cry*-negative neurons entrained very slowly to light-dark cycles (Yoshii, Hermann et al.).

Thus, *Drosophila Cry* functions as a transcriptional repressor in addition to being a circadian photoreceptor (Krishnan, Levine et al. 2001).

1.1.5.4   *Mammalian Cryptochromes*

Mammalian cryptochromes, *Cry1* and *Cry2*, were also identified as members of the DNA photolyase family. Both *Cry1* and *Cry2* were seen to bind DNA affected by UV with a high affinity, however they lacked the DNA repair activity unlike other photolyases (Campbell and Murphy 1998). Thus, the DNA binding affinity of mammalian *Cry* is considered as an evolutionary artefact (Sancar 2004).

The role of mammalian *Cry* involves regulation of circadian oscillations by tightly regulated interactions with other clock genes, thus generating interlocked feedback loops (as described in section 1.2). However, this function of *Cry* was identified only after generating *Cry1*$^{-/-}$ and *Cry2*$^{-/-}$ mouse mutants. Although, both these genes showed highly similar sequences it was surprising to determine the different and opposing phenotypes of the single mutant mice. While the *Cry1*$^{-/-}$ mice showed a shorter circadian period of 22.7hrs, the *Cry2*$^{-/-}$ mice displayed a longer circadian period of 24.7hrs compared to the circadian period of 23.7hrs in wild type mice. *Cry1*$^{-/-}$*;Cry2*$^{-/-}$ double mutants on the other hand were completely arrhythmic under constant conditions, proving the presence of *Cry* is absolutely essential in generating circadian oscillations (van der Horst, Muijtjens et al. 1999). Hence, it was then considered that the main role of mammalian *Cry* was its involvement with other clock genes to maintain the autoregulatory feedback loops.

With a prior knowledge of the involvement of *Cry* as photoreceptors in *Drosophila* and its high expression in the inner retina in mice (Miyamoto and Sancar 1998; Miyamoto and Sancar 1999; Thompson, Bowes Rickman et al. 2003), a wide variety of studies were carried out to investigate this function of mammalian cryptochromes which has ultimately resulted in a debate yet to be resolved. It was with the identification of melanopsin (opsin found in the retinal ganglion cells) that the role of *Cry* as photoreceptors was overshadowed (Provencio, Rodriguez et al. 2000). This was because elimination of melanopsin, coupled with the ablation of the classical photoreceptor rods and cones, displayed a complete loss of visual and circadian phototransduction (Hattar, Lucas et al. 2003; Panda, Provencio et al. 2003). Additionally, with a loss of either *Cry*, there is a reduced photoinduction of genes. Compared to wild-type mice, while a 2-fold reduction in photoinduction of genes is observed in *Cry2*$^{-/-}$, a 10-fold loss is observed in *Cry1*$^{-/-}$*; Cry2*$^{-/-}$ double mutants (Thresher, Vitaterna et al. 1998;

Selby, Thompson et al. 2000). These results suggest that CRY proteins do have some retinal photoreceptor function as there is less photoinduction of genes in the *Cry* null mutants.

Table 1.1 below shows a few mammalian clock genes, their *Drosophila* homologues and their function in circadian timekeeping

Table 1.1: Diversity of Clock genes among mammals and Drosophila melanogaster

Clock Gene (Mammals)	*Drosophila* Homologue	Function of Clock gene
Clock	*Clock*	Positive regulator Activates transcription of CCGs through E-boxes
Bmal1	*Cycle (Cyc)*	Positive regulator Activates transcription of CCGs through E-boxes
Per1,2	*Per*	Negative regulator Forms a heterodimer with CRY in mammals and TIM in *Drosophila*
Tim- homologous to *Tim2* in *Drosophila*	*Tim*	No circadian function of mammalian *Tim* identified *Drosophila Tim* activated by CLOCK-BMAL1 Negative regulator of PER, CRY
Caesin kinase1ε	*Doubletime (Dbt)*	Phosphorylates PER,CRY and BMAL1
Glycogen synthase kinase (GSK3)	*Shaggy (SGG)*	GSK3 involved in phosphorylation of CRY,REV-ERBa and PER SGG phosphorylates and promotes nuclear entry of TIM

1.1.6 The suprachiasmatic nucleus (SCN)

In mammals, the master pacemaker that controls and regulates circadian rhythms resides in bilaterally paired suprachiasmatic nuclei embedded in the hypothalamus. A variety of studies have been carried out with recordings of SCN neural activity with and without lesions, to show the importance of the SCN. One of the early evidences includes lesion studies carried out in the rat. It was shown that circadian rhythmicity is restored in a SCN lesioned rat, following foetal SCN transplant, suggesting the presence of the SCN is important in generating and maintaining circadian rhythms (Moore and Eichler 1972; Moore and Silver 1998). The SCN is composed of two distinct subdivisions that are both anatomically and functionally different. The differences in the subdivisions *viz* the dorsomedial "shell" and the ventrolateral "core" are known to be conserved among mammalian species (Moore 1996). Both these subdivisions also seem to have distinct functions; while the core collects inputs mainly from the retina and other brain areas, the shell on the other hand is involved in generating and relaying the circadian timing signals. Thus, maintaining the synchrony between the neurons of these two subdivisions is important.

1.1.6.1   Input to the SCN

Circadian rhythms involve entrainment to the external environment with the help of external cues such as light and temperature. While in birds and reptiles the photoreceptor molecules that are required to reset the circadian clock are present in various organs such as the pineal gland, mid-brain and eyes, in humans and mice only the eyes work as light receptors to entrain the circadian clock. With the removal of eyes or ablation of optic nerves, both mice

and humans cannot entrain to the external light cues (Schwartz, W.J. 1993). With the eye playing a role in generation of visual responses and circadian photoreception, the information is processed, once the eye receives the light input, by distinct systems. While the visual cortex, as the name suggests, processes the information received by the eye in generating visual responses, the retinohypothalamic tract (RHT) transmits information to the SCN for circadian photoreception.

Several evidences have shown that the RHT is sufficient and necessary to mediate circadian photoreception function. This is evident from studies carried out in mice carrying the retinal degeneration (*rd*) mutation. In the presence of the *rd* mutation there is inactivation of the enzyme, cGMP-phosphodiesterase, specifically found in the classical photoreceptor rods located in the outer retina. This in turn blocks the phototransduction signalling cascade of the rods and the mice are thus visually blind. However, surprisingly these mice show a normal to moderately reduced circadian photoreception (Bowes, Li et al. 1990; Yoshimura and Ebihara 1998). Similarly, humans with the condition retinitis pigmentosa, where there is a complete loss of the classical photoreceptors rods and cones, are blind with no sense of light but respond normally to the external light dark cycle and show normal circadian photoreception (Czeisler and Dijk 1995; Wee and Van Gelder 2004). Thus, it is evident that circadian entrainment is processed by a dedicated system with inner retinal neurons and central pathways entirely different from those mediating the visual perception in the outer retina.

The standard model that is responsible for circadian photoreception via the RHT in humans and mice is depicted in Figure 1.3 and is described as follows. The RHT is formed from the axons of the retinal ganglion cells (RGCs) present in the inner retina and receive signals from rods and cones in the outer retina. Most of the RGCs have their axons projecting to brain areas, via the optic nerves, generating visual images. However, a small population of

the RGCs expressing melanopsin (a classical photopigment) are the neurons that project their axons to the SCN (*via* the optic nerve) and also to other areas of the brain such as supraoptic region, anterolateral hypothalamus, subparaventricular zone and the thalamic intergeniculate leaflet (IGL) (Levine, Weiss et al. 1991). The melanopsin expressing, intrinsically photosensitive retinal ganglion cells (ipRGCs) are stimulated by light which send the signal to the SCN core via the RHT, leading to a neurotransmitter signalling cascade. RHT releases the neurotransmitter, glutamate (GLU) that activates its excitatory receptors, N-methyl-D-aspartate (NMDA) and metabotropic glutamate (mGLU) receptors. This binding of GLU and NMDA/mGLU and depolarisation of the RGC neuronal membrane triggers a Ca^{2+} influx into the SCN core neurons. Membrane depolarisation is important as at the membrane resting potential, the ion channel is blocked by extracellular Mg^{2+}, which is removed only by depolarisation. Intercellular changes in the SCN neurons with an increased Ca^{2+} influx results in the activation of various kinases such as Ca^{2+}/Calmodulin-dependent protein kinase (CaMK), mitogen activated protein kinase (MAPK), protein kinase A (PKA). This results in the subsequent activation of cAMP response element binding protein (CREB) by phosphorylation at amino acid Ser133. This phosphorylated CREB then binds to the Ca^{2+}/cAMP response elements (CRE) present in promoters of immediate early genes (IEGs) such as *c-fos*, *Per1* and *Per2*, thus activating their transcription (Meijer and Schwartz 2003; Antle and Silver 2005; Liu, Lewis et al. 2007). In addition to GLU, the RHT also releases the pituitary adenyl cyclase-activating peptide (PACAP) that mimics the effects of GLU by binding to G-protein coupled receptors, PAC1 and vasoactive intestinal peptide receptor 2 (VPAC2) (Liu, Lewis et al. 2007). The above mentioned signalling cascade occurs in the SCN core (as mentioned in the previous section that information flow is from the core to the shell). Core neurons then communicate with the SCN shell utilising neurotransmitters such as

vasoactive intestinal polypeptide (VIP), gastrin releasing peptide (GRP) and gamma amino butyric acid (GABA). Additonally, the SCN shell neurons that are GABA-ergic contain molecular clocks regulated by the autoregulatory feedback loops and communicate to various SCN targets through arginine vasopressin (AVP) and GABA (Antle and Silver 2005).

Although the main input to the SCN is received via the RHT, the SCN indirectly also receives input from geniculohypothalamic tract (GHT) that is formed from the neurons projecting from the intergeniculate leaflets (IGL) to the SCN. Neuropeptide Y (NPY) and GABA are released by neurons of the GHT. It has been identified that the presence of IGL is not completely essential for photic entrainment, however lesions in the same do result in subtle effects in phase change and period control regulation by light (Moore and Card 1994).

Apart from light being the predominant external cue for the SCN to entrain to external environment, the SCN has the ability to adapt to other forms of entrainment cues such as temperature, food, and social responses. While organisms such as *Drosophila* and mammals entrain to constant daily temperatures (Buhr, Yoo et al.), restricted feeding schedules (Stephan 1997; Stephan 2002) and repeated social interactions at the same time (Mrosovsky 1988), a change in any of the cues can cause a phase shift in the free-running activity of circadian rhythms (Ben-Shlomo and Kyriacou 2002).

Finally, in addition to the SCN, co-ordinated molecular rhythms have also been identified in a number of tissues and cell types throughout the body including the pituitary, olfactory bulbs and pineal gland (Abe, Herzog et al. 2002; Guilding and Piggins 2007).
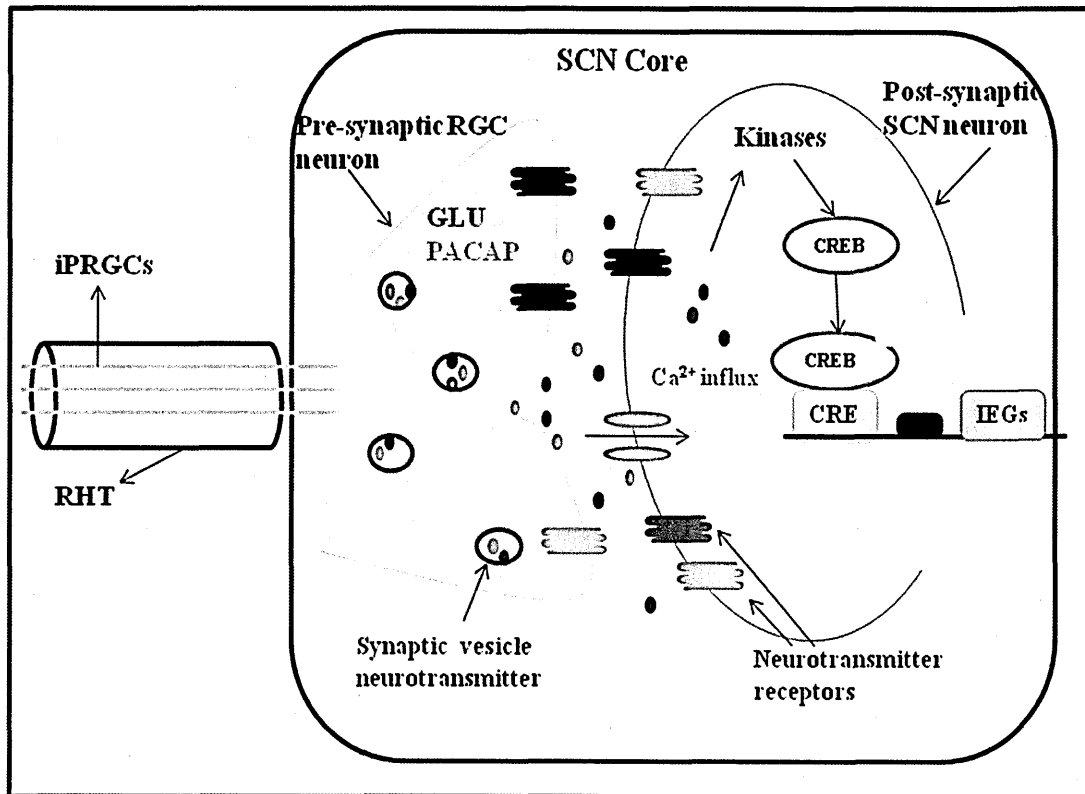
Figure 1.3: Input pathway to the suprachiasmatic nucleus via the retinohypothalamic tract.
Light is transmitted via the intrinsically photosensitive retinal ganglion gells (iPRGCs) resulting in the release of glutamate (GLU) and pituitary adenyl cyclise activating peptide (PACAP) by the presynaptic retinal ganglion cells. Binding of GLU to its NMDA receptors results in the depolarisation of the membrane leading to an increase in Ca^{2+} influx which in turn activates several kinases such as mitogen-activated protein kinase (MAPK), Ca^{2+}/Calmodulin-dependent protein kinase (CaMK), protein kinase A (PKA). This results in the phosphorylation of cAMP response element binding protein (CREB). The activated phosphorylated CREB then binds to the Ca^{2+}/cAMP response element (CRE) present in the promoters of the immediate early genes such as *c-fos*, *Per1* and *Per2*, thus initiating their transcription. The SCN core then communicates with neurons in the SCN shell that release neurotransmitters such as gamma amino butyric acid (GABA), vasoactive intestinal polypeptide (VIP), gastrin-releasing peptide (GRP). Neurons within the SCN shell are able to intiate the molecular loops once they receive the input signal from the SCN core. Adapted from Antle and Silver (2005).

23

1.1.6.2 *Intercellular organisation within the SCN*

Synchrony between the neurons of the core and the shell is co-ordinated through various neurotransmitters released in specific SCN subdivisions. With gamma-aminobutyric acid (GABA) and vasoactive intestinal polypeptide (VIP) being released by a vast majority of the SCN neurons, the core and shell also include specific neurotransmitters. The SCN core contains one or more neuropeptides that are co-localized with GABA. The two neuropeptides synthesized by the core in addition to GABA and VIP are gastrin releasing peptide (GRP) or neurotensin (NT). However a small population of cells also produce calretinin (CALR). The SCN shell on the other hand which is made of 57% of the total SCN neuronal population frequently produce arginine vasopressin (AVP) that is co-localised with GABA. There is also a small population of neurons that produce somatostatin (SS) and met-enkephalin (mENK) (Moore and Silver 1998; Abrahamson and Moore 2001).

The presence of VIP in the SCN is a pre-requisite for the activation and synchronisation of the neurons. VIP produced by ~15% of the SCN neuron population, with ~60% of the neurons expressing the VPAC2 receptor encoded by the *Vipr2* gene, is important for inter and intracellular synchronisation. This observation was made from studies in SCN organotypic slices and is also consistent with studies carried out in the $Vip^{-/-}$ and $Vipr2^{-/-}$ mice that display arrhythmic behaviour due to their inability to maintain the synchrony between the neurons (Harmar, Marston et al. 2002; Colwell, Michel et al. 2003; Aton, Colwell et al. 2005; Maywood, Reddy et al. 2006). This is further shown in the $Vipr2^{-/-}$ cells that are transiently activated, which are unable to attain synchronisation. These conclusions suggest that for the SCN to retain its pacemaker properties, synchronisation of the interceullular molecular

clockwork via the neuropeptidergic signalling cascade is necessary (Maywood, Reddy et al. 2006).

While the SCN core neurons project to other neurons located in the core, shell and other areas of the brain, the neurons from the shell are confined to the shell region. This intercellular organization suggests that the core receives the main input signal from the retina (with afferents containing glutamate (GLU) and pituitary adenyl cyclase-activating peptide (PACAP)), intergeniculate leaflet of the thalamus (IGL) (with fibres containing neuropeptide Y (NPY) and GABA) and raphe nuclei (with 5-hydroxytryptamine (5-HT) containing afferents). As compared to this complex organisation of the core, only acetylcholine (Ach), norepinephreine (NE) and histamine (HA)-projecting neurons converge into the shell (Moore and Silver 1998; Abrahamson and Moore 2001).

1.1.6.3   Output from the SCN

It has been shown that the ouput from the SCN to other brain areas and peripheral tissues are via neuronal and/or humoral signalling. The determination of specific SCN efferent neurons that are required for transmitting SCN output signals was identified by abolishing the output rhythms with tetrodotoxin (TTX) (Schwartz, Gross et al. 1987). Circadian timing information from the core and shell of SCN is processed via distinct neuronal projections that send signals to brain areas such as the medial hypothalamus that regulate sleep and to peripheral organs such as liver and pineal gland via the paraventricular nucleus (PVN) (Buijs and Kalsbeek 2001; Kalsbeek, Palm et al. 2006). Humoral signals are known to be mediated via prokineticin 2 (PK2), transforming growth factor-α (TGF-α) and cardiotrophin-like cytokine (CLC) released by the SCN. PK2 for example has E-box elements in its promoter

region and is directly regulated by the CLOCK-BMAL1 heterodimer (Albrecht and Eichele 2003). PK2 is also known to function as an SCN output molecule by transmitting the circadian locomotor activity through G-protein coupled receptors (Cheng, Bullock et al. 2002; Lin, Bullock et al. 2002; Cheng, Bittman et al. 2005)

As the master pacemaker, the SCN has the ability to synchronise and drive rhythms in peripheral organs such as the liver and pineal gland. Synchronisation is achieved via neuronal, humoral signals along with the circadian modulation of body temperature (Brown, Zumbrunn et al. 2002) and feeding (Damiola, Le Minh et al. 2000; Stokkan, Yamazaki et al. 2001). The ability to drive rhythms in peripheral organs is evident from studies in liver. By selectively disabling rhythms in the liver, it was evident that circadian gene expression in liver is regulated partly by the liver clock and partly by signals received from the SCN (Kornmann, Schaad et al. 2007)

Thus, the SCN is able to coordinate the activity of individual oscillators present in different peripheral tissues with the help of behavioural, hormonal and neuronal pathways. However, there are yet a number of gaps in our knowledge in all areas of circadian control that remain to be filled. For example there are yet a number of factors to be identified that help in synchronisation of rhythms between the SCN and peripheral organs.

1.1.7 Wheel-running activity

In mammals, circadian output can be easily measured by assessing their locomotor activity using a running wheel. Mice are individually housed in cages equipped with a running wheel in order to measure output rhythms. The activity of mice is recorded in a continuous manner throughout the circadian screening protocol, after which it is analysed by plotting a double-plotted actogram. A circadian screen usually comprises of a 12hr light:12hr dark schedule to help the mice entrain to the external environment for seven days. After entrainment, the mice are now allowed to free-run (no external light input) under constant dark conditions (DD) for 2 weeks. In this phase, the endogenous clock of the mice will set the activity of the mice. Finally, the mice are allowed to free run under constant light conditions (LL) for 2 weeks.

Below is an example of a double-plotted actogram explaining the terminologies often used in circadian studies (Figure 1.4).

Entrainment: A measure of the onset of activity relative to the "lights off" cue.

Masking Light pulse: brief 3h light pulse is presented to assess the ability to mask activity under light

A

Tau (τ): the slope of line drawn through onset of activity on consecutive days.

Phase I : 12hr Light:12hr Dark (12hr L:D cycle)

Phase II : Free-running conditions under constant darkness (DD)

Phase III : Free-running conditions under constant light (LL)

B

Phase I : 12hr Light:12hr Dark (12hr L:D cycle)

Phase shift: Shift in the onset of activity after additional light exposure. Mice free run from this point

Figure 1.4: Example of a double-plotted actogram obtained from a typical circadian screen. A) A representative actogram which is double-plotted i.e. activity of mice for two consecutive days are placed next to each other. While each horizontal line represents 48hrs of data collection, data from each day is presented beneath and next to the right of the previous day. Vertical black bars represent the wheel revolutions of a mouse. The yellow or blue shaded regions in the actogram represent the time when lights are on, while the non-shaded regions represent darkness. A typical screen includes a 12hr light:12hr dark (12hr L:D) cycle for 7 days followed by two weeks in constant darkness (DD) and finally two weeks in constant light (LL) conditions. Under LD conditions, the onset of activity co-incides with lights being switched off. The screen shown above also incorporates a light pulse, which is presented to mice to assess their ability to mask activity under light. Under DD conditions, the slope of a line drawn through the onset of activity on consecutive days determines the period or tau (τ) of a mouse (red line). Usually, phenodeviants are identified based on the deviation of τ from control mice. B) Example of a double actogram representing a second protocol where 12hrs of light is presented to the mice to delay their onset of activity for several hours (phase shift of activity in mice).

1.1.8 Mouse as a model organism

The laboratory mouse, *Mus musculus*, has emerged to be a chosen model organism in studying mechanisms underpinning complex behaviours. The reason for this is the similarity in the genetic composition between humans and mice. The easy manipulation of the mouse genome is an advantage in addition to the quicker reproduction rate. The presence of counterparts of human genes in mice with similar functionalities allows mice to be used as models of human diseases (with a hope that similar effects and similar pathogenesis of disease are observed). The suitability of using mice further increases with the availability of nearly 450 inbred strains and transgenic lines (Beck, Lloyd et al. 2000)

Due to the easy modification of the mouse genome, genetically modified mutant mice have been used for several years to study gene functions. The advantage of using mutant mice is their survival to adulthood, as some disorders are age-related and gene effects are only seen then. One is also able to characterize mutant mice at various levels from biochemical to behavioural stages.

The mouse genome can be modified in several ways. Gene knockouts (gene is inactivated and hence less expression or loss of function) are generated by gene targeting techniques and transgenesis, while tissue specific knockouts can be created by conditional mutagenesis. By using gene targeting techniques it is possible to obtain a gene with its normal functions impaired (Nguyen and Xu 2008). Briefly, this approach makes use of homologous recombination (exchange of DNA strands to exchange genetic material) in embryonic stem cells (ES cells). The process begins by mapping the genomic sequence followed by introducing mutations or alterations into a similar target sequence, forming the targeting construct. This construct is then injected into the ES cells, which are then injected into

blastocysts that are implanted into foster mothers. The chimeras thus produced are then screened for germ line transmission (Picciotto and Wickman 1998). *Per* (*Per1$^{-/-}$*, *Per2$^{-/-}$* and *Per3$^{-/-}$*) and *Cry* (*Cry1$^{-/-}$* and *Cry2$^{-/-}$*) mutants were generated by this technique to identify their role in circadian mechanisms (Albrecht, Sun et al. 1997; Shearman, Zylka et al. 1997; Zylka, Shearman et al. 1998; van der Horst, Muijtjens et al. 1999). Transgenesis is another method used usually to switch on gene expression, but can express mutant forms of genes that may also switch off gene expression. This involves injecting foreign DNA directly into the nucleus of the mouse egg (pronuclear microinjection) or injecting DNA into the embryonic stem (ES) cells. The disadvantage of these techniques (gene targeting and transgenesis) is the difficulty in achieving germ line transmission.

Although gene targeting can be effective in generating knockouts, if germ line transmission is obtained, it could also cause developmental defects. To overcome this, gene specific and tissue specific knockouts can be generated. This approach makes use of *Cre* recombinase, which is an *E.coli* bacteriophage P1 enzyme that recognises *lox*P sites present on the floxed DNA (DNA sequence flanked by two *lox*P sites). Once CRE recognises this site, the entire floxed sequence is excised, leaving one *lox*P site (by recombination). The advantage of such a technique over the classical gene targeting approach is to generate mice lacking a particular protein in a particular tissue or at a particular time. This approach can also be applied to ES cells; once the target DNA is floxed and *Cre* recombinase is introduced, the ES cells are implanted into foster mothers and the litters are then intercrossed. Although used widely in various fields of mouse genetics, one disadvantage of this technique is the limited availability of tissue-specific *Cre* lines (Picciotto and Wickman 1998).

All the above mentioned techniques involve modification of the gene sequence, which can be useful or even have adverse effects such as lethality. In such cases, approaches that

introduce random mutations throughout the genome are useful. In this case, the gene is still present with altered expression (gene may or may not be inactive depending on the mutated DNA base). X-irradiation was used initially (Silver, L.M. 1995) but was then replaced by chemical mutagens such as chlorambucil (CHL) (Russell, Hunsicker et al. 1989) and procabazine (PRC). These chemicals were further replaced by ethyl methanesulfonate (EMS) (Russell and Russell 1992; Favor 1998) and *N*-ethyl-*N*-nitrosourea (ENU) (Russell, Kelly et al. 1979). While X-rays results in deletions or inversions (Silver, L.M. 1995), ENU predominantly generates point mutations (Russell, Hunsicker et al. 1989). Easy breeding procedures coupled with developments in identification methods (new phenotyping screens and advanced sensitive techniques for identifying mutations in genes) ultimately complement the use of ENU mutagenesis in mice. ENU mutagenesis is explained in greater detail in the following section.

Generating mouse mutants has been of particular importance to circadian research. However it is important to consider that circadian mutants may have other far-reaching effects. One example includes the known associations of circadian clock genes and anxiety (Easton, Arbuzova et al. 2003; Roybal, Theobold et al. 2007), depression (McClung 2007) and neurological deficit (Plazzi, Schutz et al. 1997). Mutations in clock genes can also be the underlying cause of altered behaviour. Identification of such genes will provide an insight into causes of neurobehavioural phenotypes.

1.1.9 ENU mutagenesis

With the human genome completely sequenced, the challenge remains in identifying the functional role of each and every gene in the genome (Brown and Nolan 1998; Acevedo-Arozena, Wells et al. 2008). To achieve this goal mice are used as model organisms for reasons described in the previous section. Research has come a long way from collecting mice spontaneously mutated in colonies around the world, to using techniques developed by W and E Russell at Oak Ridge National Laboratory and M. Lyon at Harwell, to use radiation to generate mutations. However, the lack of markers to map mutations remained a rate-limiting step and there was a need to develop much more powerful methods to identify mouse mutants to exploit the full potential of this organism (Balling 2001). To satisfy these needs, the use of *N*-ethyl-*N*-nitrosourea (ENU) has been and is currently widely used. ENU is a powerful chemical mutagen which induces random mutations throughout the genome with a chance of achieving 1 mutation in 1.23Mbp of a coding DNA sequence in G1 males (Coghill, Hugill et al. 2002; Concepcion, Seburn et al. 2004; Quwailid, Hugill et al. 2004; Michaud, Culiat et al. 2005; Russell, Hunsicker et al. 2007; Acevedo-Arozena, Wells et al. 2008). Mutant mice that are generated can then be identified by screening for behavioural, physiological or biochemical anomalies. The structure of this powerful synthetic compound is shown below in Figure 1.5

$$H_3C - CH_2 - N - C - NH_2$$

with the top group being:

$$O = N$$

(attached to the central N) and the C bearing a double bond to O below.
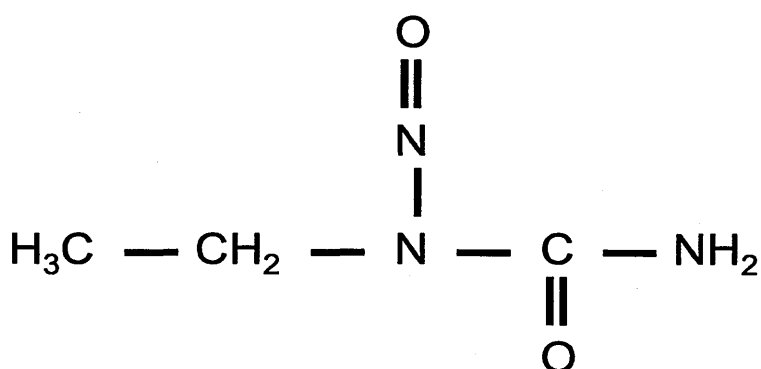
Figure 1.5: Structure of N-ethyl-N-nitrosourea (ENU)

1.1.9.1   Properties of ENU

ENU is typically injected intraperitonially in an adult male mouse where ENU induces

mutations in spermatogonial stem cells. After a period of sterility injected mice are then

crossed to a wild-type female and the resulting progeny are expected to carry potential

mutations. However, there are various limiting factors that affect the mutation rate of this

technique. The important one being the dose of ENU injected, which varies for different

strains of mice. ENU is toxic and a dose too high may result in lethality. Lower doses

however, may not be as effective in inducing mutations due to the DNA repair mechanisms of

the cell itself (Shibuya, Murota et al. 1993; Favor 1998; Godinho and Nolan 2006). One of the

many advantages of ENU includes mutagenesis resulting in multiple mutations in the same

gene. For example the gene *Fbxl3* itself is not very big (4300bps), yet multiple mutations have

been found (Godinho, Maywood et al. 2007; Siepka, Yoo et al. 2007). This has been an

advantage to geneticists in aiding them in identifying the role and functional domains of

FBXL3. Secondly, ENU can also be also be used to mutagenise ES cells (Chen, Yee et al.

2000; Coghill, Hugill et al. 2002). Mutations once identified in these germ cells, mice can be rederived from the sperm carrying independent mutations. An advantage of using germ cells is the optimisation of the ENU dose is possible, unlike in mice.

ENU, being an alkylating agent, acts through alkylation of nucleic acids by transferring its ethyl group to the nucleophilic sites on the four deoxyribonucleotides. The result of this is that mismatches and base-pair substitutions occur (Justice, Noveroske et al. 1999; Acevedo-Arozena, Wells et al. 2008). Although most of the mutations are a result of A to T transversions, AT to GC transitions can also occur. ENU mutagenesis can result in number of different possible mutations including missense, nonsense and frameshift mutations. With the possibility of generating null alleles (mutation leading to the complete loss of gene function), hypomorphs (mutation resulting in a partial loss of function), hypermorphs (mutations that result in a gain or increase of normal gene function), neomorphs (resulting in a dominant gain of gene function), antimorphs (where a dominant negative function is a result of the mutation) generated using ENU mutagenesis, it is possible to generate an allelic series in any particular gene (Noveroske, Weber et al. 2000; Quwailid, Hugill et al. 2004; Godinho and Nolan 2006; Acevedo-Arozena, Wells et al. 2008).

ENU mutagenesis is currently widely used in two complementary, yet systematic approaches to generate mouse mutants in order to study the mechanisms of gene function underlying various human diseases. The first approach is a phenotype-based approach (or forward genetics) and the second is a gene-driven approach (or reverse genetics).

1.1.9.2   Forward Genetics

As the name suggests, this approach follows the basic principle of identifying mutants based on the phenotype they express without any prior assumptions made about the gene or genes involved in the resulting behaviour. Although this is an advantage, this approach also faces a number of challenges, one of them being the robustness (including data analysis) of appropriate phenotyping screens to identify outliers and second being the identification of the relevant locus or loci that contribute to the phenotype of the mutant mice. This breeding scheme for dominant and recessive ENU screen is shown in Figure 1.6. Thus within the available phenotypic facilities and developed screens, it is possible to generate mouse models of almost any known diseases. In brief, the primary phenotyping pipeline conducted at MRC, Harwell, first identifies outliers with behavioural screens following which outliers are also screened for physiological and biochemical anomalies. Once mutants are identified, they are then screened through a much advanced pipeline including screens for identification of neurological disorders (SHIRPA, open field, rota rod, acoustic startle and PPI) followed by clinical chemistry screens (Acevedo-Arozena, Wells et al. 2008). The Harwell ENU mutagenesis program has also incorporated a screen with a particular interest to us is the circadian wheel-running screens. Progeny of mice injected with ENU are screened for deviations in their wheel-running behaviour (locomotor activity). Details of such screens have been previously described in section 1.1.7. It is due to such screens that we have been able to identify several mutants, some of which have been cloned. For example, the Afterhours mutant was identified in one such screen. Positional cloning and sequencing revealed a point mutation in the F-box protein, *Fbxl3*, causative for the *Afh* phenotype (Godinho, Maywood et

al. 2007). In summary, these screens have provided new insights into the molecular basis of

rhythms.
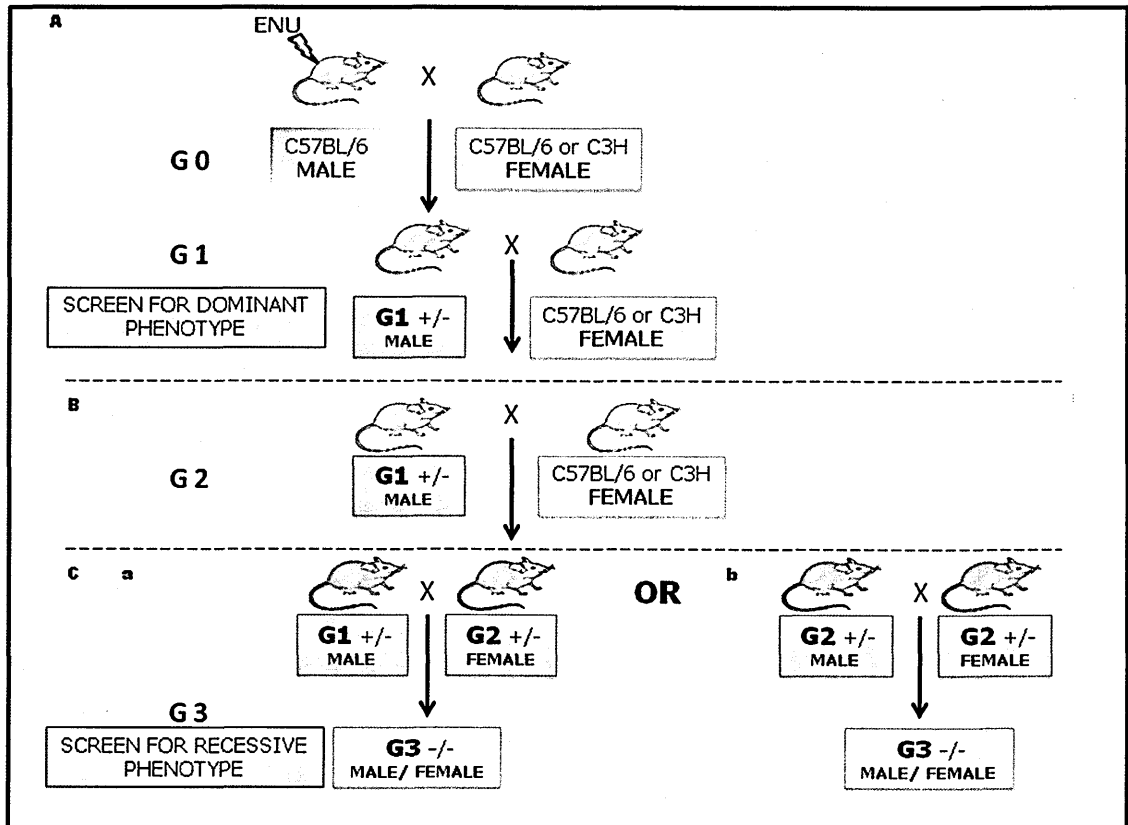
Figure 1.6: Breeding scheme to screen ENU mutagenised mice for dominant and recessive mutations. A) ENU is injected into a male mouse (C57BL/6) which is then mated with a C57BL/6 or C3H female (G0). B) Male G1 is screened and backcrossed to C57BL/6J or C3H for inheritance testing. Alternatively, for recessive screens, G1 male is crossed to wild-type female. C) The female G2 progeny obtained is mated in two different ways. a) The G1 male is mated with the G2 female or b) the G2 female is intercrossed with another G2 male. The G3 progeny (male or female) are then screened for recessive mutations.

1.1.9.3 Reverse Genetics

The reverse genetics or gene-driven approach is where one begins with a candidate gene or gene sequence with prior knowledge about its expression patterns and functions and then generates a mutant, thus providing the opportunity to completely characterise the gene. In this way, a number of genes have been identified that contribute to the genetic basis of a complex disease, through the genotype-based approach (Duerr, Taylor et al. 2006; Burton, Clayton et al. 2007; Frayling, Timpson et al. 2007; Rioux, Xavier et al. 2007; Sladek, Rocheleau et al. 2007; Todd, Walker et al. 2007). This illustrates that in addition to a phenotype-based approach, reverse genetics can also be used effectively to identify the genetic basis of complex diseases, behaviours. At the gene level, a number of methods can be utilised to generate mutants. Some of them include gene-targeting, RNA interference, gene-traps. However, ENU mutagenesis can also be effectively used in reverse genetics.

This approach makes use of screening DNA collected from ENU treated mice or from mutagenised embryonic stem cells (ES cells) (Chen, Yee et al. 2000; Coghill, Hugill et al. 2002). For such screens, MRC Harwell has an advantage as it has generated (in parallel) an archive consisting of DNA and sperm obtained from 10,000 male G1 progeny of ENU mutagenised mice that is screened using high-throughput techniques. Using this archive it is possible to obtain mutations in any gene of choice. An advantage of such a screen is that inheritance of mutation is definitely achieved. This is because mutant mice are re-derived from the same G1 mouse using the sperm frozen down at the same time as the extracted DNA in which the mutation was identified. Mutation screening to identify a single base pair change can be carried out in a number of ways. While techniques such as denaturing high-performance liquid chromatography (dHPLC) (Quwailid, Hugill et al. 2004), temperature

gradient capillary electrophoresis (TGCE) (Gao and Yeung 2000; Li, Liu et al. 2002; Murphy, Hafez et al. 2003), and targeted induced local lesions in genomes (TILLING) using the Cel1 endonucleases digestion (Oleykowski, Bronson Mullins et al. 1998; Till, Reynolds et al. 2003) have been used in the past to identify ENU-induced mutations, recent developments include much more sensitive heteroduplex analysis. The light scanner technique is based on the heteroduplex analysis as all the G1 progeny obtained will have mutations only on one chromosome, hence making identification easier. Figure 1.7 illustrates the stages involved in screening the Harwell ENU archive where following the generation of the DNA and sperm archive, a gene specific amplication of DNA is carried out. The PCR products are then analysed using the light scanner that separates outliers from the wild-type samples based on the DNA melt curve. Following this, the base pair change is identified by sequencing the DNA. Mutant mice are then re-derived using the frozen sperm from the same mouse in which the mutation was identified.
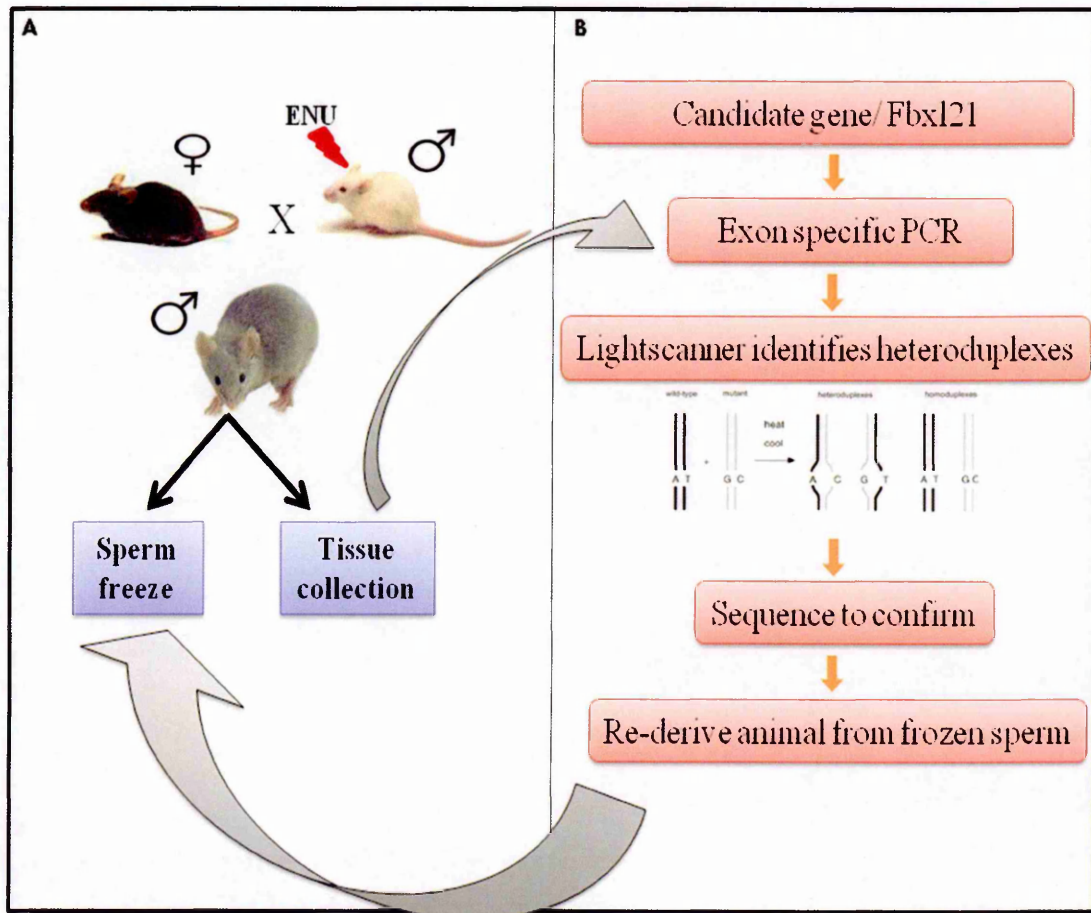
Figure 1.7: A typical ENU archive screening procedure. This procedure is used to identify mutations in any gene of choice. A) For screening, DNA from ENU mutagenised mice is extracted from tissues collected from G1 offsprings. At the same time, sperm is collected and frozen from the same male offspring to generate a sperm archive. B) Once a candidate gene is chosen, a gene specific amplification of DNA is performed. The light scanner then detects outliers isolated in the DNA heteroduplex melting curve analysis. Following this, the DNA is sequenced to determine the base-pair change. Finally, mice carrying the same mutation are re-derived using the frozen sperm from the same animal.

It can therefore be concluded that ENU mutagenesis is a powerful tool that can be used in both forward and reverse genetics in order to identify new gene functions, novel pathways underlying the mechanisms of complex diseases and finally to create new mouse models of human diseases. ENU mutagenesis can act as a perfect complement to the large-scale Knockout Mouse Project (KOMP), which aims at creating a conditional knockout for every gene in the mouse genome. ENU mutagenesis is advantageous for a project such as KOMP as it has the ability to induce and generate many types of mutations such as those that lead to truncated proteins or increase the level of gene expression, and mutations which lead to abnormal protein interactions. The best example in this case is the identification of a mutation in the *Clock* gene, whose role was then defined as the main component in circadian pacemaking. An ENU *Clock* mutant displays a very robust phenotype as compared to the subtle phenotype shown by a *Clock* knockout mouse (Antoch, Song et al. 1997; King, Vitaterna et al. 1997). Similarly, *Af4* was initially identified to be involved in lymphocyte development due to work using an *Af4* knockout mouse. It was only with the studies carried out in the *Af4* ENU mutant that this gene was shown to play a role in cerebellar degeneration in Purkinje cells (Isaacs, Oliver et al. 2003). Below are a few of the many examples of ENU mutants identified using the forward or reverse genetics approach (Table 1.2)

Table 1.2: Examples of gene functions identified in a phenotype-based or genotype-based approach using ENU mutagenesis.

Gene	Phenotype-based	Genotype-based	KO available/ Phenotype
Af4	✓ Cerebellar degeneration		✓ B/T cell developement impaired
Evi1		✓ Otitis Media	✓ Embryonic lethal
Clock	✓ Loss of circadian rhythmicity in DD		✓ Subtle phenotype
Dnchc1 (Dynein)	✓ Motor neuron degeneration		✓ Embryonic lethal
Emx2	✓ Ear ossicles abnormal		
Fbxl3	✓ Long circadian phenotype		

Adapted from (Acevedo-Arozena, Wells et al. 2008)

1.1.10   *In-vitro* analysis is complementary to ENU mutagenesis

With the identification of mutations by screening target DNA or ES cell libraries, comes the challenge of determining whether the phenotype(s) is a result of the mutation. As mentioned earlier, generating mice from ES cells can be quite tricky at times due to the difficulties in germline transmission. Hence, performing *in vitro* assays prior to generating mutants is desirable. Such assays would help us determine if the mutation is functional and would have a potential phenotypic effect.

In vitro assays in well established cell lines are widely used to determine phenotypes and primary effects of mutations in circadian biology. Cell lines such as U2OS, NIH3T3 (Akashi and Nishida 2000) and Rat-1 fibroblasts (Balsalobre, Damiola et al. 1998; Izumo, Johnson et al. 2003) are known to express all known clock genes. The protein products of these genes are also accumulated in a circadian fashion and are similar to what is observed *in vivo*. In many *in-vitro* assays, the full length DNA sequence needs to be cloned into a vector of choice following which mutations are introduced into the sequence using methods such as site-directed mutagenesis. These mutant plasmids are then overexpressed in cell lines, and effects such as protein localization or interactions between two proteins can be looked at. Any effects observed at this level could be expected to have an effect on the *in vivo* phenotype.

Real-time luciferase assays have been of great use to chronobiologists in the determination of phenodeviants *in-vitro*. This assay makes use of clock gene promoters such as *Per2, Bmal1, Rev-erbα* driving the expression of luciferase reporters. Phenodeviants that have an impaired endogenous clock can be identified based on the bioluminescence readout of the circadian oscillations generated by overexpression of mutants (Welsh, Imaizumi et al. 2005; Yamazaki and Takahashi 2005). The same methodology has also proved successful when

42

genes are knocked out using RNA interference (RNAi) (Maier, Wendt et al. 2009). Figure 1.8 (adapted from Mair et al. 2009) is an example of real time monitoring of U2OS cells stably transfected with a *Bmal1*:Luc reporter. The figure shows the difference in oscillations between the control (U2OS *Bmal1*:Luc) and cells transduced with *Cry1, Cry2, Bmal1* and *Clock* RNAi constructs. As found *in vivo*, silencing *Cry1* or *Cry2* resulted in a short and long period respectively (van der Horst, Muijtjens et al. 1999) and silencing *Bmal1* and *Clock* resulted in complete disruption of rhythms as found in *Bmal1$^{-/-}$* mice and the homozygous *Clock* ENU mutant which also show arrhythmic behaviour (Bunger, Wilsbacher et al. 2000; Liu, Welsh et al. 2007) . This confirms the use of *in-vitro* assays as a powerful tool to detect circadian phenotypes.

In-vitro assays can also be used to identify functions of clock components that are believed to play an important role in the regulation of circadian rhythms. This has been successfully shown by Maier et al. 2009 where they carried out a large-scale RNAi screen by knocking down all the known and predicted kinases, phosphatases and F-box proteins individually resulting in alteration of molecular oscillations. Although previously known that casein kinase 2 (*CK2*) is involved in the phosphorylation of the negative regulator PER2, it was only in this screen that the importance of the presence of *CK2* was identified. Real-time monitoring with downregulated levels of *CK2* by RNAi displayed disruption of circadian oscillations *in-vitro*, presumably due to accumulated levels of unphosphorylated PER2, which in turn delays the accumulation of the PER/CRY repressor complex, inhibiting their own transcription (Maier, Wendt et al. 2009)
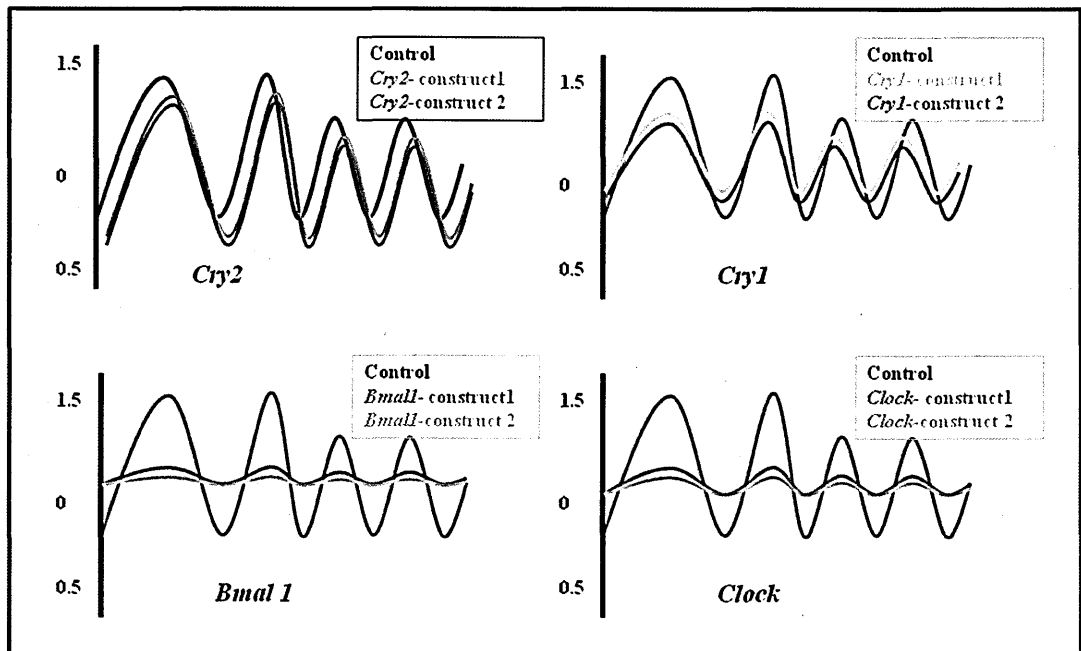
Figure 1.8: In-vitro assay confirming the circadian phenotypes of mutants. Human U2OS cells stably expressing *Bmal1*: Luc reporter was used as a control. Two RNAi constructs each for *Cry2, Cry1, Bmal1* and *Clock* were transduced into the cell lines using lentivirus. The cells were synchronised with dexamethasone and luminescence was measured. As seen, the RNAi constructs for *Cry2* (green), *Cry1* (pink) and *Bmal1* (purple) mimic the *in vivo* phenotype of the respective gene knockouts. The phenotypic effects caused due to the *Clock* RNAi constructs are also the same as observed in the ENU *Clock* homozygous mice (orange). Adapted from Maier, Wendt et al. (2009).

1.1.11   Known Circadian Mutants

The last decade has been very exciting for molecular biologists and geneticists for identifying genes and their functions and understanding the genetic contribution of many complex diseases. It has been particularly fast paced for circadian biologists, where genes regulating circadian oscillations have been identified. All this has been aided by the introduction of ENU mutagenesis screens. However, it is worth mentioning that although molecular mechanisms underlying the clock have been identified, the exact function of many other core components are yet to be identified. The identification of circadian mutants in *Drosophila melanogaster* has been extremely useful in identifying the core clock mechanisms. It was in the 1970's that the *Per* mutants were identified in *Drosophila* as part of the EMS mutagenesis screens. Three mutants were isolated by screening flies for their locomotor activity: *Per*^{0} mutant was arrhythmic, *Per*^{s} displayed a short period of 19 hours and *Per*^{1} had a long period of 29 hrs (Konopka and Benzer 1971). Studies over the course of time identified the nuclear expression of PER and the function of PER as a negative regulator of its own transcription (Hardin, Hall et al. 1990). Soon after uncovering the mechanism of the action of PER in *Drosophila*, a second mutant, *Timeless* (*Tim*), was isolated from an independent EMS screen. Studies performed on this mutant revealed interactions between PER and TIM, that TIM is required for translocation of the PER-TIM complex to the nucleus (Sehgal, Rothenfluh-Hilfiker et al. 1995) and that TIM degradation is induced by light (Hunter-Ensor, Ousley et al. 1996; Lee, Parikh et al. 1996; Myers, Wager-Smith et al. 1996; Zeng, Qian et al. 1996). Attenuated TIM degradation results in a delay or advance of the clock, depending on the light pulse as well as the nuclear translocation of PER which effects the negative feedback loop (Young 2000). Since these initial mutants were identified, many other factors have been

identified in *Drosophila* and in mammals. And both species have contributed to produce new insights.

Below are described some of the known mammalian circadian ENU mutants and their contribution to the field of circadian biology

Clock: The identification of this mutant in the early 90's was a milestone in the field of mammalian circadian biology during the time that the molecular elements of the mammalian clock were unknown. The mutant was identified in a semi-dominant screen where heterozygous G1 males were screened for their wheel running activity, first in light:dark (LD) conditions, followed by constant darkness (DD) conditions (King, Vitaterna et al. 1997). Out of 304 G1 offspring, who expressed a period length similar to wild-type animals, between 23.2-24.1hrs, there was just one outlier which exhibited a gradual lengthening of the circadian period in free-running DD conditions, which stabilised at 24.8hrs. The homozygous clock mutant however did not show sustained rhythmicity. A long extended period was apparent in the first few days in DD conditions after which they become arrhythmic (King, Vitaterna et al. 1997). This ENU mutant led to the conclusion that the *Clock* gene is necessary for sustained circadian rhythms and that at the molecular level the circadian oscillations are determined by the presence of the *Clock* gene.

The contribution of this ENU mutant provided significant information unlike the generation of a knockout mouse using the Cre-LoxP system. The *Clock* knockout, unlike the ENU mutant and the null allele of *Bmal1* that have disrupted rhythms (Bunger, Wilsbacher et al. 2000), continues to express rhythms in DD with a slight period lengthening of 20mins. However, they do show an alteration to light response during the LD cycle. The homozygous *Clock* null mutant mice initiate their activity ~2hrs before the lights were turned off (Debruyne, Noton et al. 2006). Unlike in the *Bmal1^{-/-}* mice, it was predicted that robust

rhythmicity in the *Clock* null homozygous mice was due to the presence of the *Clock* homologue, *NPAS2*, that takes over Clock function (Hogenesch, Chan et al. 1997; Zhou, Barnard et al. 1997). This was later confirmed by performing mRNA and protein studies in SCN and liver (DeBruyne, Weaver et al. 2007).

Ultimately, it can be said that if our analysis were to focus purely on the knockout phenotype, the exact function of *Clock* would not be identified due to redundancy between the homologues. However, the importance of *Clock* gene was confirmed only with the use of the ENU *Clock* mutant, suggesting that ENU mutagenesis makes a contribution to elucidate functions of genes underlying diseases or abnormal phenotypes.

Rab3a: In a screen to identify additional genes that may cause abnormal rest-activity behaviours in mice, Kapfhamer and his colleagues carried out ENU mutagenesis and screened the G1 progeny of ENU mutagenised males. Amongst 500 of the progeny screened, they identified one mouse with a short period of 23.08 hrs, which they named earlybird (*Ebd*). The earlybird phenotype was found to be caused by a point-mutation in *Rab3a* (ras-associated binding protein) resulting in a substitution of a conserved amino acid (Aspartic acid 77 Glycine; D77G) in the GTP-binding domain (Kapfhamer, Valladares et al. 2002). *Rab3a*, a member of the Rab3 family of small G proteins that are functionally redundant, plays a role in regulating neurotransmitter release and calcium dependent exocytosis (Takai, Sasaki et al. 1996; Sudhof 2004; Yang, Farias et al. 2007).

A homozygous earlybird mutant, *Ebd/Ebd*, expressed a circadian period of 22hrs in DD conditions. Expression studies carried out using whole brain extracts from *Ebd/Ebd* mice showed that the protein level of the mutated RAB3A was reduced by ~73% compared to the wild-type animals. This may suggest that the instability of the mutant protein causes the short

circadian phenotype. Similar to the *Clock* null mutant, unequal observations were made in the circadian analysis of the *Rab3a$^{-/-}$* mice. The *Rab3a$^{-/-}$* mice (generated by gene targeting) showed a shorter circadian phenotype with *Rab3a$^{+/-}$* mice displaying a period of 23.45hrs and *Rab3a$^{-/-}$* with a circadian period of 23.39hrs, ~40mins shorter than wild-type mice (Kapfhamer, Valladares et al. 2002). The phenotype observed in the knockout mice was much more subtle than the observed phenotype in the ENU generated *Ebd/Ebd*. The differences in the behaviour were suggested to be an effect of the genetic background of the mice (*Ebd/Ebd* on C3H/HeJ/C57BL/6J **Vs** *Rab3a$^{-/-}$* on 129/SvJ/C57BL/6J).

Apart from the above mentioned ENU mutants that alter circadian period, there are a few more mutants that may have effects on the clock, however, the mechanism is yet to be determined. A few of these are listed below.

__Rora__: The stability and precision of circadian oscillations are characterised due to the presence of orphan nuclear receptor proteins REV-ERB-α and retinoic acid-related orphan receptor α (*Rora*). These elements are known to suppress and activate expression of *Bmal1*, a major contributor in the regulation of circadian rhythms, respectively.

Staggerer (*sg*) is an example which has resulted due to a mutation in *Rora* gene. The mutation results in a frameshift deletion leading to a truncated RORα protein (Hamilton, Frankel et al. 1996). This mutant is shown to have cerebellar ataxia due to the incomplete development of Purkinje cells. Once the role of *Rora* in circadian regulation was determined, the *sg/sg* mice were screened for identifying deficits in locomotor activity. For this reason, the infrared (IR) beam breaking assay was used, as the lack of muscle co-ordination in the *sg/sg* mice was thought to affect the circadian wheel-running activity (Sato, Panda et al. 2004). The IR beam breaking assay revealed variable phenotypes from a shortened period (23.44 hrs+/-

0.078) of daily locomotor activity in the *sg/sg* mutants to a complete loss of free-running period or an extremely weak and undetectable circadian rhythm compared to the wild-type control mice (23.79 hrs+/-0.054) (Sato, Panda et al. 2004).

OPA1: Optic atrophy 1 (*Opa1*) is another ubiquitously expressed gene. Mutations in this gene are usually associated with autosomal dominant optic atrophy (ADOA) which is the most common optic neuropathy (Kjer 1959; Davies, Hollins et al. 2007). In this condition, the retinal ganglion cells are depleted resulting in loss of vision (Johnston, Gaster et al. 1979; Kjer, Jensen et al. 1983). A similar mutant identified in an ENU mutagenesis screen results in Q285STOP in a region which represents the beginning of the central dynamin guanosine triphosphatase (GTPase) (Davies, Hollins et al. 2007). This mutation results in a severe truncation of the OPA1 protein. Due to this truncation and loss of the retinal ganglion cells, a light pulse had no effect on the activity of mice. In normal conditions wheel running activity at night is suppressed by an acute light pulse, which was not the case the *Opa1* mutants (Davies, Hollins et al. 2007). Further studies in this mutant in turn will help us to identify the contribution of this gene in studying circadian oscillations (in terms of input pathways to the SCN), even though it is not directly involved in the mechanism of circadian regulation.

As well as the above mentioned mutants, there are a few more mutants which have been identified in a phenotype-driven or genotype-driven approach employing ENU mutagenesis. However, there are several other mutations identified that are yet to be mapped prior to identifying the mutant genes and determining their exact role in regulating circadian mechanisms. Below is a table (Table 1.3) listing some of the mutants.

Table 1.3: List of ENU circadian mutants recently identified.

Mutant	Phenotype	Mapped to	Reference
Shiftless (Sfl, Play 11)	No phase shift in response to light	**Chromosome 2** similar to melanopsin null mouse	(Hattar, Lucas et al. 2003; Panda, Provencio et al. 2003; Bacon, Ooi et al. 2004)
Setback (Sbc, Play 7)	Circadian period altered from 23.7h to 24.3 hrs due to light pulse	**Not mapped** Novel	(Bacon, Ooi et al. 2004)
Sluggish (Sgh, Play 14)	Low wheel-running activity record	**Chromosome 4/16** Novel	(Bacon, Ooi et al. 2004)
Short-circuit (Sci, Play 8)	Reduced circadian amplitude; Short circadian period in DD (21.5h-23h); Reduced or Absent phase shift	**Chromosome 8** Novel	(Bacon, Ooi et al. 2004)
Swing-shift	Activity in LD conditions (entrainment mutant)	**Not mapped** Novel	Takahashi, 2007 (unpublished)
Part-time (prtm)	Short circadian period in DD	**Chromosome 10/ Cry1** Loss of function mutation	(Siepka, Yoo et al. 2007)

1.1.12 Circadian rhythms and other physiological processes

Circadian oscillations that persist in every organism and every tissue are all controlled by one master pacemaker, the SCN, through its neuronal and humoral outputs. Circadian rhythms are important as they influence the generation of physiological and behavioural rhythms together with the generation of environment input. Genetic modification of the circadian system results in a wide range of effects depending upon the nature of the mutation and the circadian gene that is mutated. Behavioural studies in mouse mutants have been vital in providing novel insights on the associations of clock genes and behavioural phenotype. However to identify if the genetic basis of altered behaviour and physiology is primarily due to the altered SCN oscillator or if the effect secondary to specific neural dysfunction, it is necessary to identify more clock genes that will surely help us elucidate the links between circadian oscillations and physiological processes much more clearly. Described below are recent evidences showing how our body clock may influence the nervous system, metabolism, cell cycle regulation and other behaviour.

1.1.12.1 Neurological disorders

A number of evidences have shown that the primary cause of an altered emotional behaviour could be a result of disturbances in the circadian system. This has been shown in the ENU *Clock* mutant that displays various behavioural abnormalities such as mania, low anxiety, and hyperactivity (Easton, Arbuzova et al. 2003; Roybal, Theobold et al. 2007). With so many effects resulting from a single mutation, it could be hypothesised that the behavioural consequences of the *Clock* mutation are a result of either a direct effect of the mutated *Clock*

gene on core oscillator mechanisms or a secondary effect involving disturbances within the central nervous system ultimately altering the circadian clock (Barnard and Nolan 2008). Further evidences linking the circadian clock to mood regulation arise from the behavioural consequences such as anxiety due to NPY or VIP (major neurotransmitters within the SCN) dysregulation (Karl, Burne et al. 2006; Wersinger, Caldwell et al. 2007). Additionally, it has been shown that the mood stabilising agent lithium can be used to reverse the behaviour of the *Clock* mutant (Roybal, Theobold et al. 2007). Lithium is known to be a potent inhibitor of GSK3β, a major kinase involved in phosphorylation of many clock proteins. This again suggests that using agents that regulate clock proteins can alter behaviour. Another important association of circadian rhythms and behaviour is that circadian disturbances often contribute to the aetiology of syndromic disorders such as Prader-Willi syndrome (PWS). While patients suffering with PWS show sleep and behavioural disturbances (Vgontzas, Kales et al. 1996; Nixon and Brouillette 2002; Cotton and Richdale 2006), *Magel2* gene knockout mice (MAGEL2 is inactivated in PWS) show disrupted circadian rhythms and metabolism (Lee, Kozlov et al. 2000; Kozlov, Bogenpohl et al. 2007; Mercer and Wevrick 2009).

Alterations in circadian rhythms are also widely associated with a number of sleep disturbances (Barnard and Nolan 2008). For example a mutation in *Clock* could result in alteration of sleep time; its paralogue *Npas2* that takes over circadian function in the absence of *Clock*, alters sleep homeostasis (Naylor, Bergmann et al. 2000; Dudley, Erbel-Sieler et al. 2003; Barnard and Nolan 2008). Mutations in clock genes such as *Cry1* and *Cry2* also result in sleep fragmentation, change in sleep time and atypical responses after sleep deprivation (Naylor, Bergmann et al. 2000; Laposky, Easton et al. 2005; Wisor, Edgar et al. 2005). Disturbances and polymorphisms in human clock genes have also been shown to have associations with sleep and psychiatric disorders. Although polymorphisms contribute to the

morning or evening preference, extremes in such preferences may be associated with complex psychiatric disorders. With the Horne-Ostberg questionnaire that has been used for associations of clock genes with diurnal preference, studies have also revealed alterations in clock protein dynamics as a critical factor (Horne and Ostberg 1976). For example, a mutation in the CK1ε-binding domain of *Per2* identified in familial advanced sleep phase syndrome (ASPS) results in hypophosphorylation of PER2 *in-vitro* (Toh, Jones et al. 2001). Transgenic mice with this mutation show an advance in activity in the LD cycle. They further show a short free-running period in DD (Xu, Toh et al. 2007).

All this ultimately confirms the disturbances of circadian rhythms or their parameters in a range of CNS disorders, and further investigations into these areas will provide insights to identify causes and mechanisms of psychiatric and neurological disorders which can then be applied to design specific pharmaceutical targets.

1.1.12.2   Metabolism

Circadian gene expression profiling resulted in an observation that nearly 10% of the transcriptome was under circadian control, and the pathways involved were also required for basic metabolic processing (Panda, Antoch et al. 2002; Takahashi, Hong et al. 2008). Inversely, it has also been shown that genes involved in energy metabolism and cell signalling were seen to be under circadian control. For example *D-site binding protein* (*Dbp*), considered as a component of a circadian output pathway due to a dynamic change in expression levels, acts as a transcription factor regulating expression of genes involved in gluconeogenic and lipogenic pathway regulation (Lavery, Lopez-Molina et al. 1999; Gachon, Olela et al. 2006; Ripperger and Schibler 2006). Additionally, pathways such as glycolysis and cholesterol

biosynthesis were all seen to be under the regulation of circadian oscillators. Recently, genes belonging to the nuclear receptor family which are under circadian control have been shown to have diverse functions in regulating metabolic pathways. For example *Rev-erbα* is known to regulate bile acid and cholesterol synthesis by the circadian modulation of sterol regulatory element-binding protein (SREBP), which in turn leads to the cyclic expression of its downstream target genes. *Rev-erbα* activates insulin induced gene 2, *Insig2*, that encodes a protein, INSIG2, retaining SREBP in the endoplasmic reticulum, thus blocking the processing of SREBP (Dibner, Schibler et al.; Le Martelot, Claudel et al. 2009).

A clearer example of the role of *Rev-erbα* in regulating hepatic lipid homeostasis includes its interaction with histone deacetylase-3 (HDAC3), involved in chromatin remodelling. *In-vivo* studies carried out by Feng et al. (2011) showed a diurnal pattern of HDAC3 recruitment to the genome which correlated with the diurnal expression of the nuclear receptor, *Rev-erbα*. Although, the recruitment was diurnal, the level of liver HDAC3 protein did not vary. In the case of *Rev-erb*$^{-/-}$ mice, there was a repression of HDAC3 recruitment to the DNA, suggesting that the presence of REV-ERBα is important for HDAC3 recruitment. Further, it was shown that during the daytime, when there are high levels of REV-ERBα protein, it is able to recruit HDAC3, and hence a decline in histone acetylation is observed, which in turn inactivates genes such as fatty acid synthase involved in lipid biosynthesis. These observations were consistent with findings in mice lacking HDAC3. It was found that along with the loss of the repression of fatty acid synthase during the night, there were higher levels of triglycerides seen in the liver, thus explaining the role of Rev-erbα and its interaction with HDAC3 in regulating lipid homeostasis in mice (Feng, Liu et al.2011; Moore, 2011).

1.1.12.3   Cancer

Cell cycle and circadian oscillations are two important systems that are under the control of tightly regulated gene expression levels. Sharing similar concepts of periodicity (cell cycle and circadian oscillations are regulated with a period of ~24hrs) and regulatory processes (both are based on autoregulatory feedback loops), it is not surprising to find both these global systems interlinked (Hunt and Sassone-Corsi 2007). The circadian system is known to extend its regulatory control further beyond clock genes to genes involved in cell cycle regulation. While there is a circadian control over the generation of a cell cycle, circadian oscillations are self regulatory and independent of the cell cycle (Matsuo, Yamaguchi et al. 2003). Hence, attenuated expression of CCGs can have direct consequences such as the inactivation of downstream targets. It could also lead to an increase in the rate of cell proliferation with a reduced ability of performing apoptosis, thus promoting tumour formation resulting in cancer (Rana and Mahmood, 2010).

An example of a cell cycle component being regulated by the circadian clock is *Wee1,* encoding a cell cycle kinase that plays an important role in the transition of a cell from the G2-M phase of the cell cycle. Transcription of *Wee1* is activated by the binding of the CLOCK-BMAL1 to the E-box elements present in the *Wee1* promoter. In mice with a circadian deficiency, like the $Cry1^{-/-}; Cry2^{-/-}$ double knockouts, there is an elevated level of WEE1, presumably due to the lack of inhibition by the transcriptional repressors, CRY. Thus, with elevated levels of WEE1 after partial hepatectomy, there is a delay in the regeneration of liver due to the inactivation of a key mitotic regulator, cell division cycle2 (CDC2)/CyclinB1 complex, that delays the entry of cells into mitosis. Under normal conditions, CDC2/CyclinB1 complex is required to be at basal levels until the completion of the G2/M checkpoints. The

low levels of CDC2/CyclinB1 are achieved by phosphorylation of the complex by WEE1, a function critical for the completion of the G2/M checkpoints. In addition, the CDC2/CyclinB1 complex is activated by CDC25, by dephosphorylating the CDC2/CyclinB1 complex. Thus, with the activation of WEE1, the inactivation of CDC25 is also essential in promoting cells into mitosis (Matsuo, Yamaguchi et al. 2003; Oishi, Miyazaki et al. 2003; Hashimoto, Shinkawa et al. 2006).

Thus, it can be concluded that disruptions in circadian clocks could result in malfunctions of several physiological processes. Table 1.4 shows the metabolic and cancer-related phenotypes in mice with circadian deficiencies.

Table 1.4: Circadian genes and their related physiological effects

Gene	Mutant	Circadian Phenotype	Metabolic effects	Cancer-related Phenotype
Per1	*Per1*^{-/-}	Short period	No reported phenotype	**Mice:** Tumor suppressor[e] (acts with Ataxia telangiectasia mutated (ATM) and checkpoint kinase2 CHK2) **Humans:** Breast and Colon cancer[f]
Per2	*Per2*^{-/-}	Short period	Obesity, no diurnal feeding[a]	**Mice:** p53 downregulation, γ-radiation induced lymphoma[g] **Humans:** Breast cancer[f]
Cry1	*Cry1*^{-/-}	Short period	No reported phenotype	**Mice:** Spontaneous and radiation induced tumorigenesis[h]
Cry2	*Cry2*^{-/-}	Long period	No reported phenotype	**Mice:** Spontaneous and radiation induced tumorigenesis[h]
	Cry1^{-/-};*Cry2*^{-/-}	Arrhythmic	Impaired body growth[b]	**Mice:** Delayed onset of mitosis with no tumor formation[i,j] **Humans:** Prostate cancer[k,l]
Clock	*Clock*[Δ19/Δ19] (ENU induced)	Arrhythmic	Hyperglycemia, Hypercholesteroemia[c]	**Mice and Humans:** No tumor formation (spontaneous and radiation induced)[m]
Bmal1	*Bmal1*^{-/-}	Arrhythmic	**Mice:** Hypersensitive to insulin shock[d] **Humans:** Hypertension, Type 2 diabetes[d]	**Mice:** promotes tumor development with reduced expression of p53[n] (increase in expression of CDC2, Cyclin B1) **Human:** No reported phenotype

a=(Yang, Liu et al. 2009), b=(Vitaterna, Selby et al. 1999; Bur, Cohen-Solal et al. 2009), c=(Turek, Joshu et al. 2005), d=(Rudic, McNamara et al. 2004), e=(Gery, Komatsu et al. 2006), f=(Sjoblom, Jones et al. 2006), g=(Fu, Pelicano et al. 2002), h=(Lee, Donehower et al.), i=(Gauger and Sancar 2005), j=(Ozturk, Lee et al. 2009), k=(Hoffman, Zheng et al. 2009), l=(Chu, Zhu et al. 2008), m=(Antoch, Gorbacheva et al. 2008), n=(Zeng, Wu et al. 2010).

1.1.13   Thesis outline

The main aim of the thesis is to establish the regulation of interaction between *Cry* and *Fbxl3* genes and proteins. This would help us dissect the circadian functions of important clock-controlled genes, *Cry1* and *Cry2*, using the *Afh* mutant. This work has been carried out by generating $Cry^{-/-}$; $Fbxl3^{Afh/Afh}$ compound mutants. Circadian wheel-running analysis, and gene and protein expression studies have been carried out in these mutants.

Secondly, with a new F-box protein, *Fbxl21*, identified, the thesis includes some preliminary work done *in-vitro* and *in-vivo* on two mutations identified in an ENU mutagenesis screen. With studies such as interactions involving *Fbxl21* and the potential effect of the mutation carried out *in-vitro*, circadian wheel-running screens have also been carried out.

Finally, the mutants are screened through three commonly used behavioral phenotyping tests in order to investigate if they express features of psychiatric and neurological disorders known in humans. This would ultimately help identify genes that associate with human disorders and could be used as pharmaceutical drug development targets.

2 <u>CHAPTER TWO</u>: Methods and Materials

2.1 ANIMALS

2.1.1 Mouse Lines

Mouse studies carried out for this project were conducted under the guidance issued by the Medical Research Council in 'Responsibility in the Use of Animals for Medical Research' (July 1993) and under the authority of Home Office Project License Number 30/2686.

The $Cry1^{-/-}$ and $Cry2^{-/-}$ null mutants (both congenic on C57BL/6J backgrounds) were imported from the Laboratory of Molecular Biology, Medical Research Council, Cambridge (original targeted mutants were generated by Bert van der Horst) (van der Horst, Muijtjens et al. 1999). The mice imported were then re-derived and bred on the same backgrounds at the Mary Lyon Centre, Medical Research Council, Harwell after appropriate health screens. The afterhours (*Afh*) mutant was identified as a phenodeviant in an *N*-ethyl-*N*-nitrosourea (ENU) screen for alterations in circadian wheel-running activity. The *Afh* mice were maintained as a homozygous colony congenic on a C57BL/6J background. The genotyping protocols are described later in section 2.2.1 and 2.2.2. The *Fbxl21* mutants were re-derived from the Harwell Frozen Embryo and Sperm Archive and backcrossed to C57BL/6J before testing. The $Fbxl21^{V68E}$ mice were re-derived on C57BL/6J and C3H and the colony was later maintained as congenic on a C57BL/6J background. On the other hand, the $Fbxl21^{P291Q}$ mice were re-derived on BALB/C and C3H background and were later backcrossed to C57BL/6J. The $Fbxl21^{P291Q}$ mice used in studies presented here were on backcross two to the C57BL/6J. The genotyping protocols are described later in section section 2.2.2 and 2.2.3. All control mice used in studies were congenic on C57BL/6J background.

All the mice at Harwell were maintained under appropriate husbandry protocols where sentinel health screens assured cleanliness of stock in accordance with the Home Office guidelines. Mice were housed in Techniplast sealsafe IVC cages containing grade 5, dust-free autoclaved sawdust (Datesand Research, U.K.) which were checked daily and cleaned on a regular basis. Food and water was available *ad libitum* unless otherwise stated.

2.1.2 Generating Compound Mutants

Since the main aim of the project was to identify the complexity of circadian mechanisms, it was necessary to breed compound mutants. The breeding scheme shown below (Figure 2.1) was followed to generate the $Cry1^{-/-}$; $Fbxl3^{Afh/Afh}$ and $Cry2^{-/-}$; $Fbxl3^{Afh/Afh}$ compound mutants. Breeding and husbandry protocols were carried out according to the guidelines of the Home Office project license.
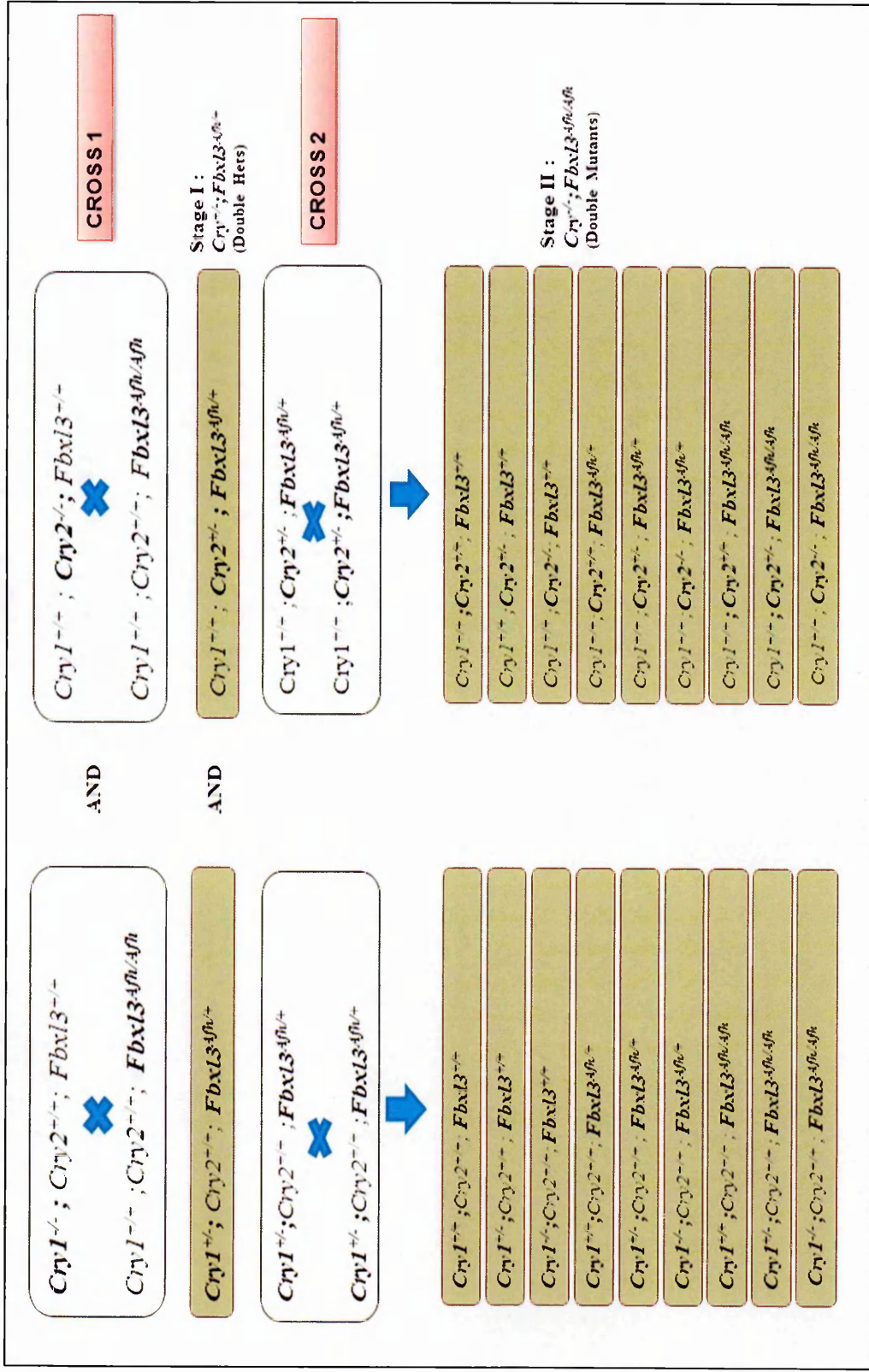
Figure 2.1: Scheme to generate Cry^{-/-}; Fbxl3^{Δfh/Δfh} compound mutants in mice. In order to generate $Cry^{-/-}$; $Fbxl3^{\Delta fh/\Delta fh}$ compound mutants, two main crosses were set up. While the unshaded boxes show the parents in the crosses, the shaded boxes show the litters generated. Cross 1 is set up by mating a $Cry^{-/-}$ single knockout with the $Fbxl3^{\Delta fh/\Delta fh}$ mice. The double heterozygous animals thus generated are further intercrossed (Cross 2) to produce a combination of genotypes. Each of the compound genotypes were screened with wild-type controls.

2.2 GENOTYPING ASSAYS

In order to genotype most mice, a crude genomic DNA extraction method was performed on ear biopsies collected from every mouse at weaning. 100μl NaOH solution (50mM) was added to the biopsy ensuring it was completely immersed in the buffer, and left in the heat block at 95°C for 1-1.5hrs to digest following which 10μl Tris (pH5) was added and vortexed thoroughly. DNA thus obtained was suitably diluted (1:4) to be used for the following assays.

2.2.1 Genotyping *Cry1* and *Cry2* Mice

Cry1 and *Cry2* knockouts were obtained by deleting a segment of the wild-type gene (deleted exon 4 and 5 for *Cry1* and exon 1 and 2 for *Cry2*) and replacing with a *Neo* gene. Hence, to genotype these mutants, two forward primers and a shared reverse primer was used. Forward primers hybridising to the deleted region were used to detect wild-type animals while primers hybridising to the *Neo* cassette were used to detect knockouts. Following the PCR, performed using the conditions and reagents mentioned in Table 2.1 and 2.2 respectively, the PCR products were analysed by gel electrophoresis on a 1% agarose gel set at 100V for 60mins which helped us identify the wild-type and mutant mice.

Table 2.1: Cry1 and Cry2 genotyping primer sequences and PCR programs

Gene	Primer Sequence		PCR Program	Product Size Wt/Ko (bp)
	Forward	Reverse		
Cry 1 wt	GTGTCTGGCTAAATGGT GG	CAGGAGGAGAAACTGACGCACT	1	1600
Cry 1 ko	TGAATGAACTGCAGGACGAG	CAGGAGGAGAAACTGACGCACT	1	2200
Cry 2 wt	CCAGAGACGGGAAATGTTCTT	GCTTCATCCACATCGGTAACTC	2	550
Cry 2 ko	GAGATCAGCAGCCTCTGTTCC	GCTTCATCCACATCGGTAACTC	2	310

PCR Program 1: 94°C for 10mins {94°C for 30secs, 61°Cfor 60secs, 72°C for 60secs} X35 times, 72°C for 10mins, store at 15°C forever

PCR Program 2: 94°C for 120secs {95°C for 30secs, 55°C for 30secs, 72°C for 90secs} X35 times, 72°C for 10mins, store at 15°C forever

Table 2.2: PCR conditions to genotype Cry1 and Cry2 mice

Gene	Master Mix volume	Primers		ddH2O (µl)	DNA (µl)	Total Reaction Volume (µl)
		Forward (µl)	Reverse (µl)			
Cry 1	Taq beads (GE Healthcare)	wt 1 (10µM) ko 1 (10µM)	wt/ko 2	20	1 (1:4)	25
Cry2	Hotshot (Cadama Medicals)	wt 0.15 (20µM) ko 0.15 (20µM)	wt/ko 0.3	4.9	2 (1:4)	15

2.2.2 Genotyping *Fbxl3^{Afh}* and *Fbxl21^{V68E}* Mice

The allelic discrimination assay was used to genotype point-mutations in *Fbxl3^{Afh}* and *Fbxl21^{V68E}*. In this assay, two sets of primer pairs and a unique set of probes overlapping the single nucleotide polymorphism (SNP) site were used. Major groove binding (MGB)-Taqman probes (Applied Biosystems) were generated with a FAM-labelled wild-type and VIC-labelled mutant sequence. Details of the primers, probes, PCR cycling conditions and reagents used are described in Table 2.3 and 2.4 respectively. The products were analysed on the real-time PCR using the ABI Prism™ 7500 software. The software was used to detect the increase in FAM and/or VIC fluorescence which would determine the genotype of the animal.

Table 2.3: F-box genotyping primer sequences, probes and PCR cycling conditions.

Gene	Primer Sequence		Probe Sequence	PCR Program
	Forward	**Reverse**		
Fbxl3(Afh)	TTGCGGGCCTCTTGATGAAG	TCCCCCAGCCCAATAGCT	Wt-FAM: CGGAACGTTGCAAAA Mut-VIC: CGGAACGTAGCAAAA	3
Fbxl21(V68E)	TTACCTCACCATGTCATATTACAGATCTT	AAGATCAGGGATGTGGAATACTTCA	Wt-FAM: CTTCGTCCGTGTGCA Mut-VIC: CTTCGTCCGAGTGCA	3

PCR Program 3: 50°C for 2mins, {95°C for 10mins, 95°C for 15mins}X40 cycles, 60°C for 1min

Table 2.4: PCR reagents to genotype the F-box mice.

Gene	Master Mix	Primers	Probe	ddH₂O (µl)	DNA(µl)	Total Reaction Volume (µl)
		Forward/Reverse (µl)	**Wt/Ko (µl)**			
Fbxl3(Afh)	Platinum qPCR Supermix UDG with Rox (Applied Biosystems) 10µl	F: 1 (25µM) R: 1 (25µM)	Wt: 1 (5µM) Ko: 1 (5µM)	4	2 (1:4)	20
Fbxl21(V68E)	Platinum qPCR Supermix UDG with Rox (Applied Biosystems) 10µl	F: 1 (25µM) R: 1 (25µM)	Wt: 1 (5µM) Ko: 1 (5µM)	4	2 (1:4)	20

2.2.3 Genotyping *Fbxl21^{P291Q}* Mice

Fbxl21^{P291Q} was genotyped using the LightScanner (Idaho Technology) where a standard PCR was performed using a primer pair, a double stranded DNA binding dye called LCGreen Plus (Idaho Technology) and a Luna Probe spanning the SNP. The probe was designed in a manner that it was complementary to the mutant allele. The PCR was performed using unequal amounts of primers so that one primer is completely used leaving several copies of the alternate strand with probe attached. Wild-type DNA should have a mismatched probe and DNA strand which should result in lower binding of the LC Green dye. Based on this principle, the PCR products were analysed by the DNA melting curves using the LightScanner and the LightScanner software. The PCR conditions and reagents are detailed below in Table 2.5 and 2.6.

Table 2.5: Genotyping primer and probe sequence for Fbxl21^{P291Q} mutants

Gene	Primer Sequence		Probe	PCR Program
	Forward	**Reverse**		
Fbxl21	ATTCTATTAAGAAACGCAGCTGGGAC	GAAGAATGCCTCAAACTCTTCTTCATAC	GACGTTCACTCTCTGGGAGTGTTTGATC	4

PCR Program 4: 95°C for 2mins,{95°C for 30sec,60°C for 30sec,72°C for 30sec}X55 times, 95°C for 30sec, 25°C for 30sec,15°C for 30sec

Table 2.6: PCR set up for Luna probe genotyping

Gene	Master Mix	Other Reagents(µl)	Primer	Probe	ddH20 (µl)	DNA(µl)	Total Reaction Volume (µl)
			Forward/Reverse (µl)	**F or R (µl)**			
Fbxl21	Hotshot(Cadama Bioscience)-5	LC Green dye: 1	F: 0.5 (20µM)	R: 0.5 (20µM)	0.9	2 (1:4)	10
			R: 0.1 (20µM)				

2.3 CIRCADIAN SCREENS

Circadian wheel-running screens were carried out on mice that were at least 6 weeks old. For these screens, mice were individually housed in cages equipped with a running wheel (Figure 2.2A). 10 such cages were then maintained in light-tight ventilated chambers. Timers were attached to every chamber that would control the light timing (Figure 2.2B). Even though the mice in the animal house wards were maintained in a 12hrs light:dark cycle, once in a circadian screen, the mice were allowed to entrain to a 12hrs light:dark (LD) schedule for a week. At the end of the week, the mice were allowed to free-run in constant darkness (DD) conditions for 2 weeks, followed by free-running conditions in constant light (LL) for 2 weeks. Circadian screens also incorporate 3hr light or dark pulses during the dark or light phases of the LD schedule. These pulses measure the ability of the mice to suppress activity in the light (light pulse) and measure amount of activity in the dark (dark pulse). Although actograms presented in this thesis are generated from screens using such light/dark pulses, they have not been considered while analysing data presented here. The activity records of mice were collected using the ClockLab software (Actimetrics). At the end of the screen, a double-plotted actogram is generated for further analysis. Apart from measuring the period length (τau) (red line), the software also measures circadian wheel-running parameters such as phase angle of entrainment, average wheel revolutions, and amplitude of oscillations.

Circadian studies were also carried out in parallel in SCN slices from the $Cry^{-/-}$;$Fbxl3^{Afh/Afh}$ compound mutants. The circadian wheel-running behaviour in $Cry^{-/-}$;$Fbxl3^{Afh/Afh}$ mice were then correlated to the data obtained from the SCN slices. This work

has been carried out by our collaborators Dr.Michael Hastings and Dr.Elizabeth Maywood

at MRC, Laboratory of Molecular Biology.
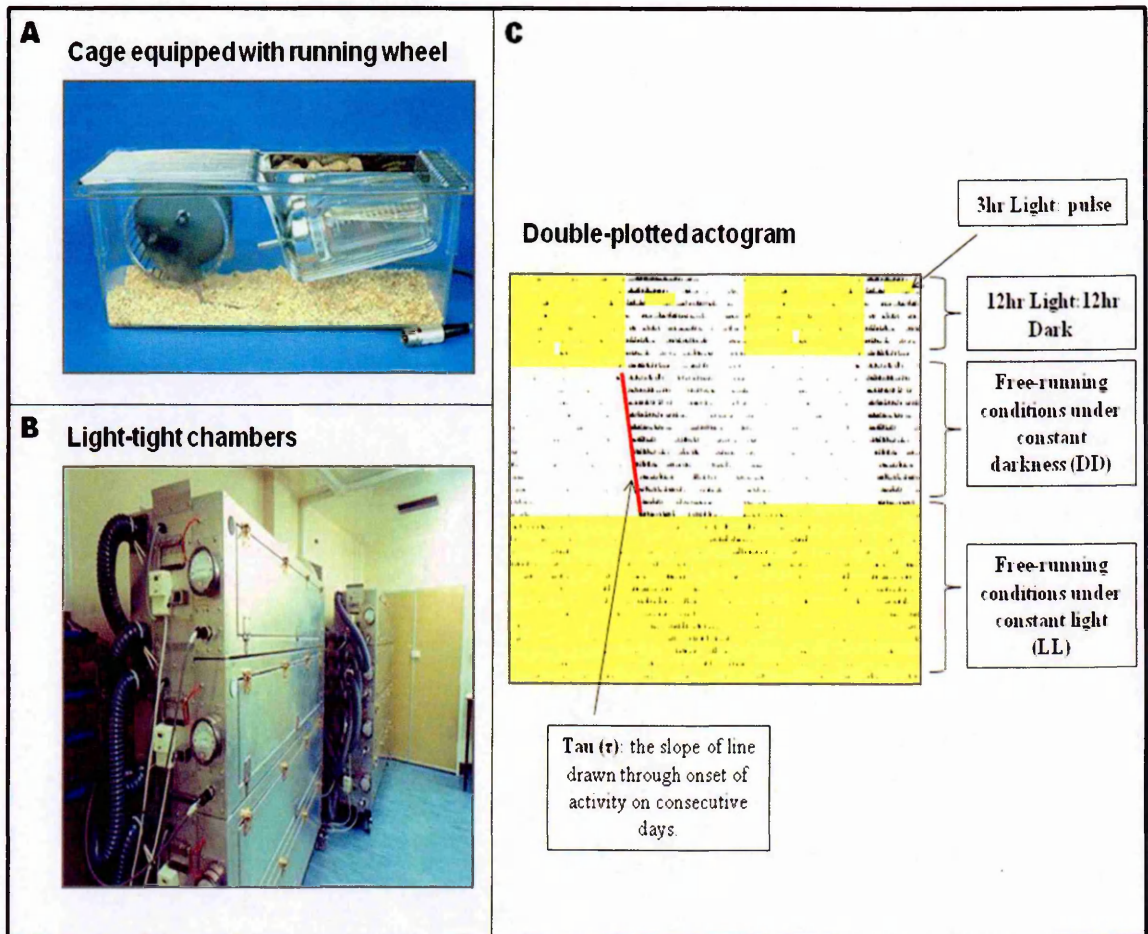
Figure 2.2: Monitoring wheel-running activity in mice. A) Example illustrating a cage equipped with a running wheel. B) 10 such cages are placed in light-tight ventilated chambers. Light conditions in the chambers are controlled by a timer. C) Example of a double-plotted actogram generated at the end of a circadian screen. The actogram shows activity of mice for 2 consecutive days. The yellow shaded regions in the actogram represent light while the unshaded areas represent darkness. The black vertical bars represent activity of mice. A typical circadian screen includes a week under 12hr L:D conditions, followed by 2 weeks under constant darkness (DD) and finally under constant light conditions (LL) for two weeks. Tau or period length (red line) is the slope of line drawn through the onset of activity on consecutive days. The screen usually also incorporates a light or dark pulse in the dark or light phase respectively of the L:D cycle. While the light pulse assesses the ability of mice to mask activity under darkness, the dark pulses measures the ability of mice to be active under light. These pulses have not been used to make any measurements and are not considered during data analysis of studies mentioned in this thesis.

2.4 CELL CULTURE

2.4.1 Cell Lines

A number of different cell lines were used during the course of the project. Molecular work was carried out on cell lines, namely U2OS (human osteosarcoma derivation from sarcoma of tibia that was moderately differentiated) (Ponten and Saksela 1967), Cos7 (derived from kidney cells of African green monkeys and developed from the CV-1 line by Yakov Gluzman in early 1980's and then transformed with SV40 virus) (Gluzman 1981), and HEK293 (derived from human kidney cells by transforming normal HEK cells with adenovirus 5 DNA) (Graham, Smiley et al. 1977). Real-time luminescence experiments required reporter cell lines. For that, U2OS and Rat-1 cells (Lindblad and Flood 1987) were stably transfected with a clock gene promoter *viz. Per2* or *Bmal1* driving the expression of the luciferase reporter. U2OS *Per2*:Luc was a kind gift from Dr. Fillipo Taminini (Erasmus University, Netherlands). Rat-1 *Per2*:Luc and Rat-1 *Bmal1*:Luc were kind gifts from Dr. Qing Jun Meng (University of Manchester). Due to the nature of cells, different media types were used to culture them. U2OS cells were cultured in McCoys 5A- media (PAA laboratories) supplemented with 1% L-glutamine (Lonza), 10% Fetal Bovine Serum (FBS) (Gibco) and 1% Penicillin-Streptomycin mixture (Lonza). Cos7, HEK293 and Rat-1 cells were cultured in Dulbecco's Modified Eagle's Medium (DMEM) (PAA laboratories) containing L-glutamine and supplemented with 10% FBS and 1% Penicillin-Streptomycin mixture. All media and plasticware were kept and used in sterile conditions. Media, Dulbecco's Phosphate Buffered Saline (PBS) (Gibco) and 0.25% Trypsin-Versene (EDTA) (Lonza) were pre-warmed in a 37^0C water bath before they came in contact with any cells.

Experiments were carried out in Class II biosafety cabinets (Microflow Peroxide) cleaned with 70% Ethanol (Fisher Scientific) prior to performing any experiments.

2.4.2 Thawing Cells

1ml frozen aliquots of cells were allowed to thaw at room temperature for 1-2mins. Cell lumps were broken by trituration with a Gilson pipette and cells were seeded into a T25cm^2 tissue culture flask (Greiner Bio One Ltd.) containing 9mls of complete media. Cells were allowed to grow overnight in a 37^{0}C incubator (Sanyo) maintained with appropriate water level and supplied with 5% CO_2. After 24hrs, in order to get rid of DMSO, old medium was removed and 10mls of fresh complete medium was added to the cells. Cells were returned to the 37^{0}C incubator with 5% CO_2 and left to grow until they became 85-90% confluent.

2.4.3 Subculturing Cells

Once the cells were 85-90% confluent, the entire media was removed from the tissue culture flask and cells were washed twice with 5mls warm PBS. 1ml of warm trypsin (GIBCO) was added to the flask, to detach cells from the flask surface, and incubated at 37^{0}C for 1-2mins. To make sure cells were completely detached; the flask was gently tapped on the sides and viewed under the light microscope (Olympus, CK2). As trypsin is harmful to the cells, it was inactivated by adding 8mls of complete media. Cell aggregates were broken by mixing the medium thoroughly by pipetting. Depending upon the extent of subculture required, an appropriate volume of cells was added to a new T75cm^2 tissue culture flask and the volume was brought up to 20mls by adding complete media. In case of 1:20 dilution, 1ml

of cells was added to 19mls of complete media while in the case of 1:10 dilution, 2ml of cells was added to 18mls of complete media in a T75cm^2 tissue culture flask. Cells were returned to the 37^{0}C incubator to grow for two days.

2.4.4 Freezing Cells

A 85-90% confluent flask or tissue culture dish was used to freeze cells. Media was removed and cells were washed twice with 10mls warm PBS. Cells were detached in the same way as mentioned in section 2.4.3. Cells were collected in a 50ml falcon tube (Greiner Bio One Ltd) and centrifuged (Beckman GS-15) at 1,000 rpm for 10mins. The supernatant was discarded and the pellet was resuspended in appropriate volumes of freezing media (6mls complete medium, 2mls dimethyl sulfoxide (DMSO) (Sigma), 2mls FBS. This was mixed well and 5mls of this mixture was added to 5mls of complete medium to make up 10mls freezing medium). The pellet was mixed thoroughly with the freezing media without formation of bubbles. Once mixed well, 1ml of the cell suspension was added to each 1.5ml cryovial (Nunc) and taken directly to -80^{0}C. From a T75cm^2 flask or a 10cm^2 tissue culture dish, usually, 10 vials of cells were frozen down.

2.4.5 Plating Cells

In order to plate cells for *in-vitro* experiments, confluent dishes or flasks of cells were first washed with warm PBS and trypsinised (in a similar way as in section 2.4.3). After the trypsin was inactivated with media, the cells were collected in a falcon tube. 50µl of cells were then mixed well with 50µl of trypan blue (diluted in PBS with a ratio of 1:2) and counted on

the haemocytometer (Neubauer haemocytometer, Fisher). Appropriate number of cells ($1X10^6$cells/10cm dish; 500,000cells/6cm dish; 200,000cells/35mm dish) were plated in media containing FBS a day prior to transfecting them.

2.4.6 Transfections

In-vitro experiments required the introduction of plasmid DNA into various cell lines. Due to different plasmid sizes, vectors into which particular full-length DNA's are inserted, differences in transfection efficiencies existed. Transfections in cell lines were carried out mainly using FuGENE® 6 transfection reagent (Roche). However, in some cases (e.g. Fbxl3-Wt-GFP and Fbxl3-G342V-GFP) transfections were carried out using jetPRIME reagent (Polyplus transfection™). Before transfecting cells with either reagents, cells were plated in required amounts in media containing FBS only, 24hrs prior to transfections so that the cells were 70-80% confluent on the day of transfections. Cells were plated either in 35mm dishes (in case of lumicycle experiments), 5cm dishes (for degradation experiments), 10cm dishes (to perform co-immunoprecipitations) or 6-well plates to check transfection efficiencies. A list of all the plasmids used is shown in Appendix 3.

2.4.6.1 Transfection using FuGENE® 6

Transfections with FuGENE® 6 were first optimised using different DNA: FuGENE®6 ratios. Commonly used ratios were 1:3, 2:3 and 1:6, where the 1:3 ratio would produce a satisfactory result with > 80% transfection efficiency. Transfections were carried out using the manufacturer's protocol. Briefly, for transfecting a 10cm dish, the total volume of transfection mixture required was 600μl. Calculated amounts of serum and antibiotic free media were first pipetted into sterile tubes into which 18μl FuGENE®6 was diluted, vortexed and incubated at room temperature for 5mins. 6μg DNA (3μg of both plasmids in case of co-transfections) was added to the media-FuGENE®6 mixture, vortexed well, centrifuged and incubated at room temperature for 15mins. At the end of 15mins, the transfection mixture was added dropwise to the dishes while swirling them constantly. The dishes were left in the incubator at 37⁰C for 24-36hrs.

2.4.6.2 Transfection using jetPRIME™

HEK293 cells were transfected using jetPRIME™ transfection reagent. Similar to any transfection protocol, the HEK293 cells were plated in required amounts 24hrs prior to transfection. A 1:2, DNA:jetPRIME™ ratio was optimised for HEK293 transfections. For a 10cm dish, 10μg DNA (5μg each in case of co-transfections) was diluted in 500μl jetPRIME™ buffer in a sterile tube, vortexed and centrifuged. 20μl jetPRIME™ reagent was then added to the diluted DNA, vortexed, centrifuged, and incubated for 10mins at room temperature. At the end of the incubation, the entire transfection mixture was added dropwise to the 10cm dishes, incubated at 37⁰C for 24-36hrs.

2.4.7 Synchronising Cells

In order to synchronise the circadian clock present in cells, medium containing 10µM Forskolin (final concentration) (Alexis biochemicals) or 100nM Dexamethasone (final concentration) (Sigma) was used. The time when the media containing forskolin or dexamethasone was added to the cells was considered as time 0. Cells were collected for protein localisation, RNA or protein extractions or prepared for lumicycle experiments at the required time points.

2.4.8 Cyclohexamide Treatment

Cyclohexamide (CHX) is a protein synthesis inhibitor. Treatment with CHX (Sigma) is particularly important to study degradation of proteins. For example: degradation of CRY by F-box proteins. For this, cells were seeded into appropriate culture dishes and transfected with desired plasmids (section 2.4.6) 48hrs prior to CHX treatment. At the start of the CHX treatment, the old medium from the cells is changed to medium containing 25µg/ml CHX (final concentration) and cells were collected at the required time point. The time of addition of CHX to the cells is considered as time 0. Cells are then collected as per requirement and used for protein extraction.

2.4.9 Isolation of Mouse Embryonic Fibroblasts

Embryonic fibroblasts were cultured from 14.5 days post coitum (dpc) embryos. Before dissecting out the embryos, the tissue culture dishes were prepared. In order to help the fibroblasts to adhere to the surface of the dish, each $15cm^2$ tissue culture dish was first coated with a mixture of 5mls PBS and 0.1% Gelatin (Invitrogen). To that, 25mls of complete DMEM supplemented with extra glutamine (25mls of 100X stock/ 500ml of media) was added and the dishes were left in the 37^0C incubator until the cells were plated. The number of dishes was dependent on the number of embryos as each embryo was plated individually according to their genotype.

Pregnant females were culled by cervical dislocation and their uteri containing the embryos were dissected out by making a small incision in the abdomen. Uteri were then dissected and embryos were kept in PBS. Embryonic head, internal organs and limbs were discarded. The tails were collected for genotyping. The caracass was washed by transferring it to a new dish containing PBS and then transferred to another dish containing 5mls trypsin. The caracass was then chopped well using sterile surgical scalpel blades (Fisher). This mixture was mixed well using a 5ml pipette and then added to a 50ml falcon and incubated for 5-10mins in a 37^0C water bath while it was constantly being swirled. In order to dissociate the cells further from the caracass, the contents were transferred into a clean petri-dish and mixed well with a 5-10ml syringe (without needle) (Plastipak BD, Fisher). The entire contents of the dish were then transferred to the 15cm2 tissue culture dish with complete DMEM and gelatin. The dishes were left in the 37^0C incubator supplied with 5%CO_2 for the cells to grow. After 24hrs, the cells were washed with 6-10mls of warm PBS in order to get rid of any debris, following which 25mls of fresh complete media was added. The cells were left to grow till they reached

85-90% confluency, after which they were split in 1:2 or 1:3 dilution in the same way as mentioned in section 2.4.3

2.5 RNA EXTRACTION FROM TISSUES AND CELLS

RNA extraction was performed with Qiazol reagent (Qiagen). To extract RNA from tissues, the tissue was first homogenised using a sterile pestle (Anachem) using Qiazol reagent. 1ml of reagent was used for approximately 50-100mg liver or cerebellar tissue. If RNA was to be extracted from cells, the cells were first washed twice with PBS (Gibco) and 2mls of qiazol reagent was directly added to a 10cm tissue culture dish. In order to ensure cell lysis, the cell lysates were passed through a Gilson pipette several times. The cell lysates were then collected in a 1.5ml eppendorf. The homogenised samples, tissue and cell lysates, were incubated for 5mins at 15-30^{0}C, following which 200μl chloroform (Fisher Scientific) per ml of qiazol was added to each sample. The contents of the tube were mixed by shaking vigorously for 15secs and incubated at 15 to 30^{0}C for 2-3mins. The tissue and cell lysates were then centrifuged (Beckman Coulter) at 12,000 rpm for 15mins at 4^{0}C. Following centrifugation, an upper aqueous layer containing RNA, an intermediate layer with DNA and a lower phenol-chloroform layer was formed. The upper aqueous layer was transferred into a fresh eppendorf and to this 500μl isopropanol (Fisher Scientific) was added, incubated at room temperature for 10mins and centrifuged at 12,000 rpm for 10mins. The pellet obtained was washed with 70% ethanol (Fisher Scientific) first by vortexing it and then by centrifugation at 7,500rpm for 5mins at 4°C. Ethanol was removed completely and the pellet was air-dried before resuspending in water. The amount of water used for resuspending depended on the size of the pellet. Once completely resuspended, RNA concentration was determined using the

NanoDrop apparatus (Thermo Scientific). Prior to quantifying the RNA, the pedestals of the nanodrop is are cleaned well to avoid contamination. The nanodrop is then calibrated with water. Then ~1-1.5µl of the RNA is placed on the pedestals of the nanodrop and the RNA concentration is determined using the NanoDrop 8000 software.

2.6 REVERSE TRANSCRIPTION

To make complementary DNA (cDNA) from RNA, SuperScript™ III First - Strand Synthesis SuperMix for qRT-PCR (Invitrogen) was used. The samples from which RNA was extracted were brought to a concentration of 1µg (per reaction) to be used for the reverse transcription reactions. The following components were added into the tube with RNA on ice:

2X RT Reaction Mix   10µl

RT Enzyme Mix   2µl

DEPC- treated water   to 20µl

The contents in the tube were gently mixed and incubated at 25^0C for 10mins following which it was incubated at 50^0C for 30mins. The reaction was terminated at 85^0C for 5mins and the contents were then cooled on ice. 1µl (2U) of *E.coli* RNase H was added to the mixture and then incubated for 20mins at 37^0C. cDNA thus prepared was stored at -20^0C until further use.

2.7 QUANTITATIVE REAL-TIME PCR

Quantitative real-time PCR was performed to determine the expression of clock genes across time points in both *Cry1⁻/⁻; Fbxl3^{Afh/Afh}* and *Cry2⁻/⁻; Fbxl3^{Afh/Afh}* double mutants. For this, liver and cerebellum tissues were collected at ZT 3,7,11,15,19 and 23 for both wild-type and mutant mice (ZT times or Zeitgeber times are relative to ZT 0 , the time of lights on). RNA was extracted from the tissues as described in section 2.5 after which cDNA was prepared as described in section 2.6. Real-time PCR was performed using *Power* SYBR® Green PCR Master Mix (Applied Biosystems). cDNA used for real-time PCR was diluted to 1:4. All the primers used to amplify clock genes and endogenous controls were designed using the Primer Express V3 software (Applied Biosystems) in a way that they would span an intron (so as to ensure that contaminating genomic DNA would not be amplified), have 60°C as their annealing temperature and were then used at a concentration of 2μM. For each clock gene, the PCR reactions were set up in triplicate for every sample at every time point. Reactions for an endogenous control (which are constitutively expressed and do not oscillate), ribosomal protein l13a (RPL13a), were set up in the same way. The following components were added to the PCR reaction set up in a MicroAmp® Fast Optical 96-Well plates (Applied Biosystems). The list of genes and primer sequences used for amplification are mentioned in *Appendix 1.*

Table 2.7: Set up with reagents and PCR cycling conditions for qRTPCR

Reagents	Primer	cDNA(μl)	ddH$_2$0 (μl)	Total Reaction Volume (μl)
	Forward/Reverse (μl)			
Power SYBR Green PCR master mix	F: 1 (2μM)	3 (1:4 diluted)	5	20
(Applied Biosystems)- 10μl	R: 1 (2μM)			

PCR program: 50^{0}C for 2mins, {95^{0}C for 10mins, 95^{0}C for 15mins}X 40cycles, 60^{0}C for 1min

The plate was sealed well with MicroAmp® Optical Adhesive Films (Applied Biosystems). The real time 7500 FAST system (Applied Biosystems) was used to run the PCR using a standard program as mentioned in the above table (table 2.7). The cycle threshold (Ct) values obtained through automatic detection by the Real time 7500 software were then used to calculate the expression of each clock gene relative to the endogenous control, RPL13a. The Ct values were used in the following series of calculations for each gene at every specified time point:

1. ΔCt = Ct$_{gene}$-Ct$_{RPL13a}$

   Here, the expression of the housekeeping gene was subtracted from the expression of the gene in question.

2. $\Delta\Delta$Ct = ΔCt$_{gene}$- ΔCt$_{calibrator\ sample}$

   The expression of every gene was made relative to a calibrator (wild-type ZT 3 sample).

3. $2^{(-\Delta\Delta Ct)}$

This would measure the fold change in expression of the gene relative to the endogenous control. This value was plotted on the graph for each gene at each time point.

2.8 PROTEIN EXTRACTION

2.8.1 Protein extraction from Tissues

Tissues (Eyes, Brain, Liver, Cortex, SCN, Kidneys, Heart and Lungs) were collected and snap-frozen at various ZT times (ZT3,7,11,15,19 and 23) in order to look at the expression of circadian proteins. RIPA buffer (1.75gms NaCl, 2mls NP40, 10mls Tris pH 7.5 1M, 2mls 10% SDS, 10mls 10% Sodium deoxycholate, 176mls H_2O) with protease and phosphotase inhibitors (Roche) was used for extracting proteins from tissues. The required amount of tissue (usually 50-70mg) was added to the FastPrep™ lysing matrix D (MP Biomedicals) that are 2ml tubes containing 1.4mm ceramic spheres and 500µl- 1ml of RIPA buffer was added directly to the beads (depending upon the amount of tissue). Tissues were lysed in a cold centrifuge (settings- between 5-10 for 20-30 seconds) (FastPrep, Bio Thermo). This step was carried out 2-3 times until the tissue is completely lysed. This causes the formation of a white froth and the entire contents of the tube were transferred to a clean eppendorf. This was further centrifuged to aid the separation of the pellet and the protein containing supernantent. Centrifugation was carried out by at 12,000 rpm for 20 mins at 4^0C. The supernatant thus formed was used for the Bradford assay for protein concentration determination (Section 2.9)

2.8.2 Protein extraction for CRY1

CRY1 levels were investigated across various time points in cerebellum. Proteins were extracted from snap-frozen tissues using 2X Laemelli Buffer (1.2gms SDS, 6mgs Bromophenol blue, 4.7ml Glycerol, 1.2ml Tris 0.5M pH 6.8, 2.1ml ddH$_2$O and reducing agent

(β-mercaptoethanol or DTT). The buffer was made in a concentration of 6X which was first diluted to 2X with water. Slices of cerebellum, weighing about 10-20mg, were collected in well-labelled eppendorfs and were homogenised on ice (without the buffer) using a sterile pestle (Sigma). To this, 100μl of 2X Laemelli buffer was added and mixed well. The proteins were allowed to solubilise by sonicating (Health-sonics) the samples for 30mins. Following sonication, the samples were centrifuged for 15mins at 4^{0}C. Required amounts of supernatant were collected and the loading buffer and sample reducing agents were added and directly loaded on the gel. Details of preparing and running samples are described later in section. It should be noted that protein supernatant was not quantified by the Bradford assay due to the nature of the lysate preparation; however equal amounts of supernatant was used. The proteins were eventually quantified using a reference protein (Actin) on a western blot.

2.8.3 Protein extraction from Cells

RIPA buffer with protease (Roche) and phosphatise (Roche) inhibitors (1 tablet each for 10ml cell extract) was used to extract proteins from cells. Media was removed and the cells were washed twice with ice-cold DPBS. Depending on the size of the dish, 150-300μl of complete RIPA buffer (150μl/6cm dish, 300μl/10cm dish) was added to the cells and was left on ice for 30mins. Cells were then scraped off using sterile cell scrapers (Greiner Bio-one), mixed well, transferred to a clean tube and centrifuged at 12,000 rpm for 30mins at 4^{0}C. The supernatant was used to read protein concentrations.

2.9 PROTEIN QUANTIFICATION

The Bradford assay was used to determine the concentration of extracted proteins from tissues and cells. A series of bovine serum albumin (BSA) dilutions were used as standards. This was done by diluting the 1mg/ml BSA stock (NEB) to known concentrations of 2.0, 1.0, 0.5, 0.25 and 0.125mg/ml. As protein extractions were performed in RIPA buffer with protease and phosphatase inhibitors, BSA serial dilutions were also prepared in the same buffer. However, due to the presence of detergents in RIPA buffer, the standards were prepared in a dilution of 1:5 RIPA: H_2O. Protein lysates from cells were either used concentrated or diluted 1:5 or 1:10 in H_2O. Protein lysates from tissues were diluted 1:20 in H_2O. To account for technical variability, each standard and sample were read in triplicate. 5µl of BSA standards or protein lysates were added in triplicate into a 96-well flat bottom plate (Greiner Bio-One Ltd). Following sample addition, 250µl of the Bradford reagent (Sigma) was added and samples were quantified on the spectrophotometer (µQuant Biotek Instruments Inc.) using the KC Junior Software.

2.10 WESTERN BLOTTING

2.10.1 Sample preparation for CRY1 protein gels

Since the protein samples from $Cry2^{-/-}$; $Fbxl3^{Afh/Afh}$ cerebellum was not quantified due to the presence of interfering components with the Bradford reagent, equal amounts of protein supernatant was used. To 5μl of protein sample, 1μl of Bromophenol blue and 0.4μl of β-mercaptoethanol (reducing agent) were added and mixed well by vortexing. The samples were brought to 10μl with double distilled water (ddH$_2$O). The samples were then denatured by heating on the heat block at 70^{0}C for 10mins, centrifuged and left on ice ready to be loaded on the gel.

2.10.2 Sample preparation for other protein gels

Once protein samples from cells and cerebellum of $Cry1^{-/-}$; $Fbxl3^{Afh/Afh}$ were quantified, they were prepared to be run on the protein gels. Amounts of protein lysates to be loaded differed from cells and tissues due to the quality of antibodies used. In case of cell lysates used for degradation and immunoprecipitation experiments, 5μg of lysates were used; 10μg of protein was used for CRY2 gels that would be used for CRY2 antibody studies. In any case of preparation, 2.5μl of 2X LDS Sample loading buffer (Invitrogen) and 1μl of reducing agent (Invitrogen) was added to the required amounts of protein lysates. The volume of protein lysates were made upto 10μl with ddH$_2$O and then denatured by heating it at 70^{0}C for 10mins and left on ice until they are loaded.

2.10.3 Running protein gels

The samples prepared with loading buffers and reducing agents were loaded on 10-well or 12- well 10-12% Bis-Tris NuPAGE precast gels (Invitrogen). The combs from the gels were removed and the gels were rinsed with water in order to get rid of the storage solutions. The wells were washed with water so that there were no air-bubbles formed that could interfere while loading the samples. The gels were set up in the gel tank according to the manufacturer's protocol (Invitrogen), creating two chambers, the middle chamber and the outer chamber. In order to check any leakage that may occur during running the gel, the middle chamber was first completely filled with 1X Running Buffer (50ml 1X MOPS Sodium Dodecyl Sulfate (SDS) running buffer (Invitrogen), 950mls distilled water). 500µl NuPAGE Antioxidant (Invitrogen) was added to the middle chamber to protect the protein. The outer chamber was completely filled with the 1X running buffer. 10µl SeeBlue Plus 2 pre-stained protein ladder (Invitrogen) was loaded on the gel after which, the samples prepared as described in 2.10.1 and 2.10.2 were loaded onto the 10 well or 12-well gels. The gel was electrophoresed at 200V for 1hr or 115V for 2hrs, depending upon the separation required using the NuPAGE power pack (Invitrogen).

2.10.4 Blotting

The proteins separated by electrophoresis were transferred to either Hybond-Polyvinylidene Fluoride (PVDF) or Hybond-ECL nitrocellulose membranes (GE Healthcare) using a semi-dry blotter (Bio-Rad). The membranes were prepared according to the size of the gels and were first activated using methanol in case of PVDF and by water in case of

nitrocellulose and left soaked in the transfer buffer (tris base (Sigma) 11.64gms, glycine(Sigma) 5.8gms, 7ml of 10% SDS solution (SDS powder-Sigma), methanol (Fisher) 400mls, water to bring upto 2litres) for 10mins. In the meanwhile, the gel plates were separated and the gel itself was trimmed to get rid of the lower tip and the wells. A corner of the gel was cut to mark the orientation of the gel. The gel was left in transfer buffer until everything was prepared for the procedure. Thick filter papers (Bio-Rad) measuring the size of the gel were prepared by soaking them in transfer buffer. The assembly of the semi-dry blotter was as follows - a single sheet of filter paper was first placed on the semi-dry blotter and excess transfer buffer and air bubbles were removed by rolling with plastic roller. The next layer was formed by the activated PVDF or nitrocellulose membrane. The air bubbles were removed using the roller. The protein gel was then overlaid on the membrane and ensured that no air bubbles were present. Finally, a sandwhich was created by placing the second sheet of filter paper soaked in transfer buffer. To completely ensure the absence of air-bubbles, the roller is used on the second filter paper. The blotter plate was carefully placed and proteins were allowed to transfer at 15V for 90mins. It must be noted that in case of using the odyssey fluorescence system, low fluorescence PVDF membrane (Thermo Scientific) was used instead of the usual PVDF membrane. However, the assembly of the blotter remained the same as described.

2.10.5   Immunodetection of blots

The PVDF membranes and nitrocellulose membranes containing the transferred proteins were prepared for immunodetection in the following ways.

2.10.5.1 Using ECL

At the end of transfer of proteins, the PVDF membrane was removed from the blotter and protected from non-specific binding by blocking the membrane in a 5% blocking reagent (dried non-fat milk (SLS) prepared in either PBS containing 0.1% Tween-20 (Sigma)(PBST) or Tris buffered saline (TBS) (Sigma) containing 0.1% Tween-20 (TBST)). This solution was referred to as blocking solution. The membrane was left in a dish with the blocking solution either at 4^0C for 24hrs or for 2hrs at room temperature on a shaking platform (See-saw rocker, Stuart Scientific). At the end of blocking, the membrane was processed for immunodetection. The membrane was probed with antibodies specific to the proteins of interest. Antibody dilutions were according to the company datasheets and were diluted in 5% blocking solution. Antibodies used were obtained from various places. The α-CRY1 and α-CRY2 primary antibodies were custom made and were a kind gift from Dr. Michael H. Hastings (Medical Research Council, Laboratory of Molecular Biology, Cambridge). The other antibodies for epitoge tags were commercially available. Details of antibodies used and incubation times are described in Table 2.8 below.

At the end of primary incubation, the membrane was washed thoroughly thrice for 15mins each with PBST or TBST on a belly dancer (Stuart Scientific) so as to remove non-specific primary antibody binding. Depending on the primary antibody used, the appropriate secondary antibody was chosen. Both the Anti-mouse IgG peroxide (Sigma) and anti-rabbit (Bio-Rad) were HRP conjugated and were used at a dilution of 1:10,000 in PBST. However, it must be noted that for CRY1 and CRY2, the secondary antibody, anti-rabbit was used at a dilution of 1:3000 in TBST. The membrane was left to incubate with secondary antibody for 1 hr at room temperature on a shaking platform. At the end of 1hr, the membrane was washed

thrice for 15mins each with PBST or TBST. Amersham™ ECL Plus Western Blot Detection Kit (GE healthcare) or Amersham™ ECL Advance Western Blot Detection Kit (GE healthcare) for detecting CRY1 and CRY2 were used to detect the secondary antibody on the membrane. Detection with ECL Plus solutions was carried out by mixing ECL Plus solution A and B in unequal amounts (975µl solution A and 25µl of solution B), whereas for detection using ECL Advance, solution A and B were mixed in a 1:1 ratio and then diluted with water in equal volumes. The ECL mixture was then spread evenly on the membrane and left to incubate for 3-4mins at room temperature. This would allow the horseradish peroxide, HRP (conjugated to the secondary antibody) and the hydrogen peroxide present in ECL solution A to oxidise luminol present in solution B which then produced luminescence. Excess ECL was drained from the membrane and placed between two acetate sheets which in turn were mounted in a dark light-proof cassette. X-ray films were used to develop the membrane. X-ray sheets were exposed to the membrane in the dark and further allowed to develop (Xograph Compact X4) to view the protein band of interest. X-ray sheets were first exposed for 10sec and then adjusted to various exposure times as desired. In some cases, the ECL treated membranes were developed using the computerised UVP ChemiDoc-It™ Imaging System for Chemiluminescent imaging (UVP) which had integrated dark room settings and used cooled CCD camera to capture images which were then stored on the computer.

2.10.5.2 Using the Odyssey System

The Odyssey® Infrared Imaging System (*LI-COR* Biosciences) allows one to detect two immunoreactivities simultaneously on the same blot. This system was used for immunodetection in some cases (*Fbxl21* interactions). As mentioned in section 2.10.4, low

fluorescence PVDF membrane was used with the Odyssey System. Once proteins were transferred on the membrane, the membrane was removed from the blotter and placed in 5% dried non-fat milk solution prepared in PBS. It must be noted that no Tween-20 was added while blocking the membrane. The membrane was blocked for 2hrs at room temperature or overnight at 4^0C whilst shaking. The primary antibodies were incubated with the membranes as described in section 2.10.5.1. Details of the antibody and conditions used are detailed in the below Table 2.8. At the end of primary antibody incubation, the membrane was washed well three times for 15mins each with PBST. Fluorescent LI-COR secondary antibodies that were compatible with the 685 and 785nm wavelength of the Odyssey system were used together. The membranes were probed with the *LI-COR* 680 (red) and/or *LI-COR* 800 (green) antibodies diluted in 1:15000 ratio prepared with the blocking solution containing Tween-20. The dishes were covered with silver foil, to protect them from light, and left on the shaking platform to get an even spread of the antibody. It must be noted that 0.001% SDS was required to be added during the secondary antibody incubation. The secondary antibody was allowed to bind to the membrane by incubating the antibody for 1hr at room temperature on a shaking platform. The membrane was then washed well for 20mins (4 washes for 5mins each) on a belly dancer and given a final wash with PBS only. It must be noted that all the steps following the addition of the secondary antibody, were performed in the dark. The membranes were then left to dry completely in the dark, and once dried, they were analysed using the Odyssey software.

2.10.5.3 Using the Snap i.d.™ Protein Detection System

In some cases, the membrane with proteins transferred in the same manner as described in section 2.10.4 was processed further using the Snap i.d. ™ Protein Detection System (Millipore). This system applied vacuum to drive the antibody to bind to the membrane unlike the conventional diffusion method. The Snap i.d.™ system was assembled as per the manufacturer's protocol where the single or double blot holders (Millipore) were wet with MilliQ water and the excess water was drained. The blotted membrane was placed on the blot holder which was then overlaid with the spacer (Millipore). A roller was used to remove the air-bubbles and once the holder was shut, it was turned over and placed on the Snap i.d. system itself. As this system was vacuum based, a lower concentration of warm blocking solution was used. The blocking solution was 0.2% dried non-fat milk prepared in PBS or TBS containing 0.1% tween-20. The blocking solution was prepared a day before and left in the 37^0C water bath overnight to warm. 30mls of blocking solution was applied to the membrane placed in the blot holder and vacuum was applied, until the blocking solution was completely drained out. Following blocking, the primary antibody was prepared in 3mls of blocking solution in the same dilution as used for conventional western blotting, detailed in Table 2.8. The primary antibody was left for incubation for 10mins after which it was washed with 0.1% PBST or TBST three times. Similar to the preparation of the primary antibody, the secondary antibody was incubated for 10mins after which it was washed out with the washing buffer, PBST or TBST. The membrane was then treated with Amersham™ ECL Plus Western Blot Detection Kit or Amersham™ ECL Advance Western Blot Detection Kit and the protein bands of interest were detected using the dark room developer or the ChemiDoc- It™ Imaging

system for Chemiluminescent imaging (UVP) which had integrated dark room settings and used cooled CCD camera to capture images which were then stored on the computer.

Table 2.8: Details of antibodies used for immunodetection of western blots

1⁰Antibody	Dilution/Duration	2⁰Antibody	Dilution/Duration
α- HA (Covance) α- MYC (Invitrogen) α- GFP (Roche)	1:1000 O/N 4⁰C	α- Mouse (Sigma)	1:10,000 1hr R.T
α- Actin (Abcam)	1:80,000 30mins R.T	α- Mouse (Sigma)	1:10,000 1hr R.T
α- HA (Sigma) α- MYC (Sigma)	1:1000 O/N 4⁰C	α- Rabbit (Bio-Rad)	1:10,000 1hr R.T
α- CRY1 (Custom made) α- CRY2 (Custom made)	1:500 O/N 4⁰C	α- Rabbit (Bio-Rad)	1:3000 1hr R.T

2.11   CO-IMMUNOPRECIPITATIONS

In order to investigate the interaction of two proteins, cell lines (Cos7 and HEK293) were doubly transfected with mammalian expression plasmids of interest. Proteins from the cells were extracted and quantified as described in section 2.8.3 and 2.9. These proteins were then used to co-immunoprecipitate (Co-ip) protein complexes using protein G Sepharose beads (Sigma). 20µl of protein G sepharose beads were washed with 500µl RIPA buffer (without inhibitors) to remove the ethanol in which the beads were stored. To the washed beads, 250µg- 500µg of protein lysate was added and the total volume was brought upto 250-500µl. The protein samples and the beads were incubated on a rotor (Stuart Scientific) for 1hr

at 4^0C. The protein-bead mixture was centrifuged at 1,000 rpm for 2 mins at 4^0C. The beads were discarded as they would contain all the non-specific binding. The supernatant was transferred into a new tube and the required amount of antibody was added. 2µg of antibody (mouse anti-HA (Covance), rabbit anti-Myc (Sigma), mouse anti-myc (Invitrogen), mouse anti-GFP (Roche)) was added to the pre-cleared protein lysate and left to incubate overnight at 4^0C on a rotor. The next day, 20µl of fresh protein G sepharose beads were washed with RIPA buffer and the protein-antibody complex was added to the freshly washed beads and incubated for 1hr at 4^0C on a rotor. At the end of incubation, the beads were centrifuged at 1,000 rpm for 2mins at 4^0C, and the supernatant was preserved as control. The beads were then washed three times with 500µl RIPA buffer complete containing protease and phosphatase inhibitors. The supernatant from all the washes was stored as controls. After the final wash, the proteins were eluted by adding 50µl NuPAGE 2X LDS Sample Loading Buffer (Invitrogen). The samples were then either stored at -20^0C without the addition of reducing agent or the western blot was performed, in which case 5µl of NuPAGE Reducing Agent (Invitrogen) was added and the samples were heated for 10mins at 70^0C. 10-15µl of the eluted protein sample was run on a protein gel, blotted and probed and immunodetected with the appropriate antibody in appropriate dilutions as described in section 2.10.2- 2.10.5.

2.12   CLONING

Although several plasmids were used, the only plasmid generated during the course of this project is the *Fbxl3*-GFP-Flag in a pIRES-hrGFP-1a vector (Stratagene). All the other plasmids used are listed in *Appendix 3.*

2.12.1   Primer Design

A variety of primers were designed to clone full length cDNA sequences of interested circadian genes into mammalian expression vectors with epitope tags. The primers were designed in a way that they had linker sequences with restriction sites for cloning at the 3' and 5' ends. Also since all the plamids cloned had a C-terminal epitope tag, primers designed included the start codon and a Kozak sequence. However, the stop codon was not included. It was important to keep in mind that the restriction enzymes chosen would not cut the insert and cut the vector only once in the entire sequence so that to avoid several pieces of vector. The primers were designed manually by including the kozak sequence (CC ACC) and excluding the native stop codon. Once designed, the primers were synthesised by Sigma Aldrich. Details of primers, plasmids and vectors are included in *Appendix 2.*

2.12.2   Full length amplification

The full-length cDNA amplification was performed using the Phusion™Flash High-Fidelity PCR Master Mix (Finnzymes) in a 20μl total reaction volume. For each reaction, 10μl Phusion™ Flash mix, 0.5μl of each primer (both forward and reverse primer were at a working concentration of 20μM), 1μl DNA (cDNA at a concentration between 50-100ng/μl)

were mixed on ice and the total reaction volume was brought to 20µl with ddH$_2$O. The PCR

reactions were carried out on a G-storm thermal cycler (GRI) using an initial denaturation step

at 98^{0}C for 10sec, followed by 30 cycles denaturation at 98^{0}C for 1sec, optimised annealing

temperature (or gradient step) for 5sec and extension at 72^{0}C for 15sec per 1kb. At the end of

the cycles, a final extension step at 72^{0}C for 1min was included in the PCR program. PCR

products were stored at 4^{0}C until further steps were carried out. Details of PCR programs used

for each primer pair are stated in the appendix

2.12.3   Gel Electrophoresis

PCR products were analysed by gel electrophoresis using 1% agarose gels containing

1X gel red nucleic acid gel stain (10,000X, Cambridge Bioscience). 1% agarose gel was

prepared by dissolving the agarose (Sigma) in 1X Tris-acetate-EDTA (TAE) buffer, boiled

well until the agarose was completely dissolved, sufficiently cooled and poured into a sealed

gel tray and allowed to solidify for 45mins. PCR products were mixed with a loading buffer

(1X Tris-borate-EDTA (TBE) buffer, 25% Glycerol and Orange G) and loaded onto the

agarose gel. To determine the size of the PCR product, a DNA ladder, 100bps (NEB) or 1Kb

Plus DNA ladder mix (Invitrogen), was also loaded on the gel. The gel was run at 100V for

1hour and later analysed using the Ultra Violet (UV) Gel Doc system (Bio-rad).

2.12.4   PCR Purification

Before the PCR products were gel extracted and ligated, they were purified to remove

all the contaminants. The QIAquick PCR Purification kit (Qiagen) was used to purify the

products. The PCR products were first transferred to a 1.5ml clean eppendorf and to one volume of the PCR product, 5 volumes of buffer PB was added and mixed well. The samples were then added to the QIAquick spin column placed in a 2ml collection tube and centrifuged (Biofuge pico. Heraeus) at room temperature for 30-60sec at maximum speed. The spin column was washed by adding 750µl buffer PE and centrifuged for 30-60secs. To get rid of the last amounts of solution, the spin column was centrifuged and supernatant was discarded. The spin column was then placed in another clean eppendorf, to which 30µl of ddH$_2$0 was added directly on the membrane and incubated for a minute after which it was centrifuged for 1minute. The purified product was quantified using the nanodrop.

2.12.5   Gel Extraction

Once PCR products were purified, they were used as a template to re-amplify the DNA (using the same Taq mix) and run on a gel, the DNA bands were gel extracted before they were used in the ligation reactions. The QIAquick Gel Extraction kit (Qiagen) was used for this purpose. It was essential to bear in mind that the quantity of DNA obtained after a gel extraction procedure was very small, and hence, it was essential to set up ten repeats of the PCR reaction and run on a 0.8% agarose gel to be used for gel extraction. Using the UV lamp, the DNA bands were precisely cut using a sharp scalpel blade. The use of UV was as minimum as possible as UV nicks and crosslinks DNA. The gel containing the DNA band was cut into pieces and placed into pre-weighed empty eppendorfs, and weighed again. This would allow us to calculate the volume of the gel. To one volume of a gel, three volumes of Buffer QG was added and immediately incubated for 10mins at 50^{0}C with intermediate vortexing every 2-3mins. This was done until the gel was completely dissolved in the buffer. If the

colour of the solution had changed during incubation, 10µl 3M sodium acetate was added and mixed well. Similar to the previous step, a 1:1 ratio of isopropanol was added i.e. to one volume of the gel, one volume of isopropanol was added to the sample. A maximum of 800µl of the mixture was added to the spin column placed in a collection tube, (both provided in the kit), and centrifuged for 1 min at room temperature. If the volume of the mixture was more than 800µl, the above step was repeated until the entire volume was centrifuged. The flow through was discarded, 500µl of buffer QG was added to the spin column and centrifuged for 1min at room temperature at maximum speed. The spin column was washed by addition of 750µl buffer PE followed by centrifugation for 1min at maximum speed. The column was then placed in a clean eppendorf and DNA was then eluted by adding 30µl ddH$_2$O, leaving it for a minute and centrifuging it for an additional minute. The eluted DNA was quantified using the nanodrop.

2.12.6   Ligation

Once the insert (amplified full length sequence) and the vector (pIRES-GFP-Flag) are purified and gel extracted, they were digested using the restriction enzymes (designed in the primer linker sequences) before they were ligated together. The right conditions for the restriction digest were found at the following website developed by New England Biolabs http://www.neb.com/nebecomm/DoubleDigestCalculator.asp . The insert and the vector were digested separately, however using the same conditions. To 2µg of insert or vector, 1µl of the chosen restriction enzymes (NEB) was added. In addition to that, according to the conditions described on the double digest calculator page, 2µl of the appropriate NEB buffer and 1µl of BSA was added. The total volume of the digest was brought upto 15-20µl with ddH$_2$O and left

to digest at the right temperature (usually 37^0C for 24hrs). The digest for the insert and vector were run on a 1% agarose gel to check if the insert and the vector were completely digested (as in section 2.12.3) and were gel extracted as in section 2.12.5 to ensure the right fragments were chosen for ligations.

Before setting up ligations, the exact molar ratios were first calculated using a web based program http://www.insilico.uni-duesseldorf.de/Lig_Input.html where the sizes of the vector and the insert were inserted and the desired ratio was calculated. Usually, molar ratios of 1:2, 1:3, 1:4, 3:1, 3:2 were tried to ligate the insert and the vector. The calculated amounts of the vector and the insert were mixed on ice and to that 0.5µl T4 ligase (NEB) and 1µl T4 ligation buffer (10X) were added, mixed well and left at 12^0C overnight in a cooling block. Ligation reactions were occasionally left at room temperature for 1 hr. The condition would differ from every insert and vector used. At the end of the incubation time allowing the insert and the vector to ligate, the product was used for transformations as described in the next section.

2.12.7   Transformation

Subcloning Efficiency™ DH5α™ Chemically Competent *Escherichia Coli (E.coli)* cells were used to transform the plasmid DNA. To ensure the viability of the cells, the initial steps of this procedure were carried on ice. 50µl of DH5α cells per transformation reaction was thawed out on wet ice. 1-10ng (1µl) of plasmid DNA or each ligation reaction was added to each vial of the competent cells and mixed well using the pipette tip. The cells containing the DNA are left on ice for 30mins after which they are heat shocked for exactly 20secs in a 42^0C water bath. The vial was then placed on ice for 2mins. 950µl of pre-warmed SOC

medium (Invitrogen) was added to the cells and left on a shaking incubator at 37^0C for 1hr.

50-100µl of the cells and DNA mixture were spread on Luria broth (LB) agar plates that

contain an appropriate antibiotic (usually ampicillin (Sigma) at 100µg/ml concentration was

used). The LB plates were inverted and left in a 37^0C incubator overnight for colonies to grow.

LB agar plates were prepared by heating a litre of water with 10gms tryptone (Sigma),

5gms yeast extract (Sigma), 5gms NaCl (Sigma) and 15gms agar until the ingredients are

dissolved. The agar was then autoclaved for 25mins. Once cooled, appropriate amounts of

ampicillin was added to get a final concentration of 100µg/ml and mixed well. The agar was

quickly poured into sterile petri dishes and then allowed to cool and set. The plates were

stored at -20^0C.

2.12.8   Plasmid Preparation

A well isolated single *E.coli* colony from a transformed plate containing the DNA of

our interest was picked and allowed to grow in LB media (LB broth is prepared in the same

way as LB agar, without agar) containing appropriate antibiotic (usually ampicillin). The

volume of growth media in which the colony was grown depended on the amount of DNA

required. Thus, it was grown either in 5mls in case of performing a plasmid minipreparation or

in 25mls in case of performing plasmid midipreparation.

2.12.9   Plasmid Minipreparation

Plasmid minipreparation was performed using the PureYield™ Plasmid Miniprep

System (Promega). The bacterial culture grown was first centrifuged for 5mins at maximum

speed at 4^{0}C and the supernatant was discarded and the pellet was resuspended in 600μl water

and mixed well. 100μl of Cell Lysis Buffer was added and mixed well by inverting 6 times.

The colour of the mixture should have changed to blue, which ensured that complete lysis of

cells had taken place. 350μl of cold neutralisation solution was added to the lysed cells, mixed

well and centrifuged at room temperature at maximum speed for 3mins. The supernatant was

transferred to a clean PureYield™ minicolumn and centrifuged at maximum speed for 15secs.

The minicolumn was washed using 200μl Endotoxin Removal Wash and spinning the tubes

again for 15secs at the maximum speed. A second wash of the minicolumn was performed

using 400μl Column Wash Solution and centrifuging the columns at maximum speed for

15secs. The DNA from the minicolumn was then eluted by placing the minicolumn in a clean

1.5ml eppendorf and adding 30μl of water directly on the filter present in the minicolumn. The

water added was left for 1min before the DNA was eluted by centrifuging the minicolumn at

maximum speed for 30secs.

2.12.10   Plasmid Midipreparation

The Plasmid Midipreparation was carried out when greater amounts of plasmids

(~100μl) was required. A single colony of required plasmid was picked from the LB plate and

allowed to grow in 25ml of LB overnight on a shaking incubator at 37^{0}C. The next day, the

plasmid midipreparation was performed using the Qiagen plasmid purification kit (Qiagen)

according to the company's datasheet. The bacterial culture was centrifuged for 15mins at

6,000rpm a 4^{0}C. The pellet was resuspended in 4mls of buffer P1. Once resuspended, 4mls

buffer P2 was added and mixed well by inverting the tube. The culture was incubated at room

temperature for 5mins after which 4mls of chilled buffer P3 was added to the bacterial culture,

mixed well and immediately added to the pre-arranged QIAfilter cartridge screwed with the cap and incubated for 10mins at room temperature. During incubation, the QIAGEN-tip was equilibrated with 4mls of QBT buffer. At the end of the 10mins incubation, the cell lysate was allowed to flow into the equilibrated tip by inserting a plunger into the QIAfilter cartridge. The cell lysate was allowed to flow by gravity. The tip was washed twice with buffer QC, using 10mls for each wash, after which the tip was transferred into a new non-polycarbonate collecting tubes. The DNA was eluted by adding 5mls of buffer QF to the tip. DNA was precipitated by adding 3.5ml isopropanol, vortexed and centrifuged (Beckmann Coulter) at 15,000g for 30mins at 4^0C. The pellet thus obtained was washed with 2mls of 70% ethanol followed by centrifuging the tube at 15,000g for 10mins at 4^0C. The supernatant was discarded and the pellet was allowed to air-dry after which, the pellet was resuspended in appropriate volume of water. Usually, 100µl of water was used to resuspend a good sized DNA pellet. The DNA was quantified using the nanodrop.

2.12.11   Sequencing

Plasmids (between 30-100ng/µl) or PCR products (between 10-50ng/µl) along with specific primers (10pmol/µl) for sequencing were sent in separate tubes to GATC where high throughput sequencing was carried out to ensure that correct ligation with the insert in the correct orientation had taken place. Sequencing results were then analysed using sequences from Ensembl and NCBI blast.

2.12.12 Storage of bacterial cultures as glycerol stocks

For preserving bacterial cultures of a correctly oriented plasmid, glycerol stocks were prepared and stored at -80^{0}C. They were prepared by thoroughly mixing 600μl of bacterial culture with 400μl of glycerol (Fisher Scientific) into a 1.5 or 2ml well labelled, sterile cryo tubes (Nunc) and stored at -80^{0}C immediately.

2.12.13 Isolation of single colonies from glycerol stock

In order to isolate a single colony from a preserved glycerol stock, the glycerol stock is first thawed out on ice. In the meanwhile, a LB plate is warmed. To isolate a colony, a sterile innoculating loop (Thermo Scientific) is dipped into the glycerol stock and immediately spread out in a back and forth motion (in the shape of a quadrant) until the culture is completely absorbed by the LB agar. The plate is then left into a 37^{0}C incubator overnight in an upside down position.

2.13 *IN-VITRO* MUTAGENESIS

This technique was used to introduce single base pair changes (mutations) into plasmids.

2.13.1   Primer Design

Primers containing desired mutations were designed using the Quick Change Primer Design software developed by Stratagene, http://www.stratagene.com/qcprimerdesign . Each of the primers were about 25bps in length and had the desired mutation. They were designed in a way that they would anneal to the same sequence on opposite strands of the plasmid. The oligonucleotides were synthesised by Sigma Aldrich. Details of primers used are mentioned in *Appendix 2.*

2.13.2   PCR

The PCR reagents used are detailed in table 2.13. Once the PCR is set up as mentioned, 1µl of *Pfu Ultra* HF DNA Polymerase (2.5U/µl) was added to each of the PCR reaction. The PCR cycling conditions are given in the table below (Table 2.9). Following temperature cycling, the reactions were cooled on ice. The parental supercoiled DNA was then digested using 1µl of restriction enzyme DpnI which was directly added to the PCR product, gently mixed and incubated for 1 hour at 37^0C. 2µl of the digested product was used for transformation (as in section 2.12.7).

Table 2.9: Reagents and PCR program for Mutagenising a plasmid

Reagents	Primer Forward/Reverse (µl)	ddH₂0 (µl)	dsDNA (µl)	Total Reaction Volume (µl)	PCR program
10X Reaction Buffer: 5µl dNTP mix: 1µl QuickSolution:3µl	F: x (125ng) R: x (125ng)	to 50	x (10ng)	50	1

PCR Program 1: 95^{0}C for 1min,{95^{0}C for 50secs, 60^{0}C for 50secs, 68^{0}C for 1min/kb of plasmid} X 18, 68^{0}C for 7mins

2.14 IMMUNOFLUORESCENCE

To determine the transfection efficiency of a particular plasmid without a fluorescent epitope tag or the cellular localisation of genes, it was necessary to perform immunofluorescence. Immunofluorescence was performed in a 8-well chamber slide (Fisher) where 20,000 cells were plated in each well of the chamber (as described in section 2.4.5), transfected with appropriate amounts of the required plasmids using Fugene6 (as described in section 2.4.6.1) and incubated in the CO_2 incubator for 24-36 hours. To perform immunofluorescence, the cell culture media was removed completely from the wells of the chamber slide first by using the pipette followed by inverting it on a blue roll. The cells were then washed with 200µl PBS which was added on the walls of each well, so that the cells would remain intact. Cells were fixed with 100µl cold 4% paraformaldehyde (PFA)(Sigma) per well of chamber slide and left at room temperature for 30mins. The PFA was removed, dried by inverting the slide on a blue roll and the cells were washed with 150µl TritonX-100, that was freshly prepared, and left to dry for 5mins. The cells were washed again with 200µl PBS twice, blocked with 200µl of 5% freshly prepared blocking solution (BSA diluted in PBS) and incubated for 1hour at room temperature. Similar to immunodetection of a western blot membrane, the cells were probed with a primary antibody diluted in 1% blocking solution (BSA in PBS). Primary antibody used was usually 10X more concentrated than in western blots. 5µg of mouse anti-myc (Invitrogen) antibody was diluted in 1% BSA blocking solution and incubated for 1 hour at room temperature. At the end of primary antibody incubation, the cells were washed thrice for 5mins each with 200µl PBS. Fluorochrome-coupled secondary antibodies {Fluorescein isothiocyanate (FITC), Tetramethylrhodamine-5-(and 6)-isothiocyanate (TRITC)} (Sigma) produced in a different animal host (to the primary

antibody) was used for immunofluorescence. The secondary antibody was diluted in freshly prepared 1% BSA blocking solution and incubated in the dark for 1 hour at room temperature. At the end of 1hour, the cells were washed three times for 5mins each with 200µl PBS. At this point, the chamber sealed on the slide was removed carefully and a drop of 4',6-diamidino-2-phenylindole stain (DAPI) (Vector shield mounting medium with DAPI, Vector Laboratories) was added to each well. A coverslip (VWR international Ltd.) was carefully overlaid taking care not to include any air bubbles and sealed with nail varnish. The slides were preserved in a darkened box laid with moist tissue to maintain humidity in the box until the slides were ready to be visualised under the confocal microscope (Leica TCS SP5) using appropriate lasers.

2.15 *IN-VITRO* LUMICYCLE ASSAY

The LumiCycle (Actimetrics) was used to investigate the effect of any mutations in any circadian genes on the clock by transfecting recombinant mammalian expression plasmids into cell lines and then imaging them in real-time. The U2OS and Rat-1 cell lines stably transfected with *Per2*:Luc (*Per2* promoter driving luciferase transcription) were used for these studies. The stable cell lines were plated (as in section 2.4.5) in 35mm dishes and were allowed to grow overnight at 37^{0}C. The cells would approximately reach 70-75% confluency the next day when particular plasmids were transfected in a 1:3 (DNA: Fugene6) ratio using Fugene6 transfection reagent. Transfection was carried out according to manufacturer's protocol (as described in 2.4.6.1). 24hrs after transfection, the cells were synchronised using forskolin (10µM final concentration) and left in the incubator for 2 hours.

During this time, the recording media was prepared in dark sterile conditions by adding 2.5mls FBS and 50µl of 0.1M luciferin (Beetle luciferin, Promega) (50mg of luciferin powder

was dissolved in 1.57ml nuclease free water in sterile conditions, aliquoted in 50μl and preserved in -80^{0}C) to 47.5mls of raw recording media. Raw recording media was prepared in sterile conditions by dissolving 1 pot of DMEM low glucose powder (Sigma) , 4gms glucose (Sigma), 10mls HEPES (1M, Sigma), 4.7mls sodium bicarbonate (7.5% Sigma) and 2.5mls penicillin-streptomycin mixture in 1 litre of milliQ water. Once all the powders were dissolved, the raw recording media was filtered using a vacuum pump and preserved in a sterile bottle at 4^{0}C. This raw media was used to make the final recording media (mentioned above).

2hrs after synchronisation, the cell culture media was thoroughly removed using a Gilson pipette and 2mls of final recording media containing luciferin was added dropwise to each lumicycle dish. The dishes were sealed immediately with a coverslip (VWR International Ltd.) that was sealed with parafilm. It was important to ensure that there were no gaps left between the coverslip and dish itself as the luciferase count would then disrupt readings. Once sealed, the dishes were placed in the lumiCycle, and the luciferase counts were monitored over 5 days using the lumiCycle analysis software (Actimetrics)

2.16 LIGHT SCANNER SCREENING

The light scanner (Idaho Technology) was used to identify mutations in a desired candidate gene in F1 progeny of ENU-mutagenised mice. The Harwell ENU archive consists of a library of ~10,000 parallel DNA and sperm samples from male F1 progeny of ENU mutagenised mice. The DNAs extracted were pooled with DNA from four animals and stored in 96-well plates at 4^{0}C. These DNA pools were screened on the light scanner to identify mutations in the F-box domain and putative CRY-binding domain of *Fbxl21*.

The first step before beginning the archive screening was to optimise the PCR and PCR conditions using the light scanner. A gradient PCR with a range of annealing temperatures between 55^0C-70^0C was performed using the PCR reagents in dark framestar 96-well plates (Cadema bioscience) as listed in the table 2.10 below. The PCR products were first analysed on the light scanner using the light scanner software and they were then analysed on a 2% agarose gel to confirm the exact annealing temperature.

After the temperature and conditions of PCR were optimised, the Harwell ENU archive DNA pools were screened to look for mutations in the two interested domains of Fbxl21. Based on the heteroduplex analysis, outliers in the DNA pools were identified i.e. if the melting curve of a particular DNA pool looked different from the others, the PCR for that particular pool was repeated using the DNA from each animal that comprised the interested pool. This way, DNA from a single animal was identified to have a mutation in our interested candidate gene, *Fbxl21*. The mutation was finally confirmed by sequencing. Based on the base pair change and preliminary *in-vitro* assays such as the LumiCycle analysis, the mutant mice were re-derived. The mice were re-derived from the frozen sperm archive created parallel to the DNA archive. A figure describing a typical Harwell ENU archive screen is shown in the previous chapter (Chapter 1, section 1.9.3).

Table 2.10: Details for screening the ENU archive

Master Mix volume	Other Reagents (µl)	Primer		ddH₂0 (µl)	DNA (µl)	Total Reaction Volume (µl)	PCR program
		Forward/Reverse (µl)					
Hotshot (Cadama Medical)-5	LC Green dye: 1	F: 0.1 (20µM)		1.8	2 (5ng/µl)	10	1
	Mineral Oil:20	R: 0.1 (20µM)					

PCR program 1: 95^{0}C for 2mins, {95^{0}C for 30secs, Appropriate annealing temperature for 30secs, 72^{0}C for 30secs} X 55 times, 95^{0}C for 30sec, 25^{0}C for 30sec, 15^{0}C for 30secs.

2.17 BEHAVIOURAL TESTS

Wild-type and mutant mice around 8-10 weeks of age were screened for three behavioural tests. Although they were age-matched, sex comparisons were not made and the data collected was considered as an entire group. 10 animals (5 males and 5 females) of each genotype (mutant and wild-type C57BL/6J) were used for each of these tests. Due to time constraints, the wild-type mice (C57BL/6J, congenic) used were not littermate controls, thus expecting variability in data. The mutants and wild-type mice were first tested in the open-field test arena, followed by acoustic startle and pre-pulse inhibition (PPI) and finally were measured for their grip strength. The tests were performed on different days giving the mice 24hrs to recover from previous tests.

2.17.1 Open Field

The open field test (OF) was carried out to investigate activity of mice in a novel environment and was used to assess a combination of locomotor activity (movement), exploratory drive and other aspects of anxiety. A standard white perspex arena (~44cm long by ~44cm wide and ~50cm high) placed one foot above the floor with a video camera fixed 1.8metres above the centre of the apparatus was used. Each arena was divided into a centre zone (~16cm of the total arena) and border area (~8cm wide border around the edges of the arena), creating an intermediate area using the EthoVision software (Noldus Ltd.) The arena was illuminated by lighting of 200lux. Each mouse was gently placed in one corner of the arena facing the wall. A stop watch was released as soon as mice were placed in the arena. The test was carried out for 30mins, giving the mice time to move and freely explore the arena.

Parameters such as time spent in the centre, time in the periphery, total distance moved, total velocity, and latency of first occurrence in the centre were recorded for the entire arena. Measurements of wild-type and mutant mice were compared and statistical significance was determined by Student's t-test.

2.17.2   Acoustic Startle and Pre-pulse Inhibition (PPI)

The acoustic startle response and PPI measures the exaggerated flinching response of mice (startle response) when an unexpected acoustic stimulus is presented. It further measures its ability to inhibit such a response when a pre-pulse is presented prior to the acoustic stimuli (PPI). Deficits in PPI have been associated with known human psychiatric disorders such as schizophrenia. Both the acoustic startle and PPI were assessed in a single session that lasted for ~1hr. Up to 12 mice at a time were tested in soundproof chambers. The chambers contain an inner chamber equipped with a loud speaker and startle platform (accelerometer) linked to a computer. To measure the startle response, the mice were given an acoustic stimulus of 110decibels (dB) that was repeated 10 times. To establish the PPI, mice were exposed to a range of pre-pulses from 65dB-75dB of 10millisecond (ms) duration followed by an 110dB acoustic stimulus lasting for 20ms. There was a 50ms interval between the pre-pulse and the acoustic stimulus. The startle response was expressed by subtracting the response to background noise (50dB). The PPI on the other hand was expressed as a percentage of inhibiting the startle response. The startle response and PPI are separately compared for wild-type and mutant mice and statistical significance was determined by Student's t-test.

2.17.3   Grip Strength

As the name suggests, grip strength is a measure of muscle strength of the forelimbs as well as the combined fore and hind limbs of mice. Defects in grip strength are usually associated with neuromuscular deficits or with defects in the cerebellar region of the brain. This test was carried out with a commercially available grip meter (Bioseb) with a single grid and was connected to a sensor. Each mouse was subjected to three trials with an interval of 5mins. The grip strength of the forelimbs was measured. The mice were placed on a platform of the grid and then gently pulled across the metal grid (caudal direction). The maximum force applied by the mice was recorded in grams at the moment the grasp is released. Although, there was no difference between the weights of mutant and wild-type mice, the data were expressed by accounting for the weight of the mice. Grip strength of wild-type and mutants were compared and statistical significance was determined by Student's t-test.

3 <u>CHAPTER THREE</u>: Investigation of *Cry⁻/⁻; Fbxl3^{Afh/Afh}* Compound Phenotypes

3.1 INTRODUCTION

3.1.1 Contribution of mammalian cryptochromes

Mammalian cryptochromes (*Cry*) are considered versatile in terms of their functions in regulating circadian rhythms. While in *Drosophila* they act as photoreceptors, this function of *Cry* is lost in mammals. However, cryptochromes are integral components of the circadian core oscillator in mammals and this was identified when the single *Cry* mutants were shown to have opposite circadian wheel-running activity phenotypes and a complete loss of rhythmicity in the absence of *Cry1* and *Cry2* (van der Horst, Muijtjens et al. 1999).

Although the two mammalian cryptochromes show 80% sequence homology amongst each other, they mostly differ in their unique C-terminal sequences (Chaves, Yagita et al. 2006). Sequence alignment of CRY1 and CRY2 proteins show no similarity between the C-terminus. Additionally, it has been recently found that *Cry1* expression is regulated by a combination of E-box elements (morning time elements) and D-box elements within *Cry1* promoter regions (Ukai-Tadenuma, Yamada et al. 2011). This combination of regulatory elements has not yet been identified in *Cry2*, confirming differences at the regulation levels of both *Cry* genes. However, both CRY proteins function as negative regulators in the mammalian clock, whereby their transcription is activated by the CLOCK-BMAL1 heterodimer.

The other importance of CRY proteins was discovered in co-localization experiments. As seen previously in Chapter 1, the formation of a PER-CRY heterodimer is necessary for feedback repression to maintain a functional circadian clock. For the purpose of formation of

114

the heterodimer, reports show the presence of CRY proteins is essential, as it is involved in translocation of PER proteins. *In-vitro* studies suggest that in the absence of CRY, PER is trapped in the cytoplasm. On the other hand, in the presence of CRY, 68% of the co-transfected cells had PER localised in the nucleus, thus showing CRY proteins play a critical role in nuclear translocation of PER proteins. It is only after nuclear translocation of CRY and PER proteins, that feedback repression is initiated (Lee, Etchegaray et al. 2001). This has further been shown in studies carried out in $Cry1^{-/-}$ and $Cry2^{-/-}$ single knockouts and $Cry1^{-/-}$; $Cry2^{-/-}$ double mutant mice. In the single mutants, due to the presence of either CRY protein, PER is able to form the heterodimer, resulting in persistent rhythms, although not similar to wild-type rhythms. However, in the absence of both CRY proteins, PER proteins are unable to translocate to the nucleus and accumulate in the cytoplasm, due to which there is no feedback repression resulting in instantaneous arrhythmicity (van der Horst, Muijtjens et al. 1999). Hence, to maintain the equilibrium between the positive and negative loops, the regulation of *Cry* genes and subsequent CRY proteins is most important.

Finally, all the above mentioned functions of CRY proteins are tightly regulated by posttranslational modifications such as phosphorylation, ubiquitination and subsequent degradation to sustain circadian oscillations to a 24hr period. F-box proteins play a vital role in this mechanism, as there are specific F-box proteins that target specific substrates for proteasomal degradation. The specific F-box proteins targeting CRY as substrates were unknown until the identification of the ENU mutants, afterhours *(Afh)* (Busino, Bassermann et al. 2007; Godinho, Maywood et al. 2007) and overtime (*Ovt*) (Siepka, Yoo et al. 2007). Both these mutants were identified by different research groups as circadian phenodeviants with a period of 26.73hrs and 25.8hrs respectively in constant dark (DD) conditions. Mapping revealed that the mutations were due to point mutations in the secondary motif, LRRs, of the

F-box protein, *Fbxl3*. Expression studies showed that the long period phenotype was a result of reduced interaction between CRY and FBXL3, due to which CRY proteins were spared from proteasomal degradation. As a result of this, higher CRY protein levels were observed during the subjective day compared to low CRY levels in wild-type mice. Consequently, the CRY proteins caused an extended transcriptional repression, resulting in a long period (Godinho, Maywood et al. 2007; Siepka, Yoo et al. 2007).

3.1.2 Aims of chapter

The aim of this chapter was to identify the effect of the *Afh* mutation on *Cry1* and *Cry2* by generating $Cry^{-/-};Fbxl3^{Afh/Afh}$ compound mutants which should lead to overexpression of the alternative CRY proteins. While a null hypothesis would predict equal effects of the *Afh* mutation on *Cry1* and *Cry2*, alternatively it could also be that both the cryptochromes are not equally affected by *Fbxl3*. However with prior knowledge of FBXL3 interacting with both CRY1 and CRY2, it may be that the *Afh* mutation would result in period lengthening by stabilisation of either CRY proteins in the double mutants. To investigate this, the compound mutants were screened for their circadian wheel-running behaviour. Additionally, since the *Afh* mutation was reported to have effects at the transcriptional and translational level (extended transcriptional repression due to stabilisation of CRY proteins), we wanted to investigate the expression profiles of various clock genes and their protein products in the compound mutants. Apart from identifying the effects of the *Afh* mutation, gene expression studies in the compound mutants would also contribute to our understanding of the functions of each *Cry* gene, namely if they have the same ability in repressing clock genes and thus controlling the clock through feedback repression.

This work has been done in collaboration with Dr. Michael H. Hastings, MRC, Laboratory of Molecular Biology, Cambridge, United Kingdom. While we carried out the *in vivo* experiments and molecular analysis, SCN slice data was obtained from Dr. Michael Hastings' lab.

3.2 RESULTS

3.2.1 Wheel running analysis for *Cry⁻/⁻; Fbxl3^{Afh/Afh}* Compound Mutants

In order to investigate the effects of the *Fbxl3^{Afh}* mutation on *Cry1* and *Cry2* individually, all combinations of *Cry⁻/⁻; Fbxl3^{Afh}* compound mutants were generated as shown in section 2.1.2. 10 animals for each combination of the genotypes were screened for wheel running activity. The complete wheel running protocol that lasted for almost a month consisted of animals being kept in a 12hr L:D schedule for 7 days following which they were allowed to free run in constant darkness (DD) for 2 weeks and finally allowed to free run in constant light (LL) conditions for the last 2 weeks of the screen.

Figure 3.1 and Figure 3.4 show nine representative double plotted actograms representing each of the genotypes generated from a *Cry1⁻/⁻* to *Fbxl3^{Afh/Afh}* and *Cry2⁻/⁻* to *Fbxl3^{Afh/Afh}* cross respectively. Each of the actograms is a representation of a group (males and females) of 10 animals and the τ values mentioned are obtained as a mean±SEM of the 10 animals. In both the figures the top panels are actograms from animals that are *Cry^{+/+}*, the middle panels are from animals with a heterozygous *Cry* (*Cry^{+/-}*) background, whereas the bottom panels are actograms from animals where both the copies of *Cry* are absent (*Cry^{-/-}*). While the graphical representation of τ obtained from the *Cry1⁻/⁻; Fbxl3^{Afh/Afh}* DD and LL are shown in Figure 3.2 and 3.3 respectively, the τ from *Cry2⁻/⁻; Fbxl3^{Afh/Afh}* in DD and LL are graphically representated in Figure 3.5 and 3.6 respectively.

In Figure 3.1 it is clearly seen that, whereas wild-type animals have τ_{DD} of 23.68hrs± 0.094, we see an increase in period length in the *Afh/Afh* mice having a τ_{DD} of 26.48 hrs± 0.161, as reported earlier by (Godinho, Maywood et al. 2007). On the other hand compared to

the wild-type mice the $Cry1^{+/-}$ mice have a τ_{DD} of 23.5hrs±0.103 which increases to 24.17hrs

±0.098 and 25.31hrs±0.178 (p<0.001) in $Cry1^{+/-};Fbxl3^{Afh/+}$ and $Cry1^{-/-};Fbxl3^{Afh/Afh}$ mice

respectively. As reported previously the loss of $Cry1$ accelerates the clock, as seen in $Cry1^{-/-}$

with a τ_{DD} of 22.89hrs±0.07 (van der Horst, Muijtjens et al. 1999). This period is seen to

lengthen with the addition of Afh mutation to 23.4hrs±0.107 and 24.19hrs±0.164 in $Cry1^{-/-}$

$;Fbxl3^{Afh/+}$ and $Cry1^{-/-};Fbxl3^{Afh/Afh}$ respectively. A similar increase in period length of the $Cry1^{-/-}$

$^{-/-};Fbxl3^{Afh/Afh}$ compound mutants is seen with the addition of the Afh mutation under LL

conditions. The trend in the period lengths are clearly seen in the graphical representations of

τ_{DD} and τ_{LL} in Figure 3.2 and 3.3 respectively. The decrease in period length (accelerated

clock) is seen with the gradual loss of $Cry1$ under wild-type $Fbxl3$ condition and an increase in

period length is seen with the gradual addition of an Afh mutation. Thus, the combined effects

of the loss of the $Cry1$ and addition of Afh mutation can be seen in the last three bars of

Figure 3.2, where under an Afh/Afh background the gradual loss of a copy of $Cry1$ results in a

significant (p<0.001) and propotional acceleration of the clock, hence a shorter period, albeit

with greater τ_{DD} than under wild-type $Fbxl3$ condition. Figure 3.3 shows a similar trend in

period length of $Cry1^{-/-};Fbxl3^{Afh/Afh}$ compound mutants under LL conditions.

The same effect of increasing period length with the addition of the Afh mutation is

seen in the $Cry2^{-/-};Fbxl3^{Afh/Afh}$ compound mutants. Figure 3.4 shows representative actograms

of these compound mutants. From a period length of 24.24hrs±0.084 seen in $Cry2^{-/-};Fbxl3^{+/+}$

mice, the period length increases to 24.75hrs±0.112 and 27.83hrs±0.310 in $Cry2^{-/-};Fbxl3^{Afh/+}$

and $Cry2^{-/-};Fbxl3^{Afh/Afh}$ mutants respectively. The graphical representation of the change in

phenotypes in DD is clearly seen in Figure 3.5.

Thus by investigating the circadian wheel-running behaviour of the compound mutants

the null hypothesis assuming equal effects of Afh on $Cry1$ and $Cry2$ can be accepted.

However, when the increase in period length between the single $Cry^{-/-}$ and $Cry^{-/-};Fbxl3^{Afh/Afh}$ double mutants are compared, there is unequal period lengthening in a $Cry1$-driven and Cry-2 driven clock. As seen in Figure 3.7, while an increase of 1 hr is observed in $Cry2$-driven clock ($Cry1^{-/-};Fbxl3^{Afh/Afh}$) (Figure 3.7A), there is a significant period lengthening of 3.59hrs ($p<0.001$) in a $Cry1$-driven clock (Figure 3.7B), suggesting differential abilities of CRY1 and CRY2 in the feeback repression process which is further investigated through gene expression studies.

Apart from the increase in period lengths, striking observations were made in the $Cry2^{-/-};Fbxl3^{Afh/Afh}$ mutants; one is their free-running activity during the LD schedule of the circadian screen. Unlike the wild-types, which show robust activity only during the dark phase of the LD cycle, the $Cry2^{-/-}; Fbxl3^{Afh/Afh}$ double mutants free-run through the LD cycle (with activity in the light phase) and are unable to entrain to the cycle (Figure 3.4). The second observation made in these mice, is their variable behaviour under constant light conditions. Although $Fbxl3^{Afh/Afh}$ mice (with wild type $Cry1$ and $Cry2$ present) show disturbed activity or splitting in LL after the first few days in LL, this activity seems to be disrupted gradually with the loss of $Cry2$ (Figure 3.4), unlike with the loss of $Cry1$ under the same conditions. In $Cry2^{+/-}; Fbxl3^{Afh/+}$ mice, there seems to be a decrease in period length for the first few days in LL which then increases with time. This activity seems to be lost with the addition of two mutated copies of $Fbxl3$ ($Cry2^{+/-}; Fbxl3^{Afh/Afh}$) and these mice seem arrhythmic in LL. Similarly, in $Cry2^{-/-}; Fbxl3^{Afh/+}$ mice, splitting of activity is seen LL conditions and behaviour becomes arrhythmic with the addition of the second copy of the Afh mutation ($Cry2^{-/-}; Fbxl3^{Afh/Afh}$). This is a consistent finding and it is interesting to investigate the potential functions of $Cry2$ in the retina and regulation of the clock under LL conditions.

Apart from the wheel running activity carried out *in vivo*, parallel studies were carried out in SCN slices, which also show a similar trend in phenotypes, with increasing period length in both *Cry1$^{-/-}$;Fbxl3$^{Afh/Afh}$* and *Cry2$^{-/-}$;Fbxl3$^{Afh/Afh}$* compound mutants compared to the respective *Cry* null mice, confirming the effect of the *Fbxl3$^{Afh/Afh}$* mutation on both *Cry1* and *Cry2 (Appendix4,5)*. Once the wheel running analysis was performed *in vivo*, it was interesting to see if the same effect as seen *in vivo* correlates to effects of the *Afh* mutation *in vitro* by using SCN slices from compound mutants. The data from the independent set of studies were then analysed to determine the Pearsons correlation coefficient (R^2). The correlation between the data collected in slices in DD and the *in vivo* behaviour is shown in figure 3.8 and 3.9 for *Cry1$^{-/-}$;Fbxl3$^{Afh/Afh}$* and *Cry2$^{-/-}$;Fbxl3$^{Afh/Afh}$* mutants respectively. When a R^2 value lies between the range of 0.5 to 1.0, then a strong co-relation between the two data sets is thought to be present. It is clear that there is a strong correlation (*Cry1$^{-/-}$;Fbxl3$^{Afh/Afh}$* R^2=0.82, p>0.05 ; *Cry2$^{-/-}$Fbxl3$^{Afh/Afh}$* R^2=0.84,p>0.05) observed between the wheel running activity and the SCN slice in both the sets of the compound mutants, although not highly significant. Hence, it could be said that, by carrying out experiments *in- vitro* in the SCN slice, the period length of animals *in vivo* could be predicted based on the values obtained from SCN slices.

Figure 3.1: Circadian wheel running activity for Cry1^{-/-}; Fbxl3^{Afh/Afh} Compound Mutants. The figure shows nine representative double plotted actograms of Cry1^{-/-};Fbxl3^{Afh/Afh} compound mutants which were allowed to entrain to a 12hr L:D (yellow blocks denote light and white blocks denote darkness) schedule for 7 days following which they were allowed to free run in constant darkness (DD) (white block) for 2 weeks and finally a constant light (LL) (yellow block) schedule was set up for 2 weeks. 10 animals of each genotype were screened for their circadian wheel-running analysis and the values mentioned are means±SEM for each group of animals. Some of the actograms show a 3hr light pulse during the dark phase of the LD schedule. The light pulse measures the ability of mice to inhibit activity in the presence of light. However, the light and dark pulses are a part of our circadian screens with no relevance to the study mentioned in this thesis. Statistical significance was determined by one way ANOVA with Bonferroni post hoc analysis.

From left to right, the top panel confirm the Afh/+ and Afh/Afh phenotype with a tau$_{DD}$ of 24.26hrs ±0.036 and 26.48hrs±0.169 respectively. The middle panel includes actograms of animals heterozygous for Cry1. It is seen that with the addition of the Afh mutation, the period lengthens from 23.5hrs±0.103 in Cry1^{+/-}; Fbxl3^{+/+} to 25.31hrs±0.178 in Cry1^{+/-}; Fbxl3^{Afh/Afh} mice. With the loss of the second Cry1 copy, the period length increases significantly from 22.89hrs±0.07 in Cry1^{-/-}; Fbxl3^{+/+} to 23.4hrs±0.107hrs in Cry1^{-/-}; Fbxl3^{Afh/+}; Fbxl3^{+/-}; Fbxl3^{Afh/+}. The period further increases to 24.19hrs±0.1642 in Cry1^{-/-}; Fbxl3^{Afh/Afh} mice. The period length as expected, lengthens even more as compared to their respective tau$_{DD}$ in every compound mutant under LL. Thus compared to the wild-type and Afh/Afh mice with a tau$_{LL}$ of 25.11hrs±0.045 and 30.61hrs±0.870, the period length decreases with the loss of Cry1 alone to give a tau$_{LL}$ of 23.91hrs±0.096 in Cry1^{-/-};Fbxl3^{+/+} mice. However, compared to the Cry1^{-/-} single mutants, the period length increases to 27.61hrs±0.268 in Cry1^{-/-};Fbxl3^{Afh/Afh} mice.

Figure 3.2 Graphical representation of period length in Cry1$^{-/-}$; Fbxl3$^{Afh/Afh}$ under DD conditions. The graph is plotted for means obtained from a group of 10 animals screened for the circadian wheel running activity. SEM are plotted as error bars. The first three bars represent the period of animals with no *Afh* mutation and a gradual loss of *Cry1*. Thus, the period decreases significantly from 23.68hrs±0.094 in wild-type mice to 22.89hrs±0.07 in *Cry1*$^{-/-}$; *Fbxl3*$^{+/+}$ (p<0.001). In an *Fbxl3*$^{Afh/+}$ background, the period first lengthens to 24.26hrs±0.036 in *Cry1*$^{+/+}$;*Fbxl3*$^{Afh/+}$ which further decreases significantly to 24.17hrs±0.098 in *Cry1*$^{+/-}$;*Fbxl3*$^{Afh/+}$ and 23.4hrs±0.107 in *Cry1*$^{-/-}$;*Fbxl3*$^{Afh/+}$ (p<0.001). With the further addition of a second copy of the *Afh* mutation, in a *Fbxl3*$^{Afh/Afh}$ background, there is a further acceleration of the endogenous clock and hence the period length of the *Cry1*$^{+/+}$;*Fbxl3*$^{Afh/Afh}$ mutant significantly decreases with the gradual loss of *Cry1* to give a τ_{DD} of 25.31hrs±0.178 in *Cry1*$^{+/-}$;*Fbxl3*$^{Afh/Afh}$ and 24.19hrs±0.164 in *Cry1*$^{-/-}$;*Fbxl3*$^{Afh/Afh}$ double mutants (p<0.001). Statistical significances were determined by using one way ANOVA with Bonferroni post hoc analysis.

Figure 3.3 Graphical representation of period length in Cry1$^{-/-}$; Fbxl3$^{Afh/Afh}$ under LL conditions. The graph is plotted for means obtained from a group of 10 animals screened for the circadian wheel running activity. SEM are plotted as error bars. The first three bars represent the period of animals with no *Afh* mutation and a gradual loss of *Cry1*. Thus, the period decreases significantly from 25.11hrs±0.045 in wild-type mice to 23.91hrs±0.096 in *Cry1*$^{-/-}$; *Fbxl3*$^{+/+}$ (p<0.001). In an *Fbxl3*$^{Afh/+}$ background, the period first lengthens to 26.38hrs±0.419 in *Cry1*$^{+/+}$;*Fbxl3*$^{Afh/+}$ which further decreases to 25.92hrs±0.2033 in *Cry1*$^{+/-}$;*Fbxl3*$^{Afh/+}$ and significantly decreases to 25.2hrs±0.30 in *Cry1*$^{-/-}$;*Fbxl3*$^{Afh/+}$ (p<0.048). With the further addition of a second copy of the *Afh* mutation, in a *Fbxl3*$^{Afh/Afh}$ background, there is a further acceleration of the endogenous clock and hence the period length of the *Cry1*$^{+/+}$;*Fbxl3*$^{Afh/Afh}$ mutant decreases with the gradual loss of *Cry1* to give a τ_{LL} of 29.12hrs±0.337 in *Cry1*$^{+/-}$;*Fbxl3*$^{Afh/Afh}$ and 27.61hrs±0.268 in *Cry1*$^{-/-}$;*Fbxl3*$^{Afh/Afh}$ double mutants (p<0.001). Statistical significances were determined by using one way ANOVA with Bonferroni post hoc analysis.

Figure 3.1: Circadian wheel running activity for Cry1⁻/⁻; Fbxl3^{Afh/Afh} compound mutants.
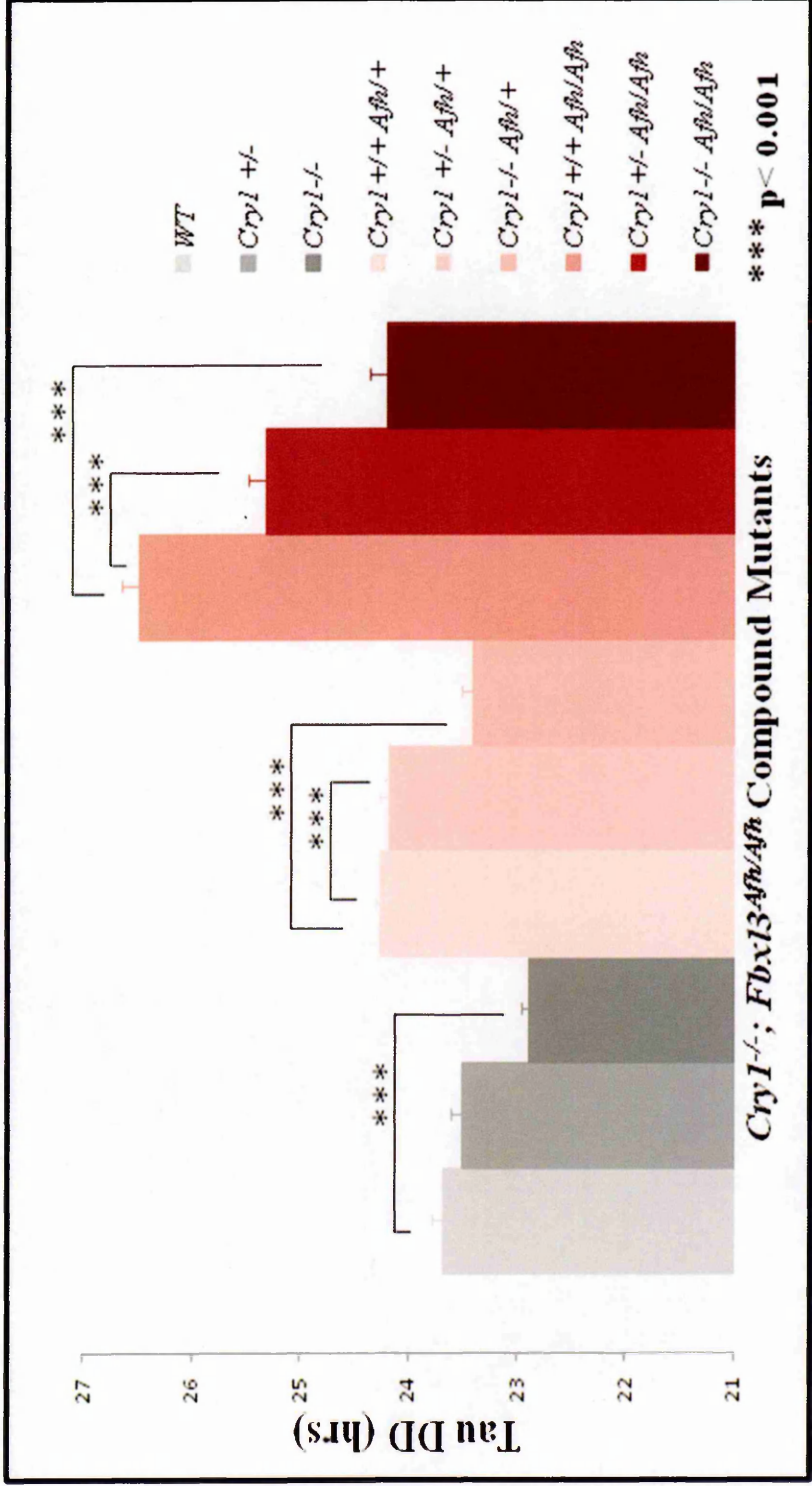
Figure 3.2: Graphical representation of period length in Cry1⁻/⁻ ; Fbxl3^Afh/Afh under DD conditions
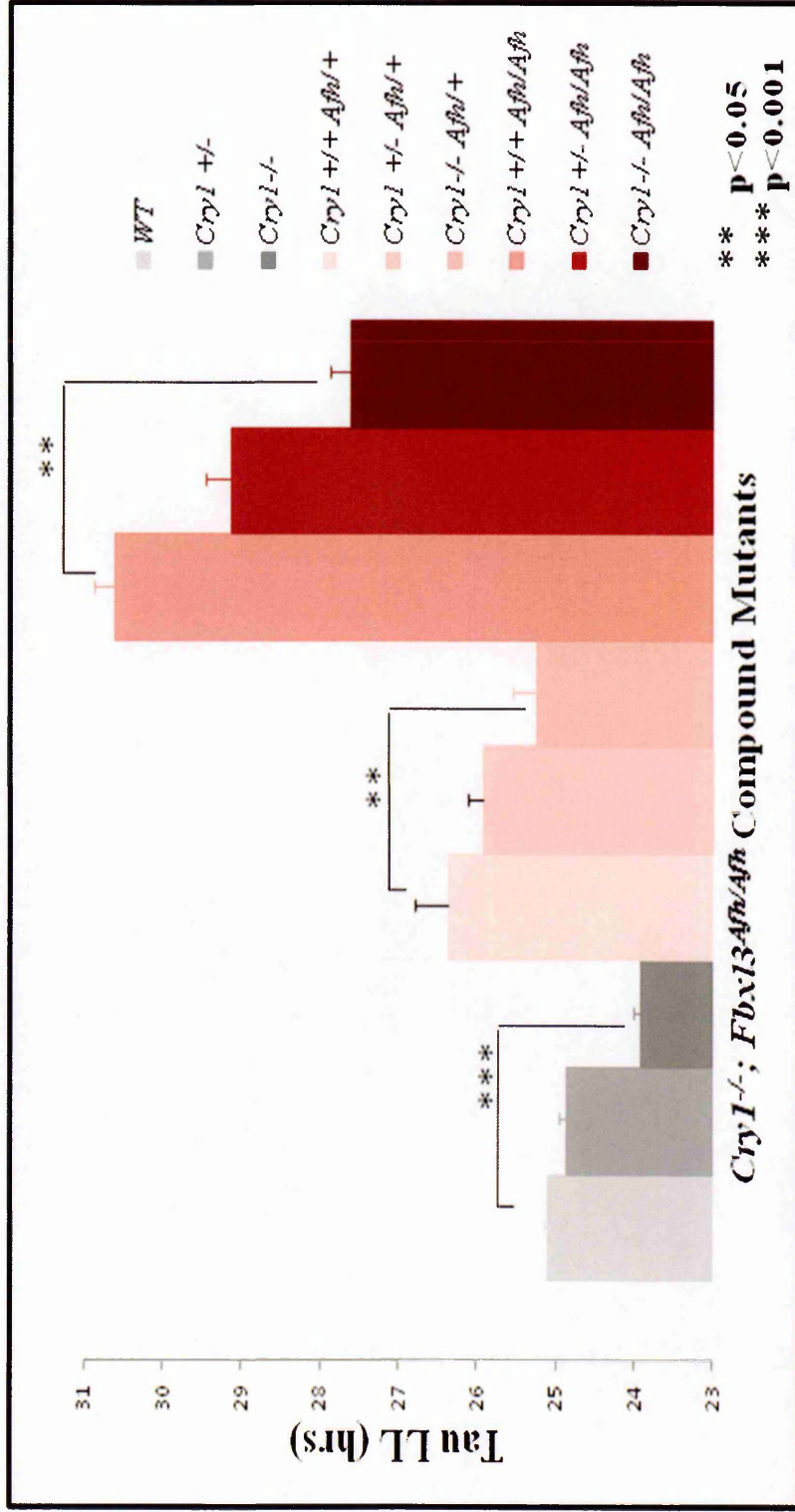
Figure 3.3: Graphical representation of period length in Cry1⁻/⁻; Fbxl3^Afh/Afh under LL conditions.

Figure 3.4: Circadian wheel running activity for Cry2$^{-/-}$; Fbxl3$^{Afh/Afh}$ Compound Mutants. The figure shows nine representative double plotted actograms of Cry2$^{-/-}$;Fbxl3$^{Afh/Afh}$ compound mutants which were allowed to entrain to a 12hr L:D schedule for 7 days following which they were allowed to free run in constant darkness (DD) for 2 weeks and finally a constant light (LL) schedule was set up for 2 weeks. 10 animals of each genotype were screened for their circadian wheel-running analysis and the values mentioned are a mean±SEM for each group of animals. Some of the actograms show a 3hr light pulse during the dark phase of the LD schedule. The light pulse measures the ability of mice to inhibit activity in the presence of light. However, the light pulses are a part of our circadian screens with no relevance to the study mentioned in this thesis. Statistical significance was determined by one way ANOVA with Bonferroni post hoc analysis.

From left to right, the top panel confirm the Afh/+ and Afh/Afh phenotype with a tau$_{DD}$ of 24.26hrs±0.036 and 26.48hrs±0.169 respectively. The middle panel includes actograms of animals heterozygous for Cry2. It is seen that with the addition of the Afh mutation, the period lengthens from 23.94hrs±0.049 in Cry2$^{+/-}$; Fbxl3$^{+/+}$ to 26.99hrs±0.19 in Cry2$^{+/-}$; Fbxl3$^{Afh/Afh}$ mice. In a Cry2$^{-/-}$ background, the addition of the Afh mutation gradually increases the period length from 24.24hrs±0.084 in Cry2$^{-/-}$; Fbxl3$^{+/+}$ to 24.75hrs±0.112hrs in Cry1$^{-/-}$; Fbxl3$^{Afh/+}$ p<0.001. The period significantly increases further to 27.83hrs±0.310 in Cry2$^{-/-}$; Fbxl3$^{Afh/Afh}$ mice. The period length, as expected, lengthens even more as compared to their respective Tau$_{DD}$ in every compound mutant under LL. Thus compared to the wild-type and Afh/Afh mice with a τ$_{LL}$ of 25.11hrs±0.045 and 30.61hrs±0.870, the period length increases with the loss of Cry2 alone to give a τ$_{LL}$ of 25.96hrs±0.24 in Cry2$^{+/-}$;Fbxl3$^{+/+}$ mice. The loss of one copy of Cry2 in the Fbxl3$^{Afh/+}$ background causes arrhythmicity in the Cry2$^{+/-}$;Fbxl3$^{Afh/Afh}$ mice. This arrhythmicity is maintained in the Cry2$^{-/-}$; Fbxl3$^{Afh/Afh}$ double mutants. Further, the effect of the loss of Cry2 is seen even in the Cry2$^{-/-}$;Fbxl3$^{Afh/+}$ which show splitting of activity under LL conditions. Another observation made is regarding the double mutants that are unable to entrain to the 12hr L:D cycle of the circadian screen, suggesting a possible role of Cry2 in the retina.

Figure 3.5 Graphical representation of period length in Cry2$^{-/-}$; Fbxl3$^{Afh/Afh}$ under DD conditions. The graph is plotted for means obtained from a group of 10 animals screened for the circadian wheel running activity. SEM are plotted as error bars. The first three bars represent the period of animals with no *Afh* mutation and a gradual loss of *Cry2*. Thus, the period increases significantly from 23.68hrs±0.094 in wild-type mice to 24.24hrs±0.084 in *Cry2$^{-/-}$; Fbxl3$^{+/+}$* (p<0.001). In an *Fbxl3$^{Afh/+}$* background, the period first lengthens to 24.26hrs±0.036 in *Cry2$^{+/+}$;Fbxl3$^{Afh/+}$* which further increases to 24.59hrs±0.060 in *Cry2$^{+/-}$;Fbxl3$^{Afh/+}$* and 24.75hrs±0.112 in *Cry2$^{-/-}$;Fbxl3$^{Afh/+}$* (p<0.001). With the further addition of a second copy of the *Afh* mutation, in a *Fbxl3$^{Afh/Afh}$* background, there is a further delay of the endogenous clock and hence the period length of the *Cry2$^{+/+}$; Fbxl3$^{Afh/Afh}$* mutant significantly increases with the gradual loss of *Cry2* to give a τ_{DD} of 26.99hrs±0.19 in *Cry2$^{+/-}$;Fbxl3$^{Afh/Afh}$* and 27.83hrs±0.310 in *Cry2$^{-/-}$;Fbxl3$^{Afh/Afh}$* double mutants (p<0.001). Statistical significances were determined by using one way ANOVA with Bonferroni post hoc analysis.

Figure 3.6 Graphical representation of period length in Cry2$^{-/-}$; Fbxl3$^{Afh/Afh}$ under LL conditions. The graph is plotted for means obtained from a group of 10 animals screened for the circadian wheel running activity. SEM are plotted as error bars. The first three bars represent the period of animals with no *Afh* mutation and a gradual loss of *Cry2*. Thus, the period decreases significantly from 25.11hrs±0.045 in wild-type mice to 25.96hrs±0.24 in *Cry2$^{-/-}$; Fbxl3$^{+/+}$* (p<0.020). In an *Fbxl3$^{Afh/+}$* background, the period first lengthens to 26.38hrs±0.419 in *Cry2$^{+/+}$;Fbxl3$^{Afh/+}$* ,decreases to 24.59hrs±0.104 in *Cry1$^{+/-}$;Fbxl3$^{Afh/+}$* (p<0.05) and significantly increases to 27.53hrs±0.415 in *Cry2$^{-/-}$;Fbxl3$^{Afh/+}$* (p<0.001), although these mice show splitting of activity in LL. With the further addition of a second copy of the *Afh* mutation, in a *Fbxl3$^{Afh/Afh}$* background, there are variable phenotypes observed. With a loss of a *Cry2* copy, i.e. in *Cry2$^{+/-}$;Fbxl3$^{Afh/Afh}$*, the mice are arrhythmic in LL and this arrhythmic behaviour is also seen in *Cry2$^{-/-}$;Fbxl3$^{Afh/Afh}$* double mutants. Another interesting observation made in the *Cry2$^{-/-}$;Fbxl3$^{Afh/Afh}$* compound mutants is the ability to entrain to the 12hrL:D cycle is lost in the *Cry2$^{-/-}$;Fbxl3$^{Afh/Afh}$* double mutants. The variations in these mutants suggest a possible role of *Cry2* in the retina. Statistical significances were determined by using one way ANOVA with Bonferroni post hoc analysis.
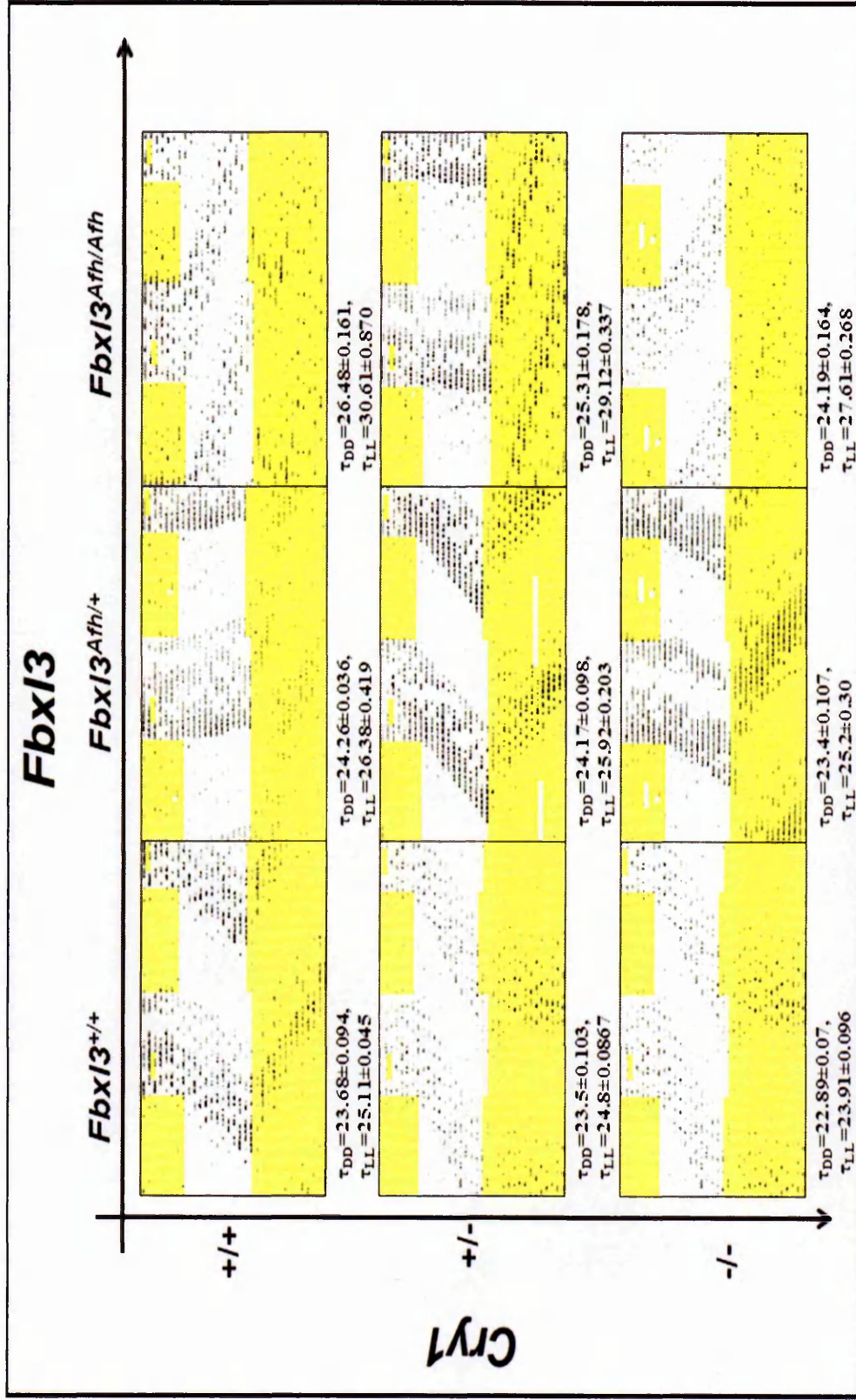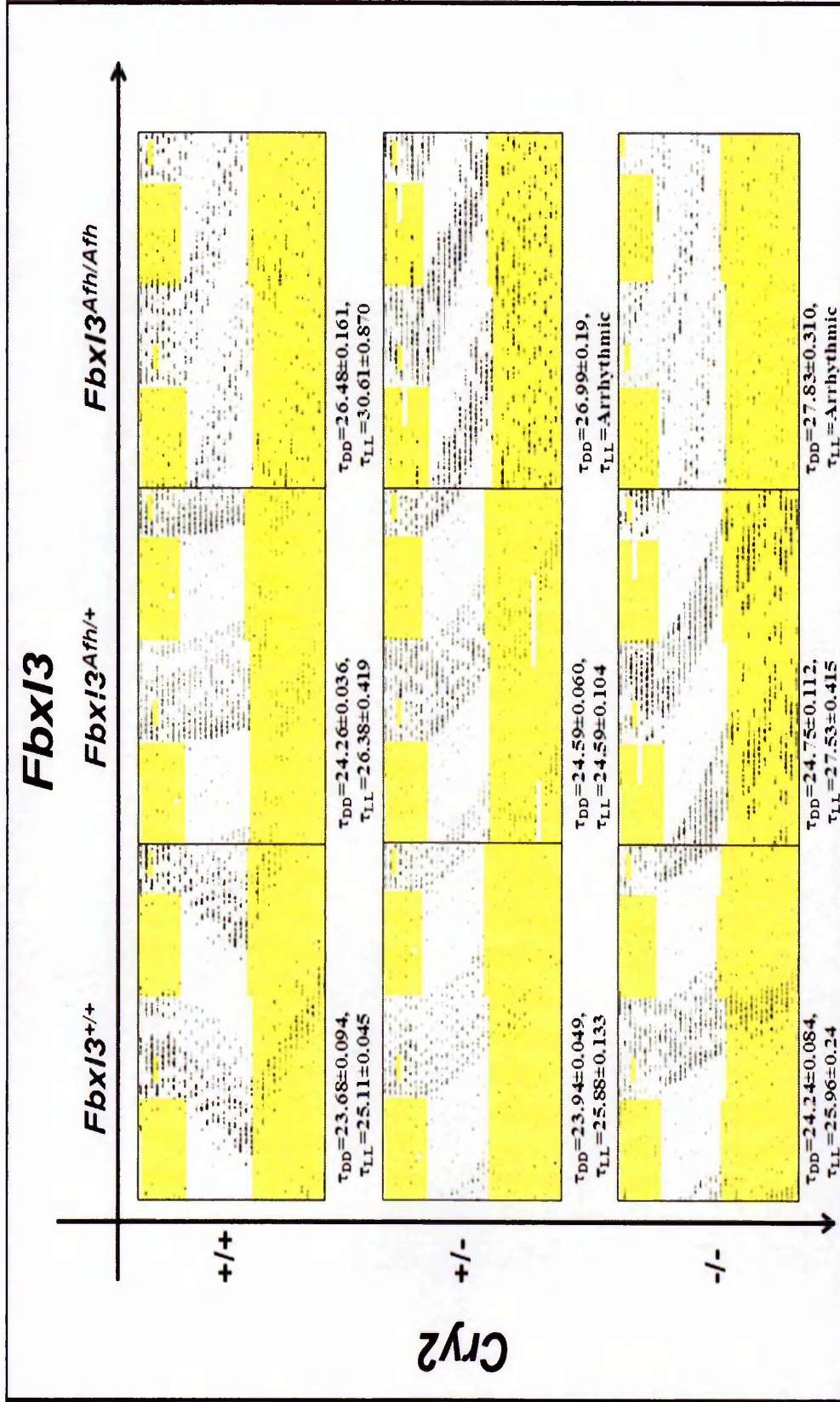
Figure 3.4: Circadian wheel running activity for Cry2⁻/⁻; Fbxl3^Afh/Afh Compound Mutants
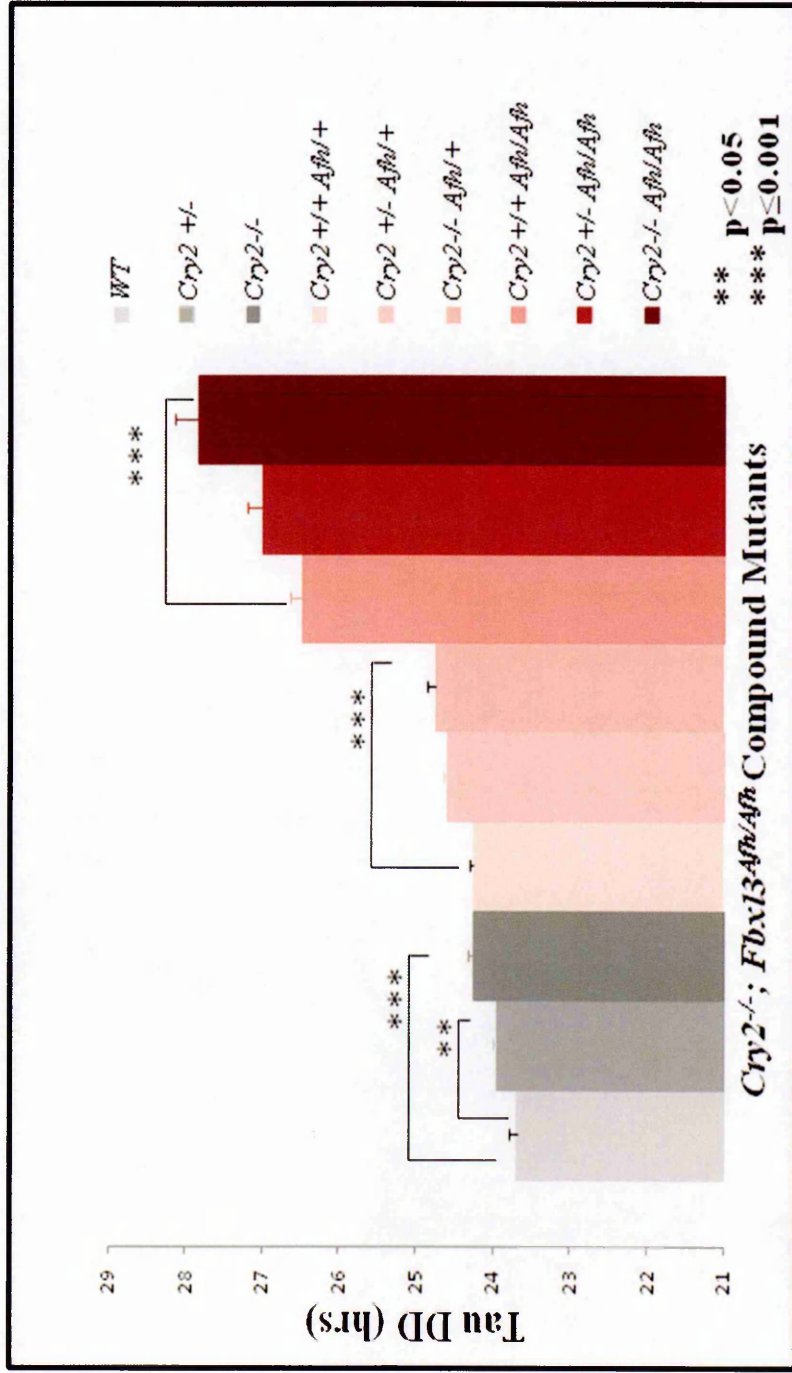
Figure 3.5: Graphical representation of period length in Cry2⁻/⁻; Fbxl3^{Afh/Afh} under DD conditions.
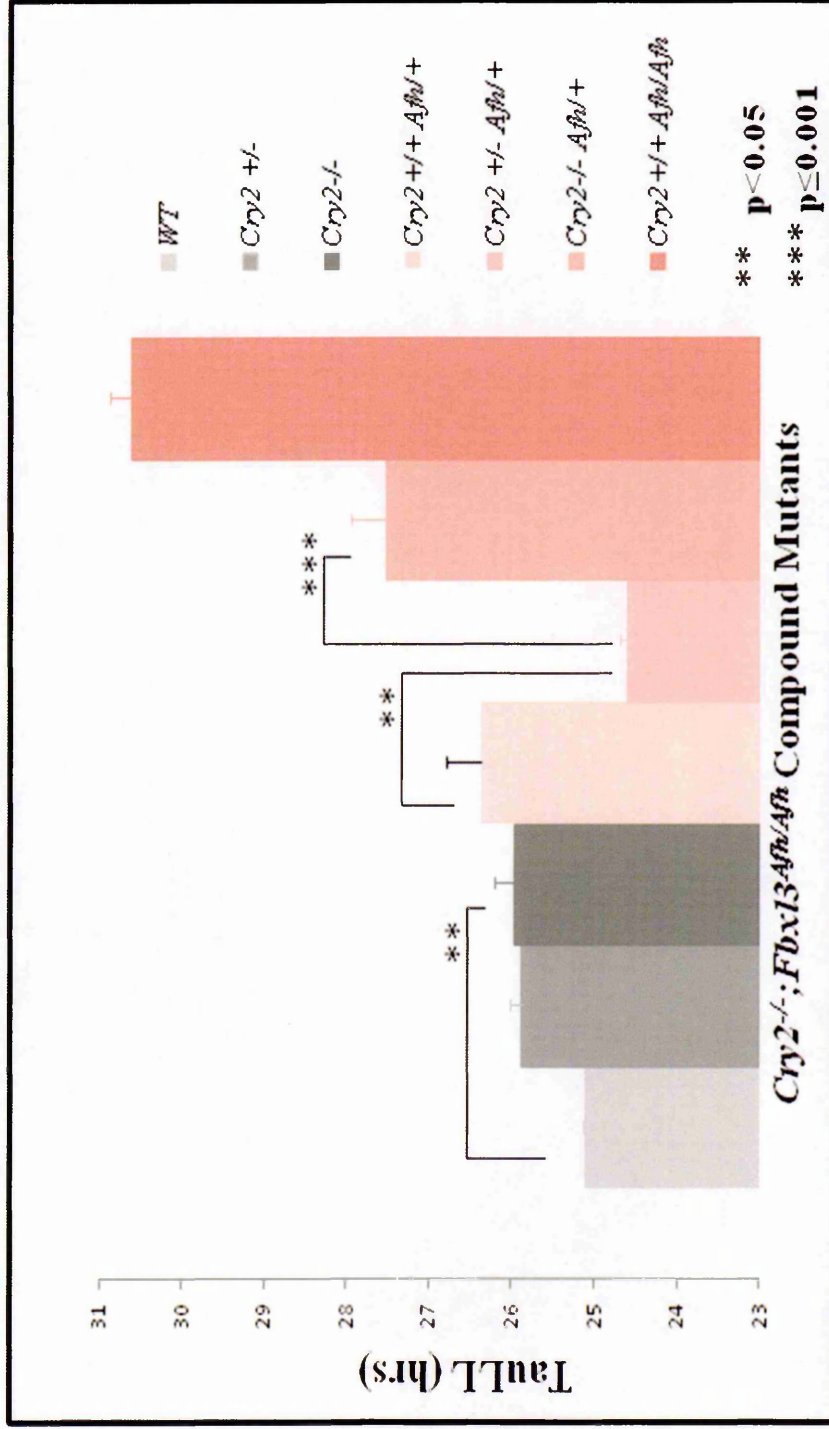
Figure 3.6: Graphical representation of period length in Cry2$^{-/-}$; Fbxl3$^{Afh/Afh}$ under LL conditions
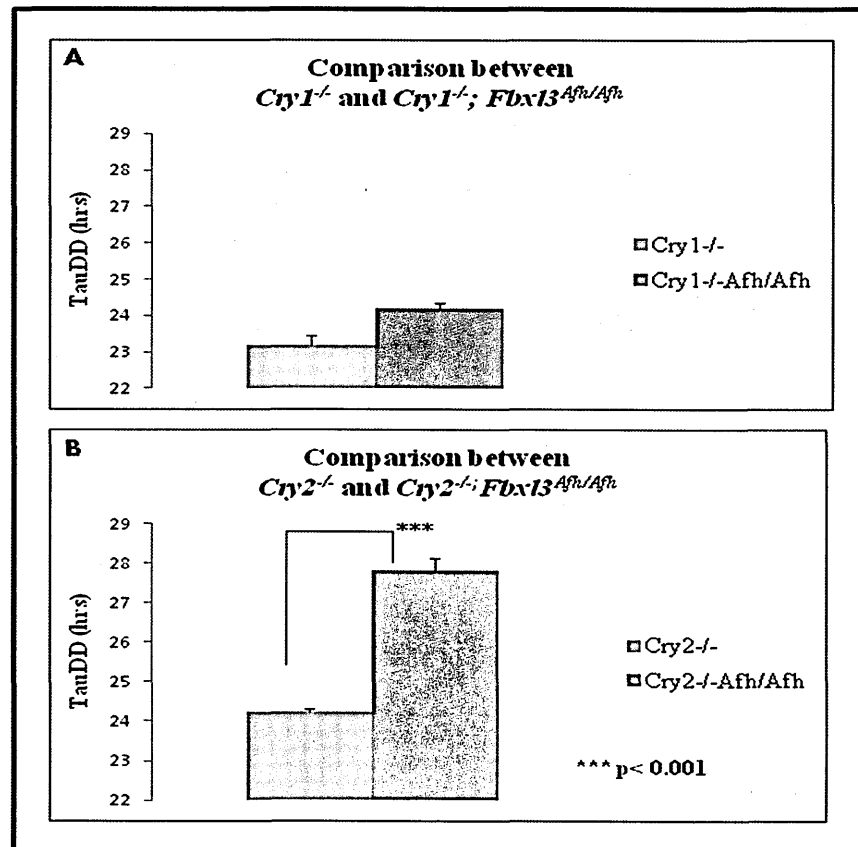
Figure 3.7: Comparison between the *Cry$^{-/-}$* ***single knockouts and*** *Cry$^{-/-}$; Fbxl3$^{Afh/Afh}$* ***double mutants.***
The difference in Tau$_{DD}$ is measured to observe the effect of the *Afh* mutation on the period length in the *Cry$^{-/-}$; Fbxl3$^{Afh/Afh}$* double mutant. Additionally, the effect of overexpressing either CRY protein can be clearly observed in the above graph. A) Compared to the *Cry1$^{-/-}$* knockout with a TauDD of 22.89±0.07, the *Cry1$^{-/-}$; Fbxl3$^{Afh/Afh}$* only shows an increase of period length by 1 hour (TauDD=24.199±0.164) which is not significant. B) Compared to the Tau$_{DD}$ of 24.24±0.049 in *Cry2$^{-/-}$* knockout mice, the addition of the *Afh* significantly increases the period of *Cry2$^{-/-}$;Fbxl3$^{Afh/Afh}$* double mutants to 27.83±0.310. Thus, compared to a 1hr difference obtained by CRY2 upregulation, CRY1 overexpression shows a significant increase of 3.59hrs (p<0.001) on the period length, suggesting that *Cry1* is a stronger transcriptional repressor than *Cry2*. The graph shown above is obtained from a mean of 10 animals (males and females). The SEM are represented as error bars. Statistical significance is determined by a one-way ANOVA.
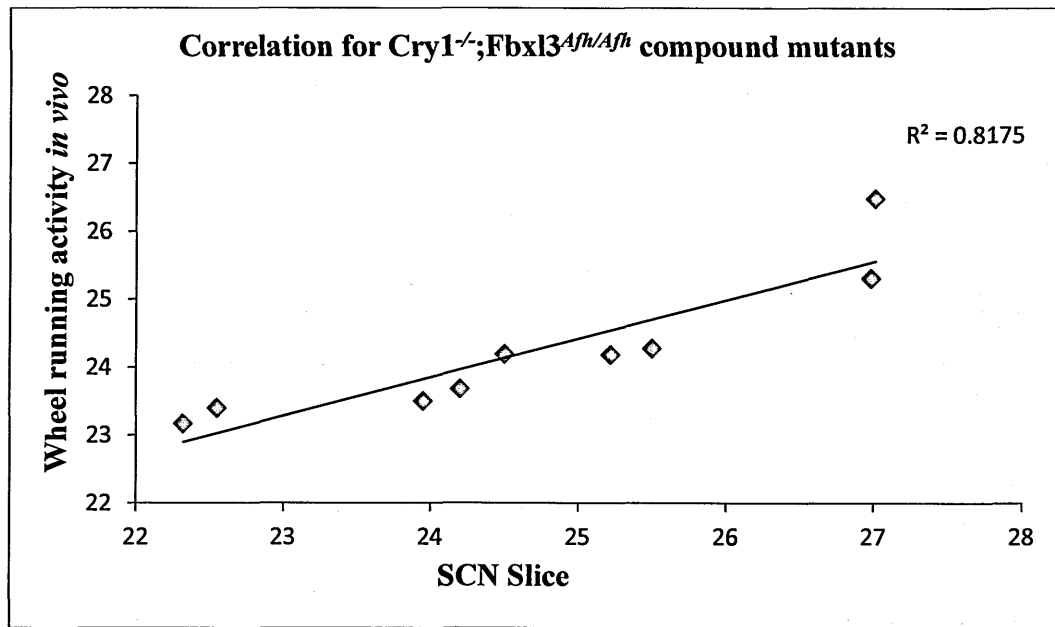
Figure 3.8: Correlation between period length in-vitro in SCN slices and in vivo wheel-running behaviour in the Cry1$^{-/-}$; Fbxl3$^{Afh/Afh}$ compound mutants. Once period lengths are independently obtained *in-vitro* and *in vivo*, the Pearson's correlation coefficient (R^2) is determined. The R^2 value shows that the two sets of data can be highly correlated and that a phenotype observed in the SCN slices can also be observed *in vivo*.
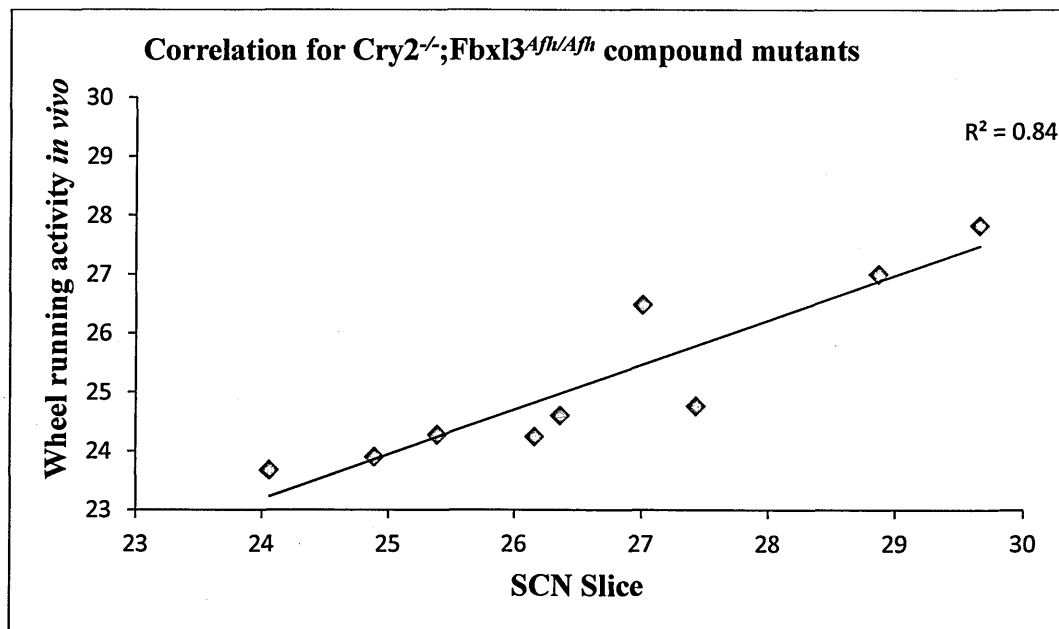
Figure 3.9: Correlation between period length in-vitro in SCN slices and in vivo wheel-running behaviour in the Cry2$^{-/-}$; Fbxl3$^{Afh/Afh}$ compound mutants. Once period lengths are independently obtained *in-vitro* and *in vivo*, the Pearson's correlation coefficient (R^2) is determined. The R^2 value shows that the two sets of data can be correlated and that a phenotype observed in the SCN slices can also be observed *in vivo*.

3.2.2 Other circadian parameters

Apart from the wheel running behavioural analysis carried out in the $Cry^{-/-}$; $Fbxl3^{Afh/Afh}$ compound mutants, other parameters such as average wheel revolutions, amplitude of oscillations in each of the light and dark phases of the circadian screen were analysed. All the parameters have been defined in the earlier chapter in section 1.1.7. Broadly, there were no significant differences observed (by One-way ANOVA with Bonferroni post hoc test) in many of the parameters analysed in each of the combination of the compound mutants.

However, as we saw a lack of entrainment in the $Cry2^{-/-}$; $Fbxl3^{Afh/Afh}$ double mutant, the phase angle of entrainment could not be measured. Compared to the wild-types, the $Cry1^{-/-}$; $Fbxl3^{Afh/Afh}$ and $Cry2^{-/-}$; $Fbxl3^{Afh/Afh}$ compound mutants did show significant differences in some of the wheel running parameters measured. Under LD conditions, the compound mutants, except $Cry1^{-/-}$; $Fbxl3^{Afh/Afh}$ and $Cry2^{-/-}$; $Fbxl3^{Afh/Afh}$, were similar to the wild-type animals. The $Cry1^{-/-}$; $Fbxl3^{Afh/Afh}$ mice were seen to have a significantly higher mean wheel revolutions in the LD phase (p=0.03, One way ANOVA with Bonferroni post hoc analysis) (Table 3.2). These animals continued to display higher wheel revolutions even under constant light conditions (p=0.03, One way ANOVA with Bonferroni post hoc analysis) (Table 3.6) suggesting that the $Cry1^{-/-}$; $Fbxl3^{Afh/Afh}$ mice may be hyperactive and hence it would be interesting to assess their behaviour in the open field test (Chapter 5). The other significant difference observed amongst the compound mutants when compared to wild-type mice, was the reduction in the percentage of nocturnal activity in $Cry2^{-/-}$; $Fbxl3^{Afh/Afh}$ mice (p=0.04, One way ANOVA with Bonferroni post hoc analysis) (Table 3.3). This result was expected due to the lack of entrainment and free running phenotype observed in these mice. Parameters such

as amplitude of oscillations in DD, LL, and average wheel revolutions in DD showed no

significant differences between wild-type and $Cry^{-/-};Fbxl3^{Afh/Afh}$ double mutants.

Phase angle of entrainment LD

$Cry^{+/+};Fbxl3^{+/+}$	$Cry1^{-/-};Fbxl3^{Afh/+}$	$Cry2^{-/-};Fbxl3^{Afh/Afh}$
182.12±1.27	179.16±2.27	Free run in LD

Table 3.1: Difference of the phase angle of entrainment between $Cry^{-/-}$; $Fbxl3^{Afh/Afh}$ compound mutants. There is no difference in the phase of entrainment between the $Cry1^{-/-}$; $Fbxl3^{Afh/Afh}$ double homozygous mice and wild-type control mice. However, phase angle of entrainment could not be measured for $Cry2^{-/-}$; $Fbxl3^{Afh/Afh}$ mice as they free-run through the LD phase of the circadian phase. Although the values shown here for the wild-type controls and the $Cry^{-/-};Fbxl3^{Afh/Afh}$ compound mutants represent the mean±SEM obtained from a group of 10 animals, the free-running condition was observed in every animal screened.

Average Wheel Revolution in LD

	$Fbxl3^{+/+}$	$Fbxl3^{Afh/+}$	$Fbxl3^{Afh/Afh}$
$Cry1^{+/+}$	2649.30±618.89	2369.70±646.73	2816.54±1385.43
$Cry1^{+/-}$	3125.522±800.86	3073.56±782.90	2630.01±609.75
$Cry1^{-/-}$	1777.50±453.94	2548.43±367.01	**4544.50±1404.21****
$Cry2^{+/+}$	2649.30±618.89	2369.70±646.73	2816.54±1385.43
$Cry2^{+/-}$	1824.83±518.96	2772.04±745.23	3774.34±689.68
$Cry2^{-/-}$	1262.67±273.17	4498.16±890.38	3475.19±1923.52

**p=0.03

Table 3.2: Comparing the average wheel revolution in LD between $Cry^{-/-}$; $Fbxl3^{Afh/Afh}$ compound mutants and wild-type mice. Most of the compound mutants with the exception of $Cry1^{-/-}$; $Fbxl3^{Afh/Afh}$ double homozygous mice had similar averages of wheel revolutions in LD. The $Cry1^{-/-}$; $Fbxl3^{Afh/Afh}$ on the other hand display a significantly higher number of wheel revolutions (**p=0.03). The values of wheel revolutions mentioned here are the mean±SEM from 10 male and or female wild-type and compound mutants. One way ANOVA with Bonferroni post hoc analysis was used to test statistical significance.

% Nocturnal Activity

	$Fbxl3^{+/+}$	$Fbxl3^{Afh/+}$	$Fbxl3^{Afh/Afh}$
$Cry1^{+/+}$	90.655±0.79	89.64±0.84	77.25±3.89
$Cry1^{+/-}$	91.66±1.44	82.93±3.31	84.71±2.32
$Cry1^{-/-}$	85.28±1.79	87.22±0.97	87.24±2.55
$Cry2^{+/+}$	90.655±0.79	89.64±0.84	77.25±3.89
$Cry2^{+/-}$	90.93±1.8	85.34±0.96	92.61±16.4
$Cry2^{-/-}$	86.85±2.02	86.25±1.33	**60.65±6.79 ****

** p=0.04

Table 3.3: Comparing the nocturnal activity of the $Cry^{-/-}$; $Fbxl3^{Afh/Afh}$ compound mutants with control mice during the LD schedule. It is seen that the $Cry2^{-/-}$; $Fbxl3^{Afh/Afh}$ mutants show a significant reduction in the percentage of nocturnal activity during the LD phase (**p=0.04). This was expected as the same animals do not entrain to the LD cycle and free-run through the light and dark phase of the 12 hr L:D schedule. Apart from these mutants, there were no other significant differences observed between the wild-type and $Cry^{-/-}$; $Fbxl3^{Afh/Afh}$ compound mutants. The values shown here represent a group of 10 animals (males and/or females) and are means±SEM. Statistical significance was tested using one way ANOVA with Bonferroni post hoc test.

Average Revolution DD

	$Fbxl3^{+/+}$	$Fbxl3^{Afh/+}$	$Fbxl3^{Afh/Afh}$
$Cry1^{+/+}$	3623.91±927.9	4423.14±630.63	3551.64±1313.2
$Cry1^{+/-}$	4909.26±1451	3520.2±584.65	3882.03±690.65
$Cry1^{-/-}$	4104.48±1291.96	4057±731.32	7417.67±2108.30
$Cry2^{+/+}$	3623.91±927.9	4423.14±630.63	3551.64±1313.2
$Cry2^{+/-}$	3498.71±964.7	3103±460.79	7721.24±1274.96
$Cry2^{-/-}$	2074±492	6360.74±1621.09	5170.24±2062.01

Table 3.4: Measuring the average wheel revolution in DD in $Cry^{-/-}$; $Fbxl3^{Afh/Afh}$ compound mutants and wild-type control mice. No significant differences were observed in the average wheel revolutions of mice under DD conditions between wild-type, $Cry1^{-/-}$; $Fbxl3^{Afh/Afh}$ and $Cry2^{-/-}$; $Fbxl3^{Afh/Afh}$ double homozygous mice. The value mentioned here are mean±SEM from a group of 10 animals (mix of males and females). Statistical significance was tested using one way ANOVA with Bonferroni post hoc test.

Amplitude DD

	$Fbxl3^{+/+}$	$Fbxl3^{Afh/+}$	$Fbxl3^{Afh/Afh}$
$Cry1^{+/+}$	909.208±138.43	1073.63±74.96	820.335±93.02
$Cry1^{+/-}$	3912.21±1247.63	1024.38±92.39	3882.03±690.65
$Cry1^{-/-}$	894.13±86.68	962.18±91.33	1138.42±218.25
$Cry2^{+/+}$	909.208±138.43	1073.63±74.96	820.335±93.02
$Cry2^{+/-}$	963.20±90.6	653.96±99.5	1345.41±81.91
$Cry2^{-/-}$	748.78±80.1	1222.47±119.7	875.02±156.06

Table 3.5: Measuring the amplitude of oscillations in DD in $Cry^{-/-}$; $Fbxl3^{Afh/Afh}$ compound mutants and wild-type mice. No significant differences were observed between wild-type, $Cry1^{-/-}$; $Fbxl3^{Afh/Afh}$ and $Cry2^{-/-}$; $Fbxl3^{Afh/Afh}$ double homozygous mice when comparing their amplitude of oscillations under DD conditions. The values mentioned here are mean±SEM from a group of 10 animals (mix of males and females). One way ANOVA with Bonferroni post hoc test was used to test statistical significance.

Average Revolution in LL

	$Fbxl3^{+/+}$	$Fbxl3^{Afh/+}$	$Fbxl3^{Afh/Afh}$
$Cry1^{+/+}$	2205.25±460.71	2171.57±459.0	1771.95±400.60
$Cry1^{+/-}$	950.29±316.06	1681.94±348.97	3472.58±785.18
$Cry1^{-/-}$	2165.66±647.51	5017.29±1054.14	**4877.36±1034.87****
$Cry2^{+/+}$	909.208±138.43	1073.63±74.96	820.335±93.02
$Cry2^{+/-}$	2575.07±795.91	1325±257.622	4877.36±1034.87
$Cry2^{-/-}$	1710.20±508.70	4477.67±1286.05	2494.10±1118.44

**p=0.03

Table 3.6: Difference in the average wheel running revolution between the $Cry^{-/-}$; $Fbxl3^{Afh/Afh}$ compound mutants and control mice in constant light (LL) conditions. There was no significance between the average revolutions in $Cry2^{-/-}$; $Fbxl3^{Afh/Afh}$ double mutants and wild-type mice. While the majority of the $Cry1^{-/-}$; $Fbxl3^{Afh/Afh}$ had no significant differences compared to wild-type controls, the $Cry1^{-/-}$;$Fbxl3^{Afh/Afh}$ double mutants show high number of revolutions in LL that is significant (**p=0.03). The same animals showed a similar significant increase in the LD cycle of the circadian screen, suggesting these mice might be hyperactive. The values shown here represent a group of 10 animals (males and/or females) and are means±SEM. Statistical significance was tested using one way ANOVA with Bonferroni post hoc test.

Amplitude LL

	$Fbxl3^{+/+}$	$Fbxl3^{Afh/+}$	$Fbxl3^{Afh/Afh}$
$Cry1^{+/+}$	1102.826±104.9	539.24±35.3	613.19±46.7
$Cry1^{+/-}$	940.97±111.40	877.733±72	548.11±74.64
$Cry1^{-/-}$	766.785±59.57	1014.5±108.6	1122.73±258.9
$Cry2^{+/+}$	1102.826±104.9	539.24±35.3	613.19±46.7
$Cry2^{+/-}$	1226.42±246.99	358.5±57.32	Arrhythmic
$Cry2^{-/-}$	569.01±68.8	655.28±43.22	Arrhythmic

Table 3.7: Comparing the amplitude of oscillations in LL between $Cry^{-/-}$; $Fbxl3^{Afh/Afh}$ compound mutants and wild-type mice. There were no significant differences observed between wild-type, $Cry1^{-/-}$; $Fbxl3^{Afh/Afh}$ and $Cry2^{-/-}$; $Fbxl3^{Afh/Afh}$ double homozygous mice when comparing their amplitude of oscillations under LL conditions. The values mentioned here are the mean±SEM from 10 male and/ or female wild-type and compound mutants. One way ANOVA with Bonferroni post hoc analysis was used to test statistical significance.

3.2.3 Gene Expression Analysis in *Cry-/-; Fbxl3^{Afh/Afh}* Compound Mutants

The wheel running activity carried out in the *Cry^{-/-}; Fbxl3^{Afh/Afh}* compound mutants showed that the *Fbxl3^{Afh}* mutation has similar effects in both *Cry1* and *Cry2* null mutants increasing the period length of their *in vivo* rhythms. In order to investigate as to how the selective stabilisation of CRY proteins due to the *Afh* mutation affects the gene expression of other clock controlled genes, we carried out gene expression studies in the cerebellum collected from the double mutants entrained to a 12hr L:D schedule for 7 days. Gene expression was investigated at zeitgeber time (ZT) 3, 7, 11, 15, 19 and 23hrs.

Quantitative real time expression studies performed in cerebellum of *Cry1^{-/-}; Fbxl3^{Afh/Afh}* double mutants (Figure 3.10) show that with the exception of *Cry2* and *Per2*, the other genes *Per1, Dbp and Bmal1* showed robust rhythmicity in the cerebellum albeit with reduced amplitude relative to the rhythms of the wild-type mice. *Cry2* expression in *Cry1^{-/-}; Fbxl3^{Afh/Afh}* is seen to be constitutive with no rhythmicity compared to wild-type *Cry2* expression. Similarly, a complete reduction of *Per2* oscillations in seen in the *Cry1^{-/-}; Fbxl3^{Afh/Afh}* cerebellum. This was surprising and may indicate possible secondary effects of *Cry2* upregulation. While a phase shift with reduction of amplitude was observed in *Dbp*, (presumably because of the effect on *Cry2* and *Per2* expression), *Bmal1* was upregulated between ZT 3 and 11 in these mice, indicating that *Cry2* could be acting as a weak transcriptional repressor.

On the other hand, expression of the clock controlled genes at the RNA level in the cerebellum of *Cry2^{-/-}; Fbxl3^{Afh/Afh}* mice (Figure 3.11) shows transcriptional inhibition coupled with a phase shift of expression in all of the investigated genes, confirming the strong repression ability of *Cry1*. The expression of *Cry1, Per1, Per2, Dbp* and *Bmal1* were

dramatically altered with a reduction in amplitude and change in the peak of expression compared to expression in wild-type cerebellum. As mentioned previously circadian mechanisms at the molecular level also involve secondary regulatory loops in addition to the core oscillator loops (Section 1.1.2). Since most of the investigated genes belonged to the core oscillator, expression levels of a component belonging to the secondary regulatory loops of the molecular oscillator, *Rev-erbα*, were then determined in the cerebellum of the *Cry$^{-/-}$; Fbxl3$^{Afh/Afh}$* mice. It was surprising to see an upregulation of *Rev-erbα* mRNA due to overexpression of *Cry2* in the *Cry1$^{-/-}$; Fbxl3$^{Afh/Afh}$* mice (Figure 3.12 A). However, the expression of *Rev-erbα* was completely dampened (no oscillation) in the *Cry2$^{-/-}$; Fbxl3$^{Afh/Afh}$* mice (Figure 3.12 B). Again this confirms the ability of *Cry1* to repress components of the secondary feedback loops, whereas the effect of *Cry2* upregulation may be secondary to its effects on other genes.

Next, in order to investigate if the repressive actions of *Cry1* are confined only to the cerebellum or if they are able to repress the genes in peripheral tissues such as liver, real-time experiments were carried out using the same conditions as for the above experiment. The liver tissues were collected from the same animals in which clock gene expression in cerebellum was analyzed. It is seen from Figure 3.13 that *Cry2* overexpression in *Cry1$^{-/-}$; Fbxl3$^{Afh/Afh}$* mice is not able to inhibit *Per2* expression in the liver compared to what was seen in the cerebellum. Expression levels of *Per2* remain unchanged, whereas a surprising, lower amplitude of *Bmal1* and a phase shift of *Per1* expression was observed. The fold change (lower amplitude) in *Bmal1* expression is ambiguous and cannot be explained on the basis of the expression of the investigated genes. Overexpression of *Cry1* in *Cry2$^{-/-}$; Fbxl3$^{Afh/Afh}$* liver (Figure 3.14) on the other hand, showed similar results as obtained with expression in cerebellum. An inhibition of

transcription with lower amplitude and phase change in the peak of expression was observed in the expression of all the clock controlled genes investigated.

The *Afh* mutation in the F-box protein, *Fbxl3*, is known to cause a reduced interaction of FBXL3 and its substrates CRY1 and CRY2 *in vivo*, resulting in stabilisation of CRY proteins and an extended transcriptional repression (Godinho, Maywood et al. 2007). Hence, in order to confirm that the effect on gene transcription observed in the previous section was related to the upregulation of the respective CRY proteins, CRY protein levels were determined in the cerebellum of $Cry^{-/-};Fbxl3^{Afh/Afh}$ compound mutants. It was expected that in the absence of CRY1, CRY2 levels will be upregulated and stabilised, and in the absence of CRY2, CRY1 levels will be upregulated. For this experiment cerebellum from the same double mutants collected across various ZT time points for real-time experiments were used. The proteins were extracted in the manner that is described in Chapter 2, section 2.8. Investigating CRY2 protein levels in $Cry1^{-/-}; Fbxl3^{Afh/Afh}$ *in vivo* determined that compared to CRY2 levels present in the wild-type, the *Afh* mutation significantly upregulates and stabilises CRY2 across time (p=0.01) (Figure 3.15). Similarly, CRY1 protein levels were also seen to be significantly upregulated and stabilised across time in the $Cry2^{-/-};Fbxl3^{Afh/Afh}$ compared to wild-type CRY1 levels (p=0.01) (Figure 3.16). A strong genotype interaction on CRY protein levels was determined by a two way ANOVA. These results ultimately show that the effects on gene transcription (transcriptional repression) are indeed related to the elevated levels of the respective CRY proteins across time.
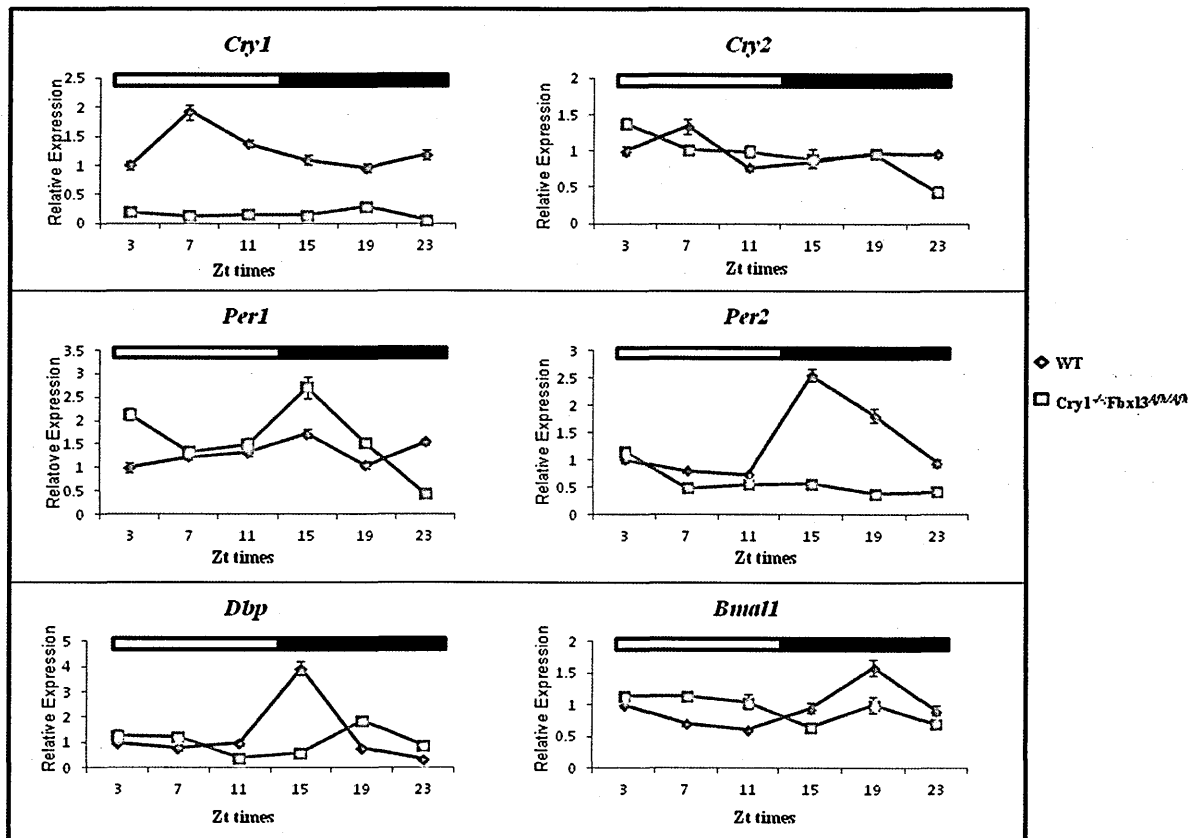
Figure 3.10: Gene expression studies in the cerebellum of Cry1^{-/-}; Fbxl3^{Afh/Afh} double mutants. To perform real-time quantitative PCR, cerebellum was dissected at various ZT times from *Cry1^{-/-}; Fbxl3^{Afh/Afh}* double mutants and wild-type controls. The expression at each time point was first calculated relative to the house-keeping gene, RPL13a, following which the expression of wild-type and mutant was made relative to expression of wild-type ZT 3. Each time point is an average of triplicate reactions, obtained from three independent samples. The SEMs are represented as error bars. The dampened levels of *Cry1* confirm the absence of the *Cry1* expression. *Cry2* levels in the double mutants are seen to be elevated and compared to the wild-type levels, *Cry2* levels in the mutant do not oscillate *in vivo*. While *Per1* had an elevated expression, *Per2* and *Dbp* show a phase shift with reduced amplitude. In contrast, *Bmal1* was seen to be upregulated, although no phase shift was observed.
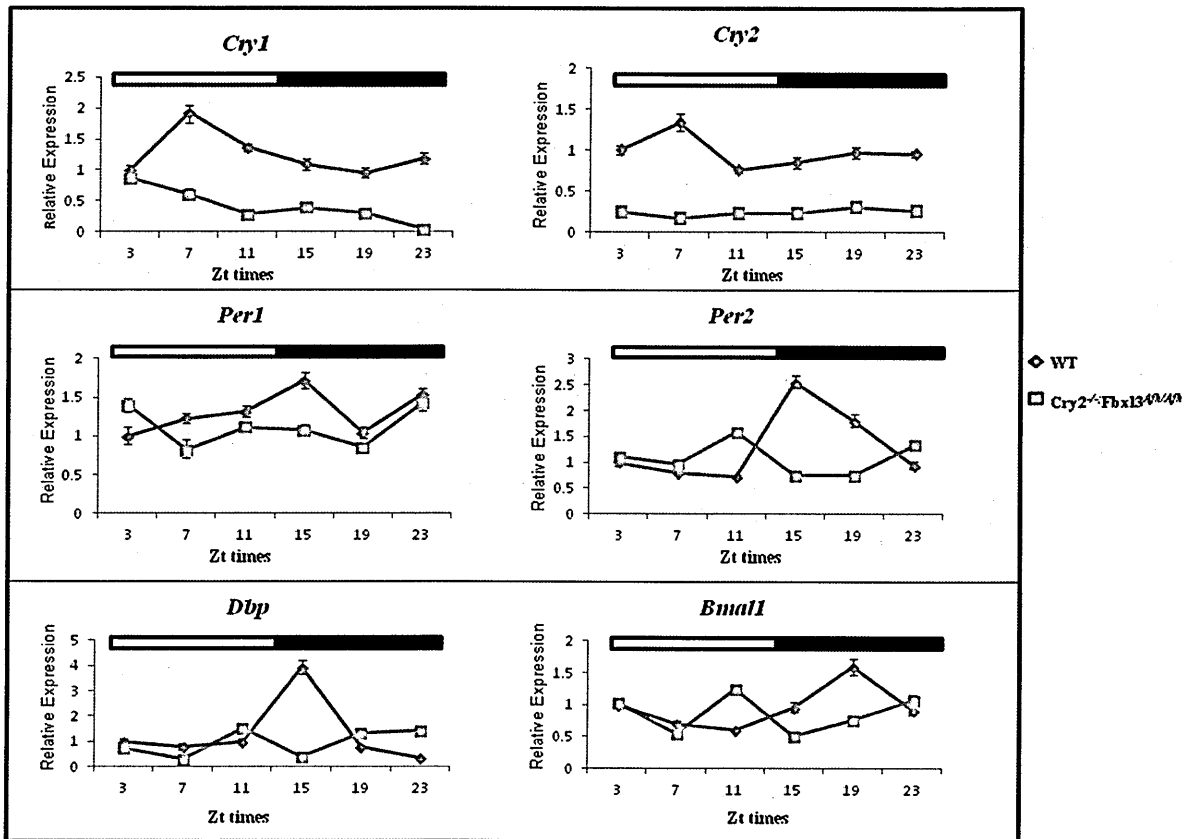
Figure 3.11: Gene expression studies in the cerebellum of Cry2^{-/-}; Fbxl3^{Afh/Afh} double mutants. To perform real-time quantitative PCR, cerebellum was dissected at various ZT times from Cry2^{-/-}; Fbxl3^{Afh/Afh} double mutants and wild-type controls. The expression at each time point was first calculated relative to the house-keeping gene, RPL13a, following which the expression of wild-type and mutant was made relative to expression of wild-type ZT 3. Each time point is an average of triplicate reactions, obtained from three independent samples. The SEMs are represented as error bars. The dampened levels of *Cry2* confirm the absence of the *Cry2* expression. *Cry1* levels in the double mutants are seen to be downregulated in the double mutants compared to *Cry1* expression levels in wild-type mice. The effect of CRY1 upregulation in these double mutants is clearly seen in the figure where expression levels of *Per1, Per2, Dbp* and *Bmal1* show a reduced amplitude with a phase shift in its expression, confirming the strong transcriptional repression ability of *Cry1*.
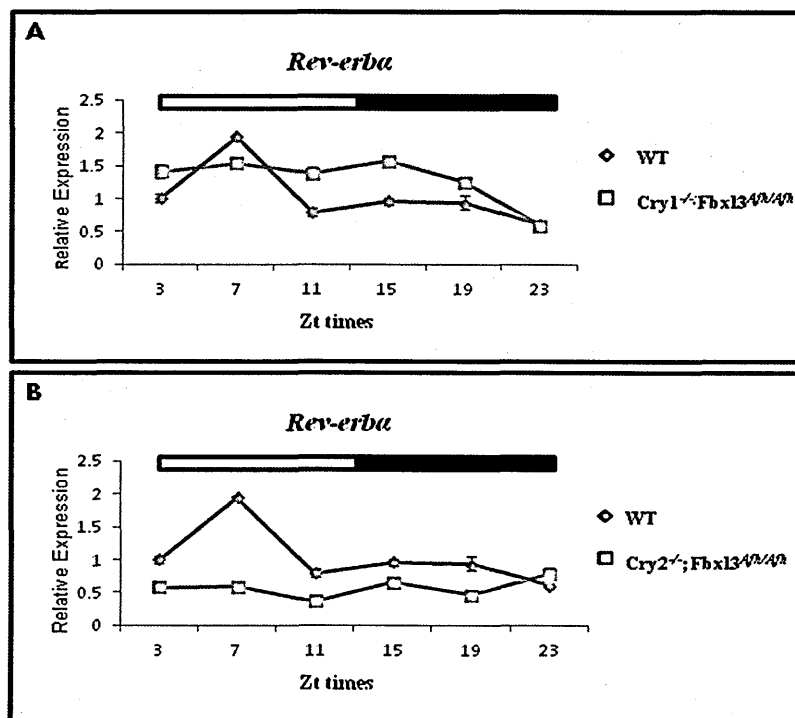
Figure 3.12: Gene expression of Rev-erba in Cry$^{-/-}$; Fbxl3$^{Afh/Afh}$ double mutants. To perform real-time quantitative PCR cerebellum dissected at various ZT times from Cry1$^{-/-}$; Fbxl3$^{Afh/Afh}$ and Cry2$^{-/-}$; Fbxl3$^{Afh/Afh}$ double mutants and wild-type controls. The expression at each time point was first calculated relative to the house-keeping gene, RPL13a, following which the expression of wild-type and mutant was made relative to expression of wild-type ZT 3. Each time point is an average of triplicate reactions, obtained from three independent samples. The SEMs are represented as error bars. A) *Rev-erba* levels in Cry1$^{-/-}$; Fbxl3$^{Afh/Afh}$ are seen to be upregulated compared to the wild-type *Rev-erba* levels. This is presumably due to the secondary effects of *Cry2* upregulation in these mutants. B) It is seen that in the absence of *Cry2*, with upregulated CRY1 levels in Cry2$^{-/-}$; Fbxl3$^{Afh/Afh}$ double mutants, there is a complete dampening of *Rev-erba* oscillations. This result again confirms the strong repressive action of *Cry1*. It is seen that *Cry1* has an ability to extend its repressive function to a component of the secondary regulatory loop as well.
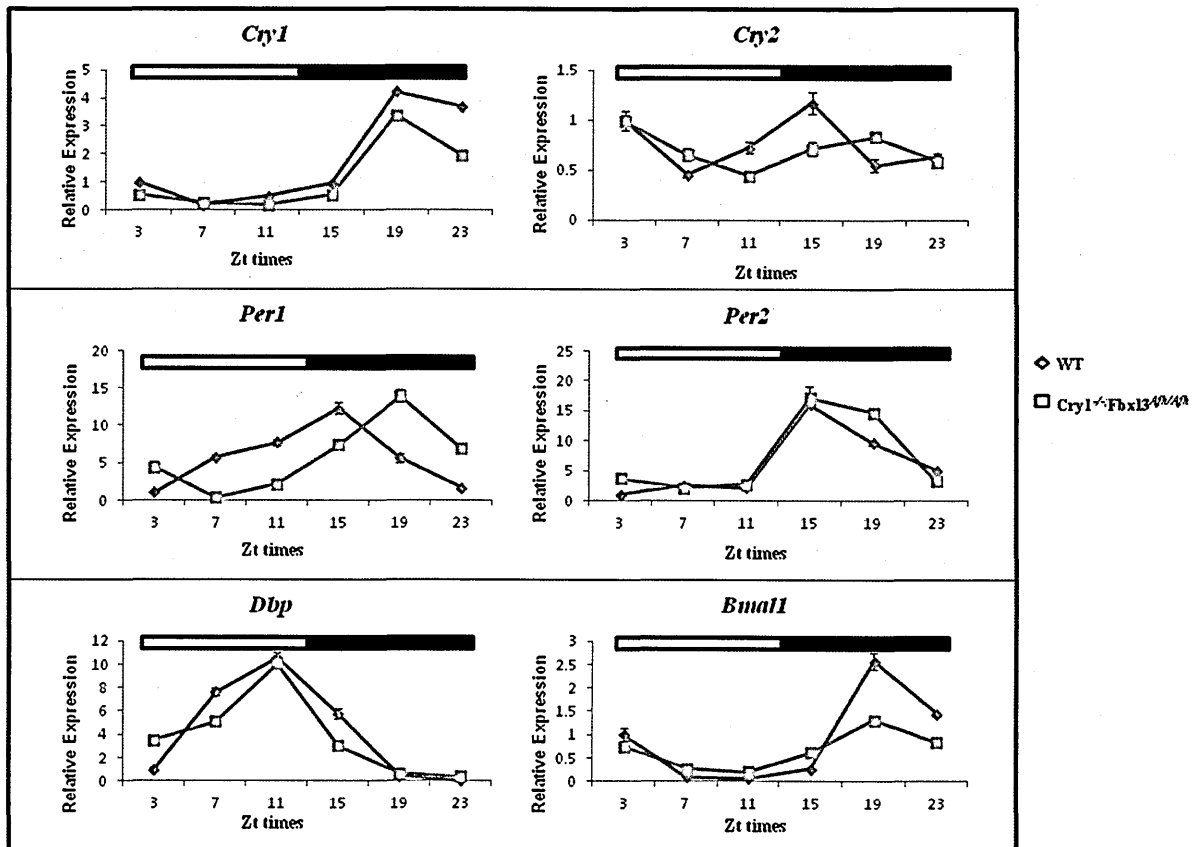
Figure 3.13: Gene expression studies in the liver of Cry1$^{-/-}$; Fbxl3$^{Afh/Afh}$ double mutants. To perform real-time quantitative PCR liver was dissected at various ZT times from Cry1$^{-/-}$; Fbxl3$^{Afh/Afh}$ double mutants and wild-type controls. The expression at each time point was first calculated relative to the house-keeping gene, RPL13a, following which the expression of wild-type and mutant was made relative to expression of wild-type ZT 3. Each time point is an average of triplicate reactions, obtained from three independent samples. The SEMs are represented as error bars. The above figure shows that overexpression of CRY2 has no effects on the expression of *Per2* and *Dbp* in the liver. While *Per1* show a phase shift in expression, *Bmal1* on the other hand oscillates with a reduced amplitude. The reason for the altered *Per1* and *Bmal1* expression is unknown. These results show that compared to the effects of *Cry2* regulation seen in the cerebellum, the expression of most clock genes remain unaltered, suggesting that the secondary effects of *Cry2* are tissue-specific.
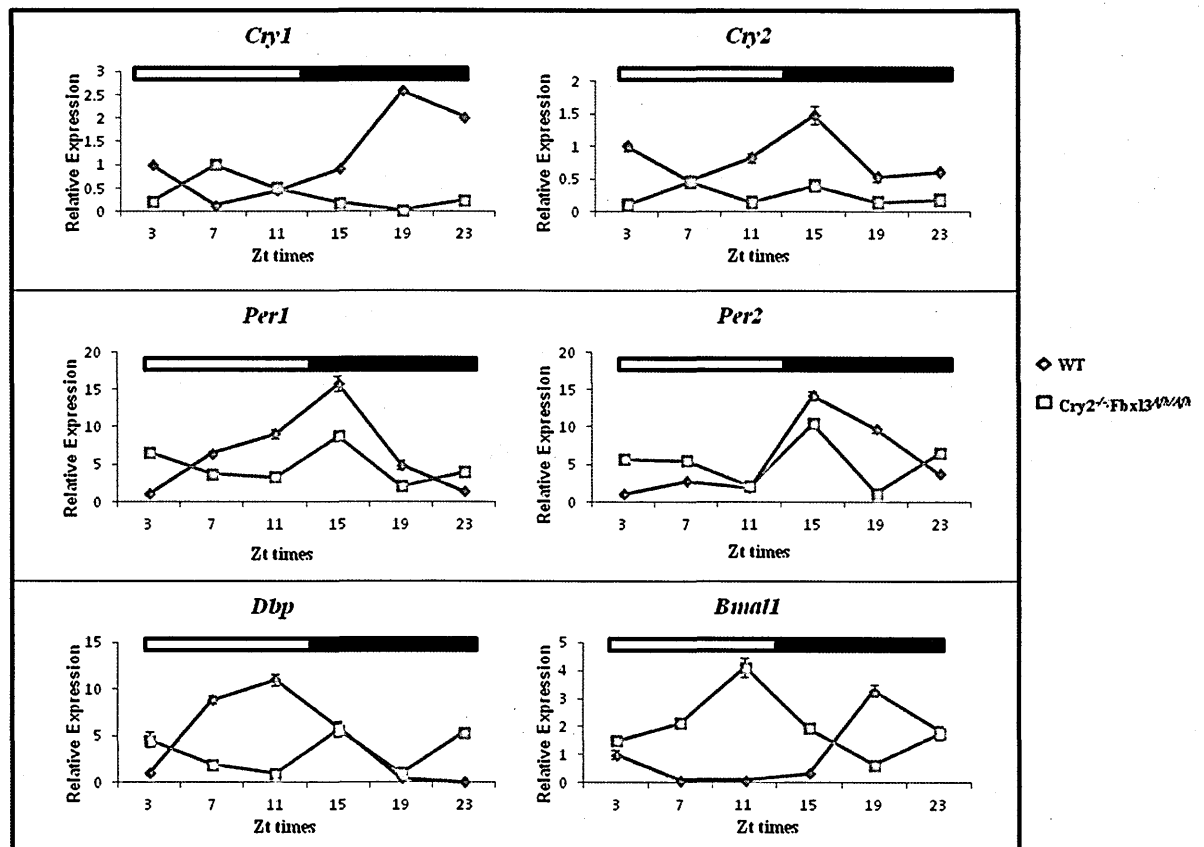
Figure 3.14: Gene expression studies in the liver of Cry2$^{-/-}$; Fbxl3$^{Afh/Afh}$ double mutants. To perform
real-time quantitative PCR liver was dissected at various ZT times from Cry2$^{-/-}$; Fbxl3$^{Afh/Afh}$ double mutants and
wild-type controls. The expression at each time point was first calculated relative to the house-keeping gene,
RPL13a, following which the expression of wild-type and mutant was made relative to expression of wild-type
ZT 3. Each time point is an average of triplicate reactions, obtained from three independent samples. The SEMs
are represented as error bars. The above figure shows that overexpression of CRY1 is able to alter the expression
of clock controlled genes in peripheral tissues as well. While the expression of *Cry1*, *Dbp* show a reduced
amplitude alongwith a phase shift, *Bmal1* show a phase shift, *Per1* and *Per2* only show a reduction in amplitude.
This again confirms that *Cry1* is not tissue-specific and is a stronger transcriptional repressor.

146

Figure 3.15: Investigating CRY2 protein expression in the cerebellum of Cry1$^{-/-}$; Fbxl3$^{Afh/Afh}$ double mutants. The levels of CRY2 proteins were determined in the cerebellum that was dissected at various ZT times from Cry1$^{-/-}$; Fbxl3$^{Afh/Afh}$ double mutants and wild-type controls. A) Proteins extracted from wild-type, Cry1$^{-/-}$; Fbxl3$^{Afh/Afh}$ double mutants were loaded on 3-12% Bis-Tris gels in equal amounts. The same amount of protein extracted from Cry2$^{-/-}$ cerebellum at ZT19 was loaded as the negative control. The proteins were then transferred onto a nitrocellulose membrane which was probed with the α-CRY2 and α-ACTIN antibodies. B) Quantified CRY2 protein levels were first normalised to the endogenous control β-actin. The normalised values were then plotted relative to CRY2 levels in the wild-type at ZT3. Each time point shown in the graph is an average of three independent samples. The SEMs are represented as error bars. The above figure shows that compared to the CRY2 levels in wild-type cerebellum, CRY2 levels are upregulated and stabilised across various ZT times in the Cry1$^{-/-}$;Fbxl3$^{Afh/Afh}$ double mutants, suggesting that the gene transcription effect seen may be due to the overexpression of CRY2 *in vivo*. The effect of the *Afh* mutation is also clearly seen with higher CRY2 protein levels during the subjective day compared to protein levels during subjective night A two-way ANOVA test reveals that the CRY2 levels in the mutants are significantly higher than the control levels and that the elevated protein levels are a result of the genotype (p =0.01)

Figure 3.16: Investigating CRY1 protein expression in the cerebellum of Cry2$^{-/-}$; Fbxl3$^{Afh/Afh}$ double mutants. The levels of CRY1 proteins were determined in the cerebellum that was dissected at various ZT times from Cry2$^{-/-}$; Fbxl3$^{Afh/Afh}$ double mutants and wild-type controls. A) Proteins extracted from wild-type, Cry2$^{-/-}$; Fbxl3$^{Afh/Afh}$ double mutants were loaded on 3-12% Bis-Tris gels in equal amounts. The same amount of protein extracted from Cry1$^{-/-}$ cerebellum at ZT 19 was loaded as the negative control, and 5µg of whole cell lysate containing Cry1-HA was loaded and used as a positive control. The proteins were then transferred onto a nitrocellulose membrane which was probed with the α-CRY1 and α-ACTIN antibodies. B) Quantified CRY1 protein levels were first normalised to the endogenous control β-actin. The normalised values were then plotted relative to CRY1 levels in the wild-type at ZT 3. Each time point shown in the graph is an average of three independent samples. The SEMs are represented as error bars. The above figure shows that compared to the CRY1 levels in wild-type cerebellum, CRY1 levels are significantly upregulated and stabilised across various ZT times in the Cry2$^{-/-}$;Fbxl3$^{Afh/Afh}$ double mutants, suggesting that the gene transcription effect seen may be due to the overexpression of CRY1 protein levels *in vivo*. The effect of the *Afh* mutation is also clearly seen with significantly higher CRY1 protein levels during the subjective day compared to protein levels during subjective night. A two-way ANOVA test reveals that upregulated CRY1 levels in the mutants are a result of the genotype (p =0.01).

3.2.3 Identification of a SNP in human *Fbxl3*

With similarities between the human and rodent circadian clocks, it is expected that mutations in the rodent clock gene might eventually lead to molecular insights into sleep or mood disorders in humans. This has been successfully shown previously by association of a mutation resulting in altered posttranslational modification of PER2 proteins with Familial Advanced Sleep Phase Syndrome (FASPS) (Toh, Jones et al. 2001). Hence, identifying polymorphisms in human clock genes still retains its importance as it may continue to improve human health. Considering that the *Afh* mutants in mice show elements of DSPS, human *Fbxl3* was sequenced to identify polymorphisms in the same. This resulted in the identification of a non-synonymous SNP only found in evening type individuals. The SNP was at position 1353 in exon 5 of the human *Fbxl3* resulting in a valine instead of glycine. Genotyping revealed that the individuals were heterozygous for the identified SNP and carry one copy of the wild-type *Fbxl3*. The equivalent of this SNP was G342V in mouse *Fbxl3*. Constructs using the mouse *Fbxl3* sequence with the appropriate mutated residue were used for further investigations mentioned later in this section. With the identification of this SNP, we tried to determine if this polymorphism could affect the rate of CRY protein degradation in humans.

For this reason, we first performed co-immunoprecipitation experiments to investigate the interaction between FBXL3-G342V and CRY1 and CRY2, the known substrates of FBXL3. The full length mouse *Fbxl3* sequence was first mutagenised with the desired nucleotide change in a manner described in section 2.13. *Cry1* or *Cry2*-HA plasmids were co-transfected with *Fbxl3*-Wt-GFP or *Fbxl3*-G342V-GFP plasmids into Cos7 cells using Fugene6 (section 2.4.6.1). The whole cell lysates were then subjected to co-immunoprecipitations in

the same way as described in section 2.11 of Chapter 2. Figure 3.17 A shows a representative western blot of the co-immunoprecipitation experiment. While Figure 3.17 B shows the interaction between FBXL3-G342V-GFP and CRY1/CRY2 when normalised to the interaction between FBXL3-Wt and CRY1/CRY2. The graph is plotted using the average obtained from three independent experiments. When normalised to FBXL3-Wt-interaction, it can be seen that, there was reduced interaction of G342V with either CRY1 or CRY2, but this was not significant (Figure 3.17 A, B)

In order to determine the effect of the *Fbxl3*-G342V mutation on the period length of mice, real time bioluminescence studies using stably transfected U2OS *Per2*:Luc cells were performed *in vitro*. Both the *Fbxl3*-Wt and *Fbxl3*-G342V plasmid were transfected into the stably transfected cells and their rhythms were monitored for a week using the LumiCycle. The period length was then analysed using the LumiCycle analysis software. No difference in the period length between *Fbxl3*-Wt and *Fbxl3*-G342V was seen *in-vitro* (Figure 3.18). The period length of *Fbxl3*-Wt and *Fbxl3*-G342V was obtained as an average±SEM of two independent experiments, each with two replicates. In U2OS *Per2*:Luc cells, while the period length of *Fbxl3*-Wt was 23.9hrs±0.045, *Fbxl3*-G342V showed a period length of 23.75hrs±0.102. The period difference between the wild-type and mutant was 0.15hrs and was non-significant (p=0.29). The difference in period was confirmed in Rat-1 *Per2*: Luc cell line, where *Fbxl3*-Wt had a period length of 22.33hrs±0.02 and *Fbxl3*-G342V had a period length of 22.25hrs±0.063. Due to the differences in cell lines, the *Fbxl3*-Wt period itself differs between the two cell lines.
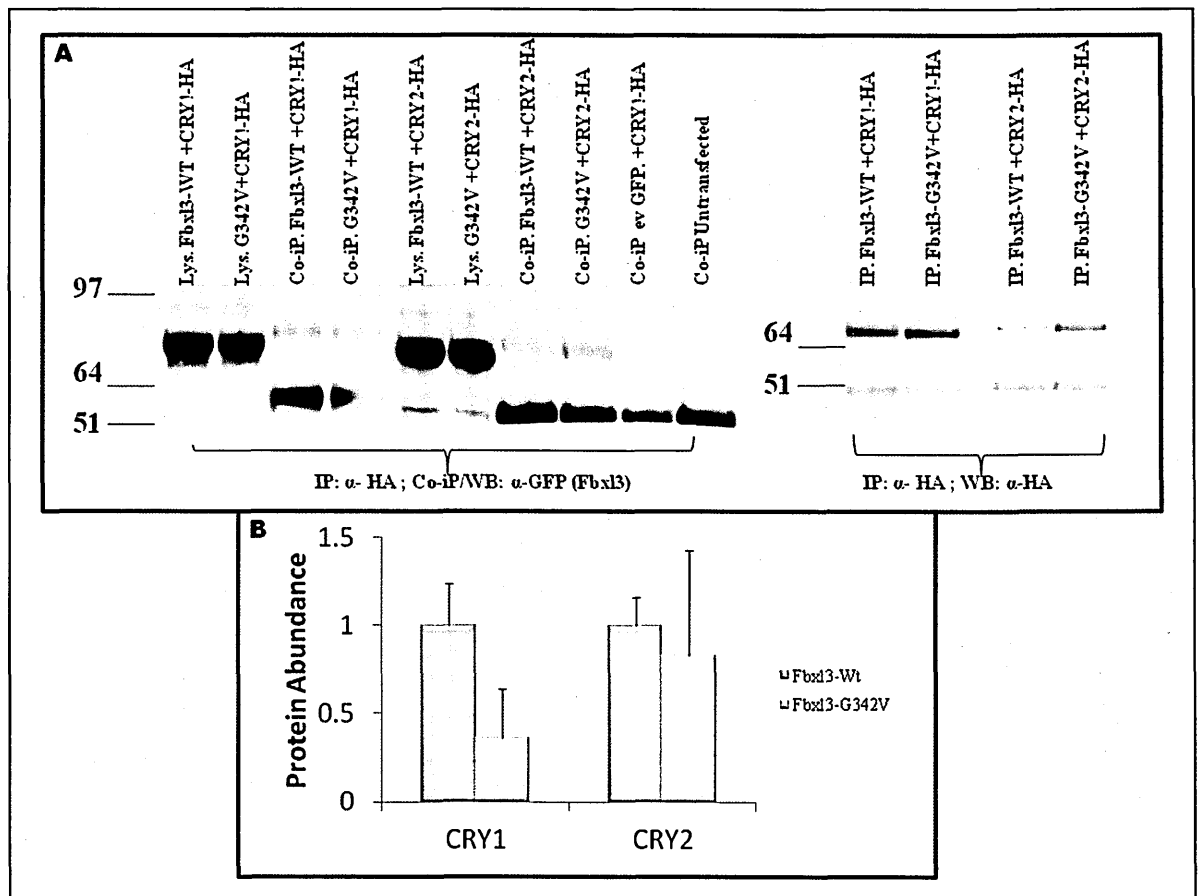
Figure 3.17: Investigating the interaction of **FBXL3-G342V** *and* **CRY1/CRY2** *in-vitro.* The *Fbxl3* SNP, G1353T identified in human *Fbxl3* was replicated in the mouse *Fbxl3* sequence (*Fbxl3*-G342V). The *Fbxl3*-Wt-GFP or *Fbxl3*-G342V-GFP plasmid was co-transfected with either *Cry1*-HA or *Cry2*-HA in Cos7 cells. Following transfection, whole cell protein lysates were collected and were subjected to a co-immunoprecipitation assay. A) shows a representative western blot. The figure shows the molecular weight marker on the left of each blot. Equal amounts (10μgs) of whole cell lysates (Lys.) from each transfection mixture was used as an input to show the presence of the *FBXL3*-Wt or G342V-GFP in the cells. Two negative controls were used for this experiment (last two lanes in the blot on left), one being an empty GFP vector (ev-GFP) co-transfected with *Cry1*-HA and the second control was untransfected whole cell lysates. Both the negative controls were processed in the same way as the experimental samples. The α-HA antibody was used to pull down CRY proteins (IP), while the α-GFP antibody was used to detect co-immunoprecipitated bands (Co-iP) showing the interaction between F-box proteins and CRY proteins. B) shows the amount of protein interaction normalised to FBXL3-Wt interaction levels. The quantified co-ip bands were first normalised to their respective IP bands, which is further normalised to the FBXL3-Wt interaction. Thus, the graph shown here represents the amount of FBXL3-G342V protein interaction with CRY1/CRY2 relative to the interaction by FBXL3-Wt. The results show no significant differences in the interaction between FBXL3-G342V and CRY1/CRY2 compared to the FBXL3-Wt interaction. The values used to plot the graph are means obtained from three independent experiments. The SEMs are represented as error bars on the graph. One-way ANOVA was used to determine statistical significance.

A — U2OS *Per2*: Luc cells

Period length: Fbxl3Wt = 23.9hrs+/-0.045; Fbxl3G342V=23.75hrs+/-0.102

B — Rat-1 *Per2*: Luc cells

Period length: Fbxl3Wt = 22.3hrs+/-0.02; Fbxl3G342V=22.25hrs+/-0.063
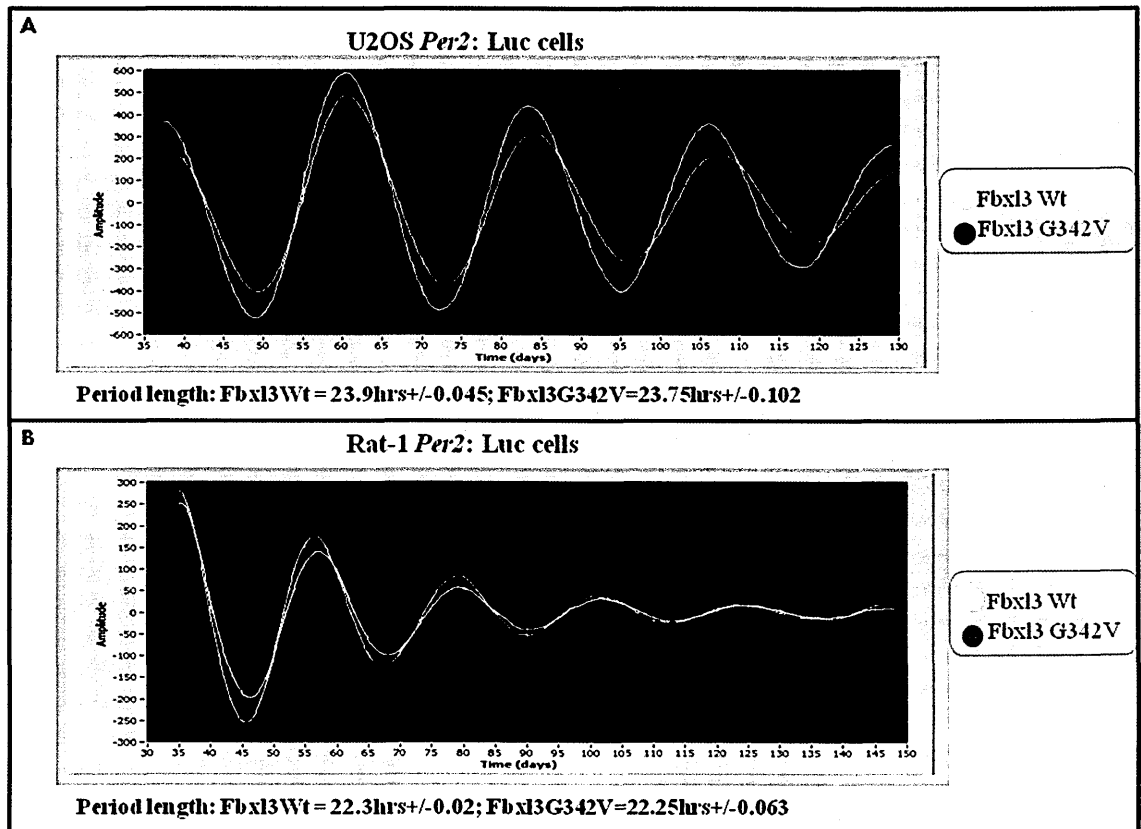
Figure 3.18: Determination of period length of Fbxl3-G342V in-vitro using the LumiCycle. The U2OS *Per2*:Luc cells and Rat-1 *Per2*:Luc fibroblasts were used for this purpose. In both the cell lines, the *Per2* promoter drives the expression of luciferase *in-vitro*. Hence with the addition of the substrate, the luminescence emitted is a read out of *Per2* oscillations *in-vitro*. The period length is then determined by the LumiCycle analysis software. The images shown here are representative of two independent experiments, each performed in duplicates. A) *Fbxl3*-Wt and *Fbxl3*-G342V plasmids were transfected into U2OS Per2:Luc cells. No significant period difference was observed in the U2OS *Per2*:Luc cell lines. While *Fbxl3*-Wt (yellow line) had a period length of 23.9hrs±0.045, the mutant *Fbxl3*-G342V (red line) had a period of 23.75hrs±0.102. B) The same experiment was carried out in Rat-1 *Per2*:Luc cell lines, where again no significant differences were identified. The *Fbxl3*-Wt (yellow line) and *Fbxl3*-G342V (red line) had a period length of 22.3hrs±0.02 and 22.25hrs±0.063 respectively.

3.3 DISCUSSION

3.3.1 *Fbxl3^{Afh}* mutation affects both cryptochromes

It has been known for a long time that the Skp/Cullin-1/F-box protein ubiquitin ligase complexes are involved in the timely degradation of clock controlled proteins. Specific F-box proteins constituting the SCF complex target specific substrates for degradation. For example, β-TRCP1 and β-TRCP2 are known to mediate the degradation of circadian regulators, period proteins, PER1 and PER2 (Ohsaki, Oishi et al. 2008). It was not until the identification of the *Fbxl3^{Afh}* mutation that specific F-box proteins targeting the important negative regulators CRY1 and CRY2 became known. A yeast two-hybrid screen initially identified FBXL3 as an interactor of Skp1, whereas later, immunoprecipitation studies combined with mass spectrometry led to the identification of FBXL3 as the ligase that targets CRY1 and CRY2 proteins for degradation (Busino, Bassermann et al. 2007; Godinho, Maywood et al. 2007). Gene and protein expression studies carried out in the SCN and liver of the *Afh* mutant revealed the suppression of *Cry1*, *Per1* and *Per2* oscillations. It also affected CRY1, PER1 and PER2 protein levels. Although the levels of the PER protein were low across circadian time, CRY1 protein levels were relatively high during the day and remained stable across time as compared to the CRY1 levels found in wild-type liver. In order to identify if the *Fbxl3^{Afh}* mutation effects both CRY1/2 proteins in a similar fashion we decided to selectively stabilise CRY1 or CRY2 by generating *Cry1^{-/-}; Fbxl3^{Afh/Afh}* and *Cry2^{-/-}; Fbxl3^{Afh/Afh}* compound mutants.

In vivo rhythms of mutants are determined by measuring their locomotor activity using running wheels. The animals are screened using a protocol involving an initial 12hr L:D schedule for seven days, followed by free-running conditions in DD and LL for 2 weeks each,

where there is no external cue given to the mice. The results are discussed in detail later in this section. For convenience, the discussion of the wheel running activity is split according to activity in the three phases LD, DD and LL.

One of the striking differences observed during our wheel running screens was evident in the activity of the compound mutants in the LD and LL schedule. In the LD schedule, there was no overt phenotype observed in the $Cry1^{-/-}$; $Fbxl3^{Afh/Afh}$ compound mutants as compared to wild-type mice. On the other hand, $Cry2^{-/-}$; $Fbxl3^{Afh/Afh}$ mice do not seem to entrain and were found to be free running in the LD schedule. This was observed in every $Cry2^{-/-}$; $Fbxl3^{Afh/Afh}$ mutant screened (n=10). Due to the free running nature of the $Cry2^{-/-}$; $Fbxl3^{Afh/Afh}$ mice in LD, it was expected that these animals would have less nocturnal activity and indeed a 20% reduction of nocturnal activity was observed in these mice compared to wild-type mice (Table 3.3). Loss of entrainment usually signifies defects in the photic input pathway that provide the SCN with the external cue via the retinohypothalamic tract (RHT). The defect can result into two possibilities, one being inability to entrain and second being that the period of these mutants is so long that they are unable to entrain, although the latter is unlikely as *Clock/Clock* homozygous mice which have a long period of 27.36hrs were able to entrain normally to the L:D cycle (Antoch, Song et al. 1997). With the majority of circadian mutants displaying deviations in period length either in DD or LL conditions, a loss of entrainment phenotype in circadian mutants is quite rare. To date there are only two examples of mice which do not entrain to the 12 L:D cycle; one being the $Math5^{-/-}$ knockout mice and the second is a spontaneous mutation identified in the Calfornia mouse, *Peromyscus californicus*. *Math5*, exclusively expressed in developing retinal ganglion cells, is known to be critical in cell differentiation of these cells. Due to the loss of *Math5*, 80% of the retinal ganglion cells are not developed. The development of cells containing melanopsin is also attenuated. These

conditions result in mice being unable to entrain even if they are kept in LD conditions for 50 days (Wee, Castrucci et al. 2002). The *Peromyscus* mice on the other hand, show robust and high amplitude rhythms under DD conditions. However, they completely fail to entrain to the 12hr L:D cycle. With no alterations in visual system, they responded to the visual stimuli and also had normal constriction of pupils in response to illumination. It was therefore suggested that these mice were unable to modulate the response of light and were only able to partially entrain to the 12hr L:D schedule (de Groot and Rusak 2002).

Wheel running activity of $Cry^{-/-}$; $Fbxl3^{Afh/Afh}$ compound mutants in DD as shown in Figure 3.1 and 3.4 reveals that the $Fbxl3^{Afh}$ mutation has a dominant effect on the clock, lengthening the period of every animal with the *Afh* mutation in the F-box protein, *Fbxl3*. Thus, in an animal with a clock that is *Cry2*-driven and carries the *Afh* mutation ($Cry1^{-/-}$; $Fbxl3^{Afh/Afh}$ mutants), period lengthening is observed. The same effect is seen in mice with a clock which is purely driven by $Cry1$ in $Cry2^{-/-}$; $Fbxl3^{Afh/Afh}$ double mutants. However in the *Afh* mutant mice, it has been shown that there is a reduced interaction between FBXL3 and CRY proteins, as a result of which CRY proteins are spared from proteasomal degradation. Therefore CRY protein levels that rise during the subjective night remain at high levels even during the subjective day resulting in a delay of transcriptional activation. If this mechanism was believed to be true in our $Cry^{-/-}$; $Fbxl3^{Afh/Afh}$, then both the mutants should have had a similar period lengthening phenotype. However, while the period length in DD increases only by 1.3hrs in $Cry1^{-/-}$; $Fbxl3^{Afh/Afh}$ double mutants (τ_{DD}=24.19hrs±0.162) compared to the $Cry1^{-/-}$ mice (τ_{DD}= 22.89hrs±0.07), the period length of $Cry2^{-/-}$; $Fbxl3^{Afh/Afh}$ double mutants (τ_{DD}=27.83hrs±0.310) shows a significant increase of 3.59 hours compared to the $Cry2^{-/-}$ mice (τ_{DD}=24.24hrs±0.084) (Figure 3.7 A,B). This suggests that stabilisation of either CRY proteins causes a period lengthening presumably due to the extended transcriptional repression

because of the *Afh* mutation (Godinho, Maywood et al. 2007). But the ability of both the CRY's to repress transcription seems to be different.

Considering the *Afh/+* and *Afh/Afh* background under DD conditions, removal of *Cry1* significantly accelerates the clock (Figure 3.2), whereas removal of *Cry2* delays the clock (Figure 3.5). This effect is only significant in the *Cry1^{-/-}* or *Cry2^{-/-}* background and not in *Cry1^{+/-}* or *Cry2^{+/-}* background which is consistent with the finding that animals heterozygous for either *Cry1* or *Cry2* and carry wild type *Fbxl3* do not show any change in period length and are similar to the wild-type mice (van der Horst, Muijtjens et al. 1999). Parallel studies were carried out in cultures from the SCN collected from each of the combination of the *Cry^{-/-}* ; *Fbxl3^{Afh/Afh}* compound mutants. The SCN cultures also showed a similar trend of period lengthening which correlated well with the *in vivo* wheel running behaviour (Appendix 4, 5). Consolidation of these results leads to a paradoxical situation; compared to mice that are homozygous for *Cry2* and wild-type for *Fbxl3^{+/+}* (*Cry2^{-/-}* ; *Fbxl3^{+/+}*) that have a long phenotype with a slower clock, the *Cry1^{-/-}* ; *Fbxl3^{Afh/Afh}* double mutants where *Cry1* is absent and there is stabilisation of CRY2 (due to the *Afh* mutation) also slows the clock resulting in an increased τ_{DD}. Hence, it is intriguing to find out why absence of CRY2 protein in *Cry2^{-/-}* mice lengthens the clock, while upregulated and stabilised levels of CRY2 in *Cry1^{-/-}* ;*Fbxl3^{Afh/Afh}* double mutants (due to spared proteasomal degradation in the presence of the *Afh* mutation) also lengthens the clock. A possible explanation for this could be attributed to the time of CRY2 protein expression. In a normal circadian cycle, clock proteins reach their peak during the night and nadir during the day. However, in *Cry2^{-/-}* mice there is no peak of CRY2 protein at night time, whereas in the *Cry1^{-/-}*; *Fbxl3^{Afh/Afh}* mice, there is less CRY2 proteins during the night and these remain at a higher level even during the daytime. This suggests that, the higher CRY2 levels during the day may have an effect on clock mechanisms resulting in a

period lengthening phenotype in both absence of CRY2 ($Cry2^{-/-}$) and upregulated levels of CRY2 ($Cry1^{-/-};Fbxl3^{Afh/Afh}$). This finding being specific to $Cry2$, suggests that the functioning of the clock is predominantly dependent on $Cry1$. This is consistent with findings in $Cry1^{-/-}$; $Cry2^{-/-}$ double mutants (van der Horst, Muijtjens et al. 1999). With no difference observed in the period length between the single Cry heterozygous animals ($Cry1^{+/-}$ and $Cry2^{+/-}$) and double heterozygous animals $Cry1^{+/-}$; $Cry2^{+/-}$ compared to wild-type mice, it was surprising to find compound mutants that carried only one $Cry2$ allele ($Cry1^{-/-}$; $Cry2^{+/-}$) displayed a period length that was shorter (τ_{DD} =21.77hrs) than the single $Cry1$ knockout mice ($Cry1^{-/-}$ τ_{DD} = 22.51hrs) in DD conditions. However, this phenotype persisted only for the initial few days, after which mice were arrhythmic. This was in contrast to compound mutants which carried only one $Cry1$ allele. In these animals ($Cry1^{+/-};Cry2^{-/-}$) an intermediate period between the $Cry1^{-/-}$ and $Cry2^{-/-}$ single knockout mice was observed. This possibly depends on the presence or absence of $Cry1$ and suggests that $Cry1$ is important for the proper functioning of the clock (van der Horst, Muijtjens et al. 1999). This in return leads us to think that it is presumably due to the presence of other interacting factors that confer different functions to $Cry2$ or regulate $Cry2$ differently. However, to investigate the roles of $Cry1$ and $Cry2$ and to dissect their individual functions gene and protein expression profiles have to be determined in the compound mutants. This is described in section 3.2.3 and 3.2.4.

Activity screens of the compound mutants in LL result in variable phenotypes, from a clear phase shift or splitting of activity in animals with an $Fbxl3^{Afh/+}$ background, to very weak rhythms or arrhythmicity as observed in $Cry2^{-/-}$; $Fbxl3^{Afh/Afh}$. Phase delays in mice are known to be associated with the expression of the clock controlled PER2 levels. It has been shown that under constant light conditions in wild-type mice, there is no degeneration of PER2 resulting in constitutive and elevated levels of PER2, thus contributing to the phase delay

(Munoz, Peirson et al. 2005). This has been proved in the $Per2^{Brdm1}$ mutant mice (a targeted *Per2* mutant), where in the absence of PER2 there is no phase delay and hence the mutant mice show a shortened endogenous period under LL conditions (Steinlechner, Jacobmeier et al. 2002). Hence, it would be interesting to investigate the expression of PER2 in the $Cry2^{-/-}$; $Fbxl3^{Afh/Afh}$ to determine if arrhythmicity observed in our double mutants is associated with PER2 protein levels. Although the effects of LL are not very dramatic in $Cry1^{-/-}$; $Fbxl3^{Afh/Afh}$ mice, huge variability is observed amongst the $Cry2^{-/-}$; $Fbxl3^{Afh/Afh}$ compound mutants, where a complete loss of synchronisation to the LD cycle and arrhythmicity in LL is observed in the $Cry2^{-/-}$; $Fbxl3^{Afh/Afh}$ double mutants and $Cry2^{+/-}$; $Fbxl3^{Afh/Afh}$ and splitting of activity in LL is observed in $Cry2^{-/-}$; $Fbxl3^{Afh/+}$. Although *Cry2* was initially considered as a photoreceptor on the basis of its homologue function in *Drosophila*, the function of mammalian *Cry* as photoreceptors has been a debate for a long time and is far from proven. *Cry2* is expressed in most tissues, however, it is expressed at the highest level in the ganglion cell layer and inner nuclear layer of the retina. In the retinal ganglion cells there are distinct subsets of cells, the ipRGCs, that project to the SCN *via* the RHT and are known to play an important role in photic entrainment and may have a role as photoreceptors (Lowrey and Takahashi 2000). It may therefore be that *Cry2* is involved in the light induced regulatory pathway in the ipRGCs. Based on previous reports in $Cry2^{-/-}$ mice that show a reduced sensitivity in the photoinduction of genes (Thresher, Vitaterna et al. 1998; Sancar 2004), it could be that the loss of *Cry2* and the subsequent reduction in the photoinduction of genes is presumably one of the reasons that $Cry2^{-/-}$; $Fbxl3^{Afh/Afh}$ double mutants free run in LD. However this needs to be investigated. Compared to wild-type mice, the $Cry2^{-/-}$ single knockout mice that we screened themselves showed variability in LL. The period length τ_{LL} 25.96 hrs±0.24 of $Cry2^{-/-}$ mice is an average of 10 animals, of which some had an extremely weak rhythm, and some animals did not show

any lengthening in LL. With the variability observed in $Cry2^{-/-}$ mice it is difficult to predict if the phenotype of the $Cry2^{-/-}$; $Fbxl3^{Afh/Afh}$ double mutants is due to the loss of $Cry2$ in $Cry2^{-/-}$; $Fbxl3^{Afh/Afh}$ double homozygous mice or due to the presence of the Afh/Afh mutation. The $Fbxl3^{Afh}$ results in stabilisation of CRY1 and CRY2 and the variability observed in the $Cry2^{-/-}$ mutants might be the cause of the arrhythmic behaviour observed in the $Fbxl3^{Afh/Afh}$ mice. Additionally, while the $Cry2^{+/-};Fbxl3^{Afh/+}$ show rhythmicity in LL, the loss of sustained rhythms in $Cry2^{+/-}$; $Fbxl3^{Afh/Afh}$ reveals the importance of the presence of $Cry2$ for maintaining a functional clock in LL. Similar results have also been observed in other mutants such as short circuit (Sci), an ENU mutant, which when crossed to $Cry2^{-/-}$ mice ($Sci^{+/-}$; $Cry2^{-/-}$), shows a phase advance in activity under LD conditions and shows no period lengthening in LL (data not shown, personal communication with Jessica K. Edwards). A second mutant identified using ENU mutagenesis, results in truncation of FBXL3, with 46 amino acids missing from the C-terminal end. Preliminary studies carried out on this mutant have shown it to have a loss of entrainment phenotype in LD, similar to the $Cry2^{-/-}$; $Fbxl3^{Afh/Afh}$ mice. While the heterozygous animals show an extreme lengthening in LL (difference between τLL and τDD is > 2.74hrs), the homozygous animals with truncated $Fbxl3$ are arrhythmic. *In-vitro* interaction studies in this mutant reveal a significant reduction in both CRY1 and CRY2 interaction (data not shown, personal communication with Christine Damrau). All these results together suggest the importance of $Cry2$ that may possibly have a role in photoreception in mice. Nevertheless, gene expression studies need to be carried out in these mice housed under LL conditions.

3.3.2 *Cry1* is a stronger transcriptional repressor

One of the aims of this thesis is to dissect the individual function of the *Cry* paralogues, *Cry1* and *Cry2* using the *Afh* mutant, the knockouts of which have opposing phenotypes. The *Fbxl3*^{Afh} mutation was seen to affect both the negative regulators of the mammalian circadian loop, *Cry1* and *Cry2*. Although both the cryptochromes are affected in the same way as seen by an increase in the period length in DD conditions, this does not help us dissect the functions of the *Cry* paralogues. It is for this reason we carried out real time gene expression studies at the RNA and protein level in the cerebellum of the *Cry*$^{-/-}$; *Fbxl3*$^{Afh/Afh}$ double mutants. Our results show that, in the absence of *Cry1* (in a *Cry2*-driven clock), there is no dramatic change in expression of the clock controlled genes, except for the repression of *Per2* which presumably leads to a phase shift in the expression of *Dbp*. The expression of *Rev-erba* is also upregulated in these mutants presumably due to secondary effects of CRY2 upregulation discussed later in this section. While on the other hand, in the absence of *Cry2*, in a *Cry1* driven clock, there is transcriptional repression of the clock controlled genes. At the protein level we would expect stabilisation of the alternative CRY proteins in *Cry1*$^{-/-}$; *Fbxl3*$^{Afh/Afh}$ and *Cry2*$^{-/-}$; *Fbxl3*$^{Afh/Afh}$ mutants, as a result of the *Afh* mutation. Thus, with stabilisation of either CRY1 or CRY2 proteins we would expect transcriptional repression of clock genes (resulting in a long period, as observed). Although we find that in *Cry*$^{-/-}$; *Fbxl3*$^{Afh/Afh}$ mutants there is an upregulation of the CRY proteins, with a significant effect of the genotype (*Cry1*$^{-/-}$; *Fbxl3*$^{Afh/Afh}$: p=0.015 and *Cry2*$^{-/-}$; *Fbxl3*$^{Afh/Afh}$; p=0.05) both the *Cry1* and *Cry2* do not repress transcription of genes to the same degree. This suggests that in addition to the stabilisation of CRY proteins, some other unknown factors (maybe the presence of secondary effects of other clock genes) also contribute to the transcriptional

repressor functions of *Cry* genes. One of major differences between *Cry1* and *Cry2* could be attributed to their sequence itself. Although CRY1 and CRY2 show 80% sequence homology amongst each other, their differences lie in their unique C-terminal sequences. Alignment of CRY protein sequences show no similarity whatsoever in the C-terminal tails. Therefore, it could be that the amino acids that constitute the C-terminus of the two CRY proteins may confer specific roles to CRY proteins. An interesting observation made in the *Cry1$^{-/-}$; Fbxl3$^{Afh/Afh}$* mutants is the complete down regulation of *Per2* transcription coupled with the upregulation of *Rev-erbα*. There are two points of discussion providing a possible explanation for the observed result. One is the interaction between *Cry2* and *Per2*, and the second is the interaction between *Per2* and *Rev-erbα*.

The result obtained with the upregulation of *Cry2* coupled with the downregulation of *Per2* is consistent with previous *in vivo* report by Oster, Yasui et al. (2002) where they have shown that the inactivation of *Cry2* is able to restore circadian rhythmicity in the *Per2^{Brdm1}* mutant mice (*Per2^{Brdm1}* mutants loose rhythmicity after a few days in DD). They show that in *Per2^{Brdm1};Cry1$^{-/-}$* mutants (*Cry2* present), the mice are instantly arrhythmic once under DD conditions, while under the same conditions, *Per2^{Brdm1};Cry2$^{-/-}$* mutants are rhythmic and have a period of 23.4hrs. Gene expression studies carried out under LD conditions in the *Per2^{Brdm1}; Cry2$^{-/-}$* mutants show the amplitude and expression of *Per1, Cry1* and *Bmal1* are similar to expression found in wild-type mice. This supports the fact that with the inactivation of *Cry2*, in the *Per2^{Brdm1}* mice, circadian rhythmicity can be restored. These results suggest that *Cry2* could act as a suppressor of *Per2 in vivo* (Oster, Yasui et al. 2002). This is in agreement with our gene expression studies performed in the *Cry1$^{-/-}$; Fbxl3$^{Afh/Afh}$* mice. However, the reason for this interaction between *Cry2* and *Per2* is unknown and is yet to be investigated.

Further, in the $Cry1^{-/-}$; $Fbxl3^{Afh/Afh}$ mutants, except for the repression of *Per2* (presumably due to the high expression of *Cry2*), all other genes including *Bmal1* are rhythmically expressed. This is in contrast to the gene expression observed in the $Per2^{Brdm1}$; $Cry1^{-/-}$ mice, where there is a loss of rhythmicity in the expression of clock genes, suggesting that *Cry1* and *Per2* are the important components of the clock and are essential to maintain rhythmicity *in-vivo* (Oster, Yasui et al. 2002).

As *Cry1* is considered to be a global repressor of genes belonging to the core and the secondary loop, it may be that the *Per2* repressive functions are confined to genes belonging to the secondary loop viz. *Rev-erbα*. It is already known that *Rev-erbα* is activated by the CLOCK-BMAL1 heterodimer, and is involved in feedback repression by inhibiting the activity of *Bmal1* (Preitner, Damiola et al. 2002, Oishi, Fukui et al. 2000; Shearman, Sriram et al. 2000; Preitner, Damiola et al. 2002; Reppert and Weaver 2002; Ueda, Chen et al. 2002; Ko and Takahashi 2006). However, recently it was shown that apart from *Cry1*, *Per2* is also able to interact with and repress *Rev-erbα in-vitro*. This is evident from the fact that when *Per2* mRNA is at peak levels, *Rev-erbα* mRNA is at low levels and vice-versa (Schmutz, Ripperger et al.). This was also confirmed *in-vivo* using the $Per1^{Brdm1}$; $Per2^{Brdm1}$ and $Cry1^{-/-}$; $Cry2^{-/-}$ double mutants, where the absence of *Per2* and *Cry1* resulted in elevated *Rev-erbα* levels. Thus it can be concluded that the gene expression profiles we see in the $Cry1^{-/-}$; $Fbxl3^{Afh/Afh}$ mice are a result of two dependent interactions. One is the interaction between *Per2* and *Cry2* and the second is the interaction between *Per2* and *Rev-erbα*. Thus upregulation of *Cry2* results in repression of *Per2* as a result of which, *Rev-erbα* is spared from repression. This in turn leads to suppression of *Bmal1* finally delaying the activation of *Per* and *Cry* genes and hence we see period lengthening. This interaction together with the effect of the *Afh* mutation, results in the $Cry1^{-/-}$; $Fbxl3^{Afh/Afh}$ phenotype.

Secondly, with *Per2* repression being specific to the cerebellum of *Cry1*$^{-/-}$*;Fbxl3*$^{Afh/Afh}$ mice, it is thought that the above interactions are tissue-specific. This is supported by the fact that in peripheral tissues such as liver, there are other nuclear receptors like PPARα which may take over the function of *Rev-erbα* (Schmutz, Ripperger et al. 2010). However, it is possible that PPARα is not able to inhibit clock components and hence, we see no repression of clock genes in *Cry1*$^{-/-}$*; Fbxl3*$^{Afh/Afh}$ liver.

3.3.3 A SNP in human *Fbxl3* shows no effects

To investigate the SNP G1353T identified in human *Fbxl3*, we first introduced the mutation in mouse *Fbxl3* (*Fbxl3*-G342V) and carried out co-immunoprecipitation between FBXL3 and its known substrates CRY1 and CRY2 following which bioluminescence studies were performed *in-vitro*. With no differences observed between the interactions of FBXL3-Wt and CRY1/CRY2 and FBXL3-G342V and CRY1/CRY2, we expected no circadian phenotype. This was further confirmed *in-vitro* in the LumiCycle studies which showed no obvious phenotype from the mutation. If the interaction between FBXL3-G342V and CRY1 is indeed compromised, high levels of transcription inhibitor CRY1 would be present resulting in a slower clock and hence a longer period, similar to the phenotype observed in mice (Busino, Bassermann et al. 2007; Godinho, Maywood et al. 2007; Siepka, Yoo et al. 2007).

Though the functions of most clock controlled genes have been characterised in mammals, the assumed functions of these genes in generating the molecular rhythms are hypothetical in humans as genes are identified on the basis of sequence similarities and there is no experimental set up to prove the hypothesis. Hence, phenotypes observed by association studies do not take into account the effect of two or more genes and are merely single gene

effects. This may be the reason that replicating associations that are already known proves difficult. Chronotype itself is a polygenetic trait influenced by factors other than the core clock components. In addition, they are influenced by combined effects of the genes that are included in the input, oscillator and output pathways (Pedrazzoli, Secolin et al.; Allebrandt and Roenneberg 2008). Thus, with variations within human subjects, the determination of the exact role of one gene based on the effect of one specific SNP identified is very difficult. It can be hypothesized that effects seen in *Fbxl3*-G1353T can be a result of subtle protein alterations. This could result in alteration of interaction rates of proteins, affecting their dimerisation and in turn altering circadian regulations, finally resulting in a different chronotype. In addition, there is a possibility of alterations present in the promoter regions of *Fbxl3* resulting in differences in phase relationship of the clock and hence differences in the daily rhythms. There have also been several reports where novel non-synonymous changes identified have had alterations in the protein structure and functions, but have been identified only in a single individual, indicating that disruptions may be due to familial inheritance (Hawkins, Meyers et al. 2008). Since the *Fbxl3* SNP, G1353T, was identified only in 20% of the individuals belonging to the eveningness and extreme eveningness category, the chronotype obtained could be a possible consequence of familial inheritance. This would have to be determined only by sequencing DNA for the particular individuals belonging to one family. Thus, combined effects of inheritance along with unknown variations in the non coding promoter regions could be the basis of the observed G1353T chronotype.

Finally, disruptions of circadian oscillations and sleep homeostasis are characterised to be a part of central nervous system disorders. Examples of SNP's in clock genes such as *Per1*, *Bmal1* and *Clock* are known to be associated with autistic disorders (Nicholas, Rudrasingham et al. 2007), bipolar disorders (Nievergelt, Kripke et al. 2006) and impaired cognitive

performance (Benedetti, Radaelli et al. 2008) respectively. However, it is thought that rather than affecting circadian rhythms directly, a SNP may have a secondary effect on behaviour and may be associated with anxiety, or depression due to the uncoupling of neuronal circuitry (Albrecht). Similarly, the G1353T SNP could also be associated with behavioural disorders causing an alteration in the circadian clockwork.

3.4 SUMMARY

While the main aim of the chapter was to identify the effects of $Fbxl3^{Afh}$ mutation, in the course of these studies, we have also obtained some other interesting findings. We have successfully shown that the $Fbxl3^{Afh/Afh}$ mutation affects both $Cry1^{-/-}$ and $Cry2^{-/-}$ in vivo, by increasing the period length under DD and LL conditions. This has been confirmed in parallel studies carried out in the SCN slices obtained from the $Cry^{-/-}$; $Fbxl3^{Afh/Afh}$ compound mutants.

An observation made during the wheel running recording was in $Cry2^{-/-}$; $Fbxl3^{Afh/Afh}$ double mutants, which show a lack of entrainment in the LD phase of the circadian screen. At the RNA level, it was seen that both $Cry1$ and $Cry2$ act as transcriptional repressors, however the effects of $Cry1$ overexpression in the $Cry2^{-/-}$; $Fbxl3^{Afh/Afh}$ mice are much stronger than the overexpression of $Cry2$ in the $Cry1^{-/-}$; $Fbxl3^{Afh/Afh}$ mice. While $Cry1$ is able to repress the expression of most clock genes in the cerebellum as well as in the liver, the ability of $Cry2$ to repress transcription lies mainly in the cerebellum and it is seen to be $Per2$-specific. Furthermore its ability to repress $Per2$ in the liver is lost. Although the suppression of $Per2$ in the cerebellum of $Cry1^{-/-}$; $Fbxl3^{Afh/Afh}$ mice could be attributed to the interaction between $Per2$, Rev-$erb\alpha$ and $Bmal1$, it is possible that nuclear receptors such as PPARα, which is liver specific, do not alter the interactions between clock components.

Although the $Fbxl3^{Afh/Afh}$ mutation is known to stabilise its substrates CRY1 and CRY2 *in vivo* resulting in an extended transcriptional repression and longer period, it could be that in the $Cry1^{-/-}$; $Fbxl3^{Afh/Afh}$ double mutants, the secondary effects of *Cry2* upregulation also contribute to the period lengthening.

Along with these studies, a SNP G1353T, previously identified in the human sequence of *Fbxl3* was seen to have an association with extreme eveningness. It was interesting for us to determine if this human polymorphism in *Fbxl3* had the same effects as the $Fbxl3^{Afh/Afh}$ mutation. We performed all the experiments by replicating the polymorphism in the mouse *Fbxl3* sequence and obtained a $Fbxl3^{G342V}$ plasmid. There was no evidence of a significantly reduced interaction of $Fbxl3^{G342V}$ with CRY1 and CRY2 *in-vitro* and there were no significant differences in the period length. Hence we would assume that the association with extreme eveningness would depend on factors such as gene-environment interactions. In addition, it could also be that rather than having a direct effect on circadian regulation, the SNP may be associated with behavioural disorders indirectly altering circadian rhythms. However, taking into consideration these results, the effects of the polymorphism cannot be concluded as yet.

Finally, we are able to refine the importance of F-box proteins and their role in the regulation of the circadian protein levels.

4 <u>CHAPTER FOUR</u>: Characterisation of Mutants in Novel F-box Proteins

4.1 INTRODUCTION

One of the fundamental goals of biological research is to identify the underlying mechanisms of complex behaviour, which is accomplished by determining the physiological function of the translated proteins. With innovations made in techniques such as sequencing and mapping, a large number of genes that might play a role in the progression of complex diseases and behaviours have been identified. However, questions such as how the identified genes act and what pathways they are involved in can be answered using a mutant and determining the effects when the gene is missing (Picciotto and Wickman 1998). Isolation of mutants is achieved by combining a forward and reverse genetics approach.

4.1.1 ENU mutants Versus Knockouts

Although both ENU mutagenesis and generating knockouts have been very useful to unveil functions of a number of genes, the contribution of ENU mutagenesis has been particularly significant for circadian biologists. One of the major advantages of ENU mutagenesis is that generation of mutant mice (re-derivation of mice from frozen sperm or ES cell archive) is much easier and faster than generating knockout mice. Further, mutants generated via knockouts, may or may not have germline transmission of the mutation. While ENU mutagenesis makes uses of the same parental sperm whose DNA carried the desired mutation, germline transmission is always achieved. Finally, studying redundancies is easier in ENU mutants than in knockouts, as by generating a knockout, there is no expression of protein. Hence if a paralogue exists, then the function is taken over by the paralogue of the

knocked out gene. Since ENU mutagenesis only generates point mutations, the mutant protein is expressed. Expression of the mutant form of protein is useful in identifying effects on localisation and interactions of protein complexes. One of the best known examples clearly showing a difference between the ENU mutant and knockout is the *Clock* mutant, where compared to the homozygous ENU *Clock* mutant that was arrhythmic in DD, the *Clock* knockout mice sustained rhythmicity. It was later revealed that the presence of rhythms was due to a functional redundancy between the *Clock* and *Npas2* paralogue pairs (Antoch, Song et al. 1997; King, Vitaterna et al. 1997) suggesting that ENU mutagenesis makes a contribution to elucidate functions of genes underlying diseases or abnormal phenotypes.

4.1.2 Identification of *Fbxl21*

The F-box protein family comprises of over 40 members, which are mainly involved in the post-translational modification processes of circadian proteins. They first undergo phosphorylation followed by ubiquitination and finally proteasomal degradation through the SCF complex (Kipreos and Pagano 2000). The F-box protein FBXL21 is one such protein found to be involved in the timely degradation of circadian proteins which is required to maintain a balance between the interlocked feedback loops. *Fbxl21*, the closest paralogue of *Fbxl3*, was first identified in sheep (Jin, Cardozo et al. 2004). It was also found that the rhythmic expression of *Fbxl21* is thought to be due to the combined effect of transactivation by E-box elements through *Clock/Bmal* and the PAR-bZIP transcription factor family (Dardente, Mendoza et al. 2008) .

In comparing both the F-box proteins, *Fbxl3* and *Fbxl21*, the striking difference identified between the two is their spatial and temporal expression in tissues. *Fbxl3* seems to

169

be expressed ubiquitously in almost all the tissues including liver. *Fbxl21*, in contrast is found to be highly specific in the SCN followed by expression in neuroendocrine structures like hypothalamus and adenohypophysis with no expression in liver (Dardente, Mendoza et al. 2008). Similar to FBXL3, FBXL21 was also shown to be capable of interacting with and degrading CRY1, the important negative regulator of circadian function (Dardente, Mendoza et al. 2008). However, the role of *Fbxl21* in circadian mechanisms is still unknown and investigations into it will be a major contribution to this field. For this reason, we used the ENU mutagenesis approach to look for mutations in *Fbxl21*. As the mechanism of *Fbxl21* regulation is not yet known, it is possible that, *Fbxl21* is regulated by its paralogue and they may or may not be functionally redundant. Thus, in order to avoid the opposing phenotypes as observed in the *Clock* mutants, the reverse genetics approach was chosen.

4.2. AIMS OF CHAPTER

The broad aim of the chapter is to identify the role of the second F-box protein *Fbxl21* in circadian time-keeping. For this reason, instead of generating a knockout mouse, we used the reverse genetics approach using ENU mutagenesis to identify mutants in *Fbxl21*. Various other questions about the expression of FBXL21, its interaction with CRY1 and CRY2 and their ability to degrade the same are some of the aspects we studied. The other important question was the redundancies between the two F-box proteins, and if one or both F-box proteins are necessary to maintain the circadian balance.

4.3 RESULTS

4.3.1 Harwell ENU archive screening

FBXL21 is a F-box protein of 434 amino acids with leucine rich repeats (LRR) as their secondary motifs. FBXL21 is the closest relative of the 428 amino acid protein FBXL3, with similarities between their domains. Like FBXL3, FBXL21 has a putative CRY-binding domain, which is 80% identical to that of the FBXL3 domain. This similarity in domains gives rise to questions regarding the function of FBXL21. For this reason, the reverse genetics approach was chosen and the Harwell ENU archive was screened to look for mutations in the gene *Fbxl21*.

Because of the similarities in the F-box domains and CRY-binding domains of FBXL3 and FBXL21, specific primers for the respective domains in *Fbxl21* were designed to screen the archive for mutations. The archive consisted of DNA samples collected from 9600 male progeny of animals treated with ENU. PCR was performed on this DNA and analysed using the light scanner which identifies heteroduplexes based on the DNA melting curve.

Several DNA pools which were outliers in their DNA melting curve in both the F-box and CRY-binding domain screens were identified. A second PCR with individual DNA samples along with wild-type DNA was repeated and analysed in the same way in order to confirm the DNA melts for the outliers. Four mutations were identified in the F-box domain, all of which were confirmed by sequencing. In the putative CRY-binding domain screen, only one mutation was identified (Figure 4.1A). Out of the four F-box mutations, one, Histidine77Histidine (H77H) was a silent mutation. Leucine36Proline (L36P) and Serine28Phenylalanine (S28F) were mutations identified close to the F-box domain and the

Valine68Glutamic acid (V68E) mutation was positioned in the middle of the F-box domain (Figure 4.1A, B). Proline291Glutamine (P291Q) was the only mutation identified in the putative CRY-binding domain screen (Figure 4.1A, B). The melting curves and sequence traces for the V68E and P291Q mutations are shown in Figure 4.2A, B. While the V68E was a T to A transversion, a C to A base pair substitution resulted in the P291Q mutation. Due to the fact that the exact position of the CRY-binding domain in FBXL21 is only predicted, it might be that the P291Q mutation may still affect FBXL21 interaction with CRY proteins (Figure 4.1).

Once sequencing confirmed the base pair change in the five mutations, we looked at the conservation of regions containing these mutations across different species. Of the five mutations, we chose only two mutations to work with. As one was a synonymous mutation, and from the remaining three mutations, L36P and S28F did not lie within the F-box consensus, these mutations were eliminated. On the other hand, the V68E and P291Q mutations were in highly conserved F-box and CRY-binding domains respectively across multiple species (Figure 4.3A). The mutations were also in regions of high conservation between the two F-box proteins, FBXL3 and FBXL21 (Figure 4.3B, C).
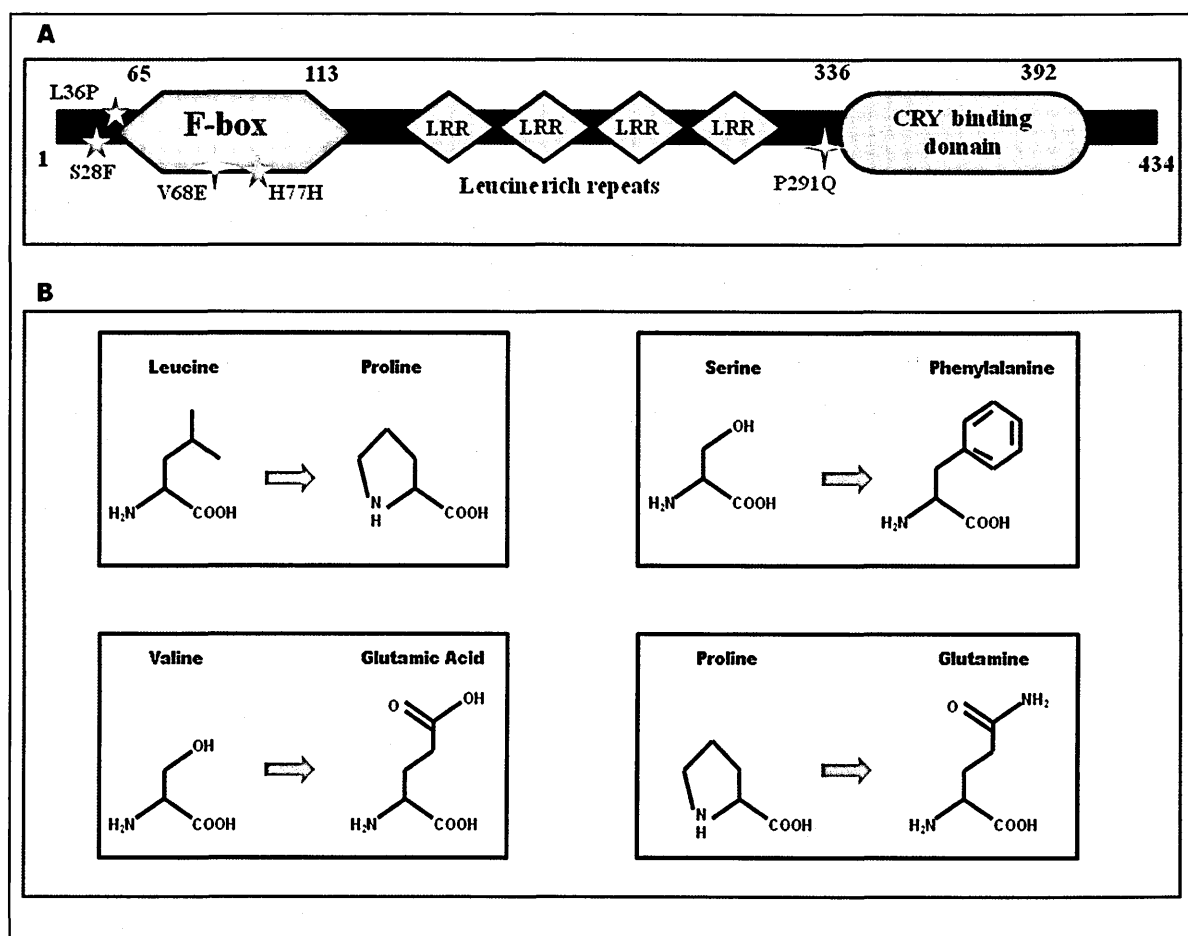
Figure 4.1: Mutations identified in the Harwell ENU archive screen. A) Representation of FBXL21 protein domains. The ENU archive was screened to identify mutations in the F-box domain and the CRY-binding domain using DNA melting curve analysis. While the green stars denote identified mutations, the red stars denote potentially functional mutations. In a total of 5 mutations, two mutations were identified in the F-box domain (H77H and V68E) and two in its vicinity (S28F and L36P). A P291Q mutation was identified in the putative CRY-binding domain. B) Amino acid changes due to identified mutations.
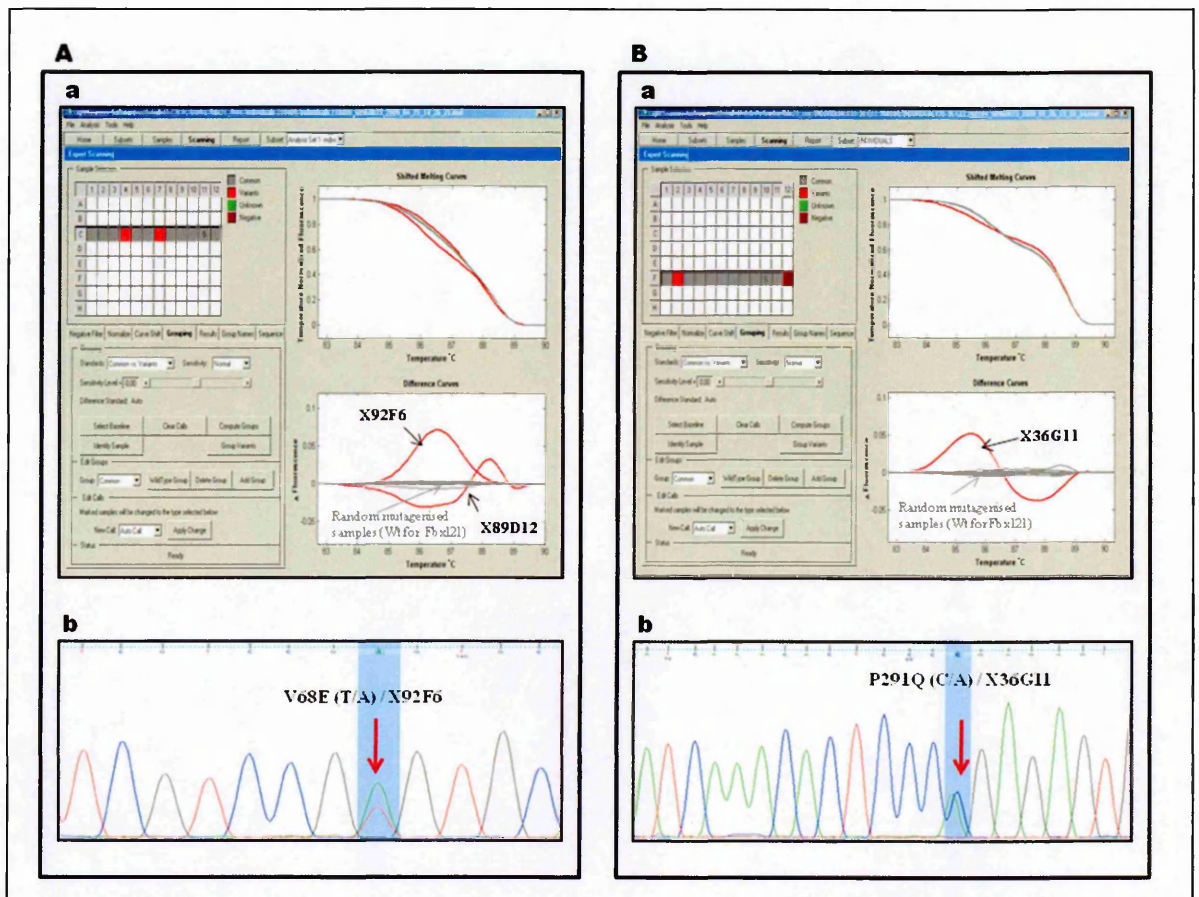
Figure 4.2: Identification of outliers in the ENU archive screen. A) PCR with specific primers for screening the F-box domain of *Fbxl21* was performed, of which there were two interesting pools of DNA. Individual DNA's (X89D12 and X92F6) were used to repeat the PCR and confirm the outliers (a). Mutations in these individual DNA's were confirmed by sequencing. V68E was identified in the X92F6 animal (b). B) The screen for identifying mutations in the CRY-binding domain was performed in the same way. a) shows X36G11 as the outlier amongst the random DNA samples. The individual was sequenced to reveal the P291Q mutation in the predicted CRY-binding domain.
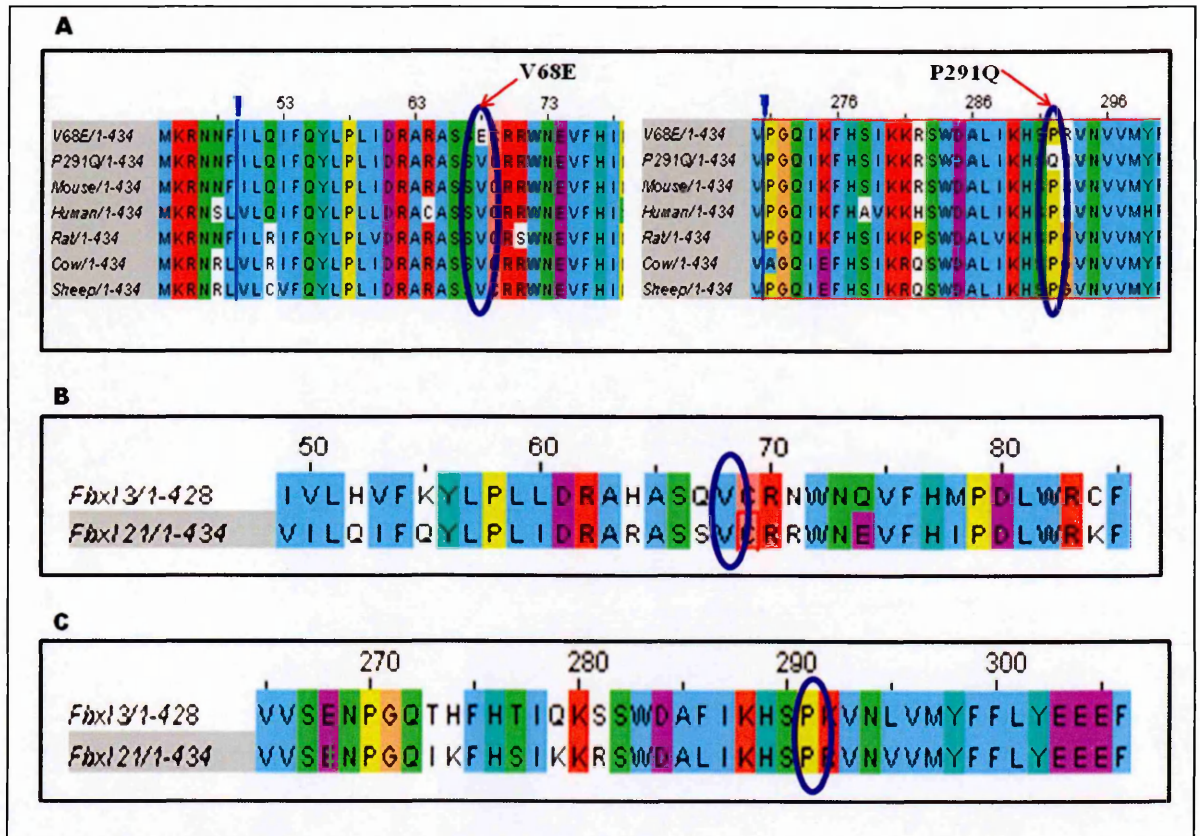
Figure 4.3: Conservation of V68E and P291Q mutations. A) Both the V68E (left panel) and P291Q (right panel) mutations lie within highly conserved regions of the F-box domain and CRY-binding domain respectively across multiple species. The blue arrow represents a break between the sequence. B) and C) show the conservation of F-box domain and the CRY-binding domain in the two F-box proteins, FBXL3 and FBXL21. It also depicts the location of the mutated amino acid.
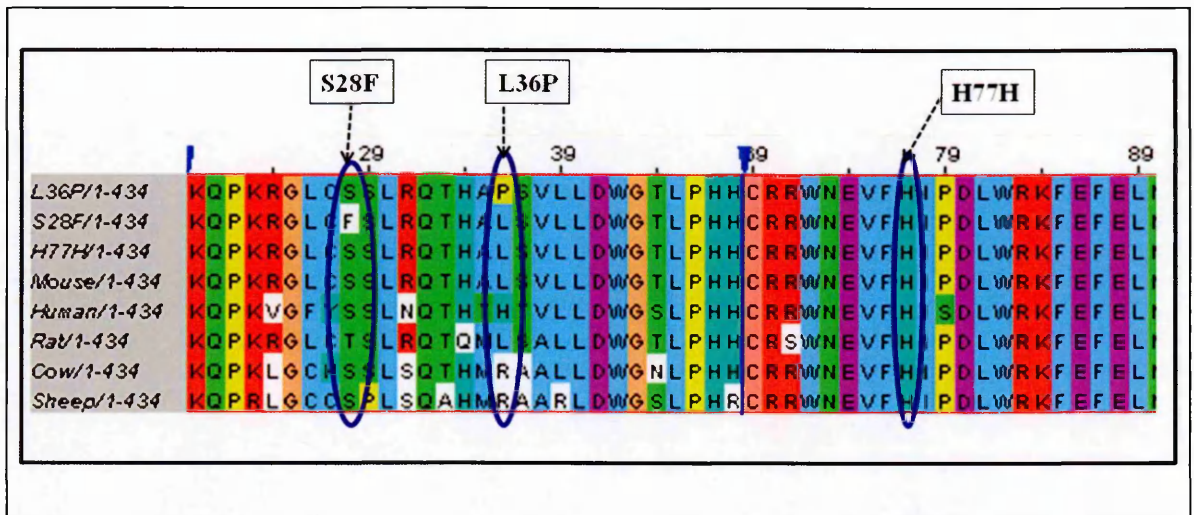
Figure 4.4: Conservation of mutations identified in the ENU archive screen. Out of the four mutations identified in the F-box domain of *Fbxl21*, only one mutation, V68E was in the middle of the F-box domain of FBXL21. The other mutations, L36P, S28F and H77H were identified in the vicinity of the F-box domain. However the sequence alignment of the mutations identified shows that the serine in S28F and histidine in H77H substituted are highly conserved across different species. The Leucine in L36P is conserved only in mice and rats and not in other species. While L36P is not thought to result in a potential functional change of FBXL21, the S28F and H77H substitutions may or may not affect FBXL21 function.

4.3.2 Localisation of FBXL21 *in-vitro*

Once mutations were identified in the F-box and CRY-binding domains of Fbxl21 the effect of these mutations on the localisation of FBXL21 was investigated. This was done by immunofluorescence performed on U2OS cells (section 2.14). Full length *Fbxl21* cDNA was cloned into the pCSII-Myc vector (a kind gift by Dr.Hughes Dardente from the University of Aberdeen). The desired mutations, V68E and P291Q were then introduced into the *Fbxl21*-wildtype (Wt) sequence using the Stratagene mutagenesis kit (Section 2.13). Wild-type and mutant *Fbxl21* plasmids were transfected into U2OS cells using Fugene6 transfection reagent (section 2.4.6). After 24hrs, the cells were synchronised with forskolin at a final concentration of 10μM (section 2.4.7). Following forskolin shock, cells were collected at various time points, washed with PBS, immediately fixed with PFA and then stored at 4°C until all the time points were collected and immunofluorescence was performed (section 2.14).

Figure 4.5 shows the localisation of FBXL21 by transfecting *Fbxl21*-Wt or mutated *Fbxl21*, V68E and P291Q. It can be seen that 6hrs after forskolin shock, FBXL21-Wt remains cytoplasmic. However, both mutant proteins V68E and P291Q are nuclear and cytoplasmic at this time (Figure 4.5A). After 12hrs of shock, this difference in FBXL21 localisation is eliminated and both FBXL21-Wt and mutated forms are nuclear as well as cytoplasmic (Figure 4.5B). The same result is obtained even after 18hrs of shock, where FBXL21-Wt and its mutated forms are both nuclear and cytoplasmic (Figure 4.5 C). Although FBXL21-Wt is restricted to the cytoplasmic compartment after 6hrs, the mutant FBXL21 is nuclear as well as cytoplasmic. Thus there appears to be an alteration in the dynamics of nucleocytoplasmic shuttling in both mutant forms of the FBXL21 protein.
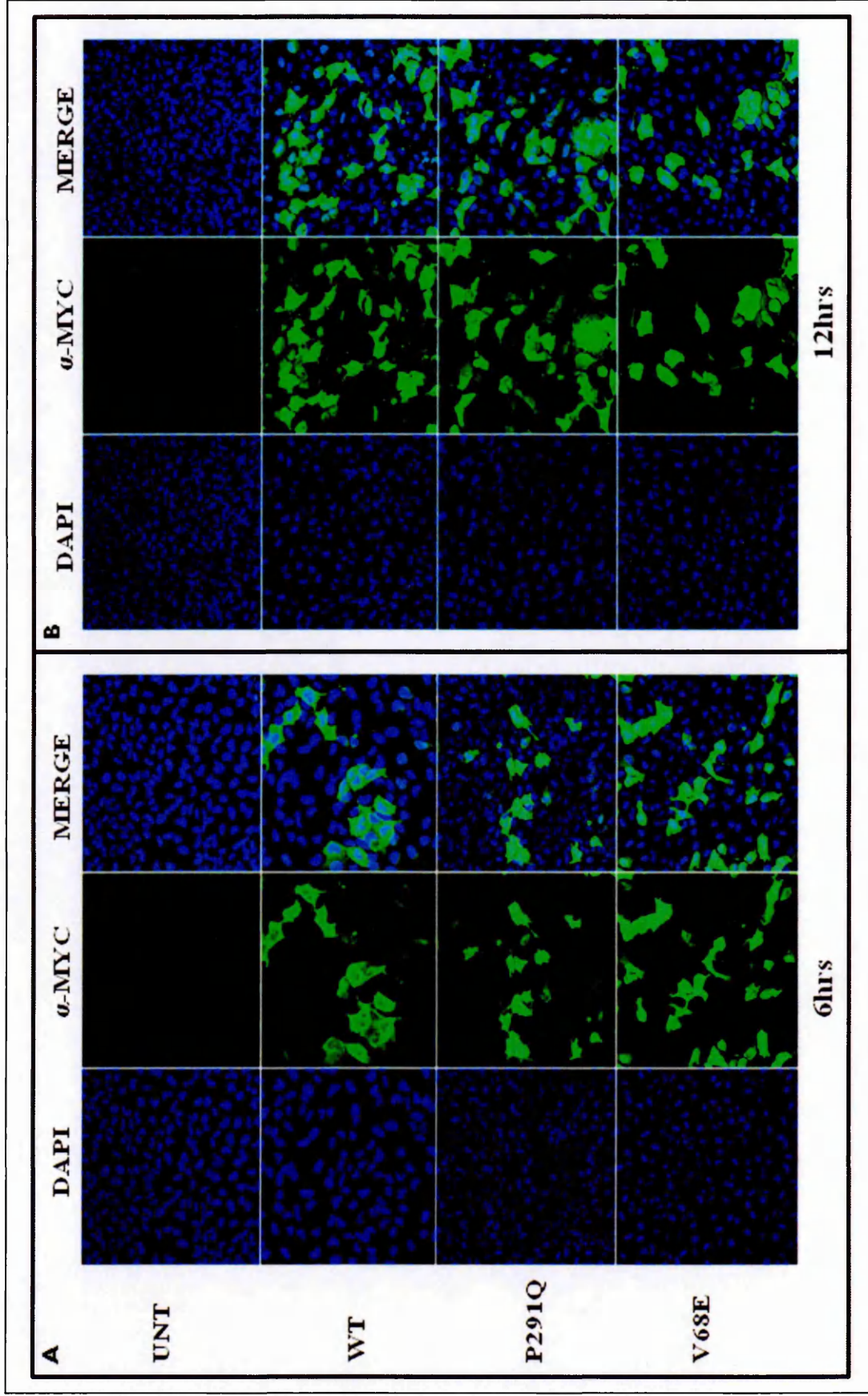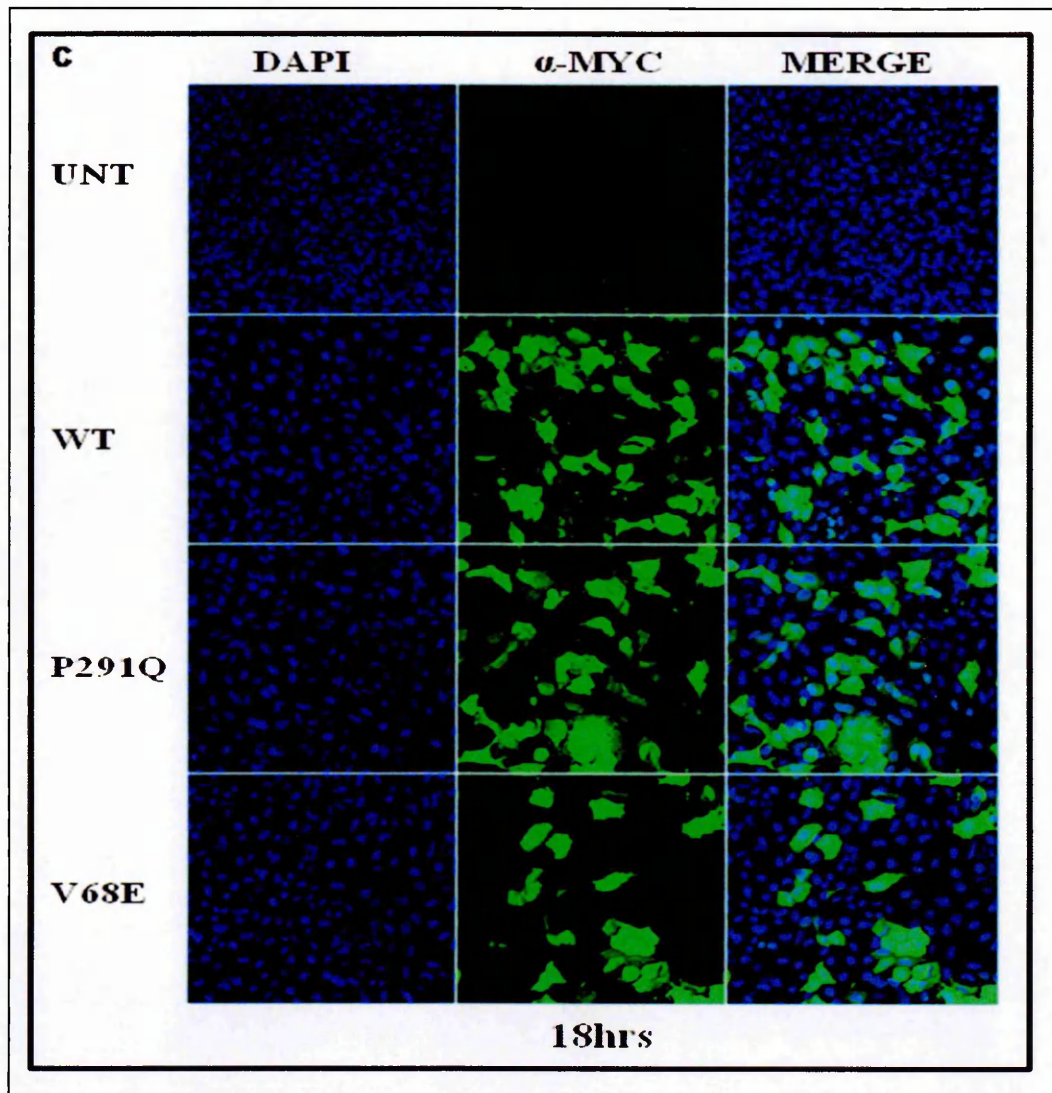
Figure 4.5: Localisation of FBXL21 in-vitro. *Fbxl21*-wild-type and mutated forms, V68E and P291Q were overexpressed in U2OS cells. While the green area in merge represents localisation in cytoplasm, aqua area in merge denotes nuclear localisation. A) After 6hrs of forskolin shock, FBXL21-Wt is retained in the cytoplasm, whereas V68E and P291Q appear to promote nuclear localisation at this time point. B) FBXL21-Wt moves into the nucleus whilst expressed in the cytoplasm as well after 12hrs of shock. Both the mutated versions are nuclear and cytoplasmic at this stage. C) There was no difference in localisation between the mutants even after 18hrs of forskolin shock.

4.3.3 Interaction of FBXL21 with CRY1 and CRY2

FBXL21 was predicted to play a role in circadian mechanisms due to its interaction with the key circadian protein, CRY1 (Dardente, Mendoza et al. 2008). However, the interaction between FBXL21 and CRY2 has not been studied. Hence, it was interesting to determine if FBXL21 interacted with both CRY1 and CRY2.

These experiments were carried out *in-vitro* using Cos7 cells. *Fbxl21*-Myc plasmids were co-transfected along with either *Cry1*-HA or *Cry2*-HA plasmid into a dish with 70-80% confluent cells using Fugene6 in a manner as described in section 2.4.6.1. 36hrs after transfection, proteins extracted from the cells were quantified (section 2.9). The protein lysates were then subjected to co-immunoprecipitations. In this experiment, the α-HA antibody was used to pull down CRY1-HA or CRY2-HA with protein G sepharose beads. The eluted proteins from the co-immunoprecipitated complexes were run on a protein gel and then probed for FBXL21 using α-Myc antibody (Invitrogen)

The results as shown in Figure 4.6A and B are a representation of five independent experiments performed that clearly show an interaction of FBXL21-Wt with both CRY1 and CRY2. Whole cell lysates (Lys) were used as an input that shows the presence of FBXL21-Myc in the protein lysates. Quantification of the blot is shown in Figure 4.6C, where the FBXL21 interactions are first quantified relative to the amount of CRY1/2 pulled down using α-HA antibody (the bands on the right hand side of both Figure 4.6A and B). Further for easier understanding, the FBXL21-Wt and CRY interactions (normalised to CRY) are set at 100% and the interactions of FBXL21-V68E/P291Q and CRY1/2 are plotted as amounts of protein present normalised to FBXL21-Wt-CRY1/2 interaction (Figure 4.6C). It can clearly be seen in the plotted graph (Figure 4.6 C) that the interaction of mutated FBXL21 with both CRY1/2

proteins is significantly reduced by ~80% *in-vitro* (One-way ANOVA with Bonferroni post hoc analysis, FBXL21-V68E-CRY1, FBXL21-P291Q-CRY1 $p \leq 0.01$, FBXL21-V68E- CRY2, FBXL21-P291Q-CRY2 $p \leq 0.001$). Thus it can be concluded that both V68E and P291Q mutations affect FBXL21-CRY interactions.

In some lanes, particularly those with cell lysates, white speckles can be observed. This is due to overexposing these bands while imaging. Due to the weak bands of FBXL21-V68E-Myc and FBXL21-P291Q-Myc, the cell lysates were overexposed. The negative controls used in this experiment should also be noted. Two negative controls, subjected to exactly the same protocol as with the experimental samples, were used. The first negative control was the protein lysate obtained from co-transfecting an empty Myc vector (evMyc) with CRY1-HA which is the same plasmid used in co-transfections with *Fbxl21*-Myc. This shows that in the absence of FBXL21 in the empty Myc vector, CRY1 is unable to bind to anything and hence, there is no band in the lane with this sample (Figure 4.6 A). The second negative control used was the protein lysate obtained from untransfected cells, which again was processed in the same way, and since no complex formation takes places, there is no band present, which ultimately proves that all the other bands present are true and not false positives (Figure 4.6 B).
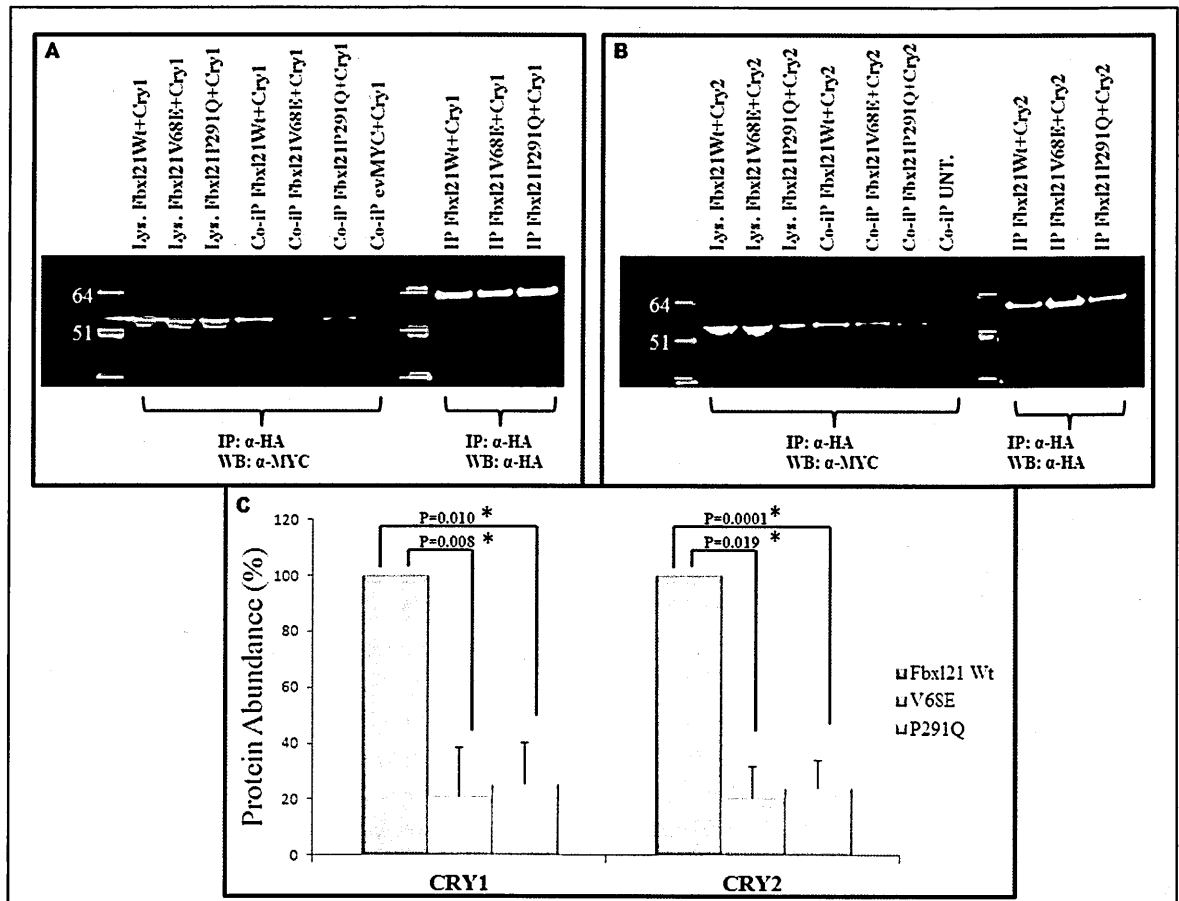
Figure 4.6: Interaction of recombinant FBXL21 with CRY1 and CRY2 in-vitro. A and B) Both these images are representative western blots performed using co-immunoprecipitated lysates. The molecular weight markers are shown on the left of each blot. The first three bands in both the blots are whole cell lysates (Lys.) that show the presence of the F-box proteins (FBXL21) in the transfection complex. The next three are co-immunoprecipitated (Co-iP) bands showing the interaction of FBXL21-Wt, V68E and P291Q with CRY1 (A) and CRY2 (B). The last three bands are the CRY proteins that are pulled down using protein G sepharose beads and α-HA antibody (IP). For performing the experiments, first CRY proteins were immunoprecipitated by using α-HA antibody following which, their interaction with FBXL21 was probed by using α-Myc antibody. The amount of interaction was first normalised to amount of CRY proteins immunoprecipitated following which, the interactions are quantified relative to FBXL21-Wt and CRY interaction. Both A and B show that FBXL21 interactions with both CRY1 and CRY2 are affected by mutations in the F-box domain and CRY-binding domain. C) Quantification of the interactions plotted as normalised to interaction of FBXL21-Wt and CRY1/2 proteins. Both the mutants show significantly reduced interaction of ~80% with both CRY1 and CRY2 proteins (One way ANOVA with Bonferroni post hoc analysis, FBXL21-V68E-CRY1 and FBXL21-P291Q-CRY1 $p \leq 0.01$, FBXL21-V68E-CRY2 and FBXL21-P291Q-CRY2 $p \leq 0.001$).

4.3.4 Degradation of CRY1 and CRY2

F-box proteins target phosphorylated substrates for polyubiquitination followed by proteasomal degradation. β-TRCP 1 and 2 are known F-box proteins that degrade PER proteins (Ohsaki, Oishi et al. 2008) and it was recently shown that FBXL3 degrades CRY proteins (Busino, Bassermann et al. 2007; Godinho, Maywood et al. 2007; Siepka, Yoo et al. 2007). Hence, due to the close homology between FBXL3 and FBXL21 and interaction of FBXL21 and CRY1/2 (as shown in Figure 4.3 and Section 4.3.3), it was necessary to determine if CRY proteins are targeted by FBXL21 as well.

For this reason, we performed *in-vitro* experiments in Cos7 cells by co-transfecting *Fbxl21*-Myc and *Cry1/2*-HA. We first determined if FBXL21-Wt is able to degrade CRY1/2 proteins. 24hrs after transfection, we treated the cells with the protein synthesis inhibitor, cyclohexamide (CHX) at a concentration of 25μg/ml and collected the cells for protein extractions at 0hrs, 2.5hrs and 5hrs after the treatment. The time CHX was added to the cells was considered as 0hrs (section 2.4.8). Once the proteins were quantified, 5μg of the protein lysates were western blotted. The levels of CRY proteins were determined by probing with α-HA antibody followed by normalisation with β-ACTIN levels (control) determined by probing with α-β-ACTIN antibody. Figure 4.7 is a representative image of five independent experiments. It can be seen from the figure that FBXL21-Wt indeed degrades both CRY1 and CRY2 proteins with different efficiencies. CRY1 protein levels do not seem to be reduced as much (~25% reduction) by FBXL21-Wt after 5hrs of CHX treatment (Left panel in Figure 4.7A, B). In contrast to this, CRY2 levels are very low (~70% reduction) after 5hrs of CHX treatment (Right panel in Figure 4.7A, B). When normalised, the above result can be clearly seen in the graph plotted where CRY protein values are normalised to CRY protein level at

0hrs (Figure 4.7 B). CRY2 protein levels are halved after 2.5hrs of CHX treatment and further

halved by 5hrs of CHX treatment, unlike CRY1 proteins. This shows that CRY2 is a better

target for FBXL21 mediated proteasomal degradation than CRY1.
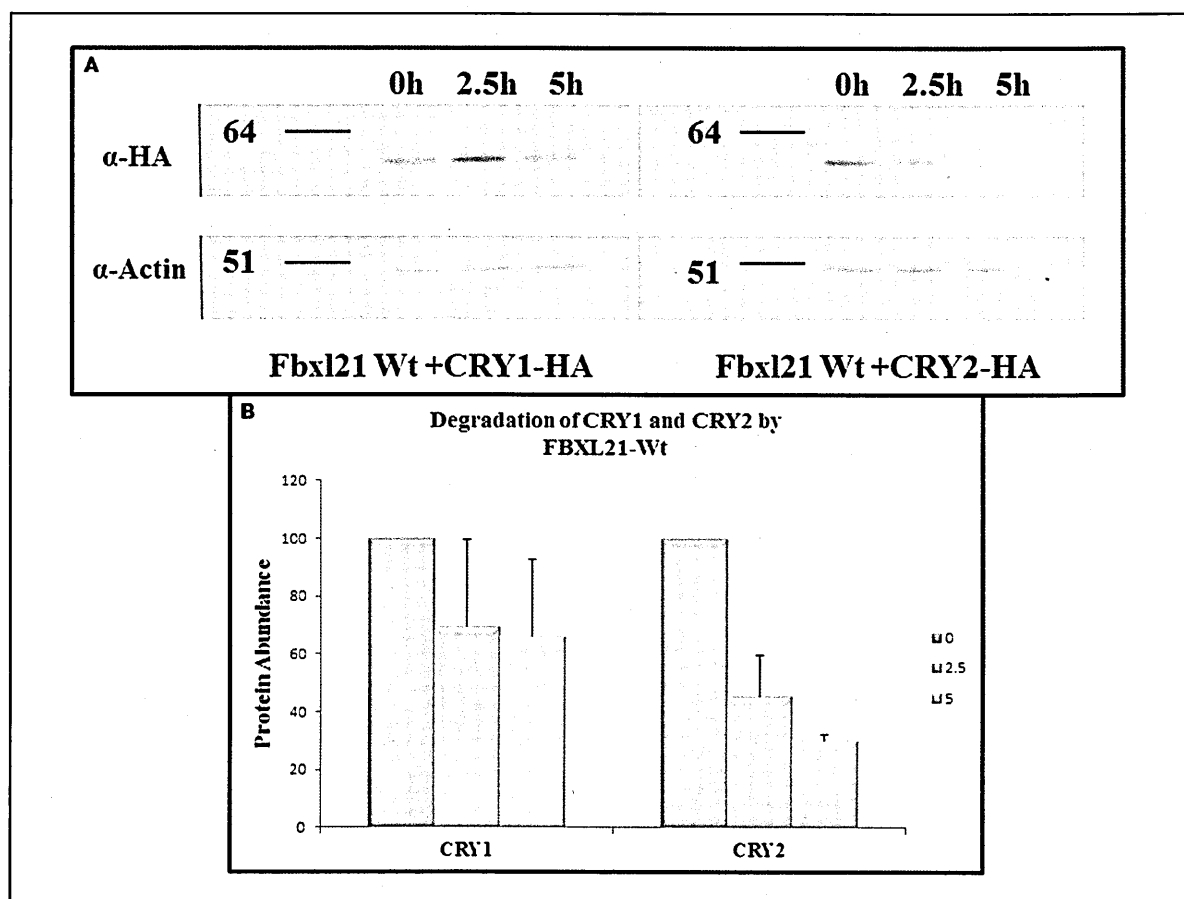
Figure 4.7: Degradation of CRY proteins by FBXL21-Wt in-vitro. A) Representative western blots showing CRY1 (left panel) and CRY2 (right panel) degradation. Protein lysates were collected from Cos7 cells co-transfected with *Fbxl21*-Wt and *Cry1*-HA or *Cry2*-HA followed by treatment with 25µg of CHX. Cells were collected at 0hrs, 2.5hrs and 5hrs after CHX treatment. The molecular weight markers are shown on the left of each blot. CRY levels were first determined by probing the membrane with α-HA antibody and were then normalised to β-ACTIN levels. B) Normalised CRY levels are plotted as values relative to CRY1 and CRY2 levels at 0hrs of CHX treatment plotted on a logarithmic scale. It shows the CRY2 levels are halved by 2.5hrs (~50% reduction) of CHX treatment and degraded even further after 5hrs (~70% reduction), which is in contrast to CRY1 levels, showing that CRY2 is a much better substrate for FBXL21-Wt than CRY1.

Once the pattern of degradation of CRY1/2 by FBXL21-Wt was identified, it was necessary to identify the degradation pattern of CRY1 and specifically CRY2 by the *Fbxl21* mutants, V68E and P291Q. The same experiment as described above was performed where *Fbxl21*-Wt or the mutant V68E and P291Q plasmids were co-transfected either with *Cry1*-HA or *Cry2*-HA. The cells were treated with CHX and proteins were extracted in the same manner (Figure 4.8A). Figure 4.8B shows that the mutated FBXL21 proteins degrade CRY1 in a similar nature as to FBXL21-Wt. When quantified and normalised to the CRY1 protein levels at 0hrs, it can be seen that both the mutations, V68E and P291Q, do reduce amounts (~30-40%) of CRY1 proteins after 2.5hrs of CHX treatment, after which there is a negligible difference in the CRY1 levels after 5hrs of CHX treatment (Figure 4.8 B Left panel). Thus, it can be said that the V68E and P291Q mutant proteins have very little effect (no statistical significance) on degradation of CRY1 proteins 2.5hrs after CHX treatment. As expected, the degradation of CRY2 by the *Fbxl21* mutants was interesting. The V68E mutation present in the F-box domain, show a very slight, non-significant difference in CRY2 protein degradation. The difference in CRY2 levels was observed after 2.5hrs of CHX treatment, where compared to 60% CRY2 degradation by FBXL21-Wt, only 40% of CRY2 was degraded by V68E protein. The CRY2 levels after 5hrs did not vary between FBXL21-Wt and V68E (Figure 4.8B right panel). An interesting observation made was the degradation of CRY2 by the P291Q mutation. Comparing CRY2 degradation (Figure 4.8B Right panel) by FBXL21-Wt, it can be seen that, the levels of CRY2 are not as low as they should be at 2.5hrs after CHX treatment. CRY2 levels seemed to be high even after 5hrs of CHX treatment (very slight degradation, ~10%) (Figure 4.8 B Right panel), suggesting an attenuation in the degradation of CRY2. Although not significant due to variability observed, the experiment shows the trend of

degradation of CRY proteins by the mutants, suggesting that the mutants may slow the rate of

CRY2 degradation *in vivo*.
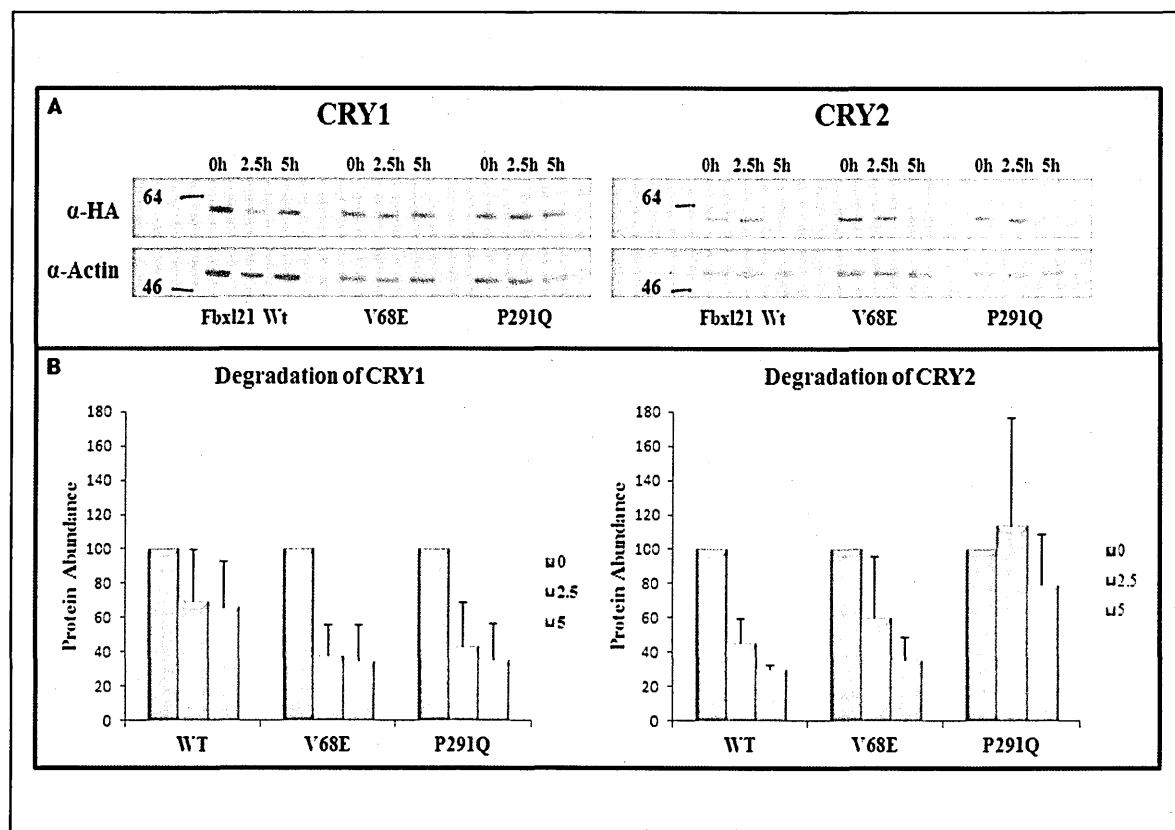
Figure 4.8: Effect of Fbxl21 mutations on CRY1 and CRY2 degradation in-vitro. A) Western blot showing degradation of CRY1 by FBXL21-Wt and the two mutants, V68E and P291Q. Cells were co-transfected with *Fbxl21* plasmids and *CRY1* or *CRY2*, treated with 25µg CHX and collected at 0hrs, 2.5hrs and 5hrs after CHX media was added to the cells. CRY proteins were detected by probing with α-HA and β-actin was used as a control and probed with α-β-actin. B) Amounts of CRY proteins were first normalised to β-actin, following which they are plotted relative to CRY levels at 0hrs on a logarithmic scale. In the left panel, it can be seen that, compared to the FBXL21-Wt, the mutants degraded CRY1 within 2.5hrs of CHX treatment, however they did not degrade them further. In case of CRY2, V68E mutation had little effect and did not degrade CRY2 as strongly at 2.5hrs as FBXL21-Wt did. However, the CRY2 levels were maintained at a higher level in the presence of P291Q mutant. Only ~10% of CRY2 protein was degraded after 5hrs of CHX treatment, suggesting that the P291Q mutant stabilises CRY2 protein *in-vitro*.

4.3.5 Determining the period length of mutants *in-vitro*

Mutations that were identified in the ENU archive screening were cloned into the pCSII vector containing a Myc epitope tag. After carrying out interaction and degradation studies, we wanted to identify alteration in the period length due to the presence of mutations in the F-box domain and CRY binding domain. For this reason, real-time bioluminescence studies were carried out using the LumiCycle (Actimeterics). The U2OS *Per2*:Luc and Rat-1 *Per2*:Luc cell lines were used for this purpose. These cell lines are stably transfected with *Per2*:Luc, where a *Per2* promoter drives the expression of luciferase reporter gene. Hence, when the luciferin substrate is added to the samples, the luminescence given out will mimic *Per2* oscillations in the cells. Thus, when a mutant plasmid is transfected into these cells, the mutant protein that is produced may affect the circadian core oscillator which reveals circadian rhythms in luminescence by reporting oscillations of *Per2*. The deviation of *Per2* oscillations in the presence of a mutant plasmid from wild-type *Per2* oscillations determines the period length of mutants.

In our experiments, the *Fbxl21*-Wt, *Fbxl21*-V68E and *Fbxl21*-P291Q plasmids were transfected into U20S *Per2*:Luc cell lines. Whilst *Fbxl21*-Wt plasmid generated a period of 23 hrs±0.08, transfection of *Fbxl21*-P291Q resulted in a period of 22.4hrs±0.09 (difference of 0.6hrs, Student's t-test p=0.05) (Figure 4.9A). The difference in period was confirmed by transfecting these same plasmids in Rat-1 *Per2*:Luc cells, which work on the same principle. Similar results were obtained by transfecting these plasmids; transfection of *Fbxl21*-Wt generated a period length of 23.7hrs±0.05, while with *Fbxl21*-P291Q a period of 22.9hrs±0.06 was determined (Student's t-test p=0.01) (Figure 4.9B).

A — U2OS Per2: Luc cells

Fbxl21 Wt
● Fbxl21 V68E
Fbxl21 P291Q

Period length: *Fbxl21*-Wt = 23.0hrs+/-0.08; *Fbxl21*-V68E=22.8hrs+/-0.155; *Fbxl21*-P291Q=22.4hrs+/-0.09

B — Rat-1 Per2: Luc cells

Fbxl21 Wt
● Fbxl21 P291Q

Period length: *Fbxl21*-Wt = 23.7hrs+/-0.05; *Fbxl21*-P291Q= 22.9hrs+/-0.06
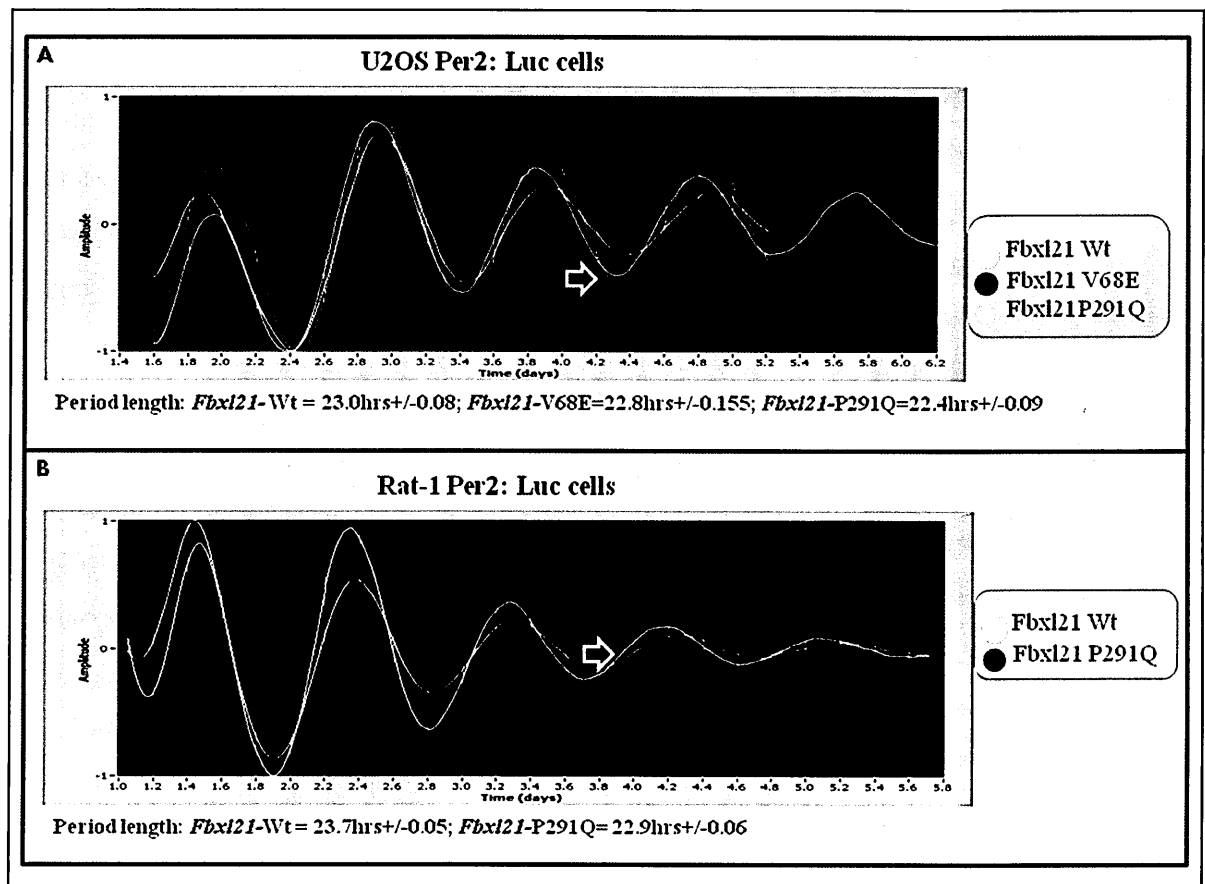
Figure 4.9: Real time bioluminescence imaging in U2OS Per2:Luc and Rat-1 Per2:Luc stably transfected cell lines using the LumiCycle. 2 dishes each of U2OS *Per2*:Luc (A) and Rat-1 *Per2*:Luc (B) cell lines were transfected with 3µg of wild-type and mutant forms of *Fbxl21* plasmids using Fugene6. Following transfections, the cells were synchronised using 10µM forskolin after which luciferin substrate was added and the dishes were placed into the LumiCycle to record the luminescence that represent the oscillations of the circadian gene *Per2*. The period length was calculated for each plasmid (wild-type and mutant) transfected and the difference in period length determines the effect of the mutants using the LumiCycle software. The Student's t-test was used to calculate statistical significance. A) In U2OS *Per2*: Luc cells, while *Fbxl21*-Wt generated a period of 23.0hrs±0.08, *Fbxl21*-V68E generated a period of 22.8hrs±0.155 and *Fbxl21*-P291Q showed a significantly shorter period of 22.4hrs±0.09 (difference of 0.6hrs, p=0.05). This phenotype was confirmed in Rat-1 *Per2*:Luc cells, where on transfecting *Fbxl21*-Wt, the period length obtained was 23.7hrs±0.05 and when *Fbxl21*-P291Q was transfected, a significantly shorter period length of 22.9hrs±0.06hrs was generated (p=0.01).

4.3.6 Circadian Wheel-running activity of *Fbxl21* mutants

All the *in-vitro* studies were carried out whilst the animals carrying the identified mutations were being re-derived using the Harwell ENU sperm archive. The animals were derived using the sperm frozen down from the same animal whose DNA carrying the mutation was identified during ENU archive screening. Once re-derived, the animals were backcrossed to C57BL/6J in order to generate the animal colony on the C57BL/6J background. Backcrossing was carried out for 9 generations to eliminate traits (coat colour, behaviour etc.) of a mixed genetic background, to remove linked mutations and generate a congenic colony on the C57BL/6J background. Although the $Fbxl21^{V68E/V68E}$ mice used in our analysis were congenic the $Fbxl21^{P291Q/P291Q}$ were only in the second backcross, and hence were expected to show traits of other genetic backgrounds. Both the $Fbxl21^{V68E/V68E}$ and $Fbxl21^{P291Q/P291Q}$ mutants were subjected to the circadian wheel-running screen as described in section 2.3, where mice were subjected to a protocol where they were kept in a 12hr light:12hr dark (LD) schedule for 7 days where their entrainment to LD cycle was assessed, following which they were left in free running conditions in constant darkness (DD) for 2 weeks followed by constant light (LL) conditions for 2 weeks. Period length, and tau (τ) in DD (τ_{DD}) and LL (τ_{LL}) conditions was then analysed using the Clock lab software.

Mice that were wild-type, heterozygous and homozygous for V68E and P291Q were screened in order to identify phenotypes associated with mutations in highly important domains of FBXL21. In case of $Fbxl21^{V68E+/-}$ and $Fbxl21^{V68E/V68E}$ animals, the τ_{DD} was 23.62hrs±0.06 and 23.83hrs±0.029 respectively (Figure 4.10A). This was not significantly different from the wild-type animals whose τ_{DD} was 23.68hrs±0.096. However, the $Fbxl21^{V68E/V68E}$ mutants seem to have a significant increase in period while free-running in LL

conditions, where the period increases from 23.83hrs±0.029 in DD to 25.67hrs±0.086 in LL (p<0.005, One-way ANOVA with Bonferroni post hoc test). Thus, the V68E mutation in the F-box domain of FBXL21 seems to have an effect in constant light. The right and left panel in figure 4.10B confirms that there is no significant difference between $Fbxl21^{+/+}$, $Fbxl21^{V68E/+}$ and $Fbxl21^{V68E/V68E}$ animals in DD (left panel) and shows the significant difference between $Fbxl21^{V68E/V68E}$ and wild-types in LL (p<0.005, One-way ANOVA with Bonferroni post hoc test) (right panel).

Mice with the P291Q mutation in the CRY-binding domain of FBXL21 were then screened to look at the effects of this mutation *in vivo*. These mice were subjected to the same protocol as the $Fbxl21^{V68E}$ mutants. The wild-type mice showed a τ_{DD} of 23.68hrs±0.096. The period length of $Fbxl21^{P291Q/+}$ was slightly but not significantly larger at 23.86hrs±0.034. A significantly shorter phenotype was observed in the $Fbxl21^{P291Q/P291Q}$ mice (τ_{DD} = 23.1hrs±0.073) compared to the wild-type mice in DD conditions (p<0.005, One-way ANOVA with Bonferroni post hoc test) (Figure 4.11A and 4.11B left panel B). The $Fbxl21^{P291Q/P291Q}$ mutants also had a significantly longer period length of ~25.87hrs±0.095 as compared to 25.1hrs±0.045 in wild-type animals in LL conditions (p<0.005, One-way ANOVA with Bonferroni post hoc test) (Figure 4.11 B right panel).

Figure 4.10: Circadian wheel-running analysis of the Fbxl21 mutant, V68E. A and B) $Fbxl21^{+/+}$, $Fbxl21^{V68E/+}$ and $Fbxl21^{V68E/V68E}$ mice were first allowed to entrain in 12hr light:dark conditions followed by which they were allowed to free run in constant dark conditions (DD). Mice heterozygous for the mutation had a τ_{DD} of 23.62hrs±0.06 and homozygous mice were no different from the heterozygotes and wild-type animals and had a τ_{DD} of 23.83hrs±0.029. Under constant light conditions (LL), while the $Fbxl21^{V68E/+}$ mice were not significantly different from wild-type mice, the $Fbxl21^{V68E/V68E}$ mutants show a significant increase in period length with a τ_{LL} of 25.67hrs±0.086 (***p<0.005).The actograms shown represent a group of 10 animals and the $\tau_{DD \text{ and }} \tau_{LL}$ values are an average±SEM obtained from 10 animals. It must be noted that a short 3hr light pulse is presented to the mice during the dark phase of the LD cycle. This was done to assess their ability to suppress activity during light conditions. The light pulses are a part of the circadian protocols carried out in the laboratory and is irrelevant to studies presented here. The graphs show the mean period length while the SEM is represented as error bars. Statistical significance is obtained from one way ANOVA using the post hoc Bonferonni test.

A

$Fbxl21^{+/+}$ (WT)

Tau DD=23.68hrs± 0.096;
Tau LL= 25.1hrs ± 0.045

$Fbxl21^{V68E/+}$(HET)

Tau DD=23.62hrs ± 0.06;
Tau LL= 25.22hrs ± 0.189

$Fbxl21^{V68E/V68E}$(HOM)

Tau DD=23.83hrs ± 0.029;
Tau LL= 25.67hrs ± 0.086

B

Wheel-running activity in DD

Wheel-running activity in LL

■ Wt
■ V68E +/-
■ V68E -/-

*** $p < 0.005$
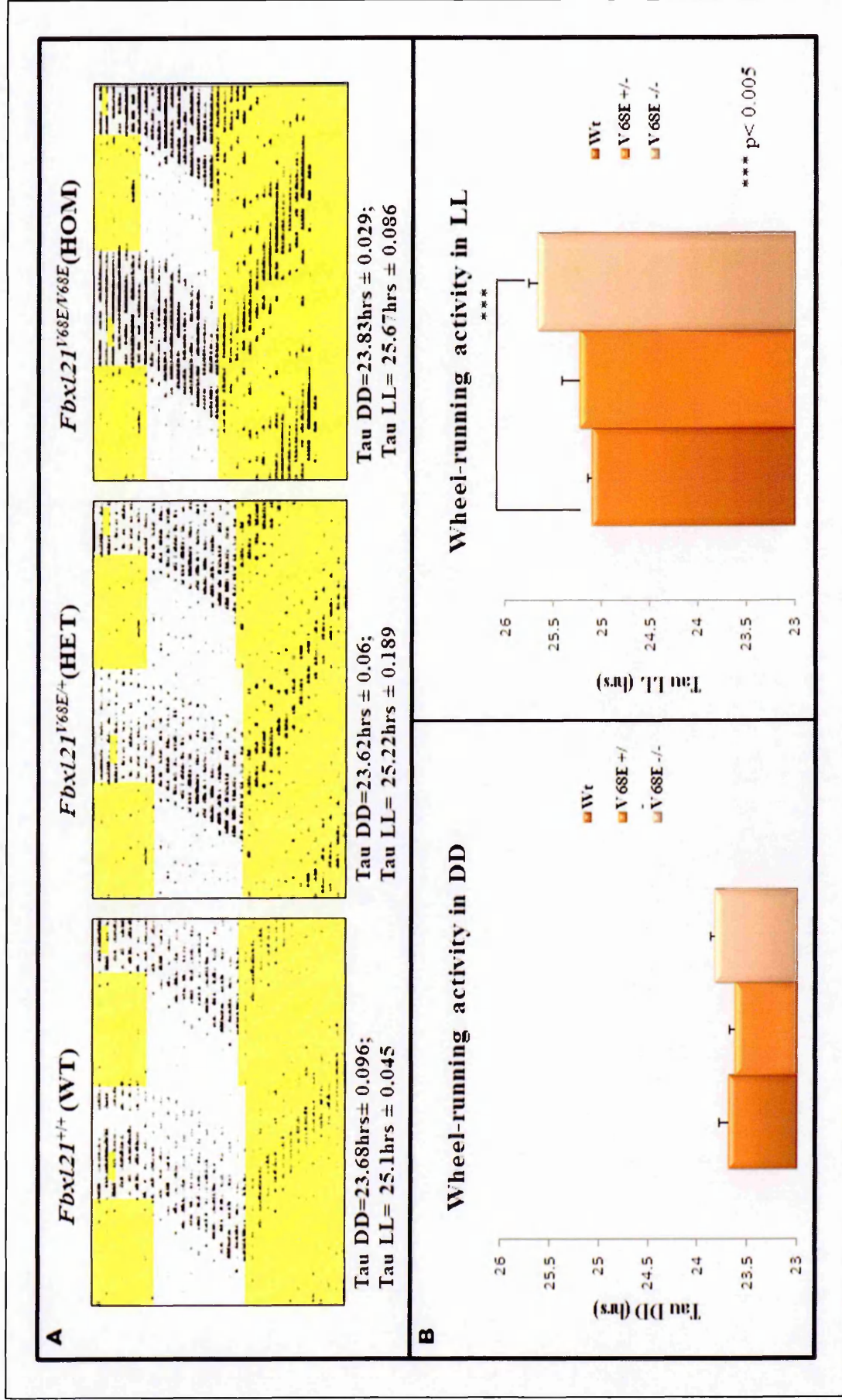
Figure 4.11: Circadian wheel running analysis of the Fbxl21 mutant, P291Q. A and B) Wild-type, heterozygous and homozygous mice for the $Fbxl21^{P291Q}$ mutation were entrained in 12hr LD conditions after which they were allowed to free run in DD for 2 weeks, and finally allowed to free run for 2 weeks under LL conditions. Their wheel running activity was recorded throughout the entire screen. The screen also included a short 3hr light pulse presented to the mice during the dark phase of the LD cycle. This was done to assess their ability to suppress activity during light conditions. The light pulses are a part of the circadian protocols carried out in the laboratory and are irrelevant to studies presented here as these were not considered during data analysis of studies presented here. Compared to the wild-type animals, the $Fbxl21^{P291Q/+}$ heterozygous mice had a slight but not significant lengthening of period resulting in τ_{DD} of 23.8hrs±0.034. However, the homozygous mice, $Fbxl21^{P291Q/P291Q}$ had a significantly shorter period length of ~23.1hrs±0.073 in DD conditions (***p<0.005). Under LL conditions there is a significant increase in period length observed in $Fbxl21^{P291Q/P291Q}$, τ_{LL}=25.87hrs±0.095 compared to the τ_{LL}=25.1hrs±0.045hrs observed in wild-type mice (***p<0.005). The actograms shown represent a group of 10 animals and the $\tau_{DD \text{ and }} \tau_{LL}$ values are means±SEM obtained from the 10 animals. The graphs shown in B are plotted as the mean period length±SEM represented as error bars. Statistical significance is obtained from one way ANOVA using the post hoc Bonferroni test.

A

Fbxl21⁺/⁺ (WT)

Fbxl21^(P291Q/-) (HET)

Fbxl21^(P291Q/P291Q) (HOM)

Tau DD=23.68hrs±0.09;
Tau LL= 25.1hrs±0.045

Tau DD=23.86hrs±0.034;
Tau LL= 25.34hrs±0.086

Tau DD= 23.10hrs±0.073;
Tau LL= 25.87hrs±0.095

B

Wheel-running activity in DD

Wheel-running activity in LL
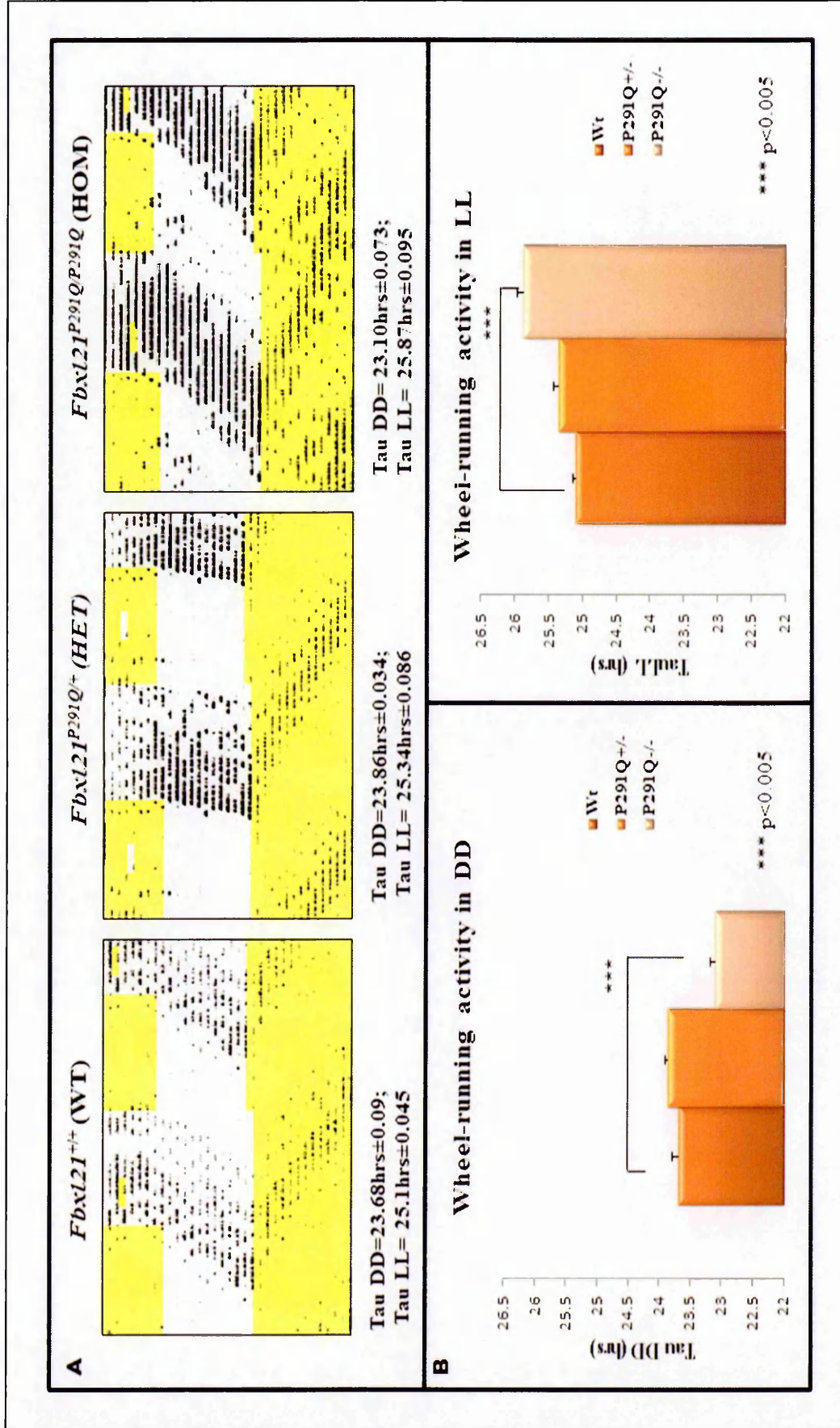
4.3.7 Investigated Circadian Parameters

Apart from the period length, τ, measured during the circadian screens, other circadian parameters such as percentage of nocturnal activity, amplitude of oscillations in DD and LL and average wheel revolution in LD, DD and LL were measured for every animal using the Clocklab software. The parameters are the same as described previously (Chapter 1). All the animals were put through the same screen of 7 days in 12hrs L:D schedule followed by 2 weeks in DD and finally 2 weeks in LL conditions. Tables 4.1 and 4.2 show the parameters measured in *Fbxl21^{V68E}* and *Fbxl21^{P291Q}* mutants respectively. Most of the parameters measured, except the average wheel revolutions in DD, were similar in *Fbxl21$^{+/+}$* and *Fbxl21$^{V68E/+}$* animals. The *Fbxl21$^{V68E/V68E}$* mutants show a significantly higher wheel revolution in LD, DD and LL conditions than the wild-type animals. The τ_{DD} of *Fbxl21$^{V68E/V68E}$* did not show any significant differences, whereas τ_{LL} was significantly higher with a high amplitude than *Fbxl21$^{+/+}$* and was 1.81hrs longer than τ_{DD} as compared to 1.42hrs lengthening in wild-type animals (One way ANOVA with Bonferroni post hoc test p=0.018).

The same parameters were measured for the *Fbxl21^{P291Q}* mutants (Table 4.2). The period length, τ_{DD} of *Fbxl21$^{P291Q/P291Q}$* animals was significantly shorter than in *Fbxl21$^{+/+}$*. The homozygous mice were also seen to have significant differences in the mean wheel revolutions in DD conditions, *Fbxl21$^{P291Q/P291Q}$* showing higher revolutions compared to the wild-type mice. Although there was no significant difference in the period length between *Fbxl21$^{P291Q/+}$* and *Fbxl21$^{+/+}$* mice under DD, these same animals showed a significantly longer period length with a low amplitude in LL conditions compared to *Fbxl21$^{+/+}$* animals. A striking result is seen in *Fbxl21$^{P291Q/+}$* where their percentage of nocturnal activity is significantly lower than the wild-type and *Fbxl21$^{P291Q/P291Q}$* animals. This could be a result of

the background of the mice. Since they are not congenic, we would expect some heterogeneity associated with the mixed genetic background in these mice.

Circadian wheel-running parameters for *Fbxl21^{V68E}* mutants

	Fbxl21$^{+/+}$	*Fbxl21$^{V68E/+}$*	*Fbxl21$^{V68E/V68E}$*
Avg. Revolution in LD	2649.301±618.89	3362.24±811.78	**8054.26±1073.99***
% of Nocturnal Activity	90.65±0.79	88.94±2.09	94.76±1.17
Avg. Revolution in DD	3623.91±927.99	**5148.37±902.72****	**10188.49±999.75***
Tau DD	23.684±0.09	23.6±0.05	23.79±0.03
Amplitude in DD	909.20±138.43	1339.365±100.99	**1440.68±92.43****
Avg. Revolution in LL	2202.25±460.71	3492.13±887.90	**5864.79±1150.27****
Tau LL	25.1±0.045	25.11±0.16	**25.60±0.17***
Amplitude in LL	1102.826±104.97	1080.39±103.95	1054.62±92.92

Table 4.1: Comparison of various wheel running parameters in Fbxl21$^{+/+}$, Fbxl21$^{V68E/+}$ and Fbxl21$^{V68E/V68E}$ animals. Most of the parameters measured were similar between the wild-type and *Fbxl21$^{V68E/+}$* mice except for average wheel revolutions in DD, which was significantly higher than in the wild-type mice. Significant differences were observed in the average wheel revolution in the LD, DD and LL phases of the circadian screen between *Fbxl21$^{V68E/V68E}$* and *Fbxl21$^{+/+}$*. In addition to the significantly higher wheel revolutions in *Fbxl21$^{V68E/V68E}$*, τ_{LL} was also seen to be significantly higher in the homozygous mice (τ_{LL}=25.60hrs±0.17). All the values represent mean+/- standard errors from 10 animals which were a mix of sexes. One way ANOVA with Bonferroni post hoc test was used to test statistical significance where *$p<0.05$, **$p\leq0.005$, ***$p\leq0.001$.

Circadian wheel-running parameters for $Fbxl21^{P291Q}$ mutants

	$Fbxl21^{+/+}$	$Fbxl21^{P291Q/+}$	$Fbxl21^{P291Q/P291Q}$
Avg. Revolution in LD	2649.301±618.89	3156.51±1048.83	5590.93±1426.62
% of Nocturnal Activity	90.65±0.79	77.22±4.44 ***	91.92±1.06
Avg. Revolution in DD	3623.91±927.99	8168.98±2143.64	11216.09±2597.49**
Tau DD	23.684±0.09	23.86±0.034	23.10±0.07***
Amplitude in DD	909.20±138.43	772.79±73.20	1053.94±86.20
Avg. Revolution in LL	2202.25±460.71	5093.60±1659.50	6380.54±2551.06
Tau LL	25.1±0.045	25.33±0.06**	25.85±0.12***
Amplitude in LL	1102.826±104.97	845.79±53.47	398.59±52.72***

Table 4.2: Comparison of the investigated circadian parameters in $Fbxl21^{+/+}$, $Fbxl21^{P291Q/+}$ and $Fbxl21^{P291Q/P291Q}$ mice. Most of the parameters measured were similar in the wild-type and $Fbxl21^{P291Q/+}$ mice except for significantly higher percentage of nocturnal activity (which may be associated with the mixed genetic background of these mice) and τ_{LL}. The $Fbxl21^{P291Q/P291Q}$ on the other hand, showed a significantly shorter period in DD (τ_{DD}=23.10hrs±0.07) compared to wild-type control mice (τ_{DD}=23.64hrs±0.09). Although with a low amplitude the τ_{LL} was also seen to be significantly higher in the heterozygous (τ_{LL}=25.33hrs±0.06) and homozygous (τ_{LL}=25.85hrs±0.12) mice. All the values represent mean±standard errors from 10 animals which were a mix of sexes. One way ANOVA with Bonferronni post hoc test was used to test statistical significance where *$p<0.05$, **$p\leq0.005$ and ***$p\leq0.001$.

197

4.3.8 Cross with *Afh* mutation to study genetic interaction

After determining the effects of *Fbxl21* mutations on the interaction of FBXL21 with CRY1 and CRY2, similar to the effect seen with the *Afh* mutation, and after determining the phenotypes of the two *Fbxl21* mutations individually, the next step was to investigate if there was a genetic interaction between the two *Fbxl* paralogues. This was done by generating $Fbxl3^{Afh/Afh}$; $Fbxl21^{V68E/V68E}$ and $Fbxl3^{Afh/Afh}$; $Fbxl21^{P291Q/P291Q}$ compound mutants and screening them to analyze their phenotypes. We screened double heterozygous and double homozygous animals for the *Afh* mutation and V68E or P291Q in the same manner as mentioned previously. The same LD, DD, LL protocol was used for this cohort of animals.

In the $Fbxl3^{Afh/Afh}$; $Fbxl21^{V68/V68E}$ compound mutants, the double heterozygous animals showed a significant lengthening of period in DD conditions, τ_{DD} =24.22hrs±0.04 (p<0.005 One way ANOVA with Bonferroni post hoc test) relative to wild-type mice (τ_{DD} =23.68hrs+/-0.09) which lengthened even more in LL with a τ_{LL} of 25.74hrs±0.119 (p<0.001, One way ANOVA with Bonferroni post hoc test) (Figure 4.12 A, B). This result can be attributed to the presence of the *Afh* allele itself. Although lengthening of period was seen in the double homozygous animals in DD (τ_{DD} =26.22hrs±0.06), their percentage of nocturnal activity during the LD schedule was significantly lower than the other genotypes (Table 4.3). Surprisingly, these animals were seen to be arrhythmic in LL (Figure 4.12 A).

In $Fbxl3^{Afh/+}$; $Fbxl21^{P291Q/+}$ double heterozygous mice, under the same conditions, the period lengthened to 24.22hrs±0.06 (p<0.001, One way ANOVA with Bonferroni post hoc analysis) (similar to the *Afh* X V68E mice), which again lengthened with a similar period of 25.86hrs±0.22 in LL conditions (p<0.001, One way ANOVA with Bonferroni post hoc analysis). These animals were seen to have splitting of activity in LL, which is not found in

the *Afh/+* mice alone. Not surprisingly, the *Fbxl21$^{Afh/Afh}$; Fbxl21$^{P291Q/P291Q}$* mice too showed an increase in period to 27.5hrs±0.173 in DD conditions and further become arrhythmic in LL, suggesting a role for *Fbxl21* under light conditions (Figure 4.13 A and B).. The fact that the period of the double mutant is even longer than that of the *Afh/Afh* alone shows that the *Afh* mutation has a significantly stronger effect on output rhythms (locomotor activity) than the *Fbxl21* mutation.

Circadian wheel-running parameters were also measured in the *Fbxl3$^{Afh/Afh}$; Fbxl21$^{V68E/V68E}$* and *Fbxl3$^{Afh/Afh}$; Fbxl21$^{P291Q/P291Q}$* compound mutants. Considering the parameters for *Fbxl3$^{Afh/Afh}$; Fbxl21$^{V68E/V68E}$* compound mice (Table 4.3), it is seen that compared to the wild-type animals, the double heterozygous and double homozygous animals show a significant increase in period length compared to wild-type mice. While the double heterozygous animals show a period length of 24.31hrs±0.02 in DD (***$p < 0.001$), the double homozygous mice show a τ_{DD}26.41hrs±0.23 (***$p < 0.001$). These phenotypes are similar to the *Afh/Afh* mutant mice alone, suggesting an epistatic role of *Fbxl3*. On the other hand, these animals showed a completely different phenotype to the *Afh/Afh* mice in LL conditions. While significant period lengthening (τ_{DD}25.741hrs±0.119) (***$p < 0.001$) along with a low amplitude of oscillations and splitting of activity was observed in the double heterozygous mice, the double homozygous mice were arrhythmic in LL. Apart from the period lengthening phenotype in the double homozygous mice, they were seen to show a reduced percentage of nocturnal activity in the LD phase of the circadian screen. The double homozygous *Fbxl3$^{Afh/Afh}$; Fbxl21$^{V68E/V68E}$* also showed a significant increase in the average wheel revolutions (6684.067±3111.89)(*$p < 0.05$) in LL which would suggest that these mice are hyperactive and hence it would be interesting to observe their behaviour in the open field test (Chapter 5)

Similar to the $Fbxl3^{Afh/Afh};Fbxl21^{V68E/V68E}$ phenotypes, the $Fbxl3^{Afh/Afh};Fbxl21^{P291Q/P291Q}$ also showed similar differences in the wheel-running parameters (Table 4.4). While, the double heterozygous $Fbxl3^{Afh/+};Fbxl21^{P291Q/+}$ and double homozygous $Fbxl3^{Afh/Afh};Fbxl21^{P291Q/P291Q}$ mice showed a significant increase in period length in DD ($Fbxl3^{Afh/+};Fbxl21^{P291Q/+}$ τ_{DD}24.28hrs±0.06; $Fbxl3^{Afh/Afh};Fbxl21^{P291Q/P291Q}$ τ_{DD}27.52hrs±0.167) compared to the wild-type animals , the double heterozygous mice show an increase in period length (τ_{LL}25.86hrs±0.22) with a reduced amplitude in LL. They also show splitting of activity in the LD phase of the screen. The double homozygous mice, on the other hand were arrhythmic in LL. Similar to the $Fbxl3^{Afh/Afh};$ $Fbxl21^{V68E/V68E}$ mice, the $Fbxl3^{Afh/Afh};Fbxl21^{P291Q/P291Q}$ mutants also showed a reduction in nocturnal activity along with hyperactivity in LL.

Figure 4.12: Circadian wheel running analysis of compound mutants generated in the Fbxl3^Afh/Afh; Fbxl21^V68E/V68E cross. A and B) Wild-type, double heterozygous and double homozygous mice for Fbxl3^Afh;Fbxl21^V68E mutation were entrained in 12hr LD conditions after which they were allowed to free run in DD for 2 weeks, followed by 2 weeks in LL conditions during which their wheel running activity was recorded. Compared to the wild-type animals, the Fbxl3^Afh/+; Fbxl21^V68E/+ double heterozygous mice had a significant lengthening of period resulting in τ_DD of 24.22hrs±0.04(***p<0.0005) and τ_LL of 25.74hrs±0.119(***p<0.001), similar to that of Fbxl3^Afh/+ and Fbxl3^Afh/Afh alone under DD conditions. Under LL, the double heterozygous animals (Fbxl3^Afh/+;Fbxl21^V68E/+) showed splitting of activity which was not observed in Afh/+ animals. Mice that were homozygous for both the Afh mutation in Fbxl3 and V68E in Fbxl21, Fbxl3^Afh/Afh; Fbxl21^V68E/V68E, significantly lengthened even more in DD (τ_DD=26.22hrs±0.06)(***p<0.0005) and were found to be arrhythmic in constant light conditions which is again not similar to Fbxl3^Afh/Afh alone. The screen also included a short 3hr light pulse or dark presented to the mice during the dark phase or light of the LD cycle respectively. The light pulse was presented to assess their ability to suppress activity during light conditions. The dark pulse on the other hand was used to assess their ability to show activity in the dark phase of the LD cycle. The light and dark pulses are a part of the circadian protocols carried out in the laboratory, however they were not considered for any measurements made during data analysis of studies presented here. The values are a representation of mean ±SEM obtained from 10 animals consisting of females and males. The SEM is represented as error bars on the graphs. Statistical significance is obtained from one way ANOVA using the post hoc Bonferroni test.

201

A

Fbxl3 +/+ ; Fbxl21 +/+ (WT)

Tau DD=23.68hrs±0.09;
Tau LL= 25.1hrs±0.045

Fbxl3 Afh/+ ; Fbxl21 T68E/+ (D.Het)

Tau DD=24.22hrs± 0.04;
Tau LL= 25.74hrs±0.119

Fbxl3 Afh/Afh ; Fbxl21 T68E/V68E (D.Hom)

Tau DD=26.22hrs±0.06;
Tau LL= Arrhythmic

B

Wheel running activity in DD

*** p<0.005

WT
Fbxl3Afh/+;Fbxl21V68E/+
Fbxl3Afh/AfhFbxl21V68E/V68E

Wheel running activity in LL

*** p< 0.001

WT
Fbxl3Afh/+;Fbxl21V68E/+
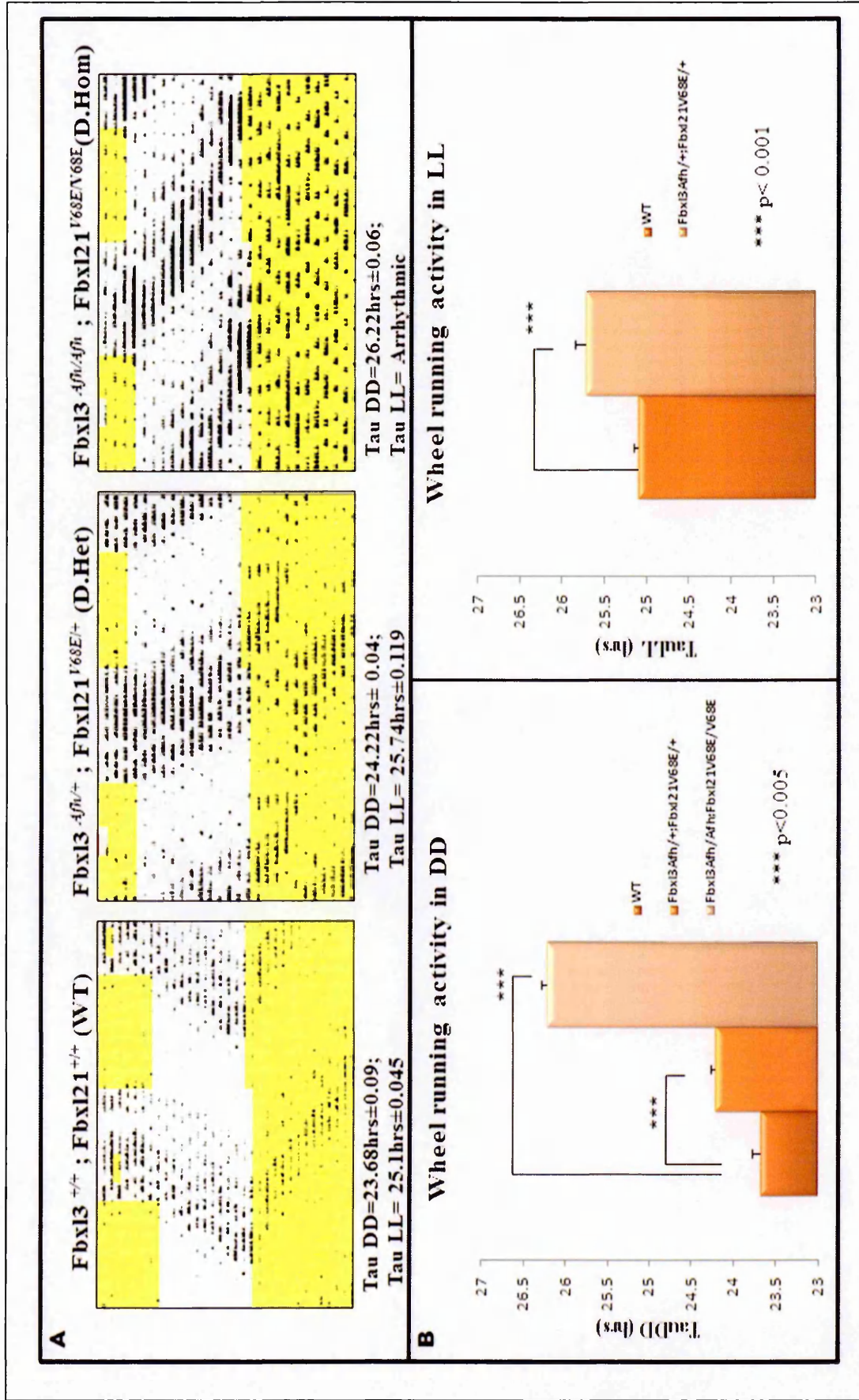
Figure 4.13: Circadian wheel running analysis of compound mutants generated in the Fbxl3$^{Afh/Afh}$; Fbxl21$^{P291Q/P291Q}$ cross. A and B) Wild-type, double heterozygous and double homozygous mice for Fbxl3^{Afh};Fbxl21^{P291Q} mutation were entrained in 12hr LD conditions after which they were allowed to free run in DD for 2 weeks, followed by 2 weeks in LL conditions during which their wheel running activity was recorded. The period length shown in the figure is a mean±SEM obtained from a group of animals. Compared to the wild-type animals, the Fbxl3$^{Af/+h}$; Fbxl21$^{P291Q/+}$ double heterozygous mice had a significant lengthening of period resulting in τ_{DD} of 24.2hrs±0.60 (***p<0.001) which significantly lengthened even more in Fbxl3$^{Afh/Afh}$;Fbxl21$^{P291Q/P291Q}$ double mutants with a τ_{DD} of 27.5hrs±0.173 (***p<0.001). The phenotypes of the compound mutants in DD were similar to Afh/Afh animals alone. Under LL conditions there was splitting of activity seen in Fbxl3$^{Afh/+}$; Fbxl21$^{P291Q/+}$ mice showing a period length of 25.86hrs±0.22. The double homozygous mice (Fbxl3$^{Afh/Afh}$; Fbxl21$^{P291Q/P291Q}$) on the other hand were seen to be completely arrhythmic in LL. This activity of the compound mutants in LL was not similar to the Afh/Afh animals alone, suggesting a potential function of Fbxl21 under LL conditions. This was a significant lengthening compared to the τ_{LL} of 25.1hrs±0.04 seen in wild-type mice. The values are a representation of mean obtained from 10 animals (for wild-type and double heterozygous) and 3 animals for Fbxl3$^{Afh/Afh}$; Fbxl21$^{P291Q/P291Q}$. Statistical significance is obtained from one way ANOVA using the post hoc Bonferonni test. . The screen also included a short 3hr light or dark pulse presented to the mice during the dark or light phase of the LD cycle respectively. The light pulse was presented to assess their ability to suppress activity during dark conditions. The dark pulse on the other hand was to assess their ability to show activity in the light phase of the LD cycle. The light and dark pulses are a part of the circadian protocols carried out in the laboratory and were not considered during data analysis of studies presented here.
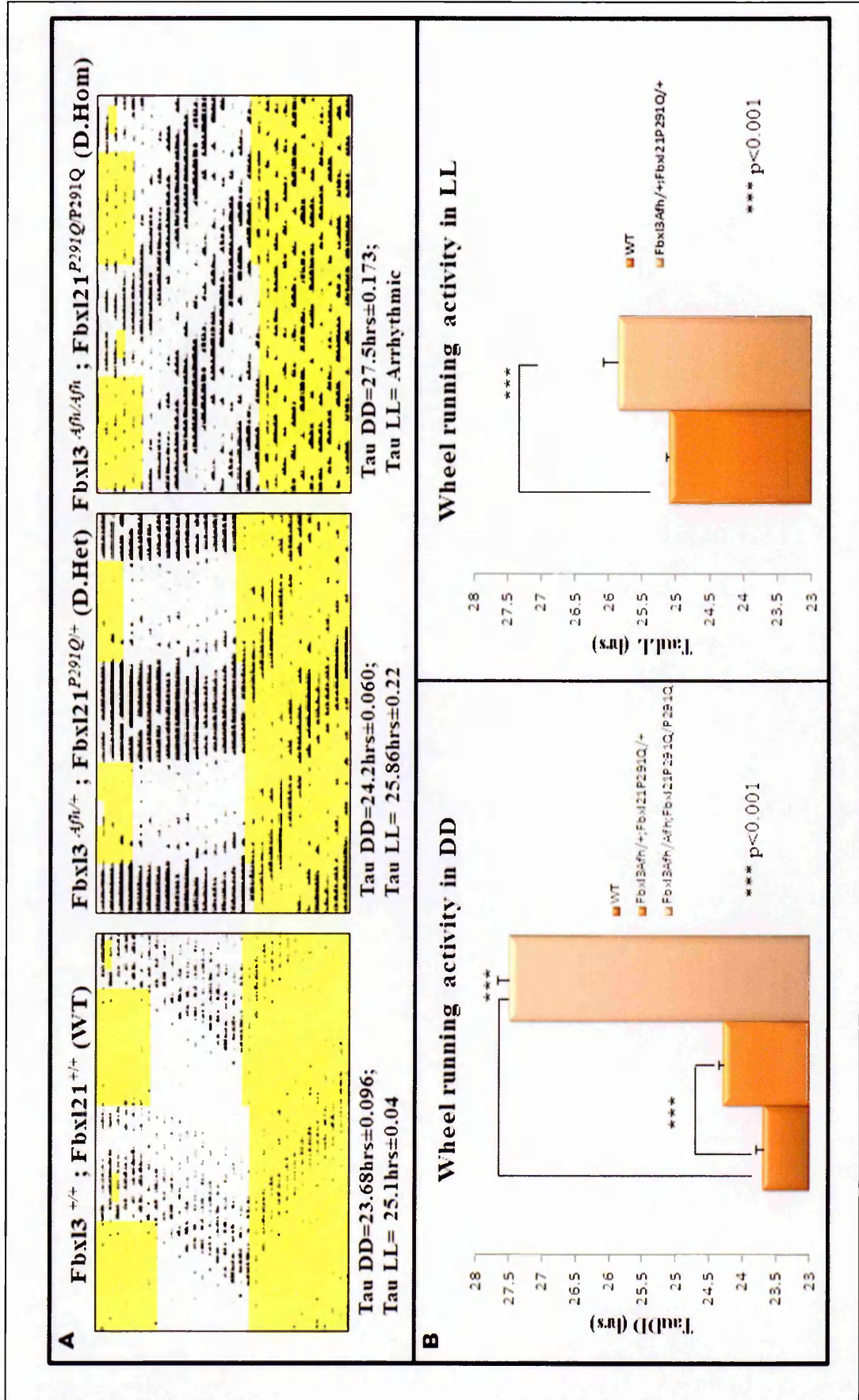
A

Fbxl3 $^{+/+}$; Fbxl21$^{+/+}$ (WT)

Tau DD=23.68hrs±0.096;
Tau LL= 25.1hrs±0.04

Fbxl3 $^{\Delta fh/+}$; Fbxl21$^{P291Q/+}$ (D.Het)

Tau DD=24.2hrs±0.060;
Tau LL= 25.86hrs±0.22

Fbxl3 $^{\Delta fh/\Delta fh}$; Fbxl21$^{P291Q/P291Q}$ (D.Hom)

Tau DD=27.5hrs±0.173;
Tau LL= Arrhythmic

B

Wheel running activity in DD

WT
Fbxl3Δfh/+;Fbxl21P291Q/+
Fbxl3Δfh/Δfh;Fbxl21P291Q/P291Q

*** p<0.001

Wheel running activity in LL

WT
Fbxl3Δfh/+;Fbxl21P291Q/+

*** p<0.001

	Fbxl3⁺/⁺;Fbxl21⁺/⁺	*Fbxl3ᴬᶠʰ/⁺;Fbxl21ⱽ⁶⁸ᴱ/⁺*	*Fbxl3ᴬᶠʰ/ᴬᶠʰ; Fbxl21ⱽ⁶⁸ᴱ/ⱽ⁶⁸ᴱ*
Avg. Revolution in LD	2649.30±618.89	2535.82±1136.78	4708.97±579.00
% of Nocturnal Activity	90.65±0.79	86.27±1.94	**80.76±2.31***
Avg. Revolution in DD	3623.91±927.99	3488.83±1257.45	8681.43±1915.28
Tau DD	23.684±0.09	**24.31±0.02***	**26.41±0.23***
Amplitude in DD	909.20±138.43	835.37±102.92	1137.58±152.37
Avg. Revolution in LL	2202.25±460.71	1861.99±605.06	**6684.067±3111.892 ***
Tau LL	25.1±0.045	**25.74±0.119****	Arrhythmic
Amplitude in LL	1102.826±104.97	**589.661±46.90*****	Arrhythmic

Table 4.3: Wheel running parameters investigated in Fbxl3ᴬᶠʰ/ᴬᶠʰ;Fbxl21ⱽ⁶⁸ᴱ/ⱽ⁶⁸ᴱ compound mutants. Parameters measured for *Fbxl3ᴬᶠʰ/⁺;Fbxl21ⱽ⁶⁸ᴱ/⁺* double heterozygous and *Fbxl3ᴬᶠʰ/ᴬᶠʰ;Fbxl21ⱽ⁶⁸ᴱ/ⱽ⁶⁸ᴱ* double homozygous mice were compared to those measured in wild-type animals. Apart from the period length in DD and LL, the parameters (except amplitude in LL) were similar in wild-type and *Fbxl3ᴬᶠʰ/⁺; Fbxl21ⱽ⁶⁸ᴱ/⁺* animals. The double heterozygous mice showed a significant increase in period length (τ_{DD}=24.31hrs±0.02)(***p<0.001) with a high amplitude. However, under LL, these mice show splitting of activity and hence although they show a significant period lengthening (τ_{LL}=25.74hrs±0.119)(**p<0.005) compared to wild-type mice (τ_{LL}=25.1hrs±0.045), their amplitude of oscillations in LL is significantly low (589.661± 46.90)(***p<0.001). In the case of *Fbxl3ᴬᶠʰ/ᴬᶠʰ; Fbxl21ⱽ⁶⁸ᴱ/ⱽ⁶⁸ᴱ* double homozygous mice, they show a reduced percentage of nocturnal activity during the LD phase of the circadian screen (* p<0.05). In DD, the double homozygous mice show a period length of 26.41hrs±0.23 (***p<0.001) that is similar to the period length of *Afh/Afh* mutants alone. Further under LL conditions these mice were seen to be more active than the double heterozygous and wild-type mice. However, they were seen to be arrhythmic in LL, suggesting a potential role of *Fbxl21* in light responsiveness. All the values represent mean±standard errors from 10 animals which were a mix of sex. One way ANOVA with Bonferronni post hoc test was used to test statistical significance with *p<0.05, **p<0.005, ***p<0.001.

	$Fbxl3^{+/+};Fbxl21^{+/+}$	$Fbxl3^{Afh/+};$ $Fbxl21^{P291Q/+}$	$Fbxl3^{Afh/Afh};$ $Fbxl21^{P291Q/P291Q}$
Avg. Revolution in LD	2649.301±618.89	3822.76±1866.70	2616.723±722.96
% of Nocturnal Activity	90.65±0.79	88.61±1.53	**67.181±4.54*****
Avg. Revolution in DD	3623.91±927.99	5014.69±1845.01	11047.19±6626.041
Tau DD	23.684±0.09	**24.28±0.06*****	**27.52±0.167*****
Amplitude in DD	909.20±138.43	928.67±125.67	1207.27±173.054
Avg. Revolution in LL	2202.25±460.71	4375.225±1486.11	**10233.59±6938.307***
Tau LL	25.1±0.045	**25.86±0.22*****	**Arrhythmic**
Amplitude in LL	1102.826±104.97	**716.31±98.93****	**Arrhythmic**

Table 4.4: Circadian wheel-running parameters determined in the $Fbxl3^{Afh/Afh};$ $Fbxl21^{P291Q/P291Q}$ compound mutants. Significant differences were observed in the period length, τ, in DD and LL conditions in both $Fbxl3^{Afh/+};$ $Fbxl21^{P291Q/+}$ and $Fbxl3^{Afh/Afh};$ $Fbxl21^{P291Q/P291Q}$ animals. While a significant period lengthening was observed in $Fbxl3^{Afh/+};$ $Fbxl21^{P291Q/+}$ (τ_{DD}=24.28±0.006) and $Fbxl3^{Afh/Afh};$ $Fbxl21^{P291Q/P291Q}$ (τ_{DD}=27.52±0.0167)(***p<0.001) under DD conditions, this was similar to the phenotype of Afh/Afh mutant mice alone. The double homozygous mice also showed a reduction in the percentage of nocturnal activity during the LD phase (67.181±4.54). Unlike the similarities between the Afh/Afh mutants and $Fbxl3^{Afh/Afh};Fbxl21^{P291Q/P291Q}$ compound mutants in DD and although there was an increase in period length of the double heterozygous animals in LL (τ_{LL}=25.86±0.022)(***p<0.001), these animals were seen to show splitting of activity in LL and the double homozygous mice were arrhythmic. The values mentioned here are a mean±SEM of 10 wild-type and double heterozygous animals and 3 double homozygous animals. Significance is tested using one way ANOVA and Bonferronni post hoc analysis where *p<0.05, **p<0.005 and ***p<0.001.

4.4 DISCUSSION

4.4.1 *Fbxl21* V68E and P291Q are potentially functional

Although forward and reverse genetics approachs using ENU mutagenesis have their share of advantages and disadvantages, they are still widely used to identify roles of particular genes in day to day mechanisms. This has been shown using the Harwell Mutagenesis Program on several occasions in various fields from development to metabolism and behaviour. It has also played a vital role in unveiling novel circadian loci that result in an abnormal circadian phenotype (Bacon, Ooi et al. 2004).

Since the reverse genetics approach supported by ENU mutagenesis is a quicker way than generating knockouts to identify underlying roles and mechanisms of genes, the Harwell ENU archive was screened for mutations in the recently identified F-box protein, *Fbxl21*. Though there was a total of five mutations identified in the two main domains, F-box domain and putative CRY-binding domain of *Fbxl21* (Figure 4.1A), the two mutations V68E and P291Q were thought to be potentially functional; as reasoned below (Figure 4.1 A and 4.2).

H77H, L36P and S28F were some of the other mutations identified in the F-box domain screen, however P291Q was the only mutation identified in the putative CRY-binding domain. One of the reasons both the mutations, V68E and P291Q were important was the amino acid conservation in the immediate region of the mutations across different species and especially between the two F-box proteins, FBXL3 and FBXL21 (Figure 4.3B, C). Also, the structural changes in the substituted amino acids made these mutations interesting to study further (Figure 4.1 B). For example, in the V68E mutation, the non-polar amino acid valine has been substituted with a negatively charged polar amino acid, thus changing the properties

of the side chain. Also the substitution of P291Q makes this mutation structurally interesting because the loss of proline results in the loss of an aliphatic side chain. Proline plays an important role in formation of beta turns in the secondary structure of proteins and hence the loss of proline may result in a change of FBXL21 protein structure and hence the change is likely to be functional.

The V68E mutation lies in the middle of the F-box domain that is important in protein-protein interactions (Feldman, Correll et al. 1997; Skowyra, Craig et al. 1997). F-box proteins have an important function of associating substrates, via their secondary motifs, to other components of the SCF complex where the substrates are polyubiquitinated and finally degraded.

Thus, a mutation in F-box proteins would potentially disrupt this entire process resulting in dysregulation of protein turnover mechanisms leading to an abnormal circadian phenotype. There are several known examples of this, a classic one being a point mutation in the leucine rich repeat domain of the F-box protein, *Fbxl3*, due to which there is reduction of interaction between the F-box protein and the substrate, resulting in stabilisation of protein levels and hence an abnormal phenotype (Godinho, Maywood et al. 2007; Siepka, Yoo et al. 2007). Another instance revealing the importance of F-boxes is *Fbxo11*, a mutation in which causes chronic otitis media (Hardisty-Hughes, Tateossian et al. 2006) where the ubquitination and protein turnover mechanisms are impaired. To our knowledge the V68E mutation is the first example of a mutation in the F-box domain of a mammalian circadian F-box protein rather than in a secondary domain. A potential consequence of this V68E mutation could be disrupting interactions between components of the SCF complex and also impaired interactions between the F-box protein and its substrates.

Cry genes are the key regulators of circadian oscillations. Both *Cry1* and *2* are known to be involved in negative regulation of transcription. There is not much information about the exact roles of these genes in the negative feedback mechanisms, however it is a known fact that they are substrates of the F-box protein, FBXL3 and due to the homology between the *Fbxl3* and *Fbxl21* in the putative CRY binding domain, the mutation P291Q was thought to be potentially functional (Busino, Bassermann et al. 2007; Godinho, Maywood et al. 2007; Siepka, Yoo et al. 2007). *In-vitro* studies have identified that a stop codon resulting in the loss of the CRY-binding domain can impair the interaction between the substrate and the proteasomal degradation pathway (Dardente, Mendoza et al. 2008). CRY proteins have the ability to inhibit the CLOCK-BMAL1 activation, and CRY's ability to inhibit activation is reduced in the presence of F-box proteins. However, it was predicted that a mutation in the F-box motif did not reduce the inhibitory effects of CRY resulting in abnormal circadian rhythmicity (Dardente, Mendoza et al. 2008).

A second reason the P291Q mutation was potentially interesting was the results of an *in-vitro* assay carried out by our collaborator Dr. Hugues Dardente at the University of Aberdeen *(Appendix 6)*. They introduced the mutation in the full-length *Fbxl21* sequence cloned into a pCSII-Myc tagged vector and performed an *in-vitro* luminometry assay. The assay was analysed as the luminescence readout of *Rev-erba*:Luc reporter. In addition to activation of *Per* and *Cry* genes, CLOCK-BMAL1 is also able to regulate the transcription of *Rev-erba* and *Rora*, components belonging to the secondary regulatory loops in mammals. In the presence of CRY1, this activation of *Rev-erba* and *Rora* is inhibited and hence a lower luminescence is obtained. On the other hand, when *Fbxl21*-Wt is co-transfected with *Cry1*, the inhibitory function of CRY1 is diminished due to the degradation of CRY1 by FBXL21, resulting in higher luminescence. However, this was not the case with the P291Q mutant

where the F-box protein was not as efficient in diminishing the inhibitory effects of CRY1 resulting in a lower luminescence readout. Hence, this mutation was thought to be a hypomorph.

In addition to this lies another complexity related to CRY1 function. Although FBXL21 binds to CRY1, it has been seen that CRY2 is a preferable target of FBXL21. However in our *in-vitro* luminometry assay when recombinant *Cry1* is co-transfected with *Fbxl21*-Wt, it has been seen that FBXL21-Wt has been able to inhibit CRY1 regulation of transcription. This leads us to think that the presence of an unknown mechanism (may be absence of *Fbxl3*) confers a role to FBXL21 in inhibiting CRY1 function. One of the reasons might be sequestration of CRY1 in the cytoplasm by FBXL21. This can be further investigated by co-transfecting *Fbxl21* and *Cry1 in vitro* and determining the localisation of CRY1 across circadian time.

4.4.2 FBXL21 shuttles between the nucleus and cytoplasm

Localisation studies help obtain a partial assessment about the function of a particular gene and regulatory events that control this localisation are crucial in maintaining the 24-hr circadian clock (Kipreos and Pagano 2000). In our localisation studies, we transiently transfected the wild-type and mutant (V68E and P291Q) Myc tagged forms of *Fbxl21* in U2OS cells, synchronised them using 10μM forskolin following which we collected the cells at specific times and performed immunofluorescence using an anti-Myc antibody.

Our results show that FBXL21-Wt is mainly cytoplasmic after 6hrs of forskolin shock whereas the mutants are nuclear and cytoplasmic at the same time (Figure 4.5A). After 12hrs, FBXL21-Wt translocates into the nucleus and is distributed between the nucleus and the

cytoplasm whereas the mutant FBXL21 remains nuclear and cytoplasmic (Figure 4.5B). There have been several evidences that the use of serum or compounds such as forskolin activate multiple signalling pathways which result in activation of the expression of circadian genes which enforce nuclear localisation of the genes (Balsalobre, Marcacci et al. 2000; Yagita, Tamanini et al. 2001). Serum shock influences intracellular pathways where the mitogen activated protein kinases, p42/44, activate the phosphorylation of Ca^{2+}/cAMP responsive element binding protein (CREB) which in turn enforces the nuclear localisation of the PER proteins. Forskolin on the other hand, directly activates the phosphorylation of CREB by elevating the cAMP levels and activating the protein kinase A pathway (Balsalobre, Brown et al. 2000; Yagita and Okamura 2000). Thus, this mechanism of synchronisation of cells with forskolin may have an effect on the mutant FBXL21 localisation.

Another possibility for differences observed in localisation studies could be due to the epitope tag (Myc) used to tag FBXL21. Discrepancies have been reported in localisation of CRY proteins due to the different epitope tags being used. When localisation of CRY-GFP was studied, CRY appeared to be mitochondrial (Kobayashi, Kanno et al. 1998). However the same protein, CRY, when tagged with V5 or HA, was seen to translocate into the nucleus (Kobayashi, Kanno et al. 1998; Thresher, Vitaterna et al. 1998). Thus, it was would be interesting to perform the immunofluorescence of FBXL21 Wt and mutant recombinant protein with different epitope tags or even by using α-FBXL21 antibody.

The difference in the localisation between the Wt and mutants may not cause any effect on the interaction of the F-box protein with its substrates. The nature of F-box proteins is such that they are found to be normally distributed equally in both the nucleus and cytoplasm and that even if the localisation of the Wt and mutant is different or identical, the binding of the F-box protein with the Skp1 component of the SCF complex is not affected as

211

ultimately the proteasomal degradation occurs in the cytoplasm (Kipreos and Pagano 2000). Hence, we cannot state whether there may be an effect of FBXL21 localisation on substrate interaction.

4.4.3 FBXL21 interacts with cryptochromes, CRY1 and CRY2

Circadian oscillations that involve complex inter-relating networks are maintained by a balance of protein synthesis and degradation. This is very tightly regulated by the E3 ubiquitin ligases which transfer ubiquitin (Ub) molecules on substrates that are targeted for proteasomal degradation. A very well known E3 Ub ligase complex is the Skp-Cullin-F-box protein (SCF) complex, where the F-box is responsible for identifying and targeting specific substrates for proteasomal degradation (Ho, Tsai et al. 2006). Although there are several known F-box proteins, none except β-TRCP (that degrade PER proteins) (Ohsaki, Oishi et al. 2008) was known to target any circadian clock proteins until the *Fbxl3^{Afh}* mutant was identified where it was shown that the F-box protein, FBXL3, interacts with the key regulators of the negative feedback, CRY1 and CRY2 (Busino, Bassermann et al. 2007; Godinho, Maywood et al. 2007). With the identification of the second F-box protein, *Fbxl21*, it was shown that in addition to FBXL3, FBXL21 is also able to interact with CRY1 *in-vitro* (Dardente, Mendoza et al. 2008). To investigate the interaction of FBXL21 with both CRY1 and CRY2 further, *in-vitro* studies were carried out. The interaction of the V68E and P291Q mutants with both CRY proteins was also determined.

In-vitro experiments were performed using Cos7 cells, where *Fbxl21*-Wt and mutants were transiently co-transfected with *Cry1* or *Cry2*, after which the whole cell extracts were subjected to co-immunoprecipitations as described in section 2.11. The results in Figure 4.6

show that FBXL21-Wt interacts with both CRY1 and CRY2. When the interaction of the mutants is normalised to the FBXL21-Wt interaction, it can be seen that, the interaction between the mutant FBXL21 and CRY1 and CRY2 is greatly reduced (Figure 4.6B), with significant reduction in interaction between FBXL21-V68E and P291Q and CRY2 (Figure 4.6B right panel). Considering this result along with the localisation of FBXL21 we considered whether the interaction between the FBXL21 and CRY2 is more likely to occur in the cytoplasm than in the nucleus. Further experiments such as co-localisation of FBXL21 and CRY2 across circadian time could be investigated.

Reduced interactions were expected with FBXL21-P291Q protein which is a result of a mutation in the CRY-binding domain of FBXL21. It has already been shown that an FBXL21 recombinant protein lacking the CRY-binding domain is unable to bind to CRY1, indicating that an intact CRY-binding domain is necessary for interactions with CRY proteins (Dardente, Mendoza et al. 2008). In this study, the FBXL21-P291Q mutant protein shows a rather weak interaction with both CRY1 and CRY2 when compared to the interaction with FBXL21-Wt and this is consistent with findings with the *Fbxl3*^{Afh} mutation. *Fbxl3*^{Afh} was a result of a mutation in the secondary motifs (leucine rich repeats) of the F-box protein, *Fbxl3*. This domain is mainly involved in binding the substrate to the F-box protein, which in turn interacts with the Skp-Cullin complex. Due to this mutation, there was reduced interaction between the FBXL3 and CRY proteins. As a consequence, CRY is spared from proteasomal degradation resulting in the lengthening of the circadian clock (Busino, Bassermann et al. 2007; Godinho, Maywood et al. 2007). In the interaction studies as shown in Figure 4.6B, it can also be seen that there is a reduced interaction between FBXL21-V68E and CRY1/2, which is surprising. V68E is a mutation in the F-box domain, which functions as an adapter to bind the F-box-substrate complex to the Skp-Cullin complex. The reason why the reduced interaction is

surprising is due to the fact that it is the secondary motif viz. LRR that recognises and binds to the specific phosphorylated substrate and hence a mutation in the F-box domain would be expected not to have any effect. However, one possibility could be that the V68E mutation would have an indirect effect through the Skp-Cullin complex on the interaction between FBXL21 and CRY1/2 *in-vitro*, which needs to be investigated and is beyond the scope of this body of work.

4.4.4 CRY2 is targeted for degradation by FBXL21

It is evidently known that post-translational modifications are important and control aspects of clock mechanisms by modulating protein-protein interactions. One such process is the timely degradation and protein turnover of the negative regulators such as the PER and CRY proteins, failure in which results in abnormal period lengths and circadian oscillations, as seen in the *Afh* mutant (Godinho, Maywood et al. 2007; Siepka, Yoo et al. 2007). Degradation takes place via the F-box complex, a component of the E3-Ub ligase complex, that targets phosphorylated substrates, interacts with the SCF complex, polyubiquitinates the targeted substrate which is finally degraded via the proteasome.

It is known that F-box proteins target specific phosphorylated substrates. For example β-TRCP1 and 2 targets mammalian PER proteins (Ohsaki, Oishi et al. 2008), SLIMB and JETLAG are F-box proteins that target *Drosophila* PER (Ko, Jiang et al. 2002) and TIM (Koh, Zheng et al. 2006) proteins respectively (Ko, Jiang et al. 2002) and FWD1 targets the clock protein FREQUENCY in *Neurospora* (He, Cheng et al. 2003). With previous knowledge about the function of FBXL3 and due to sequence homology and interaction between the second F-box protein, FBXL21 and CRY1/2, it was thought that FBXL21 also targets CRY.

214

In-vitro studies carried out in Cos7 cells co-transfected with *Fbxl21*-Wt and *Cry1/2*-HA followed by CHX treatment shows that FBXL21-Wt tends to target CRY2 rather than CRY1 for degradation (section 4.3.4 and figure 4.7). This complements the previous finding by Hugues Dardente et al. (2008) showing that more than FBXL21, FBXL3 tends to target CRY1 protein degradation. Levels of CRY1 are reduced drastically after 8hrs of CHX due to the presence of FBXL3, unlike in the presence of FBXL21 when there is a significantly higher amount of CRY1 (higher than with FBXL3) present at the same time. FBXL3 is known to target not only CRY1 but is also shown to degrade CRY2 in the same manner *in-vitro* (Busino, Bassermann et al. 2007). Thus, it is possible that the two FBXL paralogues target CRY2 proteins for degradation; however, CRY1 seems to be a unique substrate for FBXL3. It is worth mentioning that the initial conclusions from these studies are purely due to overexpression of F-box and CRY plasmids and the cells used for this (Cos7 cells) do not contain any clock components (Yagita, Yamaguchi et al. 2000), which rules out the possibility of interactions with other endogenous clock proteins.

The importance of F-box proteins are well understood with the help of mutations in the proteins which result in differences in protein localisation or abnormal circadian activity. β-TRCP1 and 2 are known to target phosphorylated PER2 proteins for degradation. When these β-TRCP proteins are suppressed *in-vitro* with siRNA they lead to dampening of the circadian clock. Moreover, a mutation in both *β-Trcp's* results in an increase of unphosphorylated PER2 levels due to a lack of interaction between the mutated β-TRCP and the Skp1 component of the SCF complex (Ohsaki, Oishi et al. 2008).

Another example as stated earlier is the *Fbxl3* mutation resulting in the *Afh* phenotype in mice. When the *Fbxl21*-V68E and P291Q mutants were used to investigate their effects on CRY2 degradation, as expected, the P291Q mutation had a significant effect on CRY2

degradation, whereas V68E had only a very slight effect (Figure 4.8). The CRY2 proteins were spared from proteasomal degradation and their levels were stabilised when overexpressed and treated with CHX *in-vitro*. These results suggest that there might be a specific sequence in CRY2 that enables the binding of either F-box protein, which is absent in CRY1 thus having different interactions and functional consequences. It has previously been identified that although CRY1 and CRY2 have highly similar amino acid sequences, their C-terminals remain very unique (Harada, Sakai et al. 2005), which may account for their different affinity for the two F-box proteins.

Secondly, one must also consider the fact that CRY2, being sensitive to the proteasome degradation pathway, also undergoes dual phosphorylation by two different protein kinases in a sequential manner at positions four residues apart. Thus, it could be possible that, once phosphorylated by a kinase, CRY2 undergoes degradation mediated by one F-box protein, and due to the second phosphorylation event a few residues away, it is targeted by the second F-box protein (Kurabayashi, Hirota et al.)

The V68E mutation having an effect on interaction with CRY1 and CRY2 and little effect on CRY2 degradation is consistent with the idea that the mutation will affect circadian mechanisms in an indirect manner. For example, the mutation may well affect the phosphorylation states of CRY2 (as is the case with PER2 due to the β-Trcp mutation) apart from the earlier mentioned possibilities of effects within the Skp-Cullin complex. However, all these predictions will only be valid after determining the *in vivo* phenotype of these mutant animals by investigating their circadian wheel-running behaviour.

4.4.5 *Fbxl21$^{P291Q/P291Q}$* mice show a short circadian phenotype

Although *in-vitro* studies prove extremely useful in explaining or predicting *in vivo* mechanisms or behaviour, it has been essential to verify the conclusions gathered from *in-vitro* studies *in vivo*. Thus, the typical circadian wheel running screen was carried out on the mice which were wild-type, heterozygous and homozygous for V68E and P291Q mutations for the second F-box protein, *Fbxl21*.

The wheel running screen was based on a standard protocol, where the mutant mice with all the genotypes were allowed to entrain in a 12hr LD schedule for 7 days, following which they were allowed to free-run in DD conditions for 2 weeks.

Not surprisingly, the *Fbxl21$^{V68E/+}$* and *Fbxl21$^{V68E/V68E}$* mice were no different from the wild-type *Fbxl21$^{+/+}$* mice (Figure 4.10A, B). A circadian phenotype (short or long period) usually arises from quicker degradation or slower rate of degradation of proteins such as PER or CRY that act as negative regulators of transcriptional activation (Godinho, Maywood et al. 2007; Siepka, Yoo et al. 2007; Ohsaki, Oishi et al. 2008). In case of the V68E mutation in the F-box domain of FBXL21, the only effect seen *in-vitro* was the reduced interaction between FBXL21 and CRY1/2, which had no significant effect on the degradation of the negative regulators, hence ruling out the possibility of expecting a phenotype. Thus, the reduction in interaction can be interpreted as an indirect effect of the mutation where there is an intact C-terminal domain to bind to the substrate. The effect the mutation may have is in terms of the interaction with the Skp-Cullin complex itself which needs to be investigated. FBXL21 interaction with the SCF complex might be necessary for CRY interaction. However, even reduced interaction with the SCF complex might be sufficient for CRY protein degradation.

This can be explained well with an example that has been studied well in *Neurospora* in which the F-box protein, FWD1, interacts with and degrades phosphorylated FREQUENCY (FRQ) protein. Mutagenesis studies in FRQ identified that this protein had several phosphorylation sites that are important for regulating FRQ functions. These sites were identified to be spread across different regions of FRQ protein that suggested that phosphorylation followed by ubiquitination and degradation is not solely dependent upon one phosphorylation event, and that it may be a dynamic process that is required for the fine and timely regulation of the FRQ, which in turn fine tunes the circadian clock (He, Cheng et al. 2003).

On these similar lines, the *Fbxl21$^{P291Q/P291Q}$* mutant mice show a period 0.58hrs shorter in DD conditions (Figure 4.11 A and B). This mutation has been shown to have a reduced interaction with CRY1 and CRY2, further stabilising CRY2 levels *in-vitro*. The *Cry2$^{-/-}$* mice on the other hand have no CRY2 protein which results in a longer period and is consistent with our *Fbxl21$^{P291Q/P291Q}$* phenotype (van der Horst, Muijtjens et al. 1999). The effects of the mutations *in-vitro* and consequently on the *in vivo* clock could be due to dual phosphorylation of CRY2 proteins and consequent differences in degradation mechanisms.

It is has been known that mammalian CRY2 undergoes sequential events of phosphorylation by two different kinases. CRY2 proteins are first required to be phosphorylated at the Ser557 site by a newly identified kinase, dual-specificity tyrosine-phosphorylated and regulated kinase 1A (DYRK1A). This acts as a priming phosphorylation for glycogen synthase kinase-3β (GSK-3β) that phosphorylates CRY2 at Ser553. *In-vitro* studies detect no phosphorylated CRY2 levels in the absence of DYRK1A (Harada, Sakai et al. 2005). However, it is worth mentioning that the Ser557 site is specific to CRY2 and is present in the C-terminus region of CRY2, which is unique and different from the CRY1 C-

terminus. Hence, taking this into account, the following model can be hypothesised to explain the phenotype of the $Fbxl21^{P291Q/P291Q}$ mutant due to dual phosphorylation of CRY2.

As shown in Figure 4.14, PER and CRY proteins are translated in the cytoplasm, where during the CRY2 protein accumulation stage, it undergoes phosphorylation by DYRK1A at Ser557. Ser557 phosphorylated CRY2 could then be immediately targeted by the F-box protein, FBXL21, for proteasomal degradation. DYRK1A-phosphorylated CRY2 could also be able to form a complex with PER2. The CRY2-PER2 complex then translocates into the nucleus to undergo the second phosphorylation event by GSK-3β. At the same time, it is assumed that DYRK1A phosphorylation speeds up the second phosphorylation event by GSK-3β at Ser553, which is assumed to take place in the nucleus, following which it is degraded by FBXL3. This is in agreement with the lack of nuclear function of CRY2 (as shown in Chapter 3) which has been shown to have very limited transcriptional repressor function (as CRY2 is degraded twice, once by FBXL21 in the cytoplasm and further targeted for degradation by FBXL3). It should further be noted that in the presence of CRY proteins, PER2 proteins are stabilised and spared from proteasomal degradation (Yagita, Tamanini et al. 2002). Under wild-type conditions, with the degradation of CRY2, PER2 is also degraded initiating the next transcriptional-translational feedback loop. This may also account for *Per2* repression observed in $Cry1^{-/-}$; $Fbxl3^{Afh/Afh}$ double mutants, where CRY2 levels are upregulated and stabilised. Due to the higher CRY2 levels in the double mutants, PER2 levels are also stabilised (hence lower *Per2* mRNA levels) resulting in an increase in period length.

The events that are thought to regulate CRY2 levels take place along with the phosphorylation and degradation of CRY1 by GSK-3β and FBXL3 respectively. Translated CRY1 proteins are able to interact with FBXL21 in the cytoplasm but do not undergo degradation as it is not phosphorylated by DYRK1A. The CRY1 proteins are instead thought

to be sequestered in the cytoplasm by FBXL21 through some unknown mechanisms. Alternatively, CRY1 proteins are also able to form a complex with PER2 which then translocates into the nucleus where it gets phosphorylated by GSK-3β followed by degradation by FBXL3. In case of the $Cry2^{-/-}$ mice, since CRY1 is not targeted by DYRK1A, CRY1 proteins have to be accumulated in the nucleus, where they can get phosphorylated by GSK-3β; since this is a slower process, there is slower degradation of CRY1 proteins, and hence the $Cry2^{-/-}$ phenotype (longer period). This is in contrast to $Cry1^{-/-}$, where CRY2 proteins, as described earlier, undergo dual phosphorylation which may be quicker due to the presence of DYRK1A, which degrades CRY2 proteins quicker and hence the shorter phenotype in $Cry1^{-/-}$ mice.

In the case of $Fbxl21^{P291Q/P291Q}$ mice, since CRY2 levels are stabilised, there may be accumulation of CRY2 in the cytoplasm where it first gets phosphorylated by DYRK1A followed by the faster second phosphorylation event by GSK-3β and is finally degraded by FBXL3, hence expressing a shorter circadian phenotype. It is worth mentioning that DYRK1A levels are found to be at a higher level during the increasing accumulation of CRY2 levels. On the contrary, GSK-3β levels start increasing from late night until early morning (ZT/CT 22-2).

If this hypothesis is considered true, then it will be interesting to investigate the redundancies between the two F-box proteins, *Fbxl3* and *Fbxl21*.
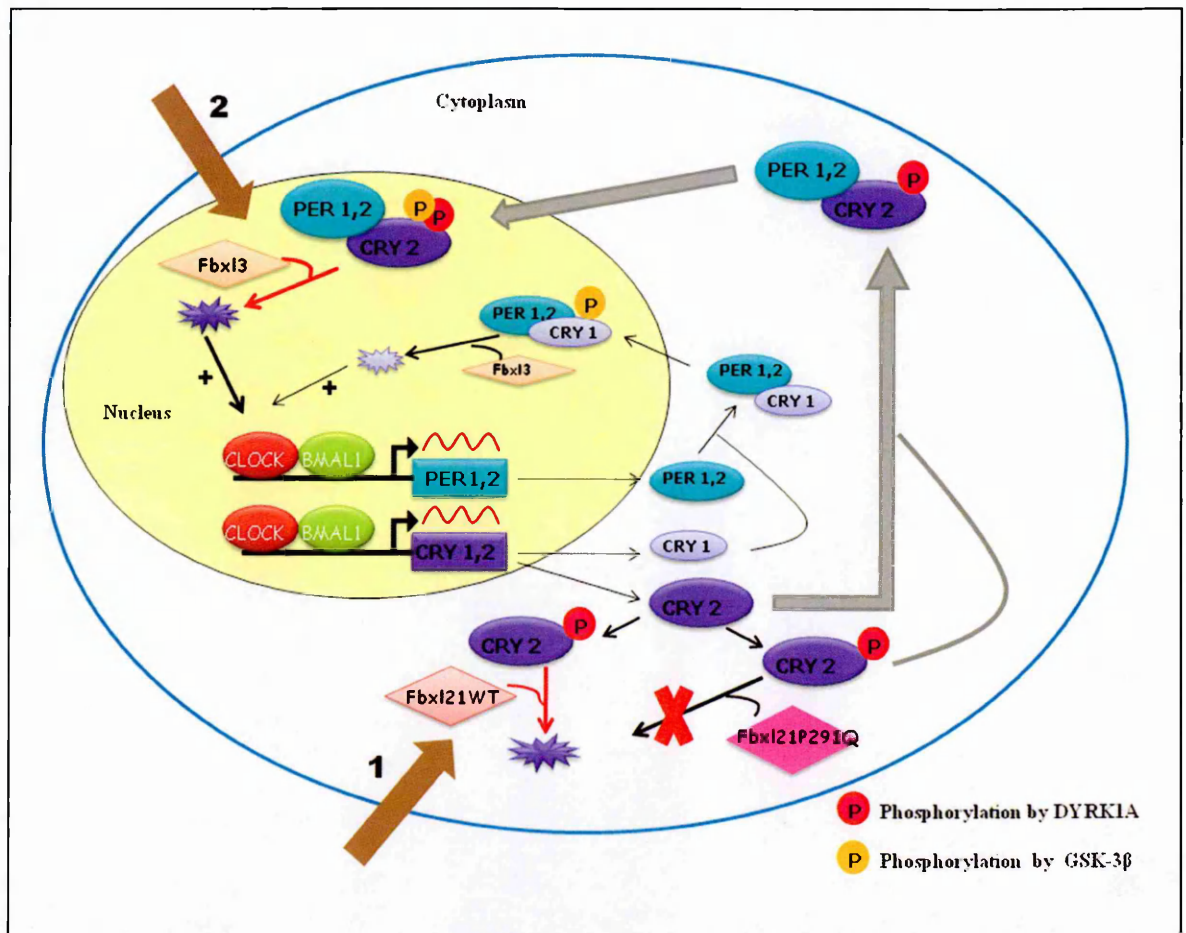
Figure 4.14: Hypothesis model of CRY2 phosphorylation. This figure is based on a hypothesis, showing dual phosphorylation of CRY2, first in the cytoplasm by DYRK1A (pink circle), that is assumed to speed up the subsequent phosphorylation by GSK-3β (yellow circle), which is then targeted by FBXL3 (orange diamond) for proteasomal degradation. DYRK1A–mediated phosphorylated CRY2 may be a target of the second F-box protein, FBXL21 (light pink diamond), for proteasomal degradation in the cytoplasm. DYRK1A-phosphorylated CRY2 is also able to form a complex with PER2 which then translocate into the nucleus to undergo GSK-3β-mediated phosphorylation followed by FBXL3 targeted degradation of CRY2. In case of the *Fbxl21*$^{P291Q/P291Q}$ (dark pink diamond), there is stabilisation of CRY2, due to which, it does not undergo degradation in the cytoplasm; while on the other hand, the GSK-3β-mediated phosphorylation is quicker, degrading CRY2 quickly, thus explaining the short period length phenotype. However, since the DYRK1A phosphorylation site is specific to CRY2, CRY1 is thought to form a complex with PER2 to translocate into the nucleus where it then undergoes phosphorylation by GSK-3β followed by FBXL3-mediated degradation. Although CRY1 is able to interact with FBXL21, it is thought that CRY1 is sequestered in the cytoplasm by some unknown mechanisms due to which FBXL21 is able to inhibit CRY1 mediated transcriptional repression.

4.4.6 Functional redundancy between the Fbxl paralogues

Most of the important mammalian circadian genes are present as paralogous pairs e.g *Per1, Per2*; *Cry1, Cry2*; *Clock* and *Npas2* in which each of the genes in every pair would have to be knocked out in order to confer arrhythmicity. However, not every gene in the pair is functionally similar; one gene may be more essential in regulation than the other. Also the effect of knockout of one gene from the pair may differ. The functional similarities that could vary between paralogues can be explained with the example of *Bmal1* and its paralogue *Bmal2*. It was hypothesized that if *Bmal1* (*Mop3*) and its paralogue *Bmal2* (*Mop9*) were not redundant then any mutations or complete absence of *Bmal1* would cause significant changes in the circadian clock. However this hypothesis was partly proved right when *Bmal1$^{-/-}$* (*Mop3$^{-/-}$*) mice were found to be arrhythmic in DD, showed no activity with no changes in the behaviour after a light pulse was administered. Thus, it was concluded that *Bmal1* and *Bmal2* did not have a redundant function. However, *Bmal1* positively regulates transcription of *Bmal2* and so in the absence of *Bmal1*, transcription of *Bmal2* is also inactivated, hence the arrhythmicity in *Bmal1$^{-/-}$* mice also expressing an epistatic interaction between the *Bmal* paralogues (Shi, Hida et al. 2010; Bunger, Wilsbacher et al. 2000). On the other hand it was shown that when *Bmal2* was constitutively expressed, it was able to rescue the phenotype of *Bmal1$^{-/-}$* mice.

In our *Fbxl3$^{Afh/Afh}$*; *Fbxl21$^{V68E/V68E}$* and *Fbxl3$^{Afh/Afh}$;Fbxl21$^{P291Q/P291Q}$* mutant mice, it was seen that under constant darkness (DD) and constant light (LL) conditions, the effect of the *Afh* mutation appears to be stronger than that of *Fbxl21* (Figure 4.12 and 4.13). Although the animals are seen to entrain well to the LD schedule, once allowed to free-run in DD followed by LL, the double heterozygous and double homozygous mice show a phenotype

similar to the *Afh* heterozygous and homozygous mice with $Fbxl3^{Afh/+}$; $Fbxl21^{V68E/+}$, $Fbxl3^{Afh/+}$;$Fbxl21^{P291Q/+}$ with a period length of 24.22hrs±0.06 for both in DD (Figure 4.12, 4.13). Under the same conditions (DD), the period length further increases to 26.22hrs±0.06 in $Fbxl3^{Afh/Afh}$; $Fbxl21^{V68E/V68E}$ mice and becomes even longer to 27.5hrs±0.173 in $Fbxl3^{Afh/Afh}$; $Fbxl21^{P291Q/P291Q}$ mice (Figure 4.12, 4.13). From these results, it can be said that under DD conditions there exists an epistatic interaction between the two *Fbxl* paralogues, where *Fbxl3* modifies the effects of *Fbxl21*. However, to test redundancies, analysis of complete gene knockouts will be necessary.

Secondly, in order to investigate if the F-box genes are regulated by their paralogues, F-box gene expression must be investigated *in vivo*. Based on the phenotype observed in the $Fbxl3^{Afh/Afh}$; $Fbxl21^{V68E/V68E}$ and $Fbxl3^{Afh/Afh}$;$Fbxl21^{P291Q/P291Q}$ compound mutants that mimic the *Afh* mutation, it is thought that *Fbxl3* is involved in the regulation of *Fbxl21* and that *Fbxl21* transcription is *Fbxl3*-dependent. To determine this, endogenous gene expression studies will have to be carried out first in the $Fbxl3^{Afh/Afh}$ mice and *Fbxl21* mutant mice followed by expression analysis in the double mutants. These studies will be similar to those carried out by Bunger et al. (2000) and Shi et al. (2010) in which it was shown that in the absence of *Bmal1*, the mRNA levels of *Bmal2* were at basal levels. Hence it was thought that in wild-type mice, *Bmal2* expression is regulated by *Bmal1* and so knocking out *Bmal1* essentially results in a $Bmal1^{-/-}$; $Bmal2^{-/-}$ condition resulting in an arrhythmic wheel running phenotype.

4.4.7 Behavioural consequences of constant light conditions

Light acts as a major circadian entraining agent in various organisms due to which under normal circumstances, the endogenous oscillations are entrained to the environmental light/dark conditions. Light is transmitted through the eye to the master pacemaker, the suprachiasmatic nucleus (SCN) which controls the autoregulatory feedback loops involving various clock genes (Reppert and Weaver 2002). The importance of light is clearly understood when an animal, if given a light pulse during early circadian night, has a delayed onset of activity while shows advanced onset of activity if given a light pulse during late circadian night. The SCN is connected to the retina through the retinohypothalamic tract (RHT) that directly reacts to the light input and hence, when the SCN-retina path is disrupted, there is a complete loss of entrainment in the LD cycle (Dijk and Archer 2009). Thus, it is interesting to find behavioural differences in LL conditions in various circadian mutants in order to find the underlying mechanisms of the light input pathway or varied functions of clock genes.

All our animals were screened using the same circadian protocol consisting of a 12hr LD schedule followed by two weeks in DD and LL conditions. While the $Fbxl21^{P291Q/P291Q}$ mutants seem to show a shorter circadian period in DD, they show a significantly longer period in LL compared to wild-type animals. The striking difference in these animals between the DD and LL phenotypes is the period lengthening in $Fbxl21^{P291Q/+}$ (Figure 4.11 A, B). Although the heterozygous and homozygous animals showed a varied phenotype in DD (slightly higher in heterozygotes), the lengthening seems to be dose dependent. A similar lengthening phenotype was also observed in the second $Fbxl21$ mutant, V68E, where the animals with two copies of the mutated F-box domain ($Fbxl21^{V68E/V68E}$) show a significantly longer period length in LL suggesting that $Fbxl21$ and their domains or their interacting

partners are light responsive and may play a role in the light input pathway of the circadian system (Figure 4.10 A, B). Saying this, it should be noted that both the *Fbxl21* mutants that are homozygous are well entrained to the 12hr LD schedule, making it difficult to predict their function, as a defect in the input pathway would result in loss of entrainment or changes in phase angles or phase shifts, which is not apparent in these mice.

An even more complex situation arises when $Fbxl3^{Afh/Afh}$; $Fbxl21^{V68E/V68E}$ and $Fbxl3^{Afh/Afh}$; $Fbxl21^{P291Q/P291Q}$ mice are screened for their circadian activity and parameters using the previously described protocol. The behaviour of these animals in LD and DD conditions are detailed in the previous section 4.4.6 and Figure 4.12, 4.13. However, in LL, the double heterozygous animals show extreme lengthening with a difference of ~2.5hrs between τ_{DD} and τ_{LL}. The double homozygous animals on the other hand are arrhythmic in LL. When analysed on a scale of 31hrs, there appears to be a very weak rhythm with a τ of ~31hrs, with low amplitude. When considered on 24hr scale, they both appear arrhythmic.

Previously studies have been carried out to understand the behaviour of mice housed under constant light conditions where it has been shown that, at the molecular level, expression of the clock genes, *Per1* and *Per2*, are affected by light (Shearman, Zylka et al. 1997). Both these genes were found to be highly expressed in the SCN and the eye in LL conditions. Further Shearman et al. (1997) showed that although both the genes were expressed in the two most important controlling regions of the circadian system, differences in expression of *Per* genes were observed. At the molecular level, the expression of *Per1* and *Per2* RNA are high during subjective day at CT3, 6, 9 and 15 in the SCN. However, this was not the case with the gene expression of *Per2* analysed in the eye, where high levels of *Per2* were found at CT 9, 15, 18 and 21 (Shearman, Zylka et al. 1997). Apart from differences in their expression, *Per1* and *Per2* were also thought to be regulated differently; *Per1* was

thought to cause phase delay, whereas differences in *Per2* regulation was thought to result in phase advance, showing that differences lay in the regulation of *Per* gene expression at the molecular level (Yan and Silver 2002; Munoz, Peirson et al. 2005). *In-situ* hybridisation, carried out in the SCN to determine gene expression of *Per1*, *Per2*, *Cry1* and *Cry2* under LL conditions show that all the genes and their protein products were rhythmic and showed circadian rhythmicity in LL. The exception to these results was the expression of *Cry2* and its protein product CRY2 which showed altered expression pattern in LL. PER2 protein levels on the other hand were also reported to be at an elevated and stabilised level across circadian time under LL, which was hypothesized to be a result of the inhibition of a kinase that is responsible for the degradation of PER2 (Munoz, Peirson et al. 2005). Thus, it was thought that the degeneration of PER2 is the contributing factor in lengthening the period in LL and that the rhythmic expression of clock genes such as *Cry1*, *Cry2* and *Per1* are PER2-independent in LL. Hence investigation of PER and CRY levels in the retina of *Fbxl3$^{Afh/Afh}$*; *Fbxl21$^{V68E/V68E}$* and *Fbxl3$^{Afh/Afh}$*; *Fbxl21$^{P291Q/P291Q}$* compound mutants would help us explain the phenotype better.

Abnormal circadian activity in LL also indicates the role of important photoreceptors and photopigments. Surprisingly it has been identified in humans and mice that rhodopsin and the other colour opsins are not essential for circadian photoreception. For example retinal degeneration (*rd*) mutant mice are visually blind but respond normally to circadian photoreception (Yoshimura and Ebihara 1998). Similarly human patients who lose all rods and cones have no consciousness of light, respond normally to environmental LD conditions (Czeisler and Dijk 1995; Wee and Van Gelder 2004). Hence, there may be one or more photopigments in the retina that may be involved in photoreception.

The other component that might attenuate the behaviour or play a role in regulation of circadian oscillations in LL is cryptochromes that act as photoreceptors in *Drosophila*. *Cry* belongs to the photolyase family and is not only expressed in photosensitive organs but is also expressed in most mouse and human tissues. It is found to be highly expressed in the retinal ganglion cells and the inner nuclear layer of the inner retina (Miyamoto and Sancar 1998). In order to identify the role of photopigments, Selby et al. (2000) generated triple mutant mice, *rd/rd; Cry1$^{-/-}$; Cry2$^{-/-}$*, that lack all the rods and most of the cones, and lack both cryptochrome genes. They then carried out a number of behavioural and molecular tests. At the behavioural level, it was shown that although *Cry1$^{-/-}$; Cry2$^{-/-}$* double mutants are arrhythmic in DD, they seem to entrain normally in LD conditions. In addition, oscillating *Per2* gene expression observed in the SCN of the double mutant mice under LD conditions suggested the presence of a phototransductive pathway. The triple mutants on the other hand were found to be arrhythmic in LD and DD. Photoresponsiveness could arise from colour opsins present in the surviving cone cells. It could also be due to incomplete retinal degeneration and/or due to the presence of a photoreceptor. For example, melanopsin, an opsin recently identified in the inner retina (Provencio, Rodriguez et al. 2000). At the molecular level, although high levels of *Per* gene were identified in the SCN of the triple mutants, a marked reduction in the light induced *c-fos* transcription was also observed. This reduction in *c-fos* levels was thought to be a compromise due to the lack of cryptochromes. It was then suggested that a functional redundancy between cryptochromes and the classical opsins exists in transducing information in the presence of light. This is thought to modulate the behaviour of mice (Selby, Thompson et al. 2000). Hence, it may be for this reason there was no difference in the *Fbxl3$^{Afh/Afh}$* ; *Fbxl21$^{V68E/V68E}$* mice in LD, and mice entrained normally to the LD cycle.

Since both the F-box mutations, *Fbxl3^{Afh}* and *Fbxl21^{V68E}/Fbxl21^{P291Q}* have an effect on the interaction and subsequently on degradation of CRY proteins, it would be essential to determine the expression of *Cry* and *Per* in the double mutants. The reason for arrhythmicity in LL could be contributed to expression of *Cry* which could result in elevated levels of CRY protein that in turn lead to extended additional inhibition itself, as *Cry* is a much stronger transcriptional repressor than *Per* (Langmesser, Tallone et al. 2008). To date, there is not much known about the effect of constant light on clock gene expression, mainly *Cry* and *Per*, which are important regulators of the feedback loop. The two contradictory evidences show that *Per2* RNA levels are low with reduced amplitude in LL that result in altered phase of PER2 (Sudo, Sasahara et al. 2003). On the other hand, another study by Munoz et al. (2005) show that, although *Per2* is rhythmic with high amplitude, there is a constitutively elevated expression of PER2 in the SCN of mice maintained under LL conditions (Munoz, Peirson et al. 2005). Hence, due to these discrepancies, there is no definite evidence of the actual mechanism that regulates expression of clock genes in mice. Thus, determining the expression of these genes in appropriate mutants will help us identify vital mechanisms and hopefully help explain the observed phenotypes under LL.

Finally, changes in the SCN cannot be ruled out as a result of constant illumination. It has been known that light stimulates the retinal ganglion cells that form the RHT and the transmitters they release affect the SCN. Histological evidence shows the RHT is widely spread throughout the ventral and dorsal side of SCN and the light responsive neurons of the SCN are located ventrally. Outside the SCN, there are very few neurons that respond to light (Meijer and Schwartz 2003) Thus, any changes in the circadian behaviour may result in functional changes of these neurons or vice-versa. Ohta et al. (2005) carried out single cell real time studies using *Per1* promoter driven GFP fluorescence to identify the changes in the SCN

228

when mice are exposed to LL. They reported robust individual cellular rhythms within the SCN dissected from mice that were arrhythmic in LL. However, the neuronal rhythms from the same mice were significantly desynchronised, suggesting that constant light changes the phase organisation of neurons within the SCN and does not abolish the function of the neurons per se. Thus, arrhythmic behaviour can be a result of damping of circadian oscillation due to the loss of cellular synchrony (Ohta, Yamazaki et al. 2005)

4.5 SUMMARY

In summary, although the exact role of *Fbxl21* is not completely understood yet, these studies have given us a deeper insight into the recently identified clock controlled gene. Having screened the Harwell ENU DNA archive, two mutations in two highly conserved domains, the F-box domain and the putative CRY-binding domain, were identified. V68E, a valine to glutamic acid substitution was identified in the F-box domain and P291Q, a proline to glutamine substitution, was identified in the predicted CRY-binding domain of *Fbxl21*.

In-vitro studies were carried out using full length *Fbxl21* sequences (both wild type and mutated) cloned into the pCSII-Myc vector. Localisation experiments showed that the mutations retained FBXL21 in nuclear and cytoplasmic compartments across circadian time, as opposed to shuttling between the nucleus and cytoplasm in wild-type conditions. The mutations also resulted in a significantly reduced interaction between CRY1 and CRY2 due to which it was predicted that degradation of these proteins would be affected, ultimately resulting in a circadian phenotype. It was surprising to see that FBXL21-Wt targeted CRY2 more than CRY1 for degradation. While the V68E mutation did not show any difference in degrading CRY1 and CRY2, the P291Q mutation led to stabilisation of CRY2, which ultimately not surprisingly resulted in a circadian phenotype *in vivo*. The *Fbxl21*$^{P291Q/P291Q}$ mice showed a significantly shorter period length with τDD of 23.10hrs±0.073 compared to *Fbxl21*$^{+/+}$ with a period length of 23.68hrs±0.094. *Fbxl21*$^{V68E/V68E}$ mice showed no differences in circadian phenotype in the wheel running screen.

As *Fbxl21* is the paralogue of a well characterised F-box gene, *Fbxl3*, which is also known to be involved in CRY degradation, it was interesting to investigate the redundancies between the two F-box paralogues. Compound mutants were generated by crossing the

Fbxl3$^{Afh/Afh}$ and *Fbxl21$^{V68E/V68E}$* or *Fbxl21$^{P291Q/P291Q}$* mice. Double heterozygous and double homozygous mutant mice were screened for their wheel running activity, which consisted of a 12hr L:D schedule for 7 days, followed by 2 weeks in DD and finally for 2 weeks in LL conditions. It was clearly seen from these screens that these mutants mimic the phenotype of the *Fbxl3$^{Afh/Afh}$* mutant alone in DD. The effect of the *Fbxl3^{Afh}* mutation is much stronger than the mutations in *Fbxl21* and there exists an epistatic interaction between the two *Fbxl* paralogues. It is thought that the ideal way to investigate the redundancies between these two paralogous pairs is by generating complete gene knockouts rather than generating mice with point mutations.

Finally, having determined these results there a number of studies yet to be carried out to understand completely how *Fbxl21* plays a role in circadian time keeping. Studies such as the modification of phosphorylation sites (specifically Ser557 targeted by DYRK1A) of CRY2 to look at the interaction between FBXL21 and CRY2/1 are needed. If the interaction is attenuated further, it is clear that FBXL21 interaction is DYRK1A dependent. Further studies also include carrying out gene expression analysis in the *Fbxl21$^{P291Q/P291Q}$* and *Fbxl3$^{Afh/Afh}$* homozygous mice in addition to gene expression studies in the *Fbxl3$^{Afh/Afh}$*; *Fbxl21$^{V68E/V68E}$* and *Fbxl3$^{Afh/Afh}$*;*Fbxl21$^{P291Q/P291Q}$* compound mutants.

5 <u>CHAPTER FIVE</u>: Behavioural Analysis of F-box Mutants

5.1 INTRODUCTION

Circadian rhythms existing in the majority of organs, such as liver, kidney, heart and other brain regions, are all under the control of the SCN. It has been known that the SCN is able to influence and control various aspects of physiology and behaviour mainly through its humoral response and neuronal circuitry. It is due to this control that any disturbances in the circadian system can have adverse effects on the behaviour of an organism. Thus, mutants with disturbed circadian oscillations may have an effect on the functioning of the central nervous system. This could be either due to primary deficits in the master pacemaker itself or deficits in the functioning of the oscillators in other areas of the brain. There have been several evidences that show associations of several neurological and psychiatric disorders with disturbances in sleep. For example, abnormal rapid eye movement (REM) sleep is observed in patients suffering from schizophrenia (Zarcone, Gulevich et al. 1968; Zarcone, Azumi et al. 1975). Various parameters of sleep are under the control of circadian timing, and behavioural, psychiatric and neurological disorders may in turn be under the indirect control of the circadian clock.

Circadian gene polymorphisms are widely studied in humans in order to identify exact clock gene functions. In humans, people with clock gene polymorphisms either have morning or evening preference that are associated with differences in response to the Horne-Ostberg questionnaire (Horne and Ostberg 1976). Additionally, people with an extreme morning or evening preference often also have complex behavioural phenotypes that are associated with psychiatric and mood disorders. Xu et al. (2005) reported that out of five patients suffering from familial advanced sleep phase syndrome (FASPS), four of these have a history or clinical

features of depression (Xu, Padiath et al. 2005). Similarly, patients suffering from the delayed sleep phase syndrome (DSPS) also show symptoms of depression (Drennan, Klauber et al. 1991; Shirayama, Shirayama et al. 2003; Xu, Padiath et al. 2005). Examples of clock gene polymorphisms occurring in core oscillator genes not only show deficits in oscillator mechanisms, but they are also linked to depressive disorders. For example the circadian clock regulator *Cry2* has been found to be associated with bipolar disorder and depression. Studies have shown that variation in *Cry2* expression levels can be associated with depression. *Cry2* RNA levels are found to be low in the blood collected from patients suffering with bipolar disorder compared to healthy controls (Lavebratt, Sjoholm et al. 2010).

It addition to the effects of circadian disturbances resulting in behavioural disorders, it could also be that dysfunctional clock mechanisms could merely be symptoms of various diseases. Evidences report the disturbances in circadian and sleep mechanisms are secondary to the primary brain circuitry deficits in the neurodegenerative Alzheimer disease (Wisor, Edgar et al. 2005; Ambree, Touma et al. 2006). Similarly, in the transgenic model of Huntington's disease, Huntington R6/2 mutant mice, altered clock gene expression and rhythms were observed (Morton, Wood et al. 2005). Examples of other disease conditions with circadian disturbances include schizophrenia, bipolar disorders and unipolar depression.

It has recently been shown that the clock gene *Fbxl21* is associated with schizophrenia in humans (Chen, Wang et al. 2008). Linkage analysis of chromosome 5q resulted in the possibility that interleukin 9 (*IL 9*) and *Fbxl21* could be associated with schizophrenia. Further analysis reported that there was no association of IL-9. However, out of 14 samples, 6 consecutive SNPs present in and around *Fbxl21* showed a significant association (Chen, Wang et al. 2008). On the other hand, *Fbxl21,* as seen in the previous chapters, is a clock gene with its protein product presumably playing a role in regulating CRY2 proteins in mice (Dardente,

Mendoza et al. 2008). Hence, it will be interesting to investigate the behavioural effects of *Fbxl21* mutations in mice.

Interestingly, studies have shown that by treating circadian disturbances, a diseased condition can also be reversed. For example, the mutant *Per2* mice that show an increased consumption of alcohol can be reversed by glutamate transporters such as *Eaat1* that alter circadian gene expression and reduce the glutamatergic activity, suggesting that neurotransmitters are able to modulate the expression and regulation of circadian genes which in turn modulate the functions of the neural circuitry processing information to other brain areas (Spanagel, Pendyala et al. 2005). Similarly, lithium that is an inhibitor of GSK3β activity is able to reverse behavioural disturbances observed in the *Clock* mutant. Lithium is able to promote the nuclear entry of clock proteins, which in turn undergo proteasomal degradation and result in activation of the positive regulators of the circadian clock (Martinek, Inonog et al. 2001; Iitaka, Miyazaki et al. 2005; Yin, Wang et al. 2006).

Hence continuous research in the field of circadian rhythms and identification of new clock genes involved in major neurological, psychiatric and other behavioural disorders will help to develop drugs that are predominantly circadian based. This in turn will contribute to the improvement of public health.

5.1.1 Aims of chapter

With associations known between circadian clock genes and behavioural and neurological disorders, the $Cry1^{-/-}; Fbxl3^{Afh/Afh}$, $Fbxl21^{V68E/V68E}$ and $Fbxl21^{P291Q/P291Q}$ mutants were screened through a primary phenotyping pipeline. A selection of tests, namely the open field, acoustic startle response, pre-pulse inhibition (PPI) and grip strength, were carried out to investigate if the mutants suffered from anxiety, sensorimotor gating deficits and motor deficits.

With $Cry1^{-/-};Fbxl3^{Afh/Afh}$ showing a significantly higher number of average wheel revolutions in LL during the circadian wheel running analysis (Chapter 3, section 3.2.2) and with known associations of human $Fbxl21$ and schizophrenia (Chen, Wang et al. 2008), it was interesting to see the behaviour of the mutant mice in the above mentioned tests.

5.2. RESULTS

5.2.1 Open field

In order to test the exploratory, locomotor and anxiety-like behaviour of mice in a novel environment, mice are put through the open field test. Mice have a natural tendency to avoid brightly illuminated and novel open areas, thus the open field arena is an anxiogenic stimulus to the mice. By measuring parameters such as time spent by the mice in the centre and periphery of the testing arena, the anxiety induced behaviour of the animal can be assessed. This test is also useful for clinicians measuring the effects of anxiogenic and anxiolytic drugs. As anxiety levels depend on environmental conditions, while performing this test it is important to maintain constant and appropriate temperature, lighting, humidity and ventilation conditions.

The open field test is carried out in an arena virtually divided into a periphery and centre with homogenous lighting intensity of 150-200lux in the centre of the arena. The mice are then allowed to explore the arena for 30mins, during which several parameters are recorded by the EthoVision software (Noldus Ltd.). Parameters measured were the time spent by the mice in the centre (sec), time spent in the periphery (sec), latency of first occurrence of mice in the centre of the arena, the total distance travelled (cm), the average speed (cm/s) and the percentage of total time spent in movement.

Mutants $Cry1^{-/-}$; $Fbxl3^{Afh/Afh}$; $Fbxl21^{V68E/V68E}$ and $Fbxl21^{P291Q/P291Q}$ were assessed for their anxiety levels and exploratory behaviour in the open field arena. A group of 10 animals (mix of males and females) for each mutant were tested and compared to the behaviour of 10 congenic C57BL/6J controls that were age matched, however were not littermate controls.

Student's t-test was used to determine any statistical significance. The $Cryl^{-/-}$; $Fbxl3^{Afh/Afh}$ mutants spent significantly more time in the centre (p=0.007) than in the periphery (Figure 5.1). Although the distance moved and the velocity of control mice and the mutant $Cryl^{-/-}$; $Fbxl3^{Afh/Afh}$ mice were similar, the mutants spent more time moving around the arena. The mutants also appeared in the centre within 30secs of the start of the test compared to the controls which appeared in the centre after ~1.5mins, suggesting a hyperactive behaviour in the $Cryl^{-/-}$; $Fbxl3^{Afh/Afh}$ mice.

There were no significant differences observed between $Fbxl21^{V68E/V68E}$ and control mice (Figure 5.2). Although the mutants spent less time in the centre, they appeared in the centre of the arena (latency of first occurrence) earlier than the control mice. The $Fbxl21^{V68E/V68E}$ mice also moved less in terms of distance moved, duration and velocity of movement.

The $Fbxl21^{P291Q/P291Q}$ mutants were significantly different from the wild-type controls in each of the measured parameters (Figure 5.3). These mice spent significantly more time in the periphery (p=0.003) than in the centre (p=0.002), with a greater latency to appear in the centre (p=0.01). Although this suggests that these mice are more anxious, they also spent less time moving and hence a lower distance was covered with a reduced velocity (total moving duration, distance and velocity p=0.002).

Figure 5.1: Behaviour of Cry1$^{-/-}$; Fbxl3$^{Afh/Afh}$ double mutants in the open field test. Parameters such as time spent in centre and periphery, total duration and distance of movement, velocity of movement and the latency of first occurrence in the centre were measured for each of the mutants. Student's t-test revealed that these mice spent significantly more time in the centre (p=0.007) than in the periphery. There were no other significant differences observed in the other parameters measured between the wild type control mice and the Cry1$^{-/-}$; Fbxl3$^{Afh/Afh}$ mice. A total of 10 mutant animals (congenic) and 10 wild-type (C57BL/6J, congenic) of the same age were tested. The 20 animals tested were a mix of males and females. The average values with SEM are represented in the graphs.

Figure 5.2: Behaviour of Fbxl21$^{V68E/V68E}$ homozygous mice in the open field test. These mice showed no significant differences compared to the C57BL/6J wild-type mice. All the parameters measured (total time spent in the centre, periphery, total duration and distance of movement, velocity of movement and the latency of first occurrence in the centre) were no different to the wild-type mice. The behaviour of 10 mutants (males and females mixed and congenic) were compared to 10 wild-type congenic mice (males and females mixed) that were of similar age. The Students t-test was used to determine statistical differences. The values represented on the graph are mean values of 10 animals of each genotype with SEM represented as error bars

Figure 5.3: Behaviour of Fbxl21$^{P291Q/P291Q}$ homozygous mice. Results show that these mice are anxious and exhibit significant differences in the parameters measured. The mutants spend significantly less time in the centre (p=0.002) than in the periphery (p=0.003). They display a lower tendency to explore a novel area (latency of first occurrence in centre p= 0.01). However, the Fbxl21$^{P291Q/P291Q}$ mutants also tend to move significantly less in terms of duration (p=0.002), distance (p=0.002) and velocity (p=0.002). The behaviour of these mice were compared to C57BL/6J wild-type mice of similar age. A total of 10 mutant animals (mixed background) and 10 wild-type (C57BL/6J, congenic) with a mix of females and males were tested. The average values with SEM are represented in the graphs. Student's t-test was used to determine statistical significance.
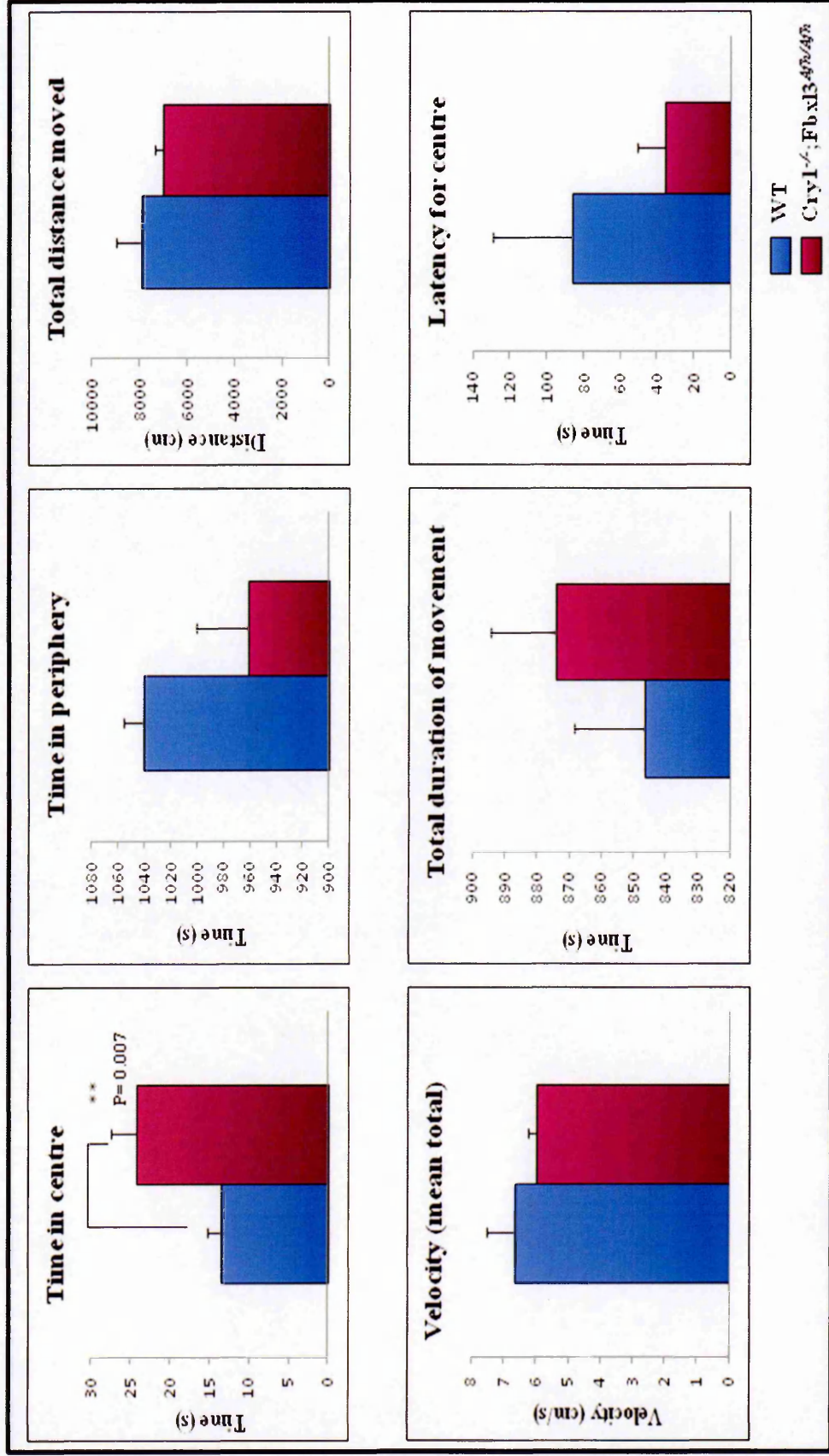
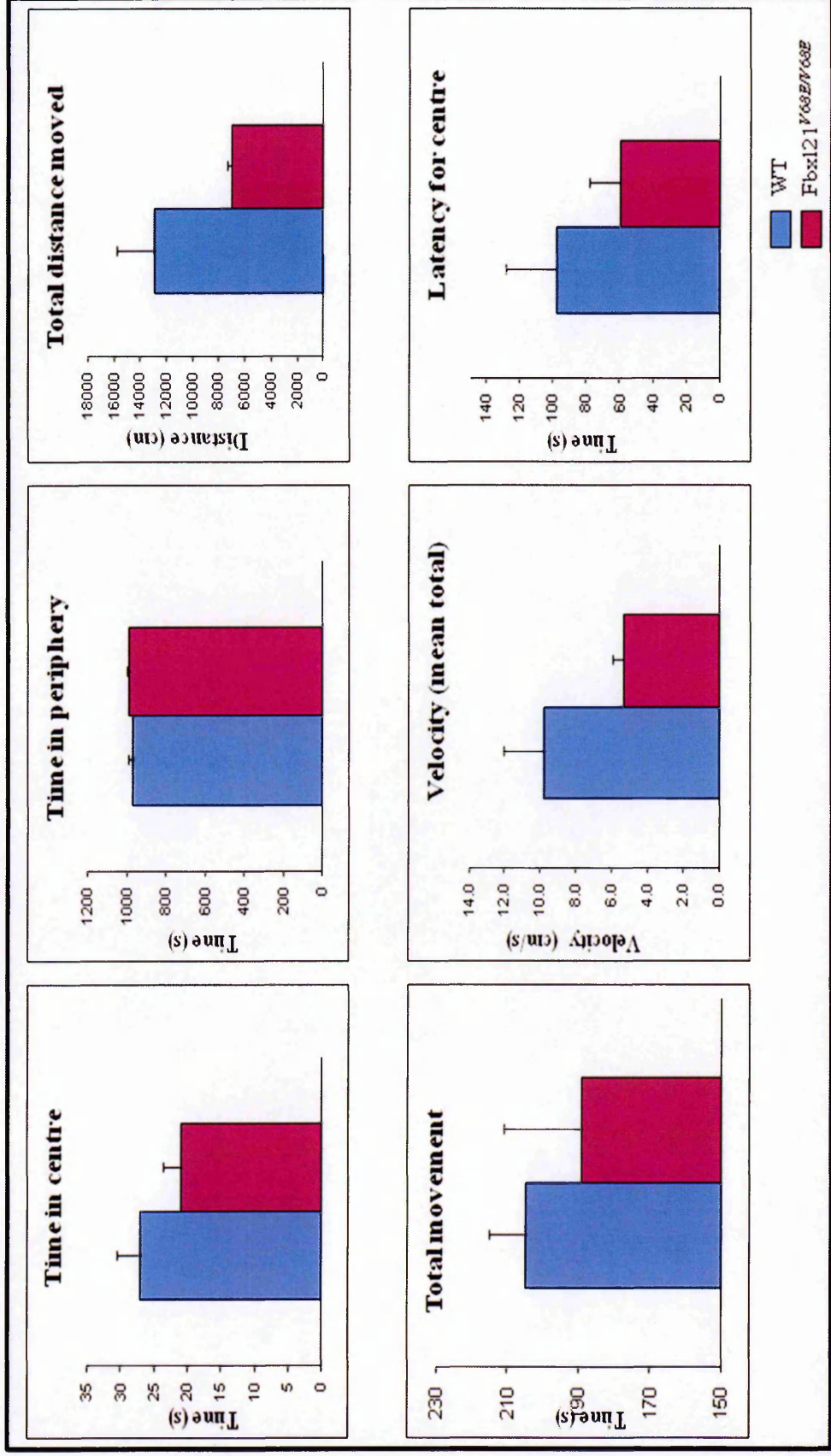*Figure 5.1: Behaviour of Cry1⁻ᐟ⁻; Fbxl3ᴬᶠʰ⁄ᴬᶠʰ double mutants in the open field test.*

Figure 5.2: Open field test in Fbxl21$^{V68E/V68E}$ mutant mice.
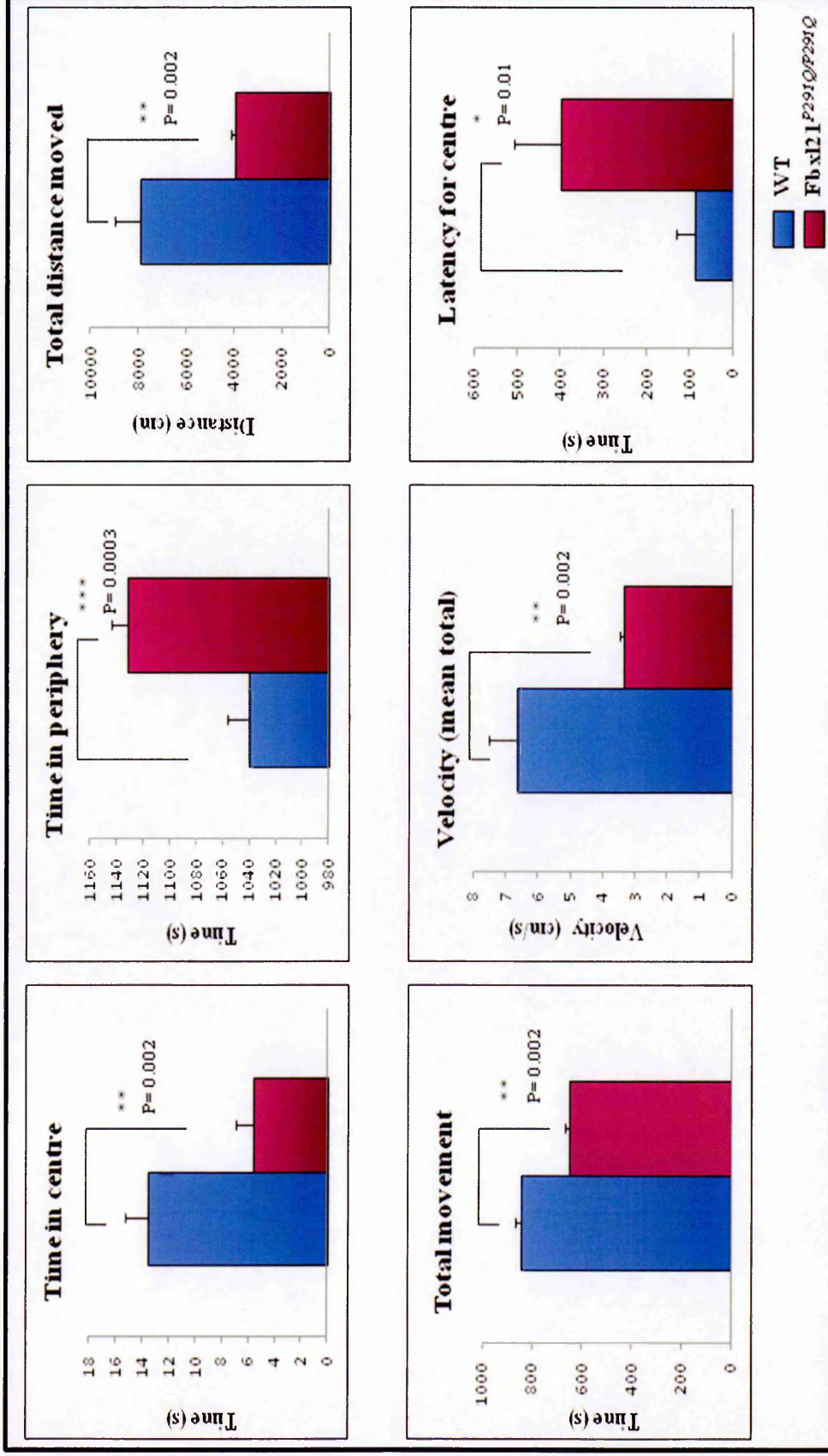
Figure 5.3: Behaviour of Fbxl21$^{P291Q/P291Q}$ *homozygous mice.*

5.2.2 Acoustic startle and Pre-pulse inhibition (PPI)

This test is used as a measure of sensorimotor gating in which a weak external stimulus (pre-pulse) reduces or inhibits the whole body startle response that is generated by an external stimulus (pulse). The stimuli presented are usually acoustic but tactile and light stimuli can also be given. Pre-pulse inhibition (PPI) is a neurological phenomenon that is found in several species from mice to humans. The test reflects the ability of an organism's nervous system to adapt to a stronger stimulus when a prior warning stimulus is presented. However, this ability is known to be attenuated not only in schizophrenic patients but also a number of other conditions. On the other hand, while a decrease in startle response reflects sensorineural deafness, an increase in startle response could be an indication of psychotic disturbances.

The test was performed in a single session where the mice were placed in sound proof chambers containing an inner chamber connected to a loud speaker and a startle platform. This chamber was connected to the computer where the startle responses of mice were recorded and finally analysed using the EthoVision software. To begin with, startle responses of mice were recorded by exposing them to acoustic stimuli at 110 decibels (dB). In the second part of the procedure, pre-pulse acoustic stimuli ranging from 65-75 decibels was presented to the mice prior to the startle pulse of 110 decibels. The percentage inhibition of startle response by a pre-pulse was then calculated.

$Cry1^{-/-}$; $Fbxl3^{Afh/Afh}$ double mutants, $Fbxl21^{V68E/V68E}$ and $Fbxl21^{P291Q/P291Q}$ homozygous mice were assessed for their startle response before and after a pre-pulse is presented. A group of 10 animals (mix of males and females) for each mutant were tested and compared to the behaviour of 10 congenic C57BL/6J controls that were age matched.

Student's t-test was used to determine significant differences. Compared to the control mice, the $Cry1^{-/-}$; $Fbxl3^{Afh/Afh}$ double mutants (Figure 5.4) showed a significantly reduced startle response ($Cry1^{-/-}$; $Fbxl3^{Afh/Afh}$ p=0.04). While no differences were observed between wild-type controls and $Fbxl21^{V68E/V68E}$ (Figure 5.5), the $Fbxl21^{P291Q/P291Q}$ (Figure 5.6) mutants showed a significantly reduced startle response ($Fbxl21^{P291Q/P291Q}$ p= 0.019). On presenting the pre-pulse before the acoustic startle, the percentage of inhibition of startle response was measured. Both the $Cry1^{-/-}$; $Fbxl3^{Afh/Afh}$ and $Fbxl21^{P291Q/P291Q}$ mutants showed a significantly greater inhibition of startle response compared to the control mice ($Cry1^{-/-}$; $Fbxl3^{Afh/Afh}$ and $Fbxl21^{P291Q/P291Q}$ p≤ 0.005) (Figure 5.4 and 5.6).

However, the differences in the PPI levels of the wild-type control mice should be noted. While the PPI levels of wild-type mice used to test $Cry1^{-/-}$; $Fbxl3^{Afh/Afh}$ and $Fbxl21^{P291Q/P291Q}$ mice range between 18-35% (Figure 5.4 and 5.6), the PPI levels of controls used for $Fbxl21^{V68E/V68E}$ mice range between 40-50% (Figure 5.5). Although the reason for this difference is unknown, it could be that if proper littermate controls are used, the $Fbxl21^{V68E/V68E}$ mice would show a similar behaviour as the $Cry1^{-/-}$; $Fbxl3^{Afh/Afh}$ and $Fbxl21^{P291Q/P291Q}$ mutants.
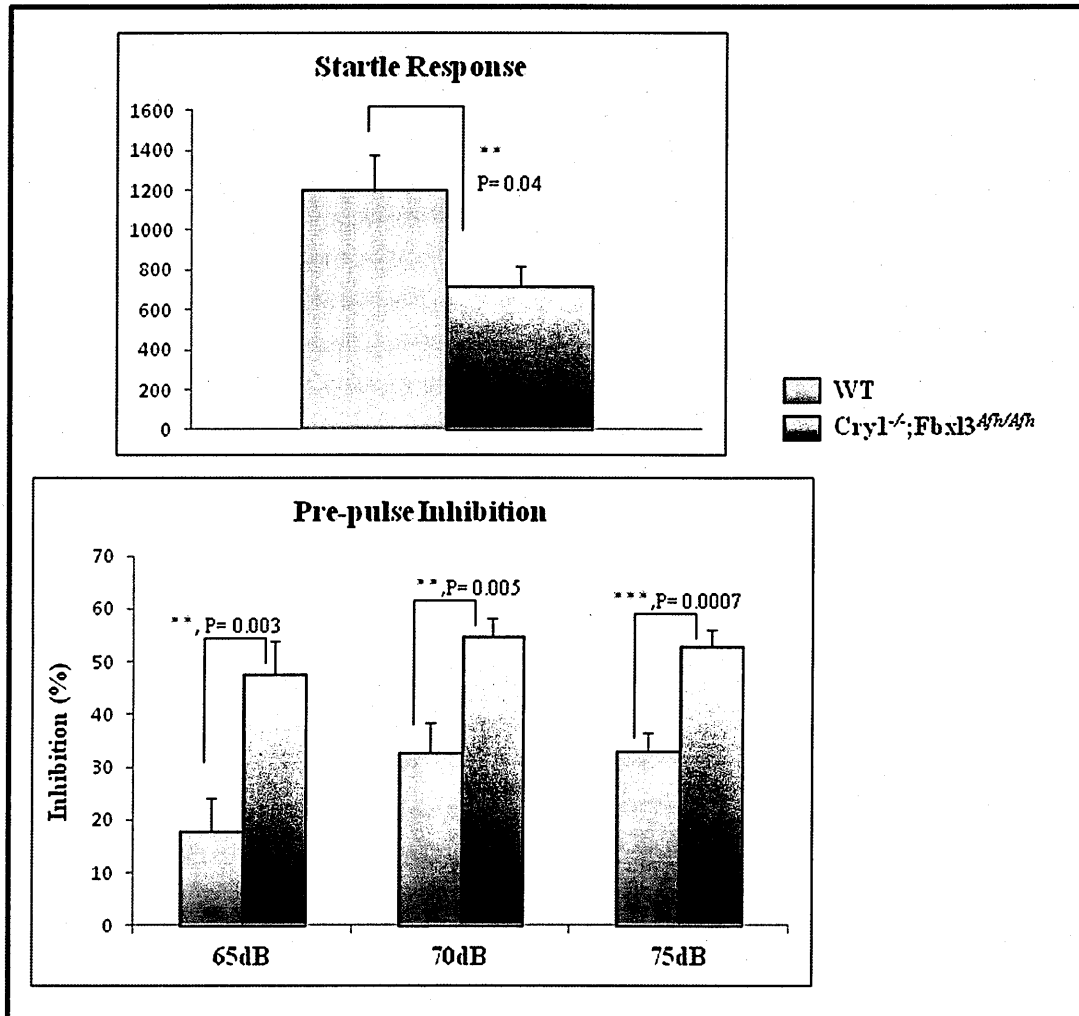
Figure 5.4: Acoustic startle response and pre-pulse inhibition in Cry1^{-/-}; Fbxl3^{Afh/Afh} double homozygous mice. These mutants showed a significantly reduced acoustic startle response at 110dB (p=0.04). However, these mice were able to significantly inhibit the startle response after the presentation of a pre-pulse ranging from 65-75dB (p≤0.005) compared to the C57BL/6J wild-type mice that were of the same age. A total of 10 mutants and 10 controls (males and females) were tested. Student's t-test was used to determine statistical differences.
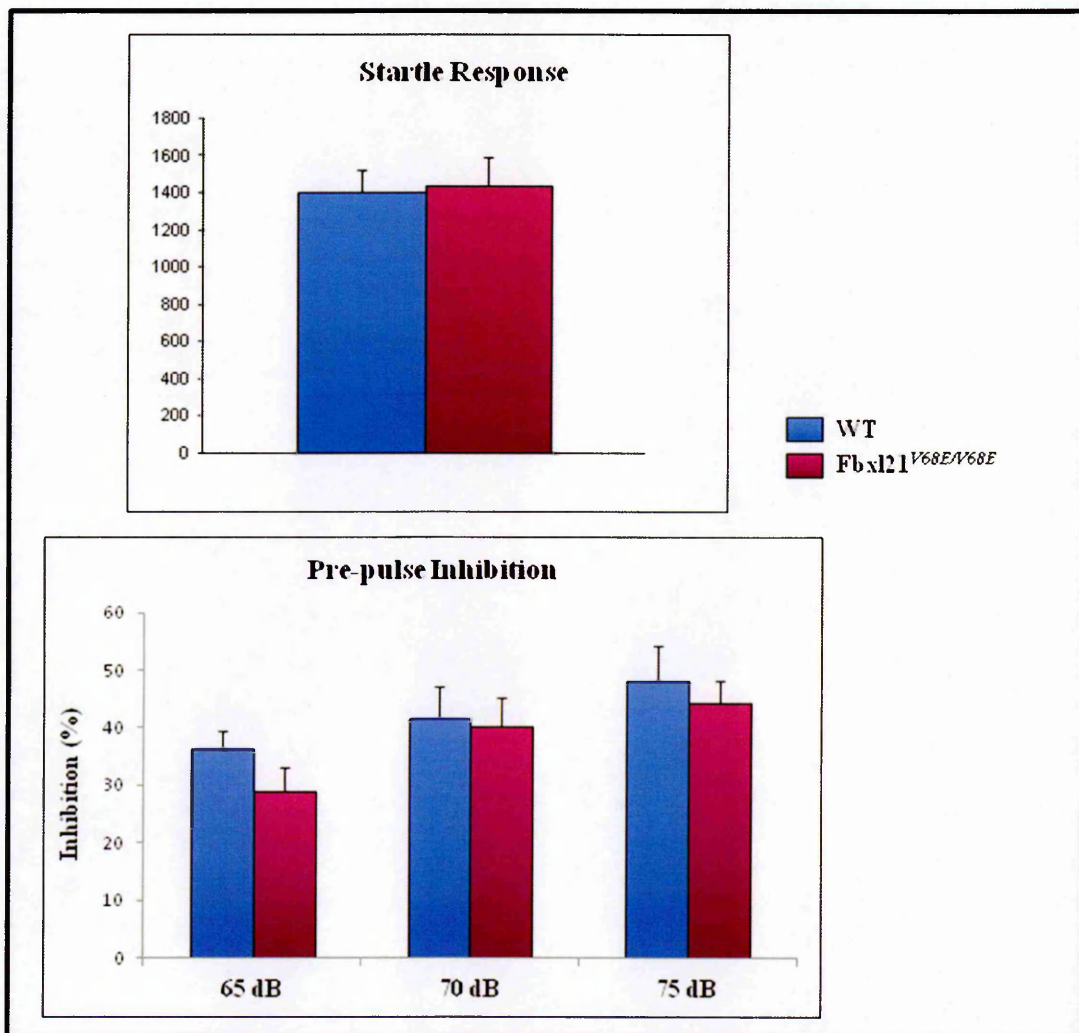
Figure 5.5: Assessing the acoustic startle response and pre-pulse inhibition in Fbxl21$^{V68E/V68E}$ mutants. There was no significant difference between the mutants and wild-type mice (C57BL/6J) in the acoustic startle response and their ability to inhibit the startle response after a pre-pulse. A total of 10 mutants and 10 controls (males and females) were tested. Student's t-test was used to determine statistical differences.
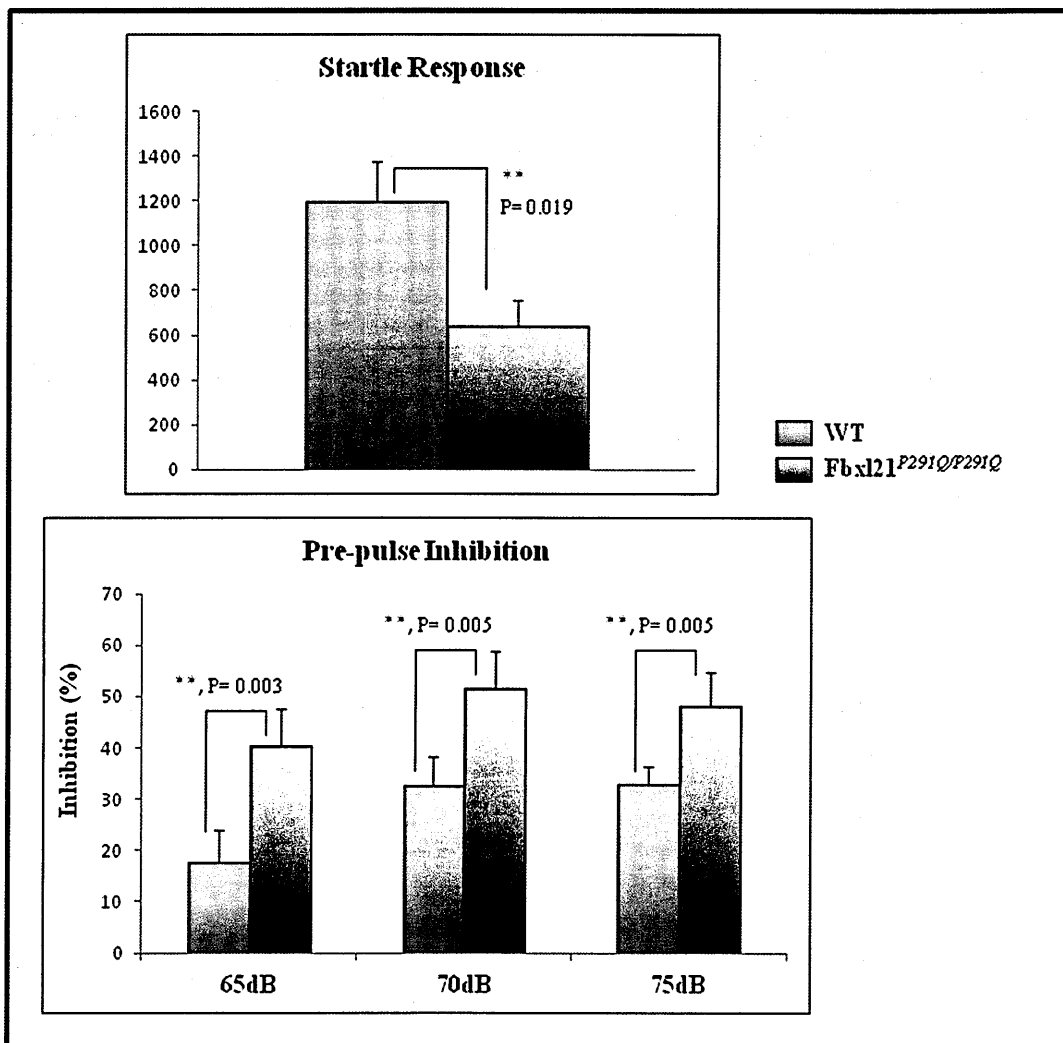
Figure 5.6: Assessment of the acoustic startle response and pre-pulse inhibition in Fbxl21^{P291Q/P291Q} mutants. These mutants showed a significantly reduced acoustic startle response at 110dB (p=0.019). Further after a range of pre-pulses (65-75dB) was presented, these mice were able to significantly inhibit the startle response (p≤ 0.005) compared to the C57BL/6J wild-type mice that were of the same age. A total of 10 mutants and 10 controls (males and females) were tested. Student's t-test was used to determine statistical differences.

5.2.3 Grip strength

Grip strength test is used as an indicator of neuromuscular function. The test can either be performed by measuring the grip strength of the two forelimbs or all the four paws.

The $Fbxl21^{V68E/V68E}$ mutants were tested for their grip strength using the Bioseb grip meter. Each animal was tested thrice with an interval of 5mins.

Since the muscle strength of the animal could vary with the weight of the animal, the animals were weighed and the mean grip was then calculated. There was no significant difference between the 2 paw grip strength of the $Fbxl21^{V68E/V68E}$ and C57BL/6J mice (Figure 5.7)
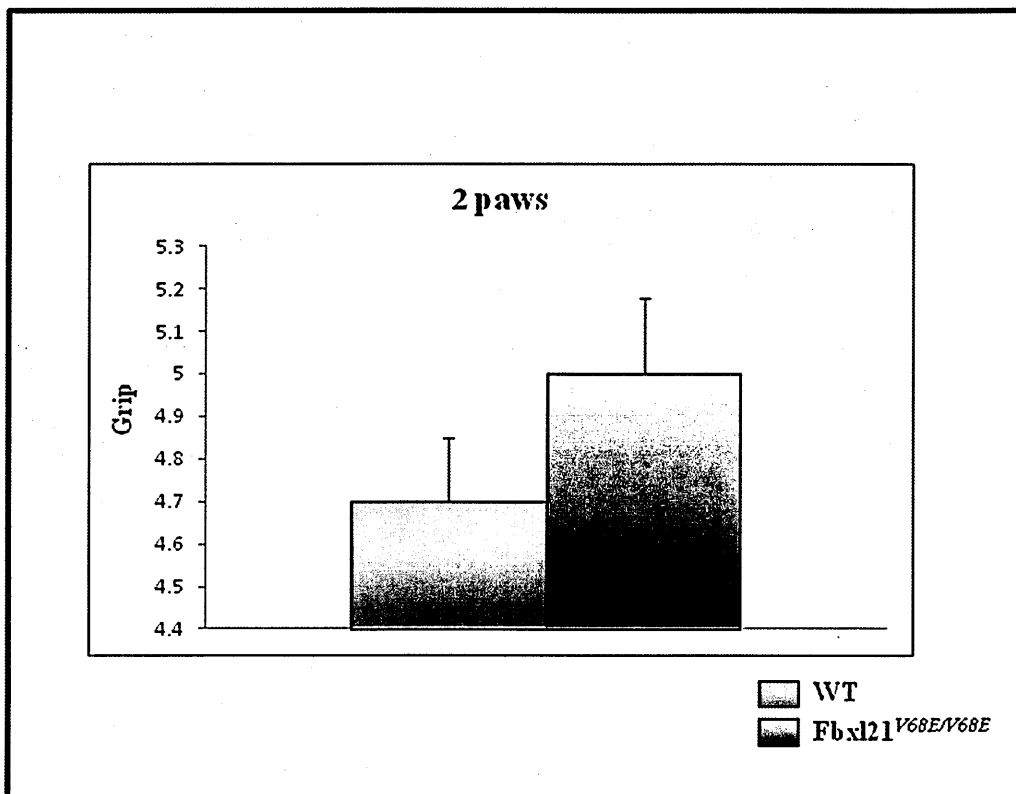
Figure 5.7: Two paw grip strength of Fbxl21$^{V68E/V68E}$ mice. There was no significant difference observed between the two paw grip strength of the *Fbxl21$^{V68E/V68E}$* and C57BL/6J wild-type mice. The represented graph is an average of three trials of each animal. Although there were no differences in body weights, they were taken into consideration during the grip strength test. The error bars represent the SEM. A cohort of 10 animals with a similar age, each for wild-type and mutant were tested. The cohort consisted of a mix of males and females. Student's t-test was used to determine statistical significance.

5.3 DISCUSSION

With several evidences showing direct or indirect associations of dysfunctional clock mechanisms with neurological and psychiatric disorders, we carried out three primary phenotyping tests in our mutant lines. The $Cry1^{-/-}$; $Fbxl3^{Afh/Afh}$ double homozygous mice and two $Fbxl21$ mutants, $Fbxl21^{V68E/V68E}$ and $Fbxl21^{P291Q/P291Q}$, were tested for their anxiety levels and were assessed for symptoms of schizophrenia (measuring their acoustic startle response and pre-pulse inhibition). While there were no significant differences observed between the control and $Fbxl21^{V68E/V68E}$ mice in the open field and PPI test, behavioural differences were observed in the other two mutants.

The $Fbxl21^{P291Q/P291Q}$ mutants displayed anxiety-related behaviour by spending significantly higher time in the periphery of the open field arena (p=0.0003). The mice were less exploratory and hence spent significantly less time moving (p= 0.002). The $Cry1^{-/-}$;$Fbxl3^{Afh/Afh}$ mutants on the other hand, were opposite to $Fbxl21$ mutants. These mutants show reduced anxiety levels. Although the mice spent significantly more time in the centre that is the anxiety-provoking area (p=0.007), parameters measured to assess the exploratory behaviour of the mice such as the latency of first occurrence was non-significantly lower than the wild-type. In order to exclude the possibility of increased locomotor activity contributing to the reduced anxiety levels, parameters such as distance travelled and total duration of movement were measured, and these remained unchanged in the mutant compared to control mice. These results were similar to the $Clock^{\Delta19/\Delta19}$ mutant generated using ENU mutagenesis, which shows reduced anxiety levels by spending more time in the centre (open field) and unprotected arm of an elevated platform (elevated plus maze) (Roybal, Theobold et al. 2007). A second clock mutant displaying low anxiety levels in an

elevated plus maze is earlybird *(Ebd)*, a mutant due to an ENU-induced point mutation in the gene *Rab3a* which regulates neurotransmitter release in the brain (Kapfhamer, Valladares et al. 2002; Yang, Farias et al. 2007).

Anxiety is a complex emotion that involves a physiological protective function to any threatening situation and involves complex interactions between different brain regions. With the brainstem nuclei being the most prominent structure playing the central role in regulating levels of arousal, the noradrenergic locus coeruleus and serotonergic nuclei are structures playing an important role in anxiety. Neurotransmitters such as GABA, serotonin (5-hydroxytryptamine (5-HT)), NPY and intracellular mediators such as adenyl cyclase type VIII are reported to be mediators of stress and anxiety related behaviour (Wood and Toth 2001). Pharmalogical studies have shown that maintaining GABA level is important in anxiety inducing situations and that upregulated GABA levels can have anxiolytic effects. This is consistent with studies carried out in mice deficient in glutamic acid decarboxylase (GAD) that regulates the synthesis of GABA. In the $GAD65^{-/-}$ mice (where an isoform of GAD is deleted), there is a reduction in the release of GABA which results in anxiety (Kash, Tecott et al. 1999). Interestingly, the projections from the serotonergic nuclei and locus coeruleus converge onto the SCN in the hypothalamus and serve as an input for synchronisation to the external environment. In addition, the above mentioned neurotransmitters (GABA, 5-HT, NPY) are involved in regulating the signalling cascade of the SCN. Hence, it is not surprising to observe anxiety related phenotypes in our circadian mutants, $Fbxl21^{P291Q/P291Q}$ and $Cry1^{-/-}; Fbxl3^{Afh/Afh}$.

Studies have shown the involvement of the GABAergic system in the modulation of acoustic startle response as well by regulating the neuronal circuitary in the brainstem (Davis, Gendelman et al. 1982; Meloni and Davis 1999). An acoustic startle response is a

stereotypic involuntary contraction of the facial and skeletal muscles in response to a sensory stimulus. This startle response is reduced when a pre-pulse is presented prior to the stimulus. However, defects in the reduction of the startle response due to pre-pulse inhibition deficits have been reported to be associated with defects in sensorimotor gating mechanisms (transmission of sensory information to motor systems) and are known to be a feature of schizophrenia and neurological disorders like Huntington's disease. In a recent report published in 2008, it was shown that the F-box gene *Fbxl21* is associated with schizophrenia in an Irish family (Chen, Wang et al. 2008). Hence, it was interesting to determine any association of *Fbxl21* and schizophrenia in mice particularly in the *Fbxl21$^{P291Q/P291Q}$* mutant mice. These mice on the other hand, along with the *Cry1$^{-/-}$; Fbxl3$^{Afh/Afh}$* mice, instead showed a significant increase in PPI (*Cry1$^{-/-}$; Fbxl3$^{Afh/Afh}$* , *Fbxl21$^{P291Q/P291Q}$* p≤0.005) between 65 and 75dB before the 110dB stimulus was presented, suggesting that the mice had no sensorimotor gating deficit.

While increase in startle response could be a reaction due to stress or fear (Zhang, Hu et al.), an decrease in startle response (as in *Cry1$^{-/-}$; Fbxl3$^{Afh/Afh}$* and *Fbxl21$^{P291Q/P291Q}$* mutants) can be indicative of deafness or sensorineural deficits. Inner ear defects are usually associated with sensorineural hearing loss (Knaus, Garcia-Calvo et al. 1994; McManus, Helms et al. 1995). It could be that the *Cry1$^{-/-}$; Fbxl3$^{Afh/Afh}$* and *Fbxl21$^{P291Q/P291Q}$* mouse mutants do not have the ability to process the conversion of sound into any neural signals in regions of the brain. There have been reports showing that circadian disturbances contribute to the aeitology of various syndromic disorders possibly due to the oscillating molecular circuits which are regulated by the clock (Barnard and Nolan 2008). One example of a mouse mutant displaying this is the Ca^{2+}-activated potassium (BK) channel knockout *Slo1$^{-/-}$*. The α-subunit of this channel is encoded by a gene *Slo1*, that is

252

ubiquitiously expressed (Knaus, Garcia-Calvo et al. 1994; McManus, Helms et al. 1995). The $Slo1^{-/-}$ line, generated by deleting the pore forming exon, displays various aspects of cerebellar dysfunction including loss of motor function co-ordination, reduction in the activity of the Purkinje cells and hearing loss that progresses with age (Ruttiger, Sausbier et al. 2004). Surprisingly, the regulation of this $Slo1$ gene is known to be under circadian control (Panda, Antoch et al. 2002).

Although hearing loss could be attributed by age, in the case of the $Cry1^{-/-}$ $;Fbxl3^{Afh/Afh}$ mutants, age-related hearing loss cannot be considered. A study evaluating hearing loss in inbred strains has shown that while most of the inbred strains develop age-related hearing loss before three months of age, strains such as BALB/cByJ and C57BL/6J do not develop hearing loss until 10 months of age (Erway, Willott et al. 1993; Willott, Turner et al. 1998; Zheng, Johnson et al. 1999). As the control mice and $Cry1^{-/-};Fbxl3^{Afh/Afh}$ double mutants used were ~51 days of age and on a C57BL/6J congenic background, hearing deficits in these mice cannot be due to age. However, in the case of $Fbxl21^{P291Q/P291Q}$ mice (~51 days) as they are on a mixed background (backcross 2), it is possible that these mice would have developed hearing loss at an early age. However, no conclusion about the progressive hearing loss condition can be made as yet, as it will need to be investigated once the colony is congenic.

One of the factors contributing to an increase in PPI is the neurotransmitter, serotonin, modulating the startle response (Dulawa, Gross et al. 2000; Dulawa, Scearce-Levie et al. 2000). With studies carried out in wild-type and 5-HT_{1B} knockout mice (5-HT1BKO), it has been shown that the serotonin system (5-HT) is a modulator of PPI. Although most studies carried out investigate reasons causing a decrease in PPI, there are evidences showing the role of the 5-HT system causing an increase in PPI. In the late

1990's Dulawa et al. (2000) reported the activation of multiple 5-HT receptors as a consequence of 5-HT release, out of which some of the activated receptors lead to an increase in PPI while some others cause a decrease in PPI. Thus, an increase in PPI is expected when receptors causing a decrease in PPI are absent, which might be one of the reasons for the observed phenotype in $Fbxl21^{P291Q/P291Q}$ mice (Dulawa, Gross et al. 2000; Dulawa, Scearce-Levie et al. 2000). In studies carried out in wild-type and 5-HT1BKO mice treated with 5-HT releasing compounds such as (+)3,4-methylenedioxy-N-methylamphetamine (MDMA) or (±)N-methyl-1-(1,3-benzodioxol-5-yl)-2- butanamine (MBDB), it was shown that an increase in PPI in the 5-HT1BKO mice (similar to the $Fbxl21^{P291Q/P291Q}$ mice) is due to the lack of the 5-HT1B receptors. Similar studies in mice lacking the 5-HT1A receptors (1AKO) report that the 5-HT1A receptors are involved in increasing PPI (Dulawa, Gross et al. 2000). Thus, although the lack of 5-HT1B receptors could be the possible reason for an increased PPI in $Fbxl21^{P291Q/P291Q}$ mutants, the reason behind either the loss of receptors or the modulations that result in loss of receptor function is yet to be identified.

A second possibility explaining the difference in $Fbxl21^{P291Q/P291Q}$ phenotypes is the time of testing. It has been previously reported that the acoustic startle response of mice is affected by the circadian clock, where mice being nocturnal animals show an increase in startle response during darkness (Chabot and Taylor 1992). Earlier reports show that the ability of animals to inhibit startle reflex by a prepulse is greatly increased during the activity phase of the animal (i.e during the night) and the reduction in prepulse inhibition during the active phase was thought to be due to the reduced processing of sensory stimulus. An increased inhibition of the startle response during the time of the test, i.e. during the light phase in the $Fbxl21^{P291Q/P291Q}$ is surprising (Delius 1970). However, the

increase in PPI in the $Cry1^{-/-};Fbxl3^{Afh/Afh}$ is not surprising, as these animals tend to be active even during the day as compared to the wild type animals. Another study carried out in rats shows that there is no effect of circadian time on the amplitude of startle response or on the ability to inhibit the startle reflex by a prepulse. This was confirmed by using apomorphine (compound that is used to induce PPI defects) that shows no difference in the startle reflex and PPI across circadian time (Weiss, Feldon et al. 1999). Hence, this point of difference remains to be a debate which is yet to be resolved.

Finally, differences in PPI observed in $Fbxl21^{P291Q/P291Q}$ mutants could be attributed to the mixed genetic background (C57BL/6J and C3H, backcross 2) of the mice. In a study involving three inbred strains, C57BL/6J, BALB/cByJ and 129S2, it has been shown that a clear difference between the amplitude of startle response to the prepulse inhibition and the level of PPI exists. The results showed that although the C57BL/6J mice had a low level of PPI, these mice showed the largest amplitude of startle response. They suggested that strain differences could be due to differences in the neurotransmitter signalling cascade (by involving strain dependent neurotransmitters) or due to the involvement of different neuronal circuitary within regions of the brain changing with the strains of mice (Aubert, Reiss et al. 2006). Hence it can be concluded that similar results in PPI cannot be obtained amongst different strains as several physiological variants contribute to final amplitude of PPI obtained.

5.4 SUMMARY

As described previously, circadian mutants are often associated with other neurological and behavioural abnormalities. For this reason, the $Cry1^{-/-}$; $Fbxl3^{Afh/Afh}$ double mutants and the two $Fbxl21$ mutants, $Fbxl21^{V68E/V68E}$ and $Fbxl21^{P291Q/P291Q}$, were subjected to a preliminary battery of phenotyping tests. While the $Fbxl21^{V68E/V68E}$ mice showed no significant differences compared to the wild-type control mice, the other two mutants revealed some interesting results.

The $Cry1^{-/-}$; $Fbxl3^{Afh/Afh}$ mice tend to have an increased exploratory behaviour in the open field test. Hence, they were seen to spend more time in the centre than in the periphery of an open field arena, which is a novel environment to these mice. On the other hand in the acoustic startle response test the $Cry1^{-/-}$; $Fbxl3^{Afh/Afh}$ mice showed a significantly reduced startle response after an acoustic startle of 110dB was presented to them. In order to test their ability to inhibit the startle response, a prepulse ranging from 65db-75db was presented to the mice. The $Cry1^{-/-}$; $Fbxl3^{Afh/Afh}$ mice were able to inhibit the startle response better than the control mice.

Since $Fbxl21$ is a known candidate for schizophrenia in humans, the $Fbxl21^{P291Q/P291Q}$ mice were expected to have a PPI deficit in inhibiting the acoustic startle response. However, these mice showed no significant deficits in sensorimotor gating and inhibition of startle response was greater than in the wild-type mice. This is similar to the findings in the mutants in *Disrupted-in-Schizophrenia* (*Disc1*). Q31L and L100P are two missense mutations identified in *Disc1*, the human form of which is a genetic risk factor for schizophrenia (Clapcote, Lipina et al. 2007). Although both these amino acids were not conserved between humans and mice, Q31L displayed a recessive major depression

phenotype, while the L100P proved to be a dominant schizophrenia mouse model (Clapcote, Lipina et al. 2007) . This shows that the behaviour of mice could depend on the exact mutation in the gene being investigated.

The open field test showed that the $Fbxl21^{P291Q/P291Q}$ were significantly more anxious and hence spent more time in the periphery of the open field arena than in the centre which is an anxiety provoking area. Additionally, these mice moved less in terms of duration and distance, suggesting a depression phenotype and/or a motor function deficit.

It would be useful to subject the $Cry1^{-/-}$; $Fbxl3^{Afh/Afh}$ and $Fbxl21^{P291Q/P291Q}$ mutants with appropriate genetic background and littermate controls to the tests already performed (Open-field, PPI). They could also be screened for additional behavioural tests such as forced swim test that is used to investigate the effects of antidepressants (Porsolt, Bertin et al. 1977), rota-rod which measures balance and motor co-ordination in rodents (Dunham and Miya 1957; Crawley 1999) and the marble burying test that is used to measures anxiety-related behaviours (Deacon 2006).

6 <u>CHAPTER SIX</u>: General Discussion

6.1 DISCUSSION

The aim of this project was to understand and identify the genetic and molecular basis of circadian rhythms. A particular focus was to dissect the functions of the two mammalian cryptochrome genes, *Cry1* and *Cry2*, using mutants previously identified in our lab. Additionally, ENU mutagenesis resulted in the identification of new mutants which have additionally been used to dissect functions of *Cry1* and *Cry2 in vivo*.

6.1.1 Summary of Results

The previous identification of the *Afh* mutation in the F-box protein, *Fbxl3*, revealed the specific F-box proteins that target CRY proteins for proteasomal degradation. The mutation results in a longer circadian period *in vivo* compared to the control mice (Busino, Bassermann et al. 2007; Godinho, Maywood et al. 2007). It was intriguing to determine if the *Afh* mutation results in a similar increase in period in the single $Cry1^{-/-}$ and $Cry2^{-/-}$ knockout mice. For this reason, $Cry1^{-/-}$; $Fbxl3^{Afh/Afh}$ and $Cry2^{-/-}$;$Fbxl3^{Afh/Afh}$ compound mutants were generated and were first screened for their circadian wheel-running behaviour. It was successfully shown that the $Fbxl3^{Afh/Afh}$ mutation affects both $Cry1^{-/-}$ and $Cry2^{-/-}$ *in vivo* by increasing their period length under DD and LL conditions of the circadian screen. However when compared to the single $Cry^{-/-}$ mutants ($Cry^{-/-}$; $Fbxl3^{+/+}$), the increase in period length in the $Cry1^{-/-}/Cry2^{-/-}$; $Fbxl3^{Afh/Afh}$ double mutants was not equal, which was thought to be due to the individual *Cry* gene function. Gene expression studies further revealed *Cry1* as a stronger transcriptional repressor than *Cry2 in vivo*. It is

thought that the role of *Cry2* as a repressor is confined to *Per2* specifically in the cerebellum. Furthermore, the *Afh* mutation is also able to upregulate and stabilise either CRY protein levels *in vivo* which presumably contribute to the extended transcriptional repression resulting in a long circadian phenotype.

Additionally the circadian screens provide an insight into the role of *Cry2* in the retina. This is due to fact that with the loss of *Cry2 in vivo*, the mice are unable to entrain to the LD cycle and are arrhythmic in constant light conditions.

The ability of ENU mutagenesis to identify mutations in a candidate gene of choice was assessed in Chapter 4. DNA from ENU mutagenised mice was screened to identify mutations in a recently identified *Fbxl3* paralogue, *Fbxl21* (Dardente, Mendoza et al. 2008). Two mutations identified in this screen, V68E (in the F-box domain) and P291Q (in the putative CRY-binding domain) were selected for the *in vivo* and *in-vitro* analysis carried out during the course of study for this thesis.

Potential functional changes were identified in the *in-vitro* analysis. The localisation of FBXL21 was seen to be affected in the presence of the mutations. In addition the mutations also resulted in a reduction of interaction between the FBXL21 and their substrates CRY1 and CRY2. Interesting conclusions were made while studying the degradation of CRY1 and CRY2 by FBXL21 *in-vitro*. It was shown that while CRY1 did interact with FBXL3, CRY2 was preferentially degraded by FBXL21. The mutant FBXL21-P291Q on the other hand spared CRY2 from proteasomal degradation *in-vitro*.

In vivo circadian wheel-running analysis further confirmed no change in the *Fbxl21$^{V68E/V68E}$* phenotype, whereas a shorter circadian phenotype was observed in the *Fbxl21$^{P291Q/P291Q}$* homozygous mice. The shorter phenotype that was a result of stabilised

CRY2 levels was found to be consistent with the $Cry2^{-/-}$ knockout mice, where a complete absence of CRY2 results in a longer period.

Since *Fbxl21* is the closest relative of *Fbxl3*, genetic interactions between the two *Fbxl* paralogues were then investigated by generating $Fbxl3^{Afh/Afh};Fbxl21^{P291Q/P291Q}$ and $Fbxl3^{Afh/Afh};Fbxl21^{V68E/V68E}$ compound mutants. Interestingly it was seen that an epistatic interaction between the two F-box proteins existed and that $Fbxl3^{Afh/Afh}$ was epistatic to *Fbxl21*. This effect of $Fbxl3^{Afh/Afh}$ was seen *in vivo* by analysing the wheel-running activity of the compound mutants which largely mimicked the $Fbxl3^{Afh/Afh}$ phenotype. In addition to this finding two differences were observed in the compound mutants: a further increase in period length in the $Fbxl3^{Afh/Afh};\ Fbxl21^{P291Q/P291Q}$ double mutants in DD, and the arrhythmic behaviour of the double mutants in LL conditions. However, the genetic interactions resulting in these observations are unknown and are beyond the scope of this work.

Finally, Chapter 5 covers the behavioural phenotyping of the $Cry1^{-/-};Fbxl3^{Afh/Afh}$ double mutants, $Fbxl21^{V68E/V68E}$ and $Fbxl21^{P291Q/P291Q}$ mutants. As expected from a higher number of wheel revolutions in LL during the circadian screen, the $Cry1^{-/-};Fbxl3^{Afh/Afh}$ double mutants were seen to be hyperactive and show a greater tendency to explore in a novel environment during the open field test. In contrast to these, the $Fbxl21^{P291Q/P291Q}$ mice were seen to be anxious and spend more time in the periphery rather than the centre of an open field arena. These mice, however, were also seen to move less than the control mice. The mutants were also assessed for their ability to inhibit their response to an acoustic startle after a pre-pulse is presented. While the $Cry1^{-/-};Fbxl3^{Afh/Afh}$ and $Fbxl21^{P291Q/P291Q}$ showed a lower startle response and an increase in the pre-pulse inhibition, it could be proposed that these mutants may possibly have a hearing deficit.

6.1.2 Contribution to the field

The project on the whole has contributed significantly to understand some of the interactions required to maintain circadian rhythms. It has particularly emphasised on the generation of compound mutants and how they contribute to our knowledge in unveiling complex mechanisms of the circadian clock.

One of the significant evidences from the study carried out is the role of *Cry2* in mammals in the presence of light. Although it has not been classified as a photoreceptor, there has been a debate about this function of *Cry2*. The consistent results obtained in previous chapters show that *Cry2* certainly has an important role in the retina and in the processing of information in the presence of light. However to gather conclusions regarding this function of *Cry2*, further investigations will have to be carried out.

The ability and contribution of ENU mutagenesis to generate circadian mutants have been shown a number of times in the past. The mutants were either identified in a forward genetics screen or were generated using a gene knockout approach (van der Horst, Muijtjens et al. 1999; Godinho, Maywood et al. 2007). However, the *Fbxl21* mutants that have been used in Chapter 4 and 5 are first evidences of circadian mutants that have been identified using the reverse genetics gene screening approach. Furthermore we have successfully been able to show the power of ENU in first identifying the mutation and further observe a circadian phenotype *in vivo*.

The study has also contributed significantly in understanding the importance of mechanisms such as clock gene redundancies and epistasis. With the core clock genes previously identified it is evident that most of these genes exist as paralog pairs. Although they may have similar functions in the regulation of rhythms, redundancy between the

paralogues may or may not exist. For example, redundancy exists between negative regulators of the secondary interlocked feedback loop, *Rev-erbα* and *Rev-erbβ*, where it was shown that the disruption of either *Rev-erb* alone does not have an effect on the transcriptional activator, *Bmal1* and hence is unable to attenuate the circadian clockwork (Liu, Tran et al. 2008). Similarly, wheel-running analysis followed by gene expression studies in the *Clock$^{-/-}$; Npas2$^{-/-}$* compound mutants revealed that *Npas2* (also called as *Mop4*) is able to substitute the function of its paralogue *Clock* in mice in order to maintain rhythmicity (DeBruyne, Weaver et al. 2007). While the above mentioned examples show redundancies, it is not always the case. With arrhythmicity observed in *Cry1$^{-/-}$; Cry2$^{-/-}$* mice, the presence of a single functional *Cry1* copy restores rhythms in these mice. This was not the case with the expression of one copy of *Cry2*, suggesting that both *Cry1* and *Cry2* act independently (van der Horst, Muijtjens et al. 1999). This has also been shown by the circadian wheel-running analysis and gene expression studies carried out in the *Cry1$^{-/-}$; Fbxl3$^{Afh/Afh}$* double mutants that have been generated during the course of the study presented in this thesis.

The investigations carried out in the *Fbxl3$^{Afh/Afh}$; Fbxl21$^{V68E/V68E}$* and *Fbxl3$^{Afh/Afh}$;Fbxl21$^{P291Q/P291Q}$* compound mutants have resulted in the identification of epistatic interactions between the two F-box proteins rather than redundancies. This has been the first *in vivo* evidence of epistatic interactions between two F-box proteins involved in similar functions of degrading CRY proteins.

The phenotyping analysis carried out in *Cry1$^{-/-}$; Fbxl3$^{Afh/Afh}$* and *Fbxl21* mutants have further shown the evidence of circadian mutants being associated with behavioural abnormalities such as hyperactivity and anxiety.

6.1.3 Future work

Although the effects of stabilising either CRY proteins under DD conditions have been successfully understood using the *Afh* mutant *in vivo*, the effects under LL require further investigations. The circadian wheel-running activity carried out in the $Cry^{-/-}$;$Fbxl3^{Afh/Afh}$ mice have revealed period lengthening in LL compared to control mice. However, the genetic basis resulting in the period change is not clear. Hence, gene expression study will have to be carried out in the $Cry^{-/-}$;$Fbxl3^{Afh/Afh}$ to fully understand the role of clock genes and in particular *Cry2*, under LL conditions.

To determine the reason behind the reduced interaction of FBXL21-V68E and CRY proteins *in-vitro* without causing a change in the circadian period, the indirect effects of the V68E mutation will have to be taken into consideration. As mentioned previously, it is possible that the V68E mutation actually affects interaction with the SCF components which ultimately results in a reduced interaction with CRY proteins. Furthermore, gene expression studies at the RNA and protein level will also have to be carried out *in vivo* in the $Fbxl21^{V68E/V68E}$, $Fbxl21^{P291Q/P291Q}$, $Fbxl3^{Afh/Afh}$;$Fbxl21^{V68E/V68E}$ and $Fbxl3^{Afh/Afh}$;$Fbxl21^{P291Q/P291Q}$ mice under both DD and LL conditions. The expression profiling in the double mutants will provide an insight into the interactions that may be taking place between *Fbxl3* and *Fbxl21*. However, to study redundancies between the F-box proteins generating complete knockouts for each of the F-box proteins will be ideal.

Since the ability of FBXL21 to degrade CRY2 is thought to be regulated by a specific kinase, DYRK1A, it will be interesting to investigate the outcome of modifying the DYRK1A-specific phoshophorylation sites *in-vitro*. The phenotype obtained after the modifications would be of particular interest especially if we assume the hypothesis

mentioned in Chapter 4 is true, where phosphorylation by DYRK1A speeds the nuclear entry of CRY. Further, it will also be interesting to investigate the localisation of CRY1 and CRY2 in the *Fbxl21* mutants over the course of circadian time. This would further confirm the ability of FBXL21 to sequester CRY1 in the cytoplasm.

Finally as we have already seen associations of *Cry1* and hyperactivity it would be interesting to screen the $Cry2^{-/-};Fbxl3^{Afh/Afh}$ double mutants through the phenotyping pipeline. Any associations found between clock genes, behavioural and neurological disorders are beneficial as the clock genes could then be used as targets for drug development by pharamaceutical industries.

6.1.4 Concluding remarks

In this thesis the genetic interactions between the negative regulators of the mammalian circadian clock, *Cry* and F-box proteins, *Fbxl3* and *Fbxl21* have been studied by generating compound mouse mutants. While the circadian effects of CRY protein upregulation was studied in the $Cry^{-/-};Fbxl3^{Afh/Afh}$ compound mutants, the gene expression profiling carried out in these mutants also confirmed the importance and role of *Cry* in regulating circadian oscillations *in vivo*. Further the ability of ENU mutagenesis to generate mutations was exploited and mutations in *Fbxl21* were identified. Analysis carried out using these mutants revealed the important role of FBXL21 to degrade CRY2. Unknown epistatic interactions between *Fbxl3* and *Fbxl21* were identified during the circadian wheel-running analysis of the *Fbxl3; Fbxl21* compound mutants. All these observations have contributed largely to our knowledge and will aid in understanding the genetic basis of the mammalian circadian clock.

7 <u>CHAPTER SEVEN</u>: References

Abe, M., E. D. Herzog, et al. (2002). "Circadian rhythms in isolated brain regions." J Neurosci 22(1): 350-6.

Abrahamson, E. E. and R. Y. Moore (2001). "Suprachiasmatic nucleus in the mouse: retinal innervation, intrinsic organization and efferent projections." Brain Res 916(1-2): 172-91.

Acevedo-Arozena, A., S. Wells, et al. (2008). "ENU mutagenesis, a way forward to understand gene function." Annu Rev Genomics Hum Genet 9: 49-69.

Ahmad, M. and A. R. Cashmore (1993). "HY4 gene of A. thaliana encodes a protein with characteristics of a blue-light photoreceptor." Nature 366(6451): 162-6.

Akashi, M. and E. Nishida (2000). "Involvement of the MAP kinase cascade in resetting of the mammalian circadian clock." Genes Dev 14(6): 645-9.

Albrecht, U. "Circadian clocks in mood-related behaviors." Ann Med 42(4): 241-51.

Albrecht, U. and G. Eichele (2003). "The mammalian circadian clock." Curr Opin Genet Dev 13(3): 271-7.

Albrecht, U., Z. S. Sun, et al. (1997). "A differential response of two putative mammalian circadian regulators, mper1 and mper2, to light." Cell 91(7): 1055-64.

Allebrandt, K. V. and T. Roenneberg (2008). "The search for circadian clock components in humans: new perspectives for association studies." Braz J Med Biol Res 41(8): 716-21.

Ambree, O., C. Touma, et al. (2006). "Activity changes and marked stereotypic behavior precede Abeta pathology in TgCRND8 Alzheimer mice." Neurobiol Aging 27(7): 955-64.

Antle, M. C. and R. Silver (2005). "Orchestrating time: arrangements of the brain circadian clock." Trends Neurosci 28(3): 145-51.

Antoch, M. P., V. Y. Gorbacheva, et al. (2008). "Disruption of the circadian clock due to the Clock mutation has discrete effects on aging and carcinogenesis." Cell Cycle 7(9): 1197-204.

Antoch, M. P., E. J. Song, et al. (1997). "Functional identification of the mouse circadian Clock gene by transgenic BAC rescue." Cell 89(4): 655-67.

Aronson, B. D., K. A. Johnson, et al. (1994). "Negative feedback defining a circadian clock: autoregulation of the clock gene frequency." Science 263(5153): 1578-84.

Aton, S. J., C. S. Colwell, et al. (2005). "Vasoactive intestinal polypeptide mediates circadian rhythmicity and synchrony in mammalian clock neurons." Nat Neurosci 8(4): 476-83.

Aubert, L., D. Reiss, et al. (2006). "Auditory and visual prepulse inhibition in mice: parametric analysis and strain comparisons." Genes Brain Behav 5(5): 423-31.

Bacon, Y., A. Ooi, et al. (2004). "Screening for novel ENU-induced rhythm, entrainment and activity mutants." Genes Brain Behav 3(4): 196-205.

Bagnall, D. J., R. W. King, et al. (1996). "Blue-light promotion of flowering is absent in hy4 mutants of Arabidopsis." Planta 200(2): 278-80.

Bai, C., P. Sen, et al. (1996). "SKP1 connects cell cycle regulators to the ubiquitin proteolysis machinery through a novel motif, the F-box." Cell 86(2): 263-74.

Balling, R. (2001). "ENU mutagenesis: analyzing gene function in mice." Annu Rev Genomics Hum Genet 2: 463-92.

Balsalobre, A., S. A. Brown, et al. (2000). "Resetting of circadian time in peripheral tissues by glucocorticoid signaling." Science 289(5488): 2344-7.

Balsalobre, A., F. Damiola, et al. (1998). "A serum shock induces circadian gene expression in mammalian tissue culture cells." Cell 93(6): 929-37.

Balsalobre, A., L. Marcacci, et al. (2000). "Multiple signaling pathways elicit circadian gene expression in cultured Rat-1 fibroblasts." Curr Biol 10(20): 1291-4.

Banerjee, R. and A. Batschauer (2005). "Plant blue-light receptors." Planta 220(3): 498-502.

Bao, S., J. Rihel, et al. (2001). "The Drosophila double-timeS mutation delays the nuclear accumulation of period protein and affects the feedback regulation of period mRNA." J Neurosci 21(18): 7117-26.

Bargiello, T. A., F. R. Jackson, et al. (1984). "Restoration of circadian behavioural rhythms by gene transfer in Drosophila." Nature 312(5996): 752-4.

Barnard, A. R. and P. M. Nolan (2008). "When clocks go bad: neurobehavioural consequences of disrupted circadian timing." PLoS Genet 4(5): e1000040.

Batschauer, A. (1993). "A plant gene for photolyase: an enzyme catalyzing the repair of UV-light-induced DNA damage." Plant J 4(4): 705-9.

Beck, J. A., S. Lloyd, et al. (2000). "Genealogies of mouse inbred strains." Nat Genet 24(1): 23-5.

Benedetti, F., D. Radaelli, et al. (2008). "Clock genes beyond the clock: CLOCK genotype biases neural correlates of moral valence decision in depressed patients." Genes Brain Behav 7(1): 20-5.

Ben-Shlomo, R. and C. P. Kyriacou (2002). "Circadian rhythm entrainment in flies and mammals." Cell Biochem Biophys 37(2): 141-56.

Bowes, C., T. Li, et al. (1990). "Retinal degeneration in the rd mouse is caused by a defect in the beta subunit of rod cGMP-phosphodiesterase." Nature 347(6294): 677-80.

Brown, S. A., G. Zumbrunn, et al. (2002). "Rhythms of mammalian body temperature can sustain peripheral circadian clocks." Curr Biol 12(18): 1574-83.

Brown, S. D. and P. M. Nolan (1998). "Mouse mutagenesis-systematic studies of mammalian gene function." Hum Mol Genet 7(10): 1627-33.

Buhr, E. D., S. H. Yoo, et al. "Temperature as a universal resetting cue for mammalian circadian oscillators." Science 330(6002): 379-85.

Buijs, R. M. and A. Kalsbeek (2001). "Hypothalamic integration of central and peripheral clocks." Nat Rev Neurosci 2(7): 521-6.

Bunger, M. K., L. D. Wilsbacher, et al. (2000). "Mop3 is an essential component of the master circadian pacemaker in mammals." Cell 103(7): 1009-17.

Bur, I. M., A. M. Cohen-Solal, et al. (2009). "The circadian clock components CRY1 and CRY2 are necessary to sustain sex dimorphism in mouse liver metabolism." J Biol Chem 284(14): 9066-73.

Burton, P. R., D. G. Clayton, et al. (2007). "Association scan of 14,500 nonsynonymous SNPs in four diseases identifies autoimmunity variants." Nat Genet 39(11): 1329-37.

Busino, L., F. Bassermann, et al. (2007). "SCFFbxl3 controls the oscillation of the circadian clock by directing the degradation of cryptochrome proteins." Science 316(5826): 900-4.

Campbell, S. S. and P. J. Murphy (1998). "Extraocular circadian phototransduction in humans." Science 279(5349): 396-9.

Ceriani, M. F., T. K. Darlington, et al. (1999). "Light-dependent sequestration of TIMELESS by CRYPTOCHROME." Science 285(5427): 553-6.

Chaves, I., K. Yagita, et al. (2006). "Functional evolution of the photolyase/cryptochrome protein family: importance of the C terminus of mammalian CRY1 for circadian core oscillator performance." Mol Cell Biol 26(5): 1743-53.

Chen, R., A. Schirmer, et al. (2009). "Rhythmic PER abundance defines a critical nodal point for negative feedback within the circadian clock mechanism." Mol Cell 36(3): 417-30.

Chen, X., X. Wang, et al. (2008). "FBXL21 association with schizophrenia in Irish family and case-control samples." Am J Med Genet B Neuropsychiatr Genet 147B(7): 1231-7.

Chen, Y., D. Yee, et al. (2000). "Genotype-based screen for ENU-induced mutations in mouse embryonic stem cells." Nat Genet 24(3): 314-7.

Cheng, M. Y., E. L. Bittman, et al. (2005). "Regulation of prokineticin 2 expression by light and the circadian clock." BMC Neurosci 6: 17.

Cheng, M. Y., C. M. Bullock, et al. (2002). "Prokineticin 2 transmits the behavioural circadian rhythm of the suprachiasmatic nucleus." Nature 417(6887): 405-10.

Chu, L. W., Y. Zhu, et al. (2008). "Variants in circadian genes and prostate cancer risk: a population-based study in China." Prostate Cancer Prostatic Dis 11(4): 342-8.

Clapcote, S. J., T. V. Lipina, et al. (2007). "Behavioral phenotypes of Disc1 missense mutations in mice." Neuron 54(3): 387-402.

Coghill, E. L., A. Hugill, et al. (2002). "A gene-driven approach to the identification of ENU mutants in the mouse." Nat Genet 30(3): 255-6.

Colwell, C. S., S. Michel, et al. (2003). "Disrupted circadian rhythms in VIP- and PHI-deficient mice." Am J Physiol Regul Integr Comp Physiol 285(5): R939-49.

Concepcion, D., K. L. Seburn, et al. (2004). "Mutation rate and predicted phenotypic target sizes in ethylnitrosourea-treated mice." Genetics 168(2): 953-9.

Crawley, J. N. (1999). "Behavioral phenotyping of transgenic and knockout mice: experimental design and evaluation of general health, sensory functions, motor abilities, and specific behavioral tests." Brain Res 835(1): 18-26.

Czeisler, C. A. and D. J. Dijk (1995). "Use of bright light to treat maladaptation to night shift work and circadian rhythm sleep disorders." J Sleep Res 4(S2): 70-73.

Damiola, F., N. Le Minh, et al. (2000). "Restricted feeding uncouples circadian oscillators in peripheral tissues from the central pacemaker in the suprachiasmatic nucleus." Genes Dev 14(23): 2950-61.

Dardente, H., J. Mendoza, et al. (2008). "Implication of the F-Box Protein FBXL21 in circadian pacemaker function in mammals." PLoS One 3(10): e3530.

Davies, V. J., A. J. Hollins, et al. (2007). "Opa1 deficiency in a mouse model of autosomal dominant optic atrophy impairs mitochondrial morphology, optic nerve structure and visual function." Hum Mol Genet 16(11): 1307-18.

Davis, M., D. S. Gendelman, et al. (1982). "A primary acoustic startle circuit: lesion and stimulation studies." J Neurosci 2(6): 791-805.

de Groot, M. H. and B. Rusak (2002). "Entrainment impaired, masking spared: an apparent genetic abnormality that prevents circadian rhythm entrainment to 24-h lighting cycles in California mice." Neurosci Lett 327(3): 203-7.

Deacon, R. M. (2006). "Digging and marble burying in mice: simple methods for in vivo identification of biological impacts." Nat Protoc 1(1): 122-4.

Debruyne, J. P., E. Noton, et al. (2006). "A clock shock: mouse CLOCK is not required for circadian oscillator function." Neuron 50(3): 465-77.

DeBruyne, J. P., D. R. Weaver, et al. (2007). "CLOCK and NPAS2 have overlapping roles in the suprachiasmatic circadian clock." Nat Neurosci 10(5): 543-5.

Delius, J. D. (1970). "Irrelevant behaviour, information processing and arousal homeostasis." Psychol Forsch 33(2): 165-88.

Denault, D. L., J. J. Loros, et al. (2001). "WC-2 mediates WC-1-FRQ interaction within the PAS protein-linked circadian feedback loop of Neurospora." EMBO J 20(1-2): 109-17.

Deng, X. W. and P. H. Quail (1999). "Signalling in light-controlled development." Semin Cell Dev Biol 10(2): 121-9.

Dibner, C., U. Schibler, et al. "The mammalian circadian timing system: organization and coordination of central and peripheral clocks." Annu Rev Physiol 72: 517-49.

Dijk, D. J. and S. N. Archer (2009). "Light, sleep, and circadian rhythms: together again." PLoS Biol 7(6): e1000145.

Dudley, C. A., C. Erbel-Sieler, et al. (2003). "Altered patterns of sleep and behavioral adaptability in NPAS2-deficient mice." Science 301(5631): 379-83.

Duerr, R. H., K. D. Taylor, et al. (2006). "A genome-wide association study identifies IL23R as an inflammatory bowel disease gene." Science 314(5804): 1461-3.

Dulawa, S. C., C. Gross, et al. (2000). "Knockout mice reveal opposite roles for serotonin 1A and 1B receptors in prepulse inhibition." Neuropsychopharmacology 22(6): 650-9.

Dulawa, S. C., K. A. Scearce-Levie, et al. (2000). "Serotonin releasers increase prepulse inhibition in serotonin 1B knockout mice." Psychopharmacology (Berl) 149(3): 306-12.

Dunham, N. W. and T. S. Miya (1957). "A note on a simple apparatus for detecting neurological deficit in rats and mice." J Am Pharm Assoc Am Pharm Assoc (Baltim) 46(3): 208-9.

Dunlap, J. C. (1999). "Molecular bases for circadian clocks." Cell 96(2): 271-90.

Easton, A., J. Arbuzova, et al. (2003). "The circadian Clock mutation increases exploratory activity and escape-seeking behavior." Genes Brain Behav 2(1): 11-9.

Edery, I., L. J. Zwiebel, et al. (1994). "Temporal phosphorylation of the Drosophila period protein." Proc Natl Acad Sci U S A 91(6): 2260-4.

Eide, E. J., E. L. Vielhaber, et al. (2002). "The circadian regulatory proteins BMAL1 and cryptochromes are substrates of casein kinase Iepsilon." J Biol Chem 277(19): 17248-54.

Eide, E. J., M. F. Woolf, et al. (2005). "Control of mammalian circadian rhythm by CKIepsilon-regulated proteasome-mediated PER2 degradation." Mol Cell Biol 25(7): 2795-807.

Emery, P., W. V. So, et al. (1998). "CRY, a Drosophila clock and light-regulated cryptochrome, is a major contributor to circadian rhythm resetting and photosensitivity." Cell 95(5): 669-79.

Erway, L. C., J. F. Willott, et al. (1993). "Genetics of age-related hearing loss in mice: I. Inbred and F1 hybrid strains." Hear Res 65(1-2): 125-32.

Favor, J. (1998). "The mutagenic activity of ethylnitrosourea at low doses in spermatogonia of the mouse as assessed by the specific-locus test." Mutat Res 405(2): 221-6.

Feldman, R. M., C. C. Correll, et al. (1997). "A complex of Cdc4p, Skp1p, and Cdc53p/cullin catalyzes ubiquitination of the phosphorylated CDK inhibitor Sic1p." Cell 91(2): 221-30.

Feng, D., T. Liu, et al. (2011). "A circadian rhythm orchestrated by histone deacetylase 3 controls hepatic lipid metabolism." Science 331(6022): 1315-9.

Frayling, T. M., N. J. Timpson, et al. (2007). "A common variant in the FTO gene is associated with body mass index and predisposes to childhood and adult obesity." Science 316(5826): 889-94.

Fu, L., H. Pelicano, et al. (2002). "The circadian gene Period2 plays an important role in tumor suppression and DNA damage response in vivo." Cell 111(1): 41-50.

Gachon, F., E. Nagoshi, et al. (2004). "The mammalian circadian timing system: from gene expression to physiology." Chromosoma 113(3): 103-12.

Gachon, F., F. F. Olela, et al. (2006). "The circadian PAR-domain basic leucine zipper transcription factors DBP, TEF, and HLF modulate basal and inducible xenobiotic detoxification." Cell Metab 4(1): 25-36.

Gallego, M. and D. M. Virshup (2007). "Post-translational modifications regulate the ticking of the circadian clock." Nat Rev Mol Cell Biol 8(2): 139-48.

Gao, Q. and E. S. Yeung (2000). "High-throughput detection of unknown mutations by using multiplexed capillary electrophoresis with poly(vinylpyrrolidone) solution." Anal Chem 72(11): 2499-506.

Gauger, M. A. and A. Sancar (2005). "Cryptochrome, circadian cycle, cell cycle checkpoints, and cancer." Cancer Res 65(15): 6828-34.

Gery, S., N. Komatsu, et al. (2006). "The circadian gene per1 plays an important role in cell growth and DNA damage control in human cancer cells." Mol Cell 22(3): 375-82.

Gluzman, Y. (1981). "SV40-transformed simian cells support the replication of early SV40 mutants." Cell 23(1): 175-82.

Godinho, S. I., E. S. Maywood, et al. (2007). "The after-hours mutant reveals a role for Fbxl3 in determining mammalian circadian period." Science 316(5826): 897-900.

Godinho, S. I. and P. M. Nolan (2006). "The role of mutagenesis in defining genes in behaviour." Eur J Hum Genet 14(6): 651-9.

Graham, F. L., J. Smiley, et al. (1977). "Characteristics of a human cell line transformed by DNA from human adenovirus type 5." J Gen Virol 36(1): 59-74.

Griffin, E. A., Jr., D. Staknis, et al. (1999). "Light-independent role of CRY1 and CRY2 in the mammalian circadian clock." Science 286(5440): 768-71.

Grima, B., A. Lamouroux, et al. (2002). "The F-box protein slimb controls the levels of clock proteins period and timeless." Nature 420(6912): 178-82.

Guilding, C. and H. D. Piggins (2007). "Challenging the omnipotence of the suprachiasmatic timekeeper: are circadian oscillators present throughout the mammalian brain?" Eur J Neurosci 25(11): 3195-216.

Hall, J. C. (1995). "Tripping along the trail to the molecular mechanisms of biological clocks." Trends Neurosci 18(5): 230-40.

Hall, J. C. (2000). "Cryptochromes: sensory reception, transduction, and clock functions subserving circadian systems." Curr Opin Neurobiol 10(4): 456-66.

Hamilton, B. A., W. N. Frankel, et al. (1996). "Disruption of the nuclear hormone receptor RORalpha in staggerer mice." Nature 379(6567): 736-9.

Harada, Y., M. Sakai, et al. (2005). "Ser-557-phosphorylated mCRY2 is degraded upon synergistic phosphorylation by glycogen synthase kinase-3 beta." J Biol Chem 280(36): 31714-21.

Hardin, P. E., J. C. Hall, et al. (1990). "Feedback of the Drosophila period gene product on circadian cycling of its messenger RNA levels." Nature 343(6258): 536-40.

Hardisty-Hughes, R. E., H. Tateossian, et al. (2006). "A mutation in the F-box gene, Fbxo11, causes otitis media in the Jeff mouse." Hum Mol Genet 15(22): 3273-9.

Harmar, A. J., H. M. Marston, et al. (2002). "The VPAC(2) receptor is essential for circadian function in the mouse suprachiasmatic nuclei." Cell 109(4): 497-508.

Harms, E., S. Kivimae, et al. (2004). "Posttranscriptional and posttranslational regulation of clock genes." J Biol Rhythms 19(5): 361-73.

Hattar, S., R. J. Lucas, et al. (2003). "Melanopsin and rod-cone photoreceptive systems account for all major accessory visual functions in mice." Nature 424(6944): 76-81.

Hawkins, G. A., D. A. Meyers, et al. (2008). "Identification of coding polymorphisms in human circadian rhythm genes PER1, PER2, PER3, CLOCK, ARNTL, CRY1, CRY2 and TIMELESS in a multi-ethnic screening panel." DNA Seq 19(1): 44-9.

He, Q., P. Cheng, et al. (2003). "FWD1-mediated degradation of FREQUENCY in Neurospora establishes a conserved mechanism for circadian clock regulation." EMBO J 22(17): 4421-30.

Helfrich-Forster, C., C. Winter, et al. (2001). "The circadian clock of fruit flies is blind after elimination of all known photoreceptors." Neuron 30(1): 249-61.

Ho, M. S., P. I. Tsai, et al. (2006). "F-box proteins: the key to protein degradation." J Biomed Sci 13(2): 181-91.

Hoffman, A. E., T. Zheng, et al. (2009). "Clock-cancer connection in non-Hodgkin's lymphoma: a genetic association study and pathway analysis of the circadian gene cryptochrome 2." Cancer Res 69(8): 3605-13.

Hogenesch, J. B., W. K. Chan, et al. (1997). "Characterization of a subset of the basic-helix-loop-helix-PAS superfamily that interacts with components of the dioxin signaling pathway." J Biol Chem 272(13): 8581-93.

Horne, J. A. and O. Ostberg (1976). "A self-assessment questionnaire to determine morningness-eveningness in human circadian rhythms." Int J Chronobiol 4(2): 97-110.

Hunt, T. and P. Sassone-Corsi (2007). "Riding tandem: circadian clocks and the cell cycle." Cell 129(3): 461-4.

Hunter-Ensor, M., A. Ousley, et al. (1996). "Regulation of the Drosophila protein timeless suggests a mechanism for resetting the circadian clock by light." Cell 84(5): 677-85.

Iitaka, C., K. Miyazaki, et al. (2005). "A role for glycogen synthase kinase-3beta in the mammalian circadian clock." J Biol Chem 280(33): 29397-402.

Ikegawa, S., M. Masuno, et al. (1999). "Cloning of translocation breakpoints associated with Shwachman syndrome and identification of a candidate gene." Clin Genet 55(6): 466-72.

Imaizumi, T., T. Kanegae, et al. (2000). "Cryptochrome nucleocytoplasmic distribution and gene expression are regulated by light quality in the fern Adiantum capillus-veneris." Plant Cell 12(1): 81-96.

Isaacs, A. M., P. L. Oliver, et al. (2003). "A mutation in Af4 is predicted to cause cerebellar ataxia and cataracts in the robotic mouse." J Neurosci 23(5): 1631-7.

Izumo, M., C. H. Johnson, et al. (2003). "Circadian gene expression in mammalian fibroblasts revealed by real-time luminescence reporting: temperature compensation and damping." Proc Natl Acad Sci U S A 100(26): 16089-94.

Jin, J., T. Cardozo, et al. (2004). "Systematic analysis and nomenclature of mammalian F-box proteins." Genes Dev 18(21): 2573-80.

Johnston, P. B., R. N. Gaster, et al. (1979). "A clinicopathologic study of autosomal dominant optic atrophy." Am J Ophthalmol 88(5): 868-75.

Justice, M. J., J. K. Noveroske, et al. (1999). "Mouse ENU mutagenesis." Hum Mol Genet 8(10): 1955-63.

Kalsbeek, A., I. F. Palm, et al. (2006). "SCN outputs and the hypothalamic balance of life." J Biol Rhythms 21(6): 458-69.

Kanai, S., R. Kikuno, et al. (1997). "Molecular evolution of the photolyase-blue-light photoreceptor family." J Mol Evol 45(5): 535-48.

Kapfhamer, D., O. Valladares, et al. (2002). "Mutations in Rab3a alter circadian period and homeostatic response to sleep loss in the mouse." Nat Genet 32(2): 290-5.

Kash, S. F., L. H. Tecott, et al. (1999). "Increased anxiety and altered responses to anxiolytics in mice deficient in the 65-kDa isoform of glutamic acid decarboxylase." Proc Natl Acad Sci U S A 96(4): 1698-703.

King, D. P., M. H. Vitaterna, et al. (1997). "The mouse Clock mutation behaves as an antimorph and maps within the W19H deletion, distal of Kit." Genetics 146(3): 1049-60.

Kipreos, E. T. and M. Pagano (2000). "The F-box protein family." Genome Biol 1(5): REVIEWS3002.

Kjer, P. (1959). "Infantile optic atrophy with dominant mode of inheritance: a clinical and genetic study of 19 Danish families." Acta Ophthalmol Suppl 164(Supp 54): 1-147.

Kjer, P., O. A. Jensen, et al. (1983). "Histopathology of eye, optic nerve and brain in a case of dominant optic atrophy." Acta Ophthalmol (Copenh) 61(2): 300-12.

Knaus, H. G., M. Garcia-Calvo, et al. (1994). "Subunit composition of the high conductance calcium-activated potassium channel from smooth muscle, a representative of the mSlo and slowpoke family of potassium channels." J Biol Chem 269(6): 3921-4.

Knippschild, U., A. Gocht, et al. (2005). "The casein kinase 1 family: participation in multiple cellular processes in eukaryotes." Cell Signal 17(6): 675-89.

Ko, C. H. and J. S. Takahashi (2006). "Molecular components of the mammalian circadian clock." Hum Mol Genet 15 Spec No 2: R271-7.

Ko, H. W., J. Jiang, et al. (2002). "Role for Slimb in the degradation of Drosophila Period protein phosphorylated by Doubletime." Nature 420(6916): 673-8.

Kobayashi, K., S. Kanno, et al. (1998). "Characterization of photolyase/blue-light receptor homologs in mouse and human cells." Nucleic Acids Res 26(22): 5086-92.

Koh, K., X. Zheng, et al. (2006). "JETLAG resets the Drosophila circadian clock by promoting light-induced degradation of TIMELESS." Science 312(5781): 1809-12.

Konopka, R. J. and S. Benzer (1971). "Clock mutants of Drosophila melanogaster." Proc Natl Acad Sci U S A 68(9): 2112-6.

Kopp, C., U. Albrecht, et al. (2002). "Homeostatic sleep regulation is preserved in mPer1 and mPer2 mutant mice." Eur J Neurosci 16(6): 1099-106.

Kornmann, B., O. Schaad, et al. (2007). "System-driven and oscillator-dependent circadian transcription in mice with a conditionally active liver clock." PLoS Biol 5(2): e34.

Krishnan, B., J. D. Levine, et al. (2001). "A new role for cryptochrome in a Drosophila circadian oscillator." Nature 411(6835): 313-7.

Kume, K., M. J. Zylka, et al. (1999). "mCRY1 and mCRY2 are essential components of the negative limb of the circadian clock feedback loop." Cell 98(2): 193-205.

Kurabayashi, N., T. Hirota, et al. "DYRK1A and glycogen synthase kinase 3beta, a dual-kinase mechanism directing proteasomal degradation of CRY2 for circadian timekeeping." Mol Cell Biol 30(7): 1757-68.

Langmesser, S., T. Tallone, et al. (2008). "Interaction of circadian clock proteins PER2 and CRY with BMAL1 and CLOCK." BMC Mol Biol 9: 41.

Lavebratt, C., L. K. Sjoholm, et al. (2010). "CRY2 is associated with depression." PLoS One 5(2): e9407.

Lavery, D. J., L. Lopez-Molina, et al. (1999). "Circadian expression of the steroid 15 alpha-hydroxylase (Cyp2a4) and coumarin 7-hydroxylase (Cyp2a5) genes in mouse liver is regulated by the PAR leucine zipper transcription factor DBP." Mol Cell Biol 19(10): 6488-99.

Le Martelot, G., T. Claudel, et al. (2009). "REV-ERBalpha participates in circadian SREBP signaling and bile acid homeostasis." PLoS Biol 7(9): e1000181.

Lee, C., J. P. Etchegaray, et al. (2001). "Posttranslational mechanisms regulate the mammalian circadian clock." Cell 107(7): 855-67.

Lee, C., V. Parikh, et al. (1996). "Resetting the Drosophila clock by photic regulation of PER and a PER-TIM complex." Science 271(5256): 1740-4.

Lee, S., L. A. Donehower, et al. "Disrupting circadian homeostasis of sympathetic signaling promotes tumor development in mice." PLoS One 5(6): e10995.

Levine, J. D., M. L. Weiss, et al. (1991). "Retinohypothalamic tract in the female albino rat: a study using horseradish peroxidase conjugated to cholera toxin." J Comp Neurol 306(2): 344-60.

Li, Q., Z. Liu, et al. (2002). "Integrated platform for detection of DNA sequence variants using capillary array electrophoresis." Electrophoresis 23(10): 1499-511.

Lin, C., D. E. Robertson, et al. (1995). "Association of flavin adenine dinucleotide with the Arabidopsis blue light receptor CRY1." Science 269(5226): 968-70.

Lin, C. and D. Shalitin (2003). "Cryptochrome structure and signal transduction." Annu Rev Plant Biol 54: 469-96.

Lin, D. C., C. M. Bullock, et al. (2002). "Identification and molecular characterization of two closely related G protein-coupled receptors activated by prokineticins/endocrine gland vascular endothelial growth factor." J Biol Chem 277(22): 19276-80.

Lindblad, W. J. and L. C. Flood (1987). "Establishment of an adult rat fibroblast cell line for studies of collagenase regulation." In Vitro Cell Dev Biol 23(6): 413-6.

Liu, A. C., W. G. Lewis, et al. (2007). "Mammalian circadian signaling networks and therapeutic targets." Nat Chem Biol 3(10): 630-9.

Liu, A. C., H. G. Tran, et al. (2008). "Redundant function of REV-ERBalpha and beta and non-essential role for Bmal1 cycling in transcriptional regulation of intracellular circadian rhythms." PLoS Genet 4(2): e1000023.

Liu, A. C., D. K. Welsh, et al. (2007). "Intercellular coupling confers robustness against mutations in the SCN circadian clock network." Cell 129(3): 605-16.

Lowrey, P. L., K. Shimomura, et al. (2000). "Positional syntenic cloning and functional characterization of the mammalian circadian mutation tau." Science 288(5465): 483-92.

Lowrey, P. L. and J. S. Takahashi (2000). "Genetics of the mammalian circadian system: Photic entrainment, circadian pacemaker mechanisms, and posttranslational regulation." Annu Rev Genet 34: 533-562.

Lu, B. S. and P. C. Zee (2006). "Circadian rhythm sleep disorders." Chest 130(6): 1915-23.

Lucas, R. J. and R. G. Foster (1999). "Circadian clocks: A cry in the dark?" Curr Biol 9(21): R825-8.

Maier, B., S. Wendt, et al. (2009). "A large-scale functional RNAi screen reveals a role for CK2 in the mammalian circadian clock." Genes Dev 23(6): 708-18.

Malhotra, K., S. T. Kim, et al. (1995). "Putative blue-light photoreceptors from Arabidopsis thaliana and Sinapis alba with a high degree of sequence homology to DNA photolyase contain the two photolyase cofactors but lack DNA repair activity." Biochemistry 34(20): 6892-9.

Marrus, S. B., H. Zeng, et al. (1996). "Effect of constant light and circadian entrainment of perS flies: evidence for light-mediated delay of the negative feedback loop in Drosophila." EMBO J 15(24): 6877-86.

Martinek, S., S. Inonog, et al. (2001). "A role for the segment polarity gene shaggy/GSK-3 in the Drosophila circadian clock." Cell 105(6): 769-79.

Mas, P., W. Y. Kim, et al. (2003). "Targeted degradation of TOC1 by ZTL modulates circadian function in Arabidopsis thaliana." Nature 426(6966): 567-70.

Matsuo, T., S. Yamaguchi, et al. (2003). "Control mechanism of the circadian clock for timing of cell division in vivo." Science 302(5643): 255-9.

Maywood, E. S., A. B. Reddy, et al. (2006). "Synchronization and maintenance of timekeeping in suprachiasmatic circadian clock cells by neuropeptidergic signaling." Curr Biol 16(6): 599-605.

McClung, C. A. (2007). "Circadian genes, rhythms and the biology of mood disorders." Pharmacol Ther 114(2): 222-32.

McManus, O. B., L. M. Helms, et al. (1995). "Functional role of the beta subunit of high conductance calcium-activated potassium channels." Neuron 14(3): 645-50.

Meijer, J. H. and W. J. Schwartz (2003). "In search of the pathways for light-induced pacemaker resetting in the suprachiasmatic nucleus." J Biol Rhythms 18(3): 235-49.

Meloni, E. G. and M. Davis (1999). "Enhancement of the acoustic startle response in rats by the dopamine D1 receptor agonist SKF 82958." Psychopharmacology (Berl) 144(4): 373-80.

Meng, Q. J., L. Logunova, et al. (2008). "Setting clock speed in mammals: the CK1 epsilon tau mutation in mice accelerates circadian pacemakers by selectively destabilizing PERIOD proteins." Neuron 58(1): 78-88.

Michaud, E. J., C. T. Culiat, et al. (2005). "Efficient gene-driven germ-line point mutagenesis of C57BL/6J mice." BMC Genomics 6: 164.

Miyamoto, Y. and A. Sancar (1998). "Vitamin B2-based blue-light photoreceptors in the retinohypothalamic tract as the photoactive pigments for setting the circadian clock in mammals." Proc Natl Acad Sci U S A 95(11): 6097-102.

Miyamoto, Y. and A. Sancar (1999). "Circadian regulation of cryptochrome genes in the mouse." Brain Res Mol Brain Res 71(2): 238-43.

Moore, D. D. (2011). "Physiology. Crise de foie, redux?" Science 331(6022): 1275-6.

Moore, R. Y. (1996). "Entrainment pathways and the functional organization of the circadian system." Prog Brain Res 111: 103-19.

Moore, R. Y. and J. P. Card (1994). "Intergeniculate leaflet: an anatomically and functionally distinct subdivision of the lateral geniculate complex." J Comp Neurol 344(3): 403-30.

Moore, R. Y. and V. B. Eichler (1972). "Loss of a circadian adrenal corticosterone rhythm following suprachiasmatic lesions in the rat." Brain Res 42(1): 201-6.

Moore, R. Y. and R. Silver (1998). "Suprachiasmatic nucleus organization." Chronobiol Int 15(5): 475-87.

Morton, A. J., N. I. Wood, et al. (2005). "Disintegration of the sleep-wake cycle and circadian timing in Huntington's disease." J Neurosci 25(1): 157-63.

Mrosovsky, N. (1988). "Phase response curves for social entrainment." J Comp Physiol A 162(1): 35-46.

Munoz, M., S. N. Peirson, et al. (2005). "Long-term constant light induces constitutive elevated expression of mPER2 protein in the murine SCN: a molecular basis for Aschoff's rule?" J Biol Rhythms 20(1): 3-14.

Murphy, K., M. Hafez, et al. (2003). "Evaluation of temperature gradient capillary electrophoresis for detection of the Factor V Leiden mutation: coincident identification of a novel polymorphism in Factor V." Mol Diagn 7(1): 35-40.

Myers, M. P., K. Wager-Smith, et al. (1996). "Light-induced degradation of TIMELESS and entrainment of the Drosophila circadian clock." Science 271(5256): 1736-40.

281

Myers, M. P., K. Wager-Smith, et al. (1995). "Positional cloning and sequence analysis of the Drosophila clock gene, timeless." Science 270(5237): 805-8.

Naylor, E., B. M. Bergmann, et al. (2000). "The circadian clock mutation alters sleep homeostasis in the mouse." J Neurosci 20(21): 8138-43.

Nguyen, D. and T. Xu (2008). "The expanding role of mouse genetics for understanding human biology and disease." Dis Model Mech 1(1): 56-66.

Nicholas, B., V. Rudrasingham, et al. (2007). "Association of Per1 and Npas2 with autistic disorder: support for the clock genes/social timing hypothesis." Mol Psychiatry 12(6): 581-92.

Nievergelt, C. M., D. F. Kripke, et al. (2006). "Suggestive evidence for association of the circadian genes PERIOD3 and ARNTL with bipolar disorder." Am J Med Genet B Neuropsychiatr Genet 141B(3): 234-41.

Noveroske, J. K., J. S. Weber, et al. (2000). "The mutagenic action of N-ethyl-N-nitrosourea in the mouse." Mamm Genome 11(7): 478-83.

Ohsaki, K., K. Oishi, et al. (2008). "The role of {beta}-TrCP1 and {beta}-TrCP2 in circadian rhythm generation by mediating degradation of clock protein PER2." J Biochem 144(5): 609-18.

Ohta, H., S. Yamazaki, et al. (2005). "Constant light desynchronizes mammalian clock neurons." Nat Neurosci 8(3): 267-9.

Oishi, K., H. Fukui, et al. (2000). "Rhythmic expression of BMAL1 mRNA is altered in Clock mutant mice: differential regulation in the suprachiasmatic nucleus and peripheral tissues." Biochem Biophys Res Commun 268(1): 164-71.

Oishi, K., K. Miyazaki, et al. (2003). "Genome-wide expression analysis of mouse liver reveals CLOCK-regulated circadian output genes." J Biol Chem 278(42): 41519-27.

Oleykowski, C. A., C. R. Bronson Mullins, et al. (1998). "Mutation detection using a novel plant endonuclease." Nucleic Acids Res 26(20): 4597-602.

Oster, H., A. Yasui, et al. (2002). "Disruption of mCry2 restores circadian rhythmicity in mPer2 mutant mice." Genes Dev 16(20): 2633-8.

Ozturk, N., J. H. Lee, et al. (2009). "Loss of cryptochrome reduces cancer risk in p53 mutant mice." Proc Natl Acad Sci U S A 106(8): 2841-6.

Panda, S., M. P. Antoch, et al. (2002). "Coordinated transcription of key pathways in the mouse by the circadian clock." Cell 109(3): 307-20.

Panda, S., I. Provencio, et al. (2003). "Melanopsin is required for non-image-forming photic responses in blind mice." Science 301(5632): 525-7.

Partch, C. L., K. F. Shields, et al. (2006). "Posttranslational regulation of the mammalian circadian clock by cryptochrome and protein phosphatase 5." Proc Natl Acad Sci U S A 103(27): 10467-72.

Pedrazzoli, M., R. Secolin, et al. "Interactions of polymorphisms in different clock genes associated with circadian phenotypes in humans." Genet Mol Biol 33(4): 627-32.

Perrotta, G., L. Ninu, et al. (2000). "Tomato contains homologues of Arabidopsis cryptochromes 1 and 2." Plant Mol Biol 42(5): 765-73.

Pevet, P., L. Agez, et al. (2006). "Melatonin in the multi-oscillatory mammalian circadian world." Chronobiol Int 23(1-2): 39-51.

Picciotto, M. R. and K. Wickman (1998). "Using knockout and transgenic mice to study neurophysiology and behavior." Physiol Rev 78(4): 1131-63.

Plazzi, G., Y. Schutz, et al. (1997). "Motor overactivity and loss of motor circadian rhythm in fatal familial insomnia: an actigraphic study." Sleep 20(9): 739-42.

Ponten, J. and E. Saksela (1967). "Two established in vitro cell lines from human mesenchymal tumours." Int J Cancer 2(5): 434-47.

Porsolt, R. D., A. Bertin, et al. (1977). "Behavioral despair in mice: a primary screening test for antidepressants." Arch Int Pharmacodyn Ther 229(2): 327-36.

Preitner, N., F. Damiola, et al. (2002). "The orphan nuclear receptor REV-ERBalpha controls circadian transcription within the positive limb of the mammalian circadian oscillator." Cell 110(2): 251-60.

Price, J. L., J. Blau, et al. (1998). "double-time is a novel Drosophila clock gene that regulates PERIOD protein accumulation." Cell 94(1): 83-95.

Provencio, I., I. R. Rodriguez, et al. (2000). "A novel human opsin in the inner retina." J Neurosci 20(2): 600-5.

Provost, G. S. and J. M. Short (1994). "Characterization of mutations induced by ethylnitrosourea in seminiferous tubule germ cells of transgenic B6C3F1 mice." Proc Natl Acad Sci U S A 91(14): 6564-8.

Quwailid, M. M., A. Hugill, et al. (2004). "A gene-driven ENU-based approach to generating an allelic series in any gene." Mamm Genome 15(8): 585-91.

Rana, S. and S. Mahmood "Circadian rhythm and its role in malignancy." J Circadian Rhythms 8: 3.

Reischl, S., K. Vanselow, et al. (2007). "Beta-TrCP1-mediated degradation of PERIOD2 is essential for circadian dynamics." J Biol Rhythms 22(5): 375-86.

Reppert, S. M. and D. R. Weaver (2001). "Molecular analysis of mammalian circadian rhythms." Annu Rev Physiol 63: 647-76.

Reppert, S. M. and D. R. Weaver (2002). "Coordination of circadian timing in mammals." Nature 418(6901): 935-41.

Rioux, J. D., R. J. Xavier, et al. (2007). "Genome-wide association study identifies new susceptibility loci for Crohn disease and implicates autophagy in disease pathogenesis." Nat Genet 39(5): 596-604.

Ripperger, J. A. and U. Schibler (2006). "Rhythmic CLOCK-BMAL1 binding to multiple E-box motifs drives circadian Dbp transcription and chromatin transitions." Nat Genet 38(3): 369-74.

Roenneberg, T. and M. Merrow (2005). "Circadian clocks - the fall and rise of physiology." Nat Rev Mol Cell Biol 6(12): 965-71.

Roybal, K., D. Theobold, et al. (2007). "Mania-like behavior induced by disruption of CLOCK." Proc Natl Acad Sci U S A 104(15): 6406-11.

Rudic, R. D., P. McNamara, et al. (2004). "BMAL1 and CLOCK, two essential components of the circadian clock, are involved in glucose homeostasis." PLoS Biol 2(11): e377.

Russell, L. B., P. R. Hunsicker, et al. (1989). "Chlorambucil effectively induces deletion mutations in mouse germ cells." Proc Natl Acad Sci U S A 86(10): 3704-8.

Russell, L. B., P. R. Hunsicker, et al. (2007). "Comparison of the genetic effects of equimolar doses of ENU and MNU: while the chemicals differ dramatically in their mutagenicity in stem-cell spermatogonia, both elicit very high mutation rates in differentiating spermatogonia." Mutat Res 616(1-2): 181-95.

Russell, L. B. and W. L. Russell (1992). "Frequency and nature of specific-locus mutations induced in female mice by radiations and chemicals: a review." Mutat Res 296(1-2): 107-27.

Russell, W. L., E. M. Kelly, et al. (1979). "Specific-locus test shows ethylnitrosourea to be the most potent mutagen in the mouse." Proc Natl Acad Sci U S A 76(11): 5818-9.

Ruttiger, L., M. Sausbier, et al. (2004). "Deletion of the Ca2+-activated potassium (BK) alpha-subunit but not the BKbeta1-subunit leads to progressive hearing loss." Proc Natl Acad Sci U S A 101(35): 12922-7.

Sanada, K., Y. Harada, et al. (2004). "Serine phosphorylation of mCRY1 and mCRY2 by mitogen-activated protein kinase." Genes Cells 9(8): 697-708.

Sanada, K., T. Okano, et al. (2002). "Mitogen-activated protein kinase phosphorylates and negatively regulates basic helix-loop-helix-PAS transcription factor BMAL1." J Biol Chem 277(1): 267-71.

Sancar, A. (2003). "Structure and function of DNA photolyase and cryptochrome blue-light photoreceptors." Chem Rev 103(6): 2203-37.

Sancar, A. (2004). "Regulation of the mammalian circadian clock by cryptochrome." J Biol Chem 279(33): 34079-82.

Sato, T. K., S. Panda, et al. (2004). "A functional genomics strategy reveals Rora as a component of the mammalian circadian clock." Neuron 43(4): 527-37.

Schmutz, I., J. A. Ripperger, et al. (2010). "The mammalian clock component PERIOD2 coordinates circadian output by interaction with nuclear receptors." Genes Dev 24(4): 345-57.

Schwartz, W. J., R. A. Gross, et al. (1987). "The suprachiasmatic nuclei contain a tetrodotoxin-resistant circadian pacemaker." Proc Natl Acad Sci U S A 84(6): 1694-8.

Sehgal, A., A. Rothenfluh-Hilfiker, et al. (1995). "Rhythmic expression of timeless: a basis for promoting circadian cycles in period gene autoregulation." Science 270(5237): 808-10.

Selby, C. P., C. Thompson, et al. (2000). "Functional redundancy of cryptochromes and classical photoreceptors for nonvisual ocular photoreception in mice." Proc Natl Acad Sci U S A 97(26): 14697-702.

Shearman, L. P., S. Sriram, et al. (2000). "Interacting molecular loops in the mammalian circadian clock." Science 288(5468): 1013-9.

Shearman, L. P., M. J. Zylka, et al. (1997). "Two period homologs: circadian expression and photic regulation in the suprachiasmatic nuclei." Neuron 19(6): 1261-9.

Shi, S., A. Hida, et al. (2010). "Circadian clock gene Bmal1 is not essential; functional replacement with its paralog, Bmal2." Curr Biol 20(4): 316-21.

Shibuya, T., T. Murota, et al. (1993). "The induction of recessive mutations in mouse primordial germ cells with N-ethyl-N-nitrosourea." Mutat Res 290(2): 273-80.

Shiromani, P. J., M. Xu, et al. (2004). "Sleep rhythmicity and homeostasis in mice with targeted disruption of mPeriod genes." Am J Physiol Regul Integr Comp Physiol 287(1): R47-57.

Siepka, S. M., S. H. Yoo, et al. (2007). "Genetics and neurobiology of circadian clocks in mammals." Cold Spring Harb Symp Quant Biol 72: 251-9.

Siepka, S. M., S. H. Yoo, et al. (2007). "Circadian mutant Overtime reveals F-box protein FBXL3 regulation of cryptochrome and period gene expression." Cell 129(5): 1011-23.

Simonneaux, V. and C. Ribelayga (2003). "Generation of the melatonin endocrine message in mammals: a review of the complex regulation of melatonin synthesis by norepinephrine, peptides, and other pineal transmitters." Pharmacol Rev 55(2): 325-95.

Sjoblom, T., S. Jones, et al. (2006). "The consensus coding sequences of human breast and colorectal cancers." Science 314(5797): 268-74.

Skowyra, D., K. L. Craig, et al. (1997). "F-box proteins are receptors that recruit phosphorylated substrates to the SCF ubiquitin-ligase complex." Cell 91(2): 209-19.

Sladek, R., G. Rocheleau, et al. (2007). "A genome-wide association study identifies novel risk loci for type 2 diabetes." Nature 445(7130): 881-5.

So, W. V. and M. Rosbash (1997). "Post-transcriptional regulation contributes to Drosophila clock gene mRNA cycling." EMBO J 16(23): 7146-55.

Soewarto, D., M. Klaften, et al. (2009). "Features and strategies of ENU mouse mutagenesis." Curr Pharm Biotechnol 10(2): 198-213.

Spanagel, R., G. Pendyala, et al. (2005). "The clock gene Per2 influences the glutamatergic system and modulates alcohol consumption." Nat Med 11(1): 35-42.

Spengler, M. L., K. K. Kuropatwinski, et al. (2009). "A serine cluster mediates BMAL1-dependent CLOCK phosphorylation and degradation." Cell Cycle 8(24): 4138-46.

Stanewsky, R., M. Kaneko, et al. (1998). "The cryb mutation identifies cryptochrome as a circadian photoreceptor in Drosophila." Cell 95(5): 681-92.

Steinlechner, S., B. Jacobmeier, et al. (2002). "Robust circadian rhythmicity of Per1 and Per2 mutant mice in constant light, and dynamics of Per1 and Per2 gene expression under long and short photoperiods." J Biol Rhythms 17(3): 202-9.

Stephan, F. K. (1997). "Calories affect zeitgeber properties of the feeding entrained circadian oscillator." Physiol Behav 62(5): 995-1002.

Stephan, F. K. (2002). "The "other" circadian system: food as a Zeitgeber." J Biol Rhythms 17(4): 284-92.

Stokkan, K. A., S. Yamazaki, et al. (2001). "Entrainment of the circadian clock in the liver by feeding." Science 291(5503): 490-3.

Sudhof, T. C. (2004). "The synaptic vesicle cycle." Annu Rev Neurosci 27: 509-47.

Sudo, M., K. Sasahara, et al. (2003). "Constant light housing attenuates circadian rhythms of mPer2 mRNA and mPER2 protein expression in the suprachiasmatic nucleus of mice." Neuroscience 121(2): 493-9.

Takahashi, J. S., H. K. Hong, et al. (2008). "The genetics of mammalian circadian order and disorder: implications for physiology and disease." Nat Rev Genet 9(10): 764-75.

Takai, Y., T. Sasaki, et al. (1996). "Rab3A small GTP-binding protein in Ca(2+)-dependent exocytosis." Genes Cells 1(7): 615-32.

Thompson, C. L., C. Bowes Rickman, et al. (2003). "Expression of the blue-light receptor cryptochrome in the human retina." Invest Ophthalmol Vis Sci 44(10): 4515-21.

Thresher, R. J., M. H. Vitaterna, et al. (1998). "Role of mouse cryptochrome blue-light photoreceptor in circadian photoresponses." Science 282(5393): 1490-4.

Till, B. J., S. H. Reynolds, et al. (2003). "Large-scale discovery of induced point mutations with high-throughput TILLING." Genome Res 13(3): 524-30.

Todd, J. A., N. M. Walker, et al. (2007). "Robust associations of four new chromosome regions from genome-wide analyses of type 1 diabetes." Nat Genet 39(7): 857-64.

Todo, T. (1999). "Functional diversity of the DNA photolyase/blue light receptor family." Mutat Res 434(2): 89-97.

Toh, K. L. (2008). "Basic science review on circadian rhythm biology and circadian sleep disorders." Ann Acad Med Singapore 37(8): 662-8.

Toh, K. L., C. R. Jones, et al. (2001). "An hPer2 phosphorylation site mutation in familial advanced sleep phase syndrome." Science 291(5506): 1040-3.

Tosini, G. and M. Menaker (1998). "The clock in the mouse retina: melatonin synthesis and photoreceptor degeneration." Brain Res 789(2): 221-8.

Turek, F. W., C. Joshu, et al. (2005). "Obesity and metabolic syndrome in circadian Clock mutant mice." Science 308(5724): 1043-5.

Ueda, H. R., W. Chen, et al. (2002). "A transcription factor response element for gene expression during circadian night." Nature 418(6897): 534-9.

Ukai-Tadenuma, M., R. G. Yamada, et al. (2011). "Delay in feedback repression by cryptochrome 1 is required for circadian clock function." Cell 144(2): 268-81.

van der Horst, G. T., M. Muijtjens, et al. (1999). "Mammalian Cry1 and Cry2 are essential for maintenance of circadian rhythms." Nature 398(6728): 627-30.

Vanselow, K., J. T. Vanselow, et al. (2006). "Differential effects of PER2 phosphorylation: molecular basis for the human familial advanced sleep phase syndrome (FASPS)." Genes Dev 20(19): 2660-72.

Vitaterna, M. H., C. P. Selby, et al. (1999). "Differential regulation of mammalian period genes and circadian rhythmicity by cryptochromes 1 and 2." Proc Natl Acad Sci U S A 96(21): 12114-9.

Vivian, J. L., Y. Chen, et al. (2002). "An allelic series of mutations in Smad2 and Smad4 identified in a genotype-based screen of N-ethyl-N- nitrosourea-mutagenized mouse embryonic stem cells." Proc Natl Acad Sci U S A 99(24): 15542-7.

Wager-Smith, K. and S. A. Kay (2000). "Circadian rhythm genetics: from flies to mice to humans." Nat Genet 26(1): 23-7.

Wee, R., A. M. Castrucci, et al. (2002). "Loss of photic entrainment and altered free-running circadian rhythms in math5-/- mice." J Neurosci 22(23): 10427-33.

Wee, R. and R. N. Van Gelder (2004). "Sleep disturbances in young subjects with visual dysfunction." Ophthalmology 111(2): 297-302; discussion 302-3.

Weiss, I. C., J. Feldon, et al. (1999). "Circadian time does not modify the prepulse inhibition response or its attenuation by apomorphine." Pharmacol Biochem Behav 64(3): 501-5.

Welsh, D. K., T. Imaizumi, et al. (2005). "Real-time reporting of circadian-regulated gene expression by luciferase imaging in plants and mammalian cells." Methods Enzymol 393: 269-88.

Willott, J. F., J. G. Turner, et al. (1998). "The BALB/c mouse as an animal model for progressive sensorineural hearing loss." Hear Res 115(1-2): 162-74.

Wisor, J. P., D. M. Edgar, et al. (2005). "Sleep and circadian abnormalities in a transgenic mouse model of Alzheimer's disease: a role for cholinergic transmission." Neuroscience 131(2): 375-85.

Wood, S. J. and M. Toth (2001). "Molecular pathways of anxiety revealed by knockout mice." Mol Neurobiol 23(2-3): 101-19.

Xu, Y., Q. S. Padiath, et al. (2005). "Functional consequences of a CKIdelta mutation causing familial advanced sleep phase syndrome." Nature 434(7033): 640-4.

Yagita, K. and H. Okamura (2000). "Forskolin induces circadian gene expression of rPer1, rPer2 and dbp in mammalian rat-1 fibroblasts." FEBS Lett 465(1): 79-82.

Yagita, K., F. Tamanini, et al. (2001). "Molecular mechanisms of the biological clock in cultured fibroblasts." Science 292(5515): 278-81.

Yagita, K., F. Tamanini, et al. (2002). "Nucleocytoplasmic shuttling and mCRY-dependent inhibition of ubiquitylation of the mPER2 clock protein." EMBO J 21(6): 1301-14.

Yagita, K., S. Yamaguchi, et al. (2000). "Dimerization and nuclear entry of mPER proteins in mammalian cells." Genes Dev 14(11): 1353-63.

Yamazaki, S. and J. S. Takahashi (2005). "Real-time luminescence reporting of circadian gene expression in mammals." Methods Enzymol 393: 288-301.

Yan, L. and R. Silver (2002). "Differential induction and localization of mPer1 and mPer2 during advancing and delaying phase shifts." Eur J Neurosci 16(8): 1531-40.

Yang, S., M. Farias, et al. (2007). "Biochemical, molecular and behavioral phenotypes of Rab3A mutations in the mouse." Genes Brain Behav 6(1): 77-96.

Yang, S., A. Liu, et al. (2009). "The role of mPer2 clock gene in glucocorticoid and feeding rhythms." Endocrinology 150(5): 2153-60.

Ye, R., C. P. Selby, et al. "Biochemical analysis of the canonical model for the Mammalian circadian clock." J Biol Chem 286(29): 25891-902.

Yin, L., J. Wang, et al. (2006). "Nuclear receptor Rev-erbalpha is a critical lithium-sensitive component of the circadian clock." Science 311(5763): 1002-5.

Yoshii, T., C. Hermann, et al. "Cryptochrome-positive and -negative clock neurons in Drosophila entrain differentially to light and temperature." J Biol Rhythms 25(6): 387-98.

Yoshimura, T. and S. Ebihara (1998). "Decline of circadian photosensitivity associated with retinal degeneration in CBA/J-rd/rd mice." Brain Res 779(1-2): 188-93.

Young, M. W. (2000). "Life's 24-hour clock: molecular control of circadian rhythms in animal cells." Trends Biochem Sci 25(12): 601-6.

Zarcone, V., K. Azumi, et al. (1975). "REM phase deprivation and schizophrenia II." Arch Gen Psychiatry 32(11): 1431-6.

Zarcone, V., G. Gulevich, et al. (1968). "Partial REM phase deprivation and schizophrenia." Arch Gen Psychiatry 18(2): 194-202.

Zeng, H., Z. Qian, et al. (1996). "A light-entrainment mechanism for the Drosophila circadian clock." Nature 380(6570): 129-35.

Zeng, Z. L., M. W. Wu, et al. (2010). "Effects of the biological clock gene Bmal1 on tumour growth and anti-cancer drug activity." J Biochem 148(3): 319-26.

Zhang, L., X. Z. Hu, et al. "Startle response related genes." Med Hypotheses 77(4): 685-91.

Zheng, Q. Y., K. R. Johnson, et al. (1999). "Assessment of hearing in 80 inbred strains of mice by ABR threshold analyses." Hear Res 130(1-2): 94-107.

Zhou, Y. D., M. Barnard, et al. (1997). "Molecular characterization of two mammalian bHLH-PAS domain proteins selectively expressed in the central nervous system." Proc Natl Acad Sci U S A 94(2): 713-8.

Zylka, M. J., L. P. Shearman, et al. (1998). "Three period homologs in mammals: differential light responses in the suprachiasmatic circadian clock and oscillating transcripts outside of brain." Neuron 20(6): 1103-10.

8 <u>CHAPTER EIGHT</u>: Appendix

Appendix 1: Genes amplified with Real time quantitative PCR

Gene Amplified	Primer Sequence
Per1 Fw	CCC CTG CCT CCC AGT GA
Per1 Rv	CTG AAA GTG CAT CCT GAT TGG A
Per2 Fw	AGC TAC ACC ACC CCT TAC AAG CT
Per2 Rv	GAC ACG GCA GAA AAA AGA TTT CTC
Cry1 Fw	GCT ATG CTC CTG GAG AGA ACG T
Cry1 Rv	TGT CCC CGT GAG CAT AGT GTA A
Cry2 Fw	TGA CCT AGA CAG AAT CAT CGA ACT G
Cry2 Rv	GGC TGA TGA GGG CCT GAA
Bmal1 Fw	CCG TGC TAA GGA TGG CTG TT
Bmal1 Rv	TTG GCT TGT AGT TTG CTT CTG TGT
Dbp Fw	GAG CCT TCT GCA GGG AAA CA
Dbp Rv	GCC TTG CGC TCC TTT TCC
Rev-erba Fw	CGT TCG CAT CAA TCG CAA CC
Rev-erba Rv	GAT GTG GAG TAG GTG AGG TC
RPL13a Fw	GGA AGC GGA TGA ATA CCA AC
RPL13a Rv	GGA TCC CAT CCA ACA CCT T

## Appendix 2: Details for cloning Fbxl3-GFP-Flag

Full length *Fbxl3* was amplified and inserted into the pIRES-hrGFP-1a (Stratagene) vector (Section 2.12.2). The details of primer sequences used to amplify *Fbxl3* are listed in the table below. Following amplification, the insert and the vector were digested with two restriction enzymes (Section 2.12.6) and then ligated using various molar ratios. Following ligation and successful sequencing confirming the orientation of the insert into the plasmid, the *Afh* and human polymorphism mutations, *Fbxl3*G342V were introduced into the same plasmid. Details of primers used for mutagenesis are also listed in the table.

Primers for full-length amplification:

Primer name	Primer Sequence
NotI_*Fbxl3*_F	GCGG CCG CCC ACCATGAAACGAGGAGGAAGA
BamHI_*Fbxl3*_R	GGAT CCGCCAAGTAGGCATCATGTC

NEB Double digest screen: Fbxl3 insert and pIRES-hrGFP-1a vector digest conditions:
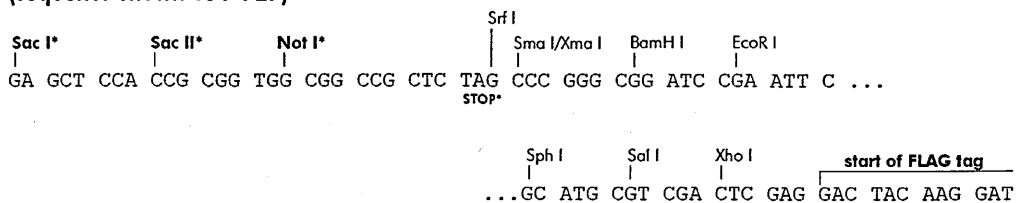
Select 1st enzyme: NotI-HF™   **Select 2nd enzyme:** BamHI-HF™   GO

Enzyme	Cat#	Temp	Supplied NEBuffer	Supplements		% Activity in NEBuffer				
				BSA	SAM	1	2	3	4	EcoRI
NotI-HF™	R3189	37°C	NEBuffer 4	Yes	No	25	100	25	100	50
BamHI-HF™	R3136	37°C	NEBuffer 4	No	No	100	50	10	100	25

Double Digest Recommendation(s) for NotI-HF™ + BamHI-HF™:

- Digest in NEBuffer 4 + BSA at 37°C.

294

Primer sequences used for Fbxl3 mutagenesis:

Primer name	Primer Sequence
Fbxl3_G342V_F	GTAGTGTGTGCCAATGTGTTGCGGCCTCTTGAT
Fbxl3_G342V_R	ATCAAGAGGCCGCAACACATTGGCACACACTAC
Fbxl3_Afh_F	GCGGAACGTAGCAAAAATTTGTC
Fbxl3_Afh_R	GACAAATTTTTGCTACGTTCCGC

Vector map of pIRES-hrGFP-1a (Stratagene) showing sites of Not1 and BamH1 used to clone Fbxl3:

The pIRES-hrGFP-1a Vector
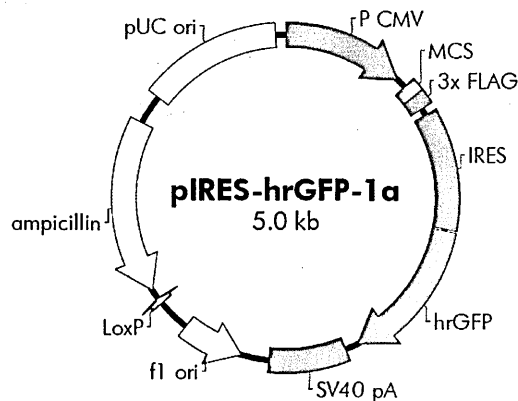
pIRES-hrGFP-1a Multiple Cloning Site Region
(sequence shown 651–727)

```
                                              Srf I
Sac I*        Sac II*       Not I*            |   Sma I/Xma I   BamH I   EcoR I
|             |             |                 |   |            |        |
GA GCT CCA CCG CGG TGG CGG CCG CTC TAG CCC GGG CGG ATC CGA ATT C ...
                                        STOP*

                        Sph I      Sal I      Xho I      start of FLAG tag
                        |          |          |          ┌──────────────
                        ...GC ATG CGT CGA CTC GAG GAC TAC AAG GAT
```

Appendix 3: List of Plasmids used

| Plasmid	3'Tag	Vector
Cry1 (kind gift from Dr.Michael H.Hastings)	HA	pcDNA 3.1
Cry2 (kind gift from Dr.Michael H.Hastings)	HA	pcDNA 3.1
Fbxl3	GFP	pcDNA3.1/CT-GFP-TOPO
Fbxl3-Afh	GFP	pcDNA3.1/CT-GFP-TOPO
Fbxl21 (kind gift from Dr.Hugues Dardente)	Myc	pCSII-Myc
Fbxl21-V68E (kind gift from Dr.Hugues Dardente)	Myc	pCSII-Myc
Fbxl21-P291Q (kind gift from Dr.Hugues Dardente)	Myc	pCSII
ev-GFP	GFP	pcDNA3
ev-Myc	GFP	

Appendix 4: Period analysis of Cry1$^{-/-}$; Fbxl3$^{Afh/Afh}$ compound mutants in-vitro
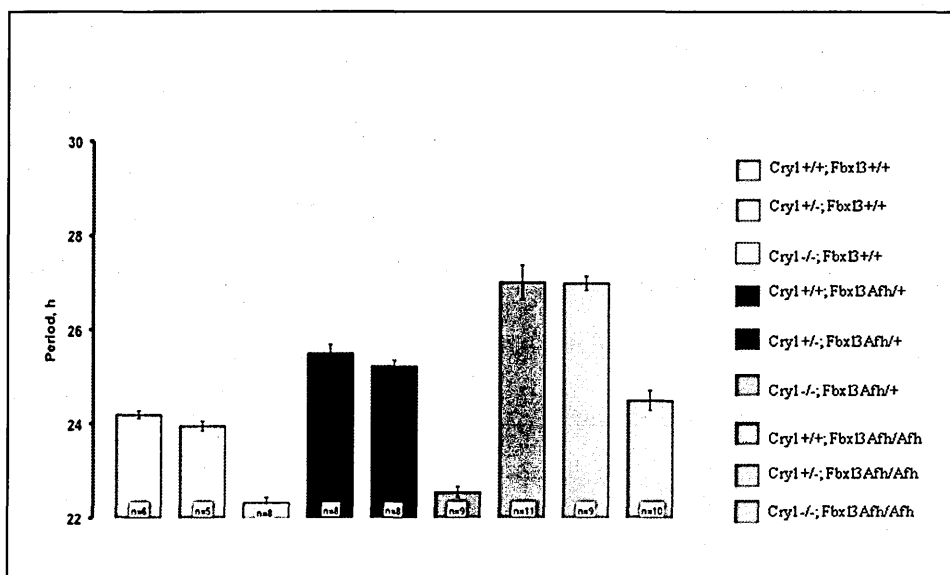
Figure 8.1: Period analysis in *Cry1$^{-/-}$;Fbxl3$^{Afh/Afh}$* compound mutants *in-vitro*. The compound mutants were crossed to a PER-driven Luc mouse line. These mice were entrained to a 12hr L;D cycle for 1 week and were then kept in constant dark conditions (DD) . The SCN from each genotype generated during the *Cry1$^{-/-}$;Fbxl3$^{Afh/Afh}$* intercross, were collected in constant darkness and organotypically cultured. The SCN slices alongwith the luciferin susbstrate were placed in the LumiCycle to measure the PER-driven bioluminescence. The figure above shows us that the period of SCN from the *Cry1$^{-/-}$;Fbxl3$^{Afh/Afh}$* mice follow a similar trend *in-vitro* to what is found *in vivo*. With the loss of a copy of *Cry* (Left to right), there is acceleration of the clock. With the addition of the *Afh* mutation, although there is period lengthening compared to the *Cry1$^{-/-}$* SCN, in the *Cry1$^{-/-}$; Fbxl3$^{Afh/Afh}$* mice, there is accereleration of the clock.

The above work was carried out by Dr. Michael Hasting and Dr. Elizabeth Maywood, MRC, Laboratory of Molecular Biology, Cambridge.
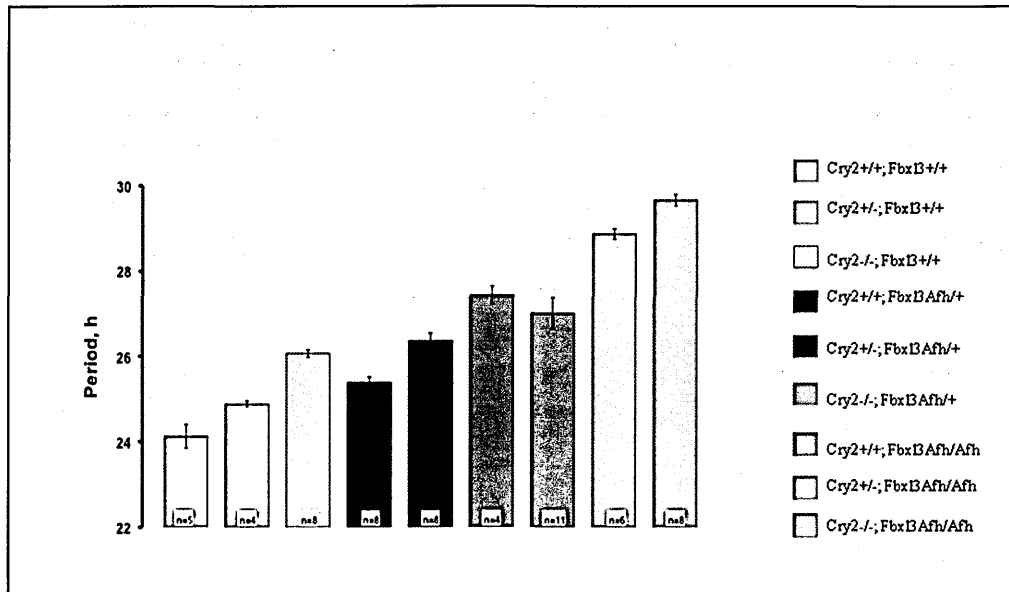
Appendix 5: Period analysis of Cry2$^{-/-}$; Fbxl3$^{Afh/Afh}$ compound mutants in-vitro

Figure 8.2: Period analysis in *Cry2$^{-/-}$; Fbxl3$^{Afh/Afh}$* compound mutants *in-vitro*. The compound mutants were crossed to a PER-driven luc mouse line. These mice were entrained to a 12hr L;D cycle for 1 week and were then kept in constant dark conditions (DD) . The SCN from each genotype generated during the *Cry2$^{-/-}$;Fbxl3$^{Afh/Afh}$* intercross, were collected in constant darkness and organotypically cultured. The SCN slices alongwith the luciferin susbstrate were placed in the LumiCycle to measure the PER-driven bioluminescence. The figure above shows us that the period of SCN from the *Cry2$^{-/-}$; Fbxl3$^{Afh/Afh}$* mice follow a similar trend *in-vitro* to what is found *in vivo*. With the loss of a copy of *Cry* (Left to right), there is delay of the clock, hence period lengthening. As the dose of the *Afh* mutation increases, there is a considerable increase in the period length. Due to the *Afh* mutation, there is overexpression of CRY1 which is a strong transcriptional repressor, thus contributing to the period lengthening phenotype.

The above work was carried out by Dr. Michael Hasting and Dr. Elizabeth Maywood, MRC, Laboratory of Molecular Biology, Cambridge.
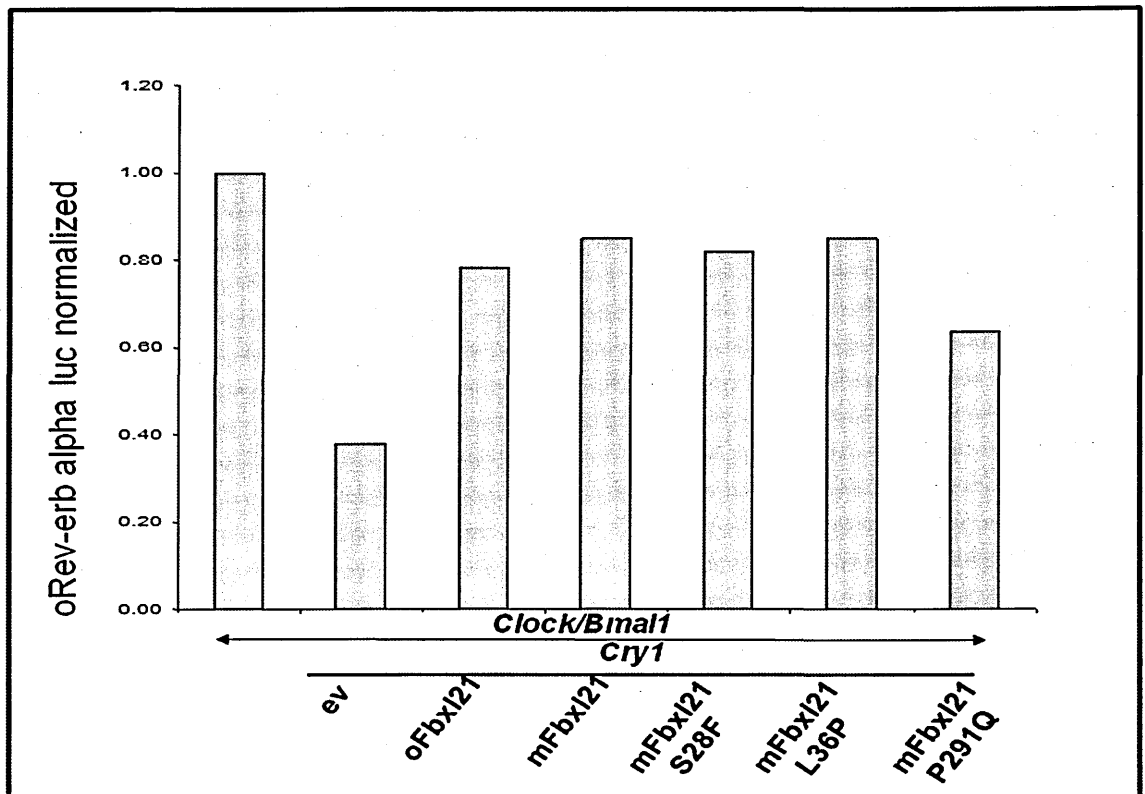
Appendix 6: In-vitro luminescence assay showing effect of Fbxl21 mutants

Figure 8.3: *In-vitro* luminescence assay showing the potential effects of mutant *Fbxl21* on the circadian clock. In this experiment, the *Rev-erbα* promoter (from sheep) is used to drive luciferase expression. This assay is used to measure the luminescence of *Rev-erbα*:Luc that is activated by the CLOCK-BMAL1 heterodimeric complex. The measure of luminescence used to plot this graph is normalised to the Rev-erbα:Luc expression that is driven by CLOCK-BMAL1 heterodimer (first bar).On the addition of *Cry1*, a transcriptional repressor, the CLOCK-BMAL1 heterodimeric activity is suppressed, as a result there is very low *Rev-erbα*:Luc read-out (second bar). Further, when *Fbxl21* is added to the CRY1-CLOCK-BMAL-1 complex, CRY1 is degraded. Hence there is an inhibition of CRY1 repression activity. As a result, the *Rev-erbα*:Luc is activated. Compared to the transactivation of *Rev-erbα*:Luc by *Fbxl21*-Wt, there is no difference in function caused by the S28F and L36P mutation. The third mutation, *Fbxl21*-P291Q shows an approximate 20% reduction in the activation of *Rev-erbα*:Luc, suggesting that this mutant is not able to degrade CRY1 as much as *Fbxl21*-Wt. Hence, this mutant is considered to be a hypomorph.